MODULATION OF MICRORNAS IN PANCREATIC CANCER BY THE DIETARY AGENT CURCUMIN

Thesis submitted for the degree of
Doctor of Philosophy
at the University of Leicester

Lara C. Lewis BSc MSc (Leicester)
Department of Cancer Studies and Molecular Medicine
University of Leicester

September 2014

Once upon a time there was a little cancer cell.....

Dedicated to my wonderful parents

Lara C. Lewis

Modulation of microRNAs in Pancreatic Cancer by the Dietary Agent Curcumin

Abstract

Pancreatic tumourigenesis is a furtive disease characterised by its lack of palpable symptoms and the inconsistency in expression of its various diagnostic markers. The early detection of pancreatic cancer is therefore problematic, with most patients presenting with advanced disease resulting in limited treatment options. MicroRNAs post-transcriptionally regulate gene expression and their aberrant expression has been linked to disease progression in various cancers including pancreatic. *In vitro* studies have shown that by manipulating microRNA expression, it is possible to inhibit proliferation, suppress metastasis and induce drug sensitivity in pancreatic cancer cells. The phytochemical curcumin, which is under investigation in combination treatment trials for pancreatic cancer, is believed to alter microRNA expression.

The work presented in this thesis aimed to identify novel, aberrantly expressed microRNAs which could potentially be used as diagnostic markers for pancreatic cancer, and to ascertain if curcumin could modulate their expression. Additionally, possible mechanisms by which curcumin may regulate the expression of key microRNAs in pancreatic cancer cells when compared to non-transformed cells were also examined.

This thesis details the identification of differentially expressed microRNAs using microarray analysis. Cell viability and growth were assessed in order to determine a dose and a treatment time with the capacity to elicit a biological response in pancreatic cancer cell lines. Validation of changes observed in microRNA expression using the microarrays was carried out using RT-qPCR. The results demonstrated that, despite being unable to validate the differential expression of various microRNAs identified by microarray analysis, curcumin did appear to modulate the expression of a number of miRNAs known to be deregulated in pancreatic cancer.

Acknowledgements

The last four years culminating in the writing of this doctoral thesis would not have been possible without the help, kindness and support of the wonderful people around me, only some of whom it is possible to mention in particular. I would like to start by thanking my supervisors, Professors Maggie Manson and Martin Bushell and Dr Howard Pringle for all their time, support and encouragement over the last four years. I am especially grateful to Matthew Blades (BBASH Bioinformatics), Mai-Kim Cheng, Lynne Howells, Nicolas Sylvius and Jack Godfry for being so generous with their time and expertise on many an occasion.

I would also like to acknowledge Elena Karpova, Kate Dudek and Katherine Clark. These inspirational women have shown me what working in scientific research is really about. Their unwavering support, encouragement and willingness to help with anything has made the last four years such an enjoyable experience. I started this journey with them as colleagues and am ending it with them as friends.

Also, huge thanks to the now defunct Biocentre and all who resided in it. I was very lucky to have the opportunity not only to work in such a nice environment, but also to work alongside such a lovely group of warm and genuine people.

The completion of a doctoral thesis however, is not a task to be undertaken lightly, with many highs and lows along the path to scientific greatness. It is therefore of paramount importance to surround yourself with like minded people with whom you can share this experience and I was lucky enough to do just that. A big thank you goes to Sian Evans, Eva Jordan, Charlotte Daly and Alex Geddes. We laughed, we cried, we ate loads of Boosts. I would also like to thank Gregg Hudson and Alex Palmer for all their help and support throughout the last year.

To my brother Philip, Abuelita Dora, Abuelito Felicisimo, Grandma Stella and Grandpa Ron thank you for being the best family ever. Finally I would like to thank my parents for their love, support and encouragement. I would never have been able to do this without you both.

List of Contents

Table of Contents

Table of Figures

Table of Tables

Abbreviations

5-FU	5-Fluorouracil
5-HETE	5-hydroxyeicosatetraenoic acid
aaRs	Aminoacyl-tRNA synthetases
ABL Buffer	Antibody lysis buffer
ACF	Aberrant crypt foci
Ago	Argonaute
AhR	Aryl hydrocarbon receptor
AIB1	Amplified in breast1
AICR	American Institute for Cancer Research
AKT	Ak mouse strain thymoma (also known as PKB)
AMO	Anti-miRNA oligonucleotide
AP-1	Activator protein-1
AR-CAG	Androgen receptor-CAG repeat
ARE	Antioxidant responsive element
ATCC	American Type Culture Collection
ATF	Activating transcription factor
BB	Blocking buffer
BCA	Bicinchoninic acid
BCL2	B cell lymphoma 2
bHLHZ	Basic helix-loop-helix-leucine zipper
BRAF	v-Raf murine sarcoma viral oncogene homolog B
BRCA2	Breast cancer 2, early onset
CA19-9	Carbohydrate antigen 19-9
CA-50	Carbohydrate antigen 50
CAT-1	Cationic amino acid transporter
CCK	Cholecystokinin
CDKI	Cyclin-dependent kinase inhibitor
CDKN2A	Cyclin-dependent kinase inhibitor 2A
cDNA	Complementary DNA
CEA	Carcinoembryonic antigen
CIN	Chromosome instability
CLL	Chronic lymphocytic leukaemia

COX-2	Cyclooxygenase-2
CRC	Colorectal cancer
CSC	Cancer stem cell
CT	Computerised tomography
CYP	Cytochrome P450 enzymes
DDR	DNA damage repair
DGCR8	DiGeorge critical region 8
DIM	3,3' diindolylmethane
DMEM	Dulbecco's modified eagle's medium
DMSO	Dimethyl sulfoxide
DNA	Deoxyribonucleic acid
dsRBDs	Double-stranded RNA-binding domains
dsRNA	Double-stranded RNA
Dupan-2	Sialyl-lcat-N-tetraose
ECL	Enhanced chemiluminescence
EGCG	Epigallocatechin gallate
EGFR	Epidermal growth factor receptor
eIF4E	Eukaryotic translation initiation factor 4E
EMT	Epithelial-to-mesenchymal transition
ERCP	Endoscopic retrograde cholangio pancreatography
EUROPAC	European registry of hereditary pancreatitis and familial pancreatic cancer
EUS	Endoluminal ultrasound
EZH2	Enhancer of zeste homologue 2
FANCC	Fanconi anemia, complementation group C
FANCG	Fanconi anemia, complementation group G
FCS	Fetal calf serum
FDG	Fluorodeoxyglucose
FDR	False discovery rate
FNA	Fine needle aspiration
GEF	Guanine-nucleotide exchange factor
GEMM	Genetically engineered mouse models
GEO	Gene expression omnibus
GF	Growth factors

GIN	Genetic instability
GOI	Gene of interest
GST	Glutathione S-transferase
GTP	Guanosine triphosphate
HCO_3^-	Bicarbonate ions
HCV	Hepatitis C virus
ICC	Interclass correlation coefficient
IGF-I	Insulin-like growth factor I
IKK	IκB kinase
IPMN	Intraductal papillary mucinous neoplasms
IRES	Internal ribosome entry site
Keap1	Kelch-like ECH-associating protein 1
KRAS	Kirsten rat sarcoma viral oncogene homolog
KPC	LSL-KrasG12D/+;LSL-Trp53R172H/+;Pdx1-Cre
LNA	Locked nucleic acid
LOH	Loss of heterozygosity
m^7G	7-methyguanosine
MAPK	Mitogen-activated protein kinase
Max	Myc-associated factor X
MCN	Mucinous cystic neoplasms
MEK1/2	MAPK/ERK kinase
MEKK1	MAPK kinase kinase-1
MET	Mesenchymal-to-epithelial transition
MIN	microsatellite instability
MIQE	Minimum Information for Publication of Quantitative Real-Time PCR Experiments
MK5/MAPKAPK5	MAP kinase-activated protein kinase 5
MKK4	MAPK kinase-4
miRNAs	MicroRNAs
MLH1	mutL homolog 1
MMP-9	Matrix metalloproteinase 9
MRCP	Magnetic resonance cholangio pancreatography
MRI	Magnetic resonance imaging
mRNA	Messenger RNA

MSH2	mutS homolog 2
MYB	Myb proto-oncogene protein
MW	Molecular weight
NF-κB	Nuclear factor kappa-light-chain-enhancer of activated B cells
NHS	National Health Service
NIK	NF-κB-inducing kinase
NP	Normal pancreas
Nrf2	Nuclear-factor-(erythroid-derived 2)-related factor 2
NT	No treatment
O/N	Overnight
(P)	Phosphorylate
PABP	Poly(A)-binding protein
PACT	Protein activator of the interferon induced protein kinase
PALB2	Partner and localizer of BRCA2
PanIN	Pancreatic intraepithelial neoplasia
P-bodies	Processing bodies
PBS	Phosphate buffered saline
PBST	Phosphate buffered saline tween-20
PC	Pancreatic cancer
PCA	Principle component analysis
PCR	Polymerase chain reaction
PDAC	Pancreatic ductal adenocarcinoma
PDK1	3-phosphoinositide-dependent protein kinase-1
Pdx1	pancreas/duodenum homeobox protein 1
PET	Positron emission tomography
PGE_2	Prostaglandin E2
Pi	Propidium iodide
PI3K	Phosphoinositide-3-kinase
PIK3CA	Phosphatidylinositol-4,5-bisphosphate 3-kinase, catalytic subunit alpha
PKB	Protein kinase B
PKC	Protein kinase C
Poly(A)	Poly adenylated

Pre-miRNA	Precursor microRNA
Pri-miRNA	Primary microRNA
PS	Phosphotidylserine
pSTAT3	Phosphorylated signal transducer and activator of transcription 3
PTEN	Phosphatase and tensin homolog
QC	Quality control
qPCR	Quantitative polymerase chain reaction
Ral-GDS	Ral guanine nucleotide dissociation stimulator
Rb-1	Retinoblastoma-1
RIN	RNA integrity number
RISC	RNA induced silencing complex
RG	Reference gene
RNA	Ribonucleic acid
RNAi	RNA interference
RNaseH	Ribonuclease H
RPMI-1640	Roswell Park Memorial Institute medium
ROS	Reactive oxygen species
RREB1	Ras-responsive element-binding protein
RT	Room temperature
RT-qPCR	Real-time reverse transcription quantitative polymerase chain reaction
SAM	Significance analysis of microarrays
SDS-PAGE	Sodium dodecyl sulphate polyacrylamide gels
SEL1L	Sel-1-like
siRNA	Small interfering RNA
SMAD4	SMAD family member 4
snRNA	small nuclear RNAs
Sp1	Specificity protein 1
SSC	Saline-sodium citrate
STK11	Serine/threonine kinase 11
TAUS	Transabdominal ultrasonography
TF	Transcription factor
TGF- β	Transforming growth factor - β

TNF- α	Tumour necrosis factor – α
TP53	Tumour protein 53
TSG	Tumour suppressor gene
TSP	Tumour suppressor protein
TRBP	TAR RNA-binding protein
Ub	Ubiquitylate
VEGF	Vascular endothelial growth factor
WCRF	World Cancer Research Fund
WHO	World Health Organisation
UTR	Untranslated region
UV	Ultraviolet
VDR	Vitamin D receptor
Zeb	Zinc finger E box-binding homeobox

Chapter 1. Introduction

1.1. Cancer

1.1.1. The Effect of Cancer on Society

Cancer is a leading cause of mortality throughout the world with over a third of the population developing this disease. There are in excess of 200 types of human cancer with breast, lung, prostate and bowel accounting for over half of all cases. In the UK alone 331,487 people were diagnosed in 2011, and over 14 million new cases were observed worldwide in 2012. Sadly over 25% of deaths in the UK can be attributed to cancer with 159,000 deaths occurring in 2011(Cancer Research UK, 2014a; Siegel et al, 2013).

There are many cancer associated risk factors, and while the inheritance of alleles which increase susceptibility to certain cancers is unavoidable, there are many avoidable environmental factors which may have pronounced effects on cancer development. These include chemical carcinogens, ultraviolet (UV) radiation, dietary (high fat) and lifestyle choices (tobacco/alcohol), which together are associated with >40% of cases in the UK. With such a multitude of risk factors it is not hard to comprehend why there is a greater than 1 in 3 chance of acquiring this aggressive disease. Aging, however, is an unavoidable major factor, with over a third of patients diagnosed aged over 75 (Moiseeva and Manson, 2009; Surh, 2003; Cancer Research UK, 2014a; Yokota, 2000; Weinberg, 2013).

1.1.2. Cancer as a Multistep Disease

Tumourigenesis is a complicated multistep process which advances over a substantial period of time as a result of the accumulation of genetic aberrations (Figure 1.1). Combined effects from DNA mutations and epigenetic regulation have considerable impact on many genes associated with malignant development. There are a substantial number of barriers that must be overcome for normal cells to become cancer cells, with various abnormalities required for pre-malignant cells to progress to advanced tumours (Surh, 2003; Yokota, 2000; Klein, 2009; Weinberg, 2013).

Abnormal genetic and epigenetic alterations accumulate throughout the lifespan of an individual; nevertheless in the majority of cases, a damaged site will not undergo

enough alterations for a neoplastic phenotype to develop. It is only in the minority of cases that sufficiently extensive changes result in the development of a malignant tumour (Figure 1.1.) (Weinberg, 2013). Understanding the genetic and epigenetic events occurring throughout tumour progression could enable the identification of stage-specific prognostic markers for certain cancers which could also act as potential therapeutic targets (Surh, 2003).

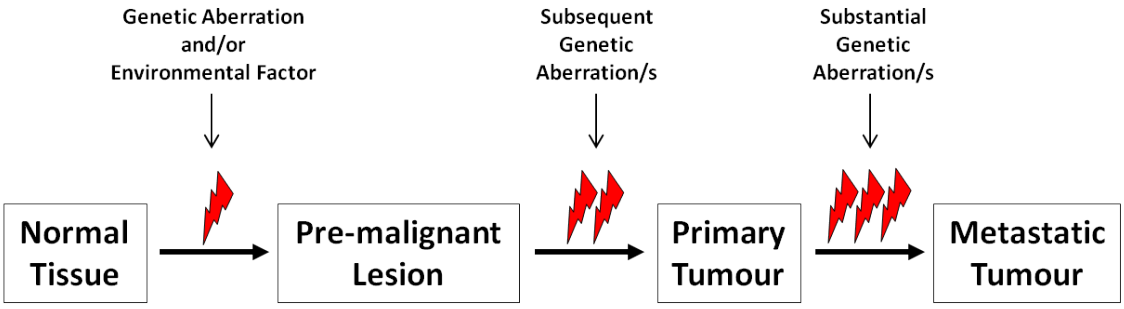

Figure 1.1: Multi-step Cancer Progression. The development of an aggressive tumour is a multi-step process. Either genetic aberrations leading to monoclonal expansion or environmental factors leading to polyclonal expansion allow the development of a pre-malignant lesion. Further genetic aberrations drive the development of this early lesion into a primary tumour, which progresses into a metastatic tumour as a result of additional mutations (Yokota, 2000; Klein, 2009). Figure adapted from (Yokota, 2000).

In order to drastically reduce the mortality rate, early detection allowing more effective treatment is necessary (Harrison, 2011). The importance of early disease recognition is demonstrated by the success of national screening programmes, including those for breast, cervical and colorectal cancers, which in part account for the improving survival over the past decade in relation to these cancer subtypes (Harrison and Benziger, 2011; Cairns et al, 2010; Public Health England 2013). There are treatments available for use in the early stages of cancer development. However, where metastatic progression is likely, such therapies can become ineffective (Ali et al, 2010).

1.1.3. Epithelial-to-Mesenchymal Transition and Cancer Stem Cells

Although not universally accepted, cancer progression is associated with the acquisition of epithelial-to-mesenchymal transition (EMT), a multi-step process which facilitates tumour cell metastasis (Thompson et al, 2005; Cardiff, 2005; Tarin et al, 2005). EMT defines the process by which the cell loses its epithelial phenotype and becomes more mesenchymal. This includes increased migratory and invasive potential, loss of polarity,

as well as reduced cell-cell and cell-substratum contact. Loss of the cell adhesion protein E-Cadherin and increased expression of various EMT transcription factors (TF) including Snail1/2 and Zinc finger E box-binding homeobox (Zeb) 1/2 are fundamental events commonly observed in EMT. These TFs have been shown to correlate with both patient relapse and survival in diverse cancers, including breast and colorectal, supporting a strong involvement of EMT in poor patient prognosis (Dykxhoorn, 2010; Thiery et al, 2009; Levayer and Lecuit, 2008).

The development of EMT is also associated with resistance or reduced sensitivity of tumour cells to chemotherapeutics (Thiery et al, 2009). Aggressive cancers, such as those of the pancreas often reach advanced stages of metastasis prior to a diagnosis. Treatments used at this stage of disease include the chemotherapeutic agent gemcitabine, however this drug and others are often of little benefit (Surh, 2003; Ali et al, 2010; Li et al, 2009). The reverse process mesenchymal-to-epithelial transition (MET) is also thought to occur in cancer (Thiery et al, 2009). In order for cancer treatment to progress, novel agents with the ability to suppress cancer progression or even reverse or prevent the development of tumour cells are required (Mann et al, 2009).

Evidence suggests that in order for a tumour to develop, a subpopulation of the cells must acquire ‘stem cell’ like properties, with these cells identified as cancer stem cells (CSC). These ‘self-renewing’ CSCs enable the advancement in growth of the tumour, providing it with the ability to become invasive and metastatic. CSCs are often attributed with the development of both EMT and drug resistance, making them and the signalling pathways involved in their development worthy targets for novel therapeutics (Wicha, 2011; Wang et al, 2010a).

1.1.4. Pancreatic Cancer

1.1.4.1. Anatomy of the Pancreas

The pancreas is made up of sections known as the head, body and tail and is found alongside the liver, small intestine and stomach (Figure 1.2) (Bardeesy and Depinho, 2002; Domínguez-Bendala, 2009). It is an exocrine-endocrine glandular organ; the exocrine pancreas is made up of ducts and acini and produces digestive enzymes, with

the endocrine pancreas comprising of the Islets of Langerhans which secrete hormones, including insulin and glucagon (Figure 1.3) (Hezel et al, 2006; Park et al, 2011a).

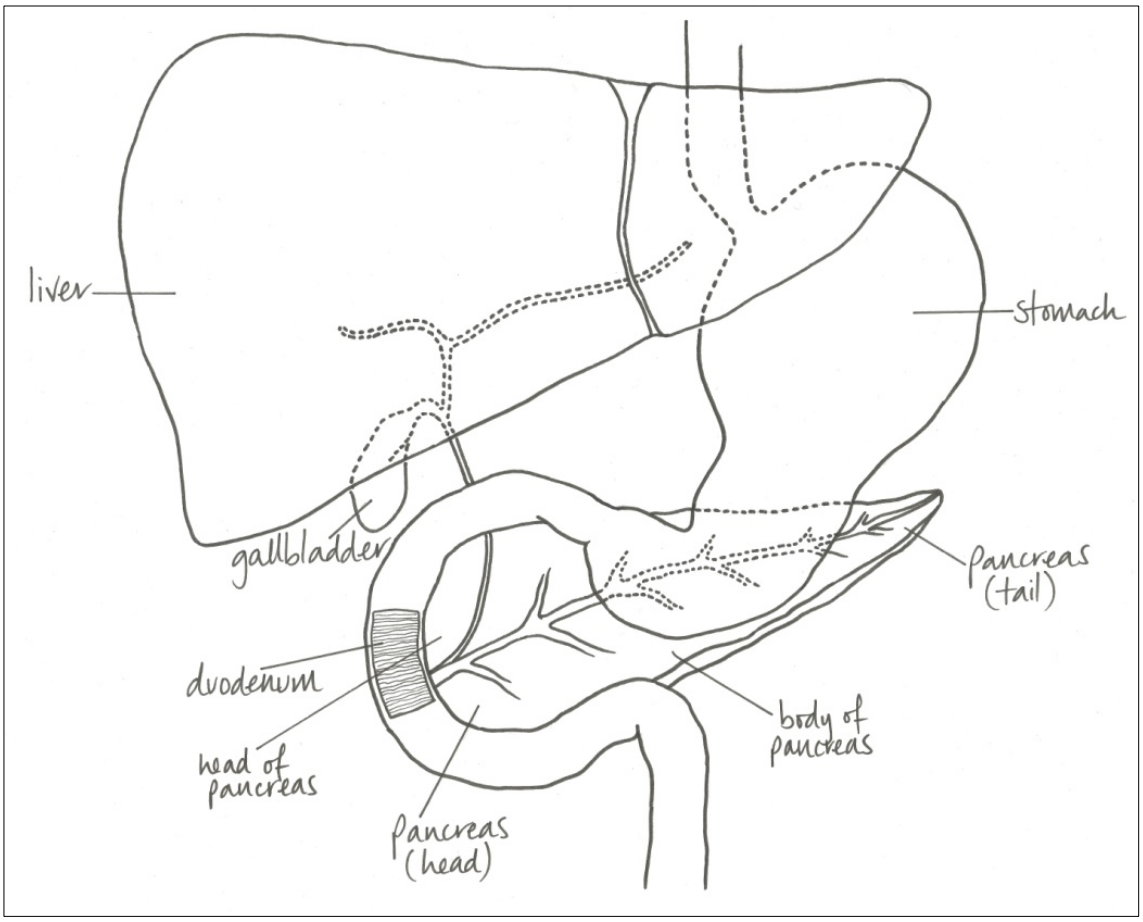

Figure 1.2: The Pancreas. The pancreas has both an exocrine (secretion of enzymes for carbohydrate, protein and lipid digestion) and an endocrine (production of hormones for glucose homeostasis) function. It is an organ within the gastrointestinal tract which is located beneath the stomach and is connected to the duodenum. The common bile duct is also connected to the pancreas, running through the head of the gland. This organ has three vaguely defined regions; the head which is connected to the duodenum and common bile duct, the slender end called the tail and the body of the pancreas which connects the head and the tail (Bardeesy and Depinho, 2002; Domínguez-Bendala, 2009; Hezel et al, 2006). Illustration by Alexandra Palmer (Bardeesy and Depinho, 2002).

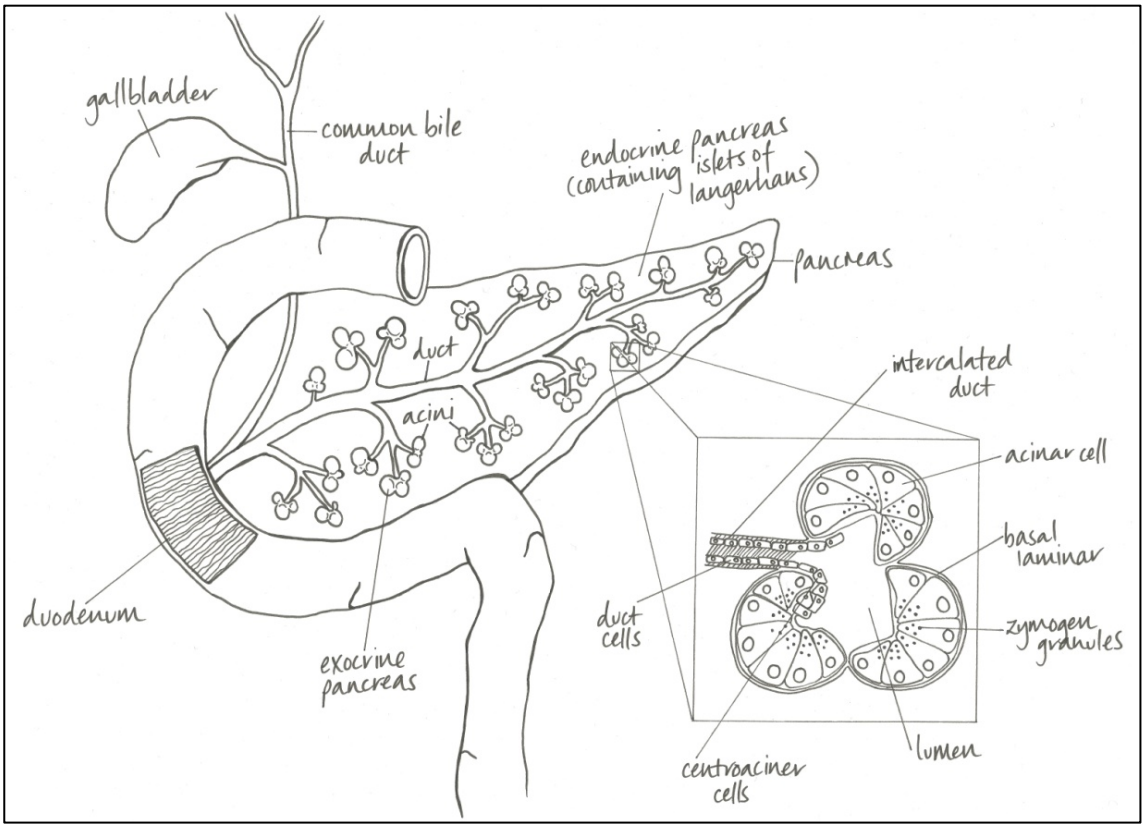

Figure 1.3: The Exocrine Pancreas. Pancreatic acini contain various cell types necessary to carry out their exocrine function, of which acinar cells are the most abundant. These cells contain secretary zymogen granules which store most enzymes involved in digestion. Zymogen granules vary in quantity depending on the stage of digestion, with more in fasting animals. The acini are linked by intercalated ducts which infiltrate the lumen of each acinus, and centroacinar cells constitute the intracinar part of these ducts. Each acinus is surrounded by a basal lamina. Large networks of ducts work to connect all pancreatic acini with larger interlobular ducts producing intralobular ducts, and from these intercalated ducts occur as offshoots (Bardeesy and Depinho, 2002; Domínguez-Bendala, 2009; Hezel et al, 2006; Mescher and Junqueira, 2013). Illustration by Alexandra Palmer (Bardeesy and Depinho, 2002).

The extensive capillary network present within the pancreas is greatly beneficial in regard to its exocrine function, enabling the secretion of water, ions and various proteases in their inactive forms which travel to the small intestine (Mescher and Junqueira, 2013). The fluid in which these secretions travel is highly alkaline due to high levels of bicarbonate ions (HCO_3^-) which neutralise the acidic chyme within the stomach, resulting in less acidic pH for optimum enzyme activity (Domínguez-Bendala, 2009; Mescher and Junqueira, 2013). Within the duodenum these proteases are activated by enteropeptidases; the protease trypsinogen is cleaved to produce active trypsin which goes on to activate the other digestive proteases originating from the pancreas. Activity of the exocrine pancreas is controlled largely by the polypeptide hormones cholecystokinin (CCK) and secretin which are produced within the small

intestine. CCK acts to promote zymogen secretion from the acinar cells and secretin encourages the secretion of both water and HCO_3^- ions from the centroacinar and intercalated duct cells. In addition, the parasympathetic nerve fibres also encourage both types of secretion (Domínguez-Bendala, 2009; Mescher and Junqueira, 2013).

The endocrine pancreas is made up of small groups of cells known as islets of Langerhans, which are encapsulated in fibrous connective tissue and surrounded by the acini and ducts of the exocrine pancreas. Each islet can contain as little as a few cells and anywhere up to several hundred, with an estimated 1 million residing in the pancreas (Mescher and Junqueira, 2013). Islets contain five specialised cell types which are known to secrete hormones involved in glucose homeostasis and the regulation of metabolism (Table 1.1) (Domínguez-Bendala, 2009; Hezel et al, 2006).

Table 1.1: The Hormones Produced Within the Endocrine Pancreas.

Cell Type	Quantity (%)	Hormone	Position within the Pancreas	Hormone Function
Alpha (α)	~20	Glucagon	Usually in periphery	Acts on tissues to make energy stored in glycogen and fat available through glycogenolysis and lipolysis; increases blood glucose content
Beta (β)	~70	Insulin	Centrally located	Acts on several tissues to cause entry of glucose into cells and promotes decrease of blood glucose levels
Delta (δ)	5-10	Somatostatin	scattered	Inhibits release of other islet cell hormones through local paracrine action
PP	Rare	Pancreatic Polypeptide	Head of pancreas	Control of gastric secretion. Control of secretion of the exocrine pancreas
Epsilon(ε)	Rare	Ghrelin	-	-

This Table highlights the five major hormone producing cell types which reside in the endocrine pancreas (Domínguez-Bendala, 2009; Mescher and Junqueira, 2013). Table adapted from (Mescher and Junqueira, 2013).

The main function of the endocrine pancreas is to maintain glucose homeostasis around 70mg/dL. This occurs through the secretion of glucagon and insulin into the blood stream (Table 1.1). Insulin decreases blood glucose levels by activating uptake into cells

and glucagon acts to convert glycogen into glucose through glycogenolysis, thereby increasing blood glucose levels (Domínguez-Bendala, 2009; Mescher and Junqueira, 2013). Various endocrine hormones within the pancreas act in a paracrine manner to regulate hormone release within islet cells and the activity of exocrine acinar cells. Sympathetic and parasympathetic nerve endings are also present within the endocrine pancreas in association with a small number of α, β and δ cells and can act to regulate secretion of insulin and glucagon as part of the control system which maintains blood glucose levels (Mescher and Junqueira, 2013).

1.1.4.2. Pancreatic Cancer Statistics

In 2010 pancreatic cancer (PC) was the tenth most common cancer in the UK, with pancreatic ductal adenocarcinoma (PDAC) accounting for over 90% of all cases (other types of PC are discussed in section 1.1.4.5) (Cancer Research UK, 2014b; Park et al, 2011a; Hamilton et al, 2000; Ballehaninna and Chamberlain, 2013). This disease related to aging is principally detected in adults, with over 75% of cases observed in patients over the age of 65 (Cancer Research UK, 2014b; Bergmann et al, 2007). Within the UK, PC is known to be the fifth greatest cause of cancer related death. In 2010 8,463 patients were diagnosed with PC, and in 2011 8,320 deaths were documented as a result of this aggressive disease (Cancer Research UK, 2014b). The high mortality is due mainly to the lack of symptoms related with disease onset commonly resulting in the absence of a diagnosis before aggressive local invasion and metastasis of the tumour (Park et al, 2011a; Li et al, 2007). Due to late onset of symptoms, once diagnosed, most individuals with PDAC will have a maximal survival of 12 months, with a less than 5% chance of surviving up to 5 years (Table 1.2) (Park et al, 2011a; Jemal et al, 2010). Long term survival can only be contemplated for an individual fortunate enough to have a primary localised tumour treatable via curative resection at the time of diagnosis (Park et al, 2011a; Bergmann et al, 2007).

Table 1.2: Pancreatic Cancer Survival Statistics in England and Wales.

	1 year Survival		5 year Survival		10 year Survival	
	1971-1975	**2005-2009**	**1971-1975**	**2005-2009**	**1971-1975**	**2005-2009**
Male	6%	17.4%	2%	3.6%	2%	2.8%
Female	7%	19.8%	2%	3.8%	2%	2.6%

These data highlight the minimal improvement in survival for patients diagnosed with PC since the 1970's (Cancer Research UK, 2014b).

1.1.4.3. Risk Factors Associated with Pancreatic Cancer

Risk factors such as smoking, alcohol consumption and high-fat/high-meat based diets have been implicated in PC development (Hamilton et al, 2000; Bergmann et al, 2007). In the UK alone smoking was shown to account for almost 30% of cases in 2011 (Cancer Research UK, 2014b; Parkin, 2011). Pancreatitis, inflammation of the pancreas, occurs when proenzymes involved in carbohydrate digestion become activated within the pancreas, leading to digestion of pancreatic tissues (Mescher and Junqueira, 2013). The chance of developing PC if already suffering from chronic pancreatitis is thought to increase 10-20 fold, with further risk elevation associated with increased duration of pancreatitis (Lowenfels et al, 1993; Duell et al, 2012). Other medical conditions are also thought to be risk factors. It was found that patients with diabetes were approximately 40% more likely to develop this malignancy compared with non-diabetics (Cancer Research UK, 2014b; Elena et al, 2013). Increased risk was also observed in patients with gastric ulcers, ulcerative colitis, Crohns disease and periodontal disease, as well as in individuals with previous cancerous lesions (Cancer Research UK, 2014b; Luo et al, 2007; Hemminki et al, 2009; Hemminki et al, 2008; Michaud et al, 2008; Shen et al, 2006). It has also been suggested that occupational exposure to agents such as insecticides, aluminium, acrylamide, nickel and halogenated hydrocarbons, as well as chlorinated hydrocarbon solvents and ionising radiation, are risk factors (Hamilton et al, 2000; Ojajarvi et al, 2000).

1.1.4.4. Presentation, Investigation, Diagnosis and Treatment of Pancreatic Cancer

1.1.4.4.1. Disease Presentation and Diagnosis

The vague non-specific nature of symptoms, makes diagnosing PC extremely difficult. Abdominal and mid-back pains are probably some of the most frequently observed symptoms (Vincent et al, 2011; Gullo et al. 2001). Unexplained weight loss is often associated with patients having feelings of early satiety and nausea-related vomiting (Hamilton et al, 2000). Weight loss, and as a result, anorexia, were found to occur in approximately 7% of patients at diagnosis (Gullo et al, 2001). Other typical symptoms associated with the presentation of PC include jaundice, pruritus (itching of skin) and the development of diabetes mellitus (late-onset diabetes) (Hamilton et al, 2000; Vincent et al, 2011; Gullo et al, 2001).

At present there are a variety of tests available for the diagnosis and staging of PC. These include transabdominal ultrasonography (TAUS), computerised tomography (CT), magnetic resonance imaging (MRI), endoscopic retrograde cholangio pancreatography (ERCP) and endoluminal ultrasound (EUS) as the main imaging modalities, as well as positron emission tomography (PET), laparoscopy and the determination of various tumour markers (Hamilton et al, 2000; Kelly and Conlon, 2014; Kulig et al, 2014). TAUS and CT are the most commonly employed imaging techniques. They can detect small masses (<2cm), determine if pancreatic and bile ducts are dilated and observe hepatic metastases (Warshaw and Fernandez-del Castillo, 1992). Various other modalities available to aid in the diagnosis and prognosis of PC are outlined in Table 1.3.

The European registry of hereditary pancreatitis and familial pancreatic cancer (EUROPAC) is involved in researching inherited causes of pancreatitis and PC. It screens patients over the age of 40 who have either hereditary pancreatitis or where PC is prevalent within a family and the individual may be at risk of developing familial PC. Those who fit the criteria have a blood test for fasting glucose and CA19-9 and a CT scan or EUS test every three years. An ERCP is also carried out and a sample of the pancreatic juices is obtained. The latter is examined for any changes in the *KRAS*, *TP53* and *CDKN2A* genes, which are commonly mutated in PC. If genetic changes are observed these tests will be carried out annually, to potentially diagnose the development of PC at a treatable stage. EUROPAC uses the information obtained to produce a registry of the families within Europe who are at high risk of PC. Not only can this information be beneficial for these families, but any information gathered could help improve the genetic testing available to diagnose those with PC or others at risk of developing this disease (Cancer Research UK, 2014b; University of Liverpool, 2014).

Table 1.3: Modalities used for Pancreatic Cancer Diagnosis.

Modality	Description
TAUS	• Widely available, inexpensive, non-invasive, does not use ionising radiation. • Associated with a diagnostic accuracy of between 70-94%. • Routinely used as an initial form of clinical investigation for PC. • Has the capacity to show a tumour's relationship with the surrounding structures and vasculature in real-time. • Extremely accurate when differentiating between obstructive and non-obstructive jaundice (advantageous in diagnosing a patient with PC as around 50% present with this feature).
CT	• Provides increased sensitivity and specificity when observing the tumours structure (gives 100% accuracy in association with the prediction of nonresectability).
MRI	• Less readily available than CT and TAUS. • Similar levels of accuracy as CT in regard to diagnosing and staging PC. • In most cases MRI is used in addition to other imaging techniques. • Certain circumstances (e.g. patient allergy to iodinated contrast agents) MRI may be used.
ERCP	• Used to acquire images of the biliary and pancreatic ducts to ascertain if there are any obstructive intraductal lesions and to alleviate any obstruction observed. • Magnetic resonance cholangio pancreatography (MRCP) is similar to ERCP and is often used in place of this modality.
EUS	• Used for sampling of diagnostic cytology by fine needle aspirations (FNA) of potentially neoplastic cells (CT can also be used) with around 80% sensitivity for pancreatic masses. • Tissue analysis using FNA following the diagnosis and staging of pancreatic disease is customary in order to distinguish benign disorders or to ascertain patient status prior to chemotherapy.
PET	• Often used in combination with the radioactive glucose analogue fluorodeoxyglucose (FDG). • FDG-PET works by identifying malignant tissue by its increased ability to take up FDG (FDG is taken up in a similar manner to glucose, but once inside the cell it cannot be metabolised, resulting in accumulation within tumour cells over time). • FDG-PET relies on normal cells having a normal glucose metabolism; often in PC this is not the case and may cause irregular FDG distribution producing potentially false positive results. • FDG-PET is often combined with CT in order to improve accuracy and sensitivity of tumour detection. • Occasionally used to help predict prognosis in response to treatment.
Laparoscopy	• An advanced staging technique used to identify either areas of obscure metastatic disease or re-staging of disease following adjuvant or neoadjuvant therapies. • Minimally invasive laparoscopies are carried out by inserting a device which can visualise the abdominal organs and facilitate the detection of obscure metastatic lesions unidentifiable through other imaging modalities. • CT or MRI in combination with FDG-PET is usually used to identify metastatic disease, information from these imaging methods can be used to guide laparoscopies towards genuine areas of metastatic growth and to prevent non-therapeutic laporotomies.

Table 1.3: Continued.

Modality	Description
Tumour Markers	• There are various hormones, enzymes and tumour-associated antigens used as tumour markers to diagnose or monitor PC. • The most commonly used marker is carbohydrate antigen 19-9 (CA19-9) which is used diagnostically, as elevated levels are observed in around half the cases of PC. • CA19-9 levels of >100-200U/ml are indicative of unresectability in preoperative patients, however this marker is not specific for PC and therefore can often contribute to an incorrect diagnosis. • A considerable number of other proteins/epitopes including carbohydrate antigen 50 (CA-50), carcinoembryonic antigen (CEA), sialyl-lcat-N-tetraose (Dupan-2) and SPAN-1 have also been investigated for their use as serum tumour markers. • There is no single definitive tumour marker for PC and it is widely maintained that a combination of various markers for this disease is necessary to increase diagnostic accuracy.

(Vincent et al, 2011; Kelly and Conlon, 2014; Kulig et al, 2014; Warshaw and Fernandez-del Castillo, 1992; Hanbidge, 2002; Goonetilleke and Siriwardena, 2007)

1.1.4.4.2. Pancreatic Cancer Treatment

PC is a heterogeneous disease and must be managed by a multidisciplinary team as patient response to therapy will depend on many different factors, including the stage of disease progression, cancer biology and reaction to treatment (Vincent et al, 2011).

The surgical removal (most commonly a pancreaticoduodenectomy/Whipple procedure) of a pancreatic tumour is the only potential cure, but often surgery alone will not achieve this (Ansari et al, 2011; Bardeesy and Depinho, 2002). The reported 5-year survival rate associated with resection varies significantly from 3-4% up to 27% (Hamilton et al, 2000; Katz et al, 2009). These poor survival statistics highlight the frequent relapse in most patients following a resection. This relapse is often due to the inability to detect and eliminate microscopic metastasis present within the pancreas at the time of diagnosis (Ansari et al, 2011). For this reason it is common to give either adjuvant or neoadjuvant therapy in addition to a resection to increase a patient's chance of survival.

The main forms of adjuvant therapy are chemotherapy or chemoradiation; there is insufficient evidence to determine whether the use of radiation in addition to chemotherapy is of any additional benefit (Warshaw and Fernandez-del Castillo, 1992; Neoptolemos et al, 2004; Abrams et al, 2009). Following recovery from surgery, patients are assessed using baseline CT scans and CA19-9 concentrations (Vincent et al, 2011). Gemcitabine and 5-Fluorouracil (5-FU) are two of the most commonly used

adjuvant chemotherapeutics. Various trials have favoured the use of either Gemcitabine over 5-FU or vice versa, although the majority of reports state that the efficacy of both agents is similar (Neoptolemos et al, 2009; Neoptolemos et al, 2010; Abrams et al, 2009; Redmond et al, 2010).

The use of neoadjuvant therapy is recommended for patients with borderline/early PC, whereby pre-treatment with various agents could potentially downstage their disease, subsequently allowing for a potentially curative resection. Response rates to neoadjuvant or adjuvant therapies are not high. For this reason some suggest that delaying potentially curative surgery to administer neoadjuvant therapies may be counterproductive. Others, however, believe that neoadjuvant treatment could help prevent metastatic progression by acting on microscopic metastasis associated with relapse (Vincent et al, 2011; Abrams et al, 2009; Tuveson and Neoptolemos, 2012).

For patients with locally advanced or metastatic disease who are not eligible for a resection, treatment options are limited. In most cases either chemotherapy or chemoradiation is used, with Gemcitabine often as standard treatment. There are, however, currently no effective second-line treatments and therefore palliative care is often the only option (Vincent et al, 2011).

Abraxane® is an albumin bound nanoparticle formulation of Paclitaxel (a chemotherapeutic agent), also known as *nab*-Paclitaxel. The use of Abraxane® in conjunction with Gemcitabine has been studied in various stage I/II and stage III clinical trials for the treatment of metastatic PC. The combination appears to improve overall survival compared to Gemcitabine alone, but this treatment option is not yet licensed in the UK (Von Hoff et al, 2011; Von Hoff et al, 2013; Pancreatic Cancer Action, 2014).

1.1.4.5. Types of Pancreatic Cancer

PDAC is a solid tumour, the exact origin of which has not been determined (Stanger and Dor, 2006). In the majority of cases, it is alleged that this exocrine tumour originates from mutations in the epithelial lining of the pancreatic ducts (Garcea et al, 2005b). It has also been postulated that PDAC may originate from mutations in the centroacinar cells which make up the intracinar part of the exocrine ducts (Stanger and

Dor, 2006). Over 60% of PDACs occur in the head of the pancreas between the bile duct and main pancreatic duct, with the remaining 40% affecting the body and tail (Hamilton et al, 2000; Bergmann et al, 2007). In association with PDAC, dissemination of cells into neighbouring tissues, including the lymphatics, spleen and peritoneal cavity are often observed. It is also common to witness metastatic growth in both the liver and lungs (Hezel et al, 2006).

PDAC is characterised by the presence of cancerous glandular structures which resemble the pancreatic ducts and are found enclosed within a mass of desmoplastic (fibrous or connective tissue) stroma. In well differentiated PDACs a variety of large and small duct-like structures are observed, mitotic activity is low and mucin production is intensive. The neoplastic duct-like glands contain large columnar cells containing nuclei of varying sizes which are often large and lacking in polarity, located basally within the cell. Mucin-containing neoplastic ducts, in contrast to regular pancreatic ducts, may be structurally incomplete or ruptured. With increasing tumour grade the glandular structures become moderately and then poorly differentiated mucin levels become reduced until secretion ceases and mitotic activity begins to escalate (Bergmann et al, 2007). The histopathological grading of PDACs with decreasing levels of differentiation correlate with increasing tumour grades.

In addition to the PDAC phenotype, an assortment of rare histomorphological variants are observed, including; adenosquamous carcinoma, mucinous non-cystic carcinoma, undifferentiated (anaplastic) carcinoma/undifferentiated carcinoma with osteoclast-like giant cells and signet-ring cell carcinoma. These variants all contain foci comprising of neoplastic glands with ductal differentiation, even in cases where neoplasms are poorly differentiated (Hamilton et al, 2000).

1.1.4.6. Familial Hereditary Pancreatic Cancer

Most cases of PDAC occur sporadically; however this disease has also been associated with familial pancreatic cancer syndromes, as well as genetic syndromes including hereditary pancreatitis, Familial Atypical Multiple Mole Melanoma and Peutz-Jeghers Syndrome (Hamilton et al, 2000; Bergmann et al, 2007; Hruban et al, 2010) . Certain germline mutations have been linked with an elevated risk for the development of PC,

including in the *BRCA2*[1], *CDKN2A*, *STK11*, *PALB2* and *PRSS1* genes. Mutations in the *BRCA2* gene appear to have a very strong link with inherited PC and are found in up to 17% of families diagnosed with familial PC (Vincent et al, 2011; Koorstra et al, 2008). It has been reported that up to 10% of patients with PC have first degree relatives who have also been diagnosed with this disease (Shi et al, 2009). It was estimated that persons with two family members already suffering from PC have an approximately 6.4-fold greater chance of developing this disease than those with no affected family members. For individuals with three relatives suffering from PC this increased to 32-fold (Klein et al, 2004). It is surprising, however, that these genetic syndromes are related to <20% of familial PC cases, highlighting the lack of understanding in regard to further genetic aberrations or epigenetic changes which drive familial PC (Hezel et al, 2006; Hruban et al, 2010).

1.1.4.7. Precursor Lesions in Pancreatic Cancer

Three histologically distinct forms of precursor lesion have been associated with the development of PDAC. These are pancreatic intraepithelial neoplasia (PanIN), intraductal papillary mucinous neoplasms (IPMN) and mucinous cystic neoplasms (MCN) (Figure 1.4) (Hezel et al, 2006). Increasing grades of these non-invasive lesions are thought to acquire mutations in both tumour suppressor genes (TSG) and oncogenes in a sequential manner leading to the eventual development of PC (Bergmann et al, 2007; Hruban et al, 2008a; Hruban et al, 2008b).

[1] See abbreviations list for all genes discussed

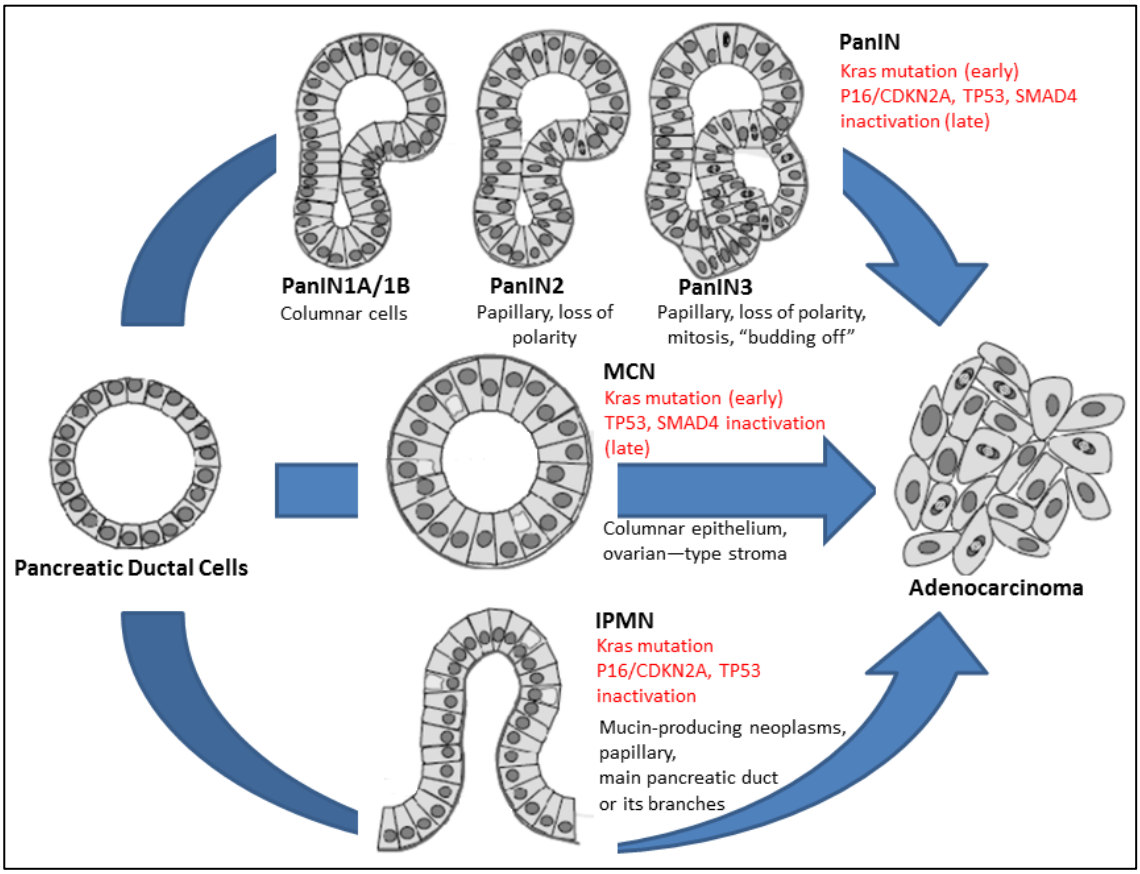

Figure 1.4: Precursor Lesions in Pancreatic Cancer.
The progression of pancreatic ductal cells from normal to adenocarcinoma can result from the development of various types of precursor lesions known as; pancreatic intraepithelial neoplasia (PanIN), intraductal papillary mucinous neoplasms (IPMN) and mucinous cystic neoplasms (MCN). Figure adapted from Jonckheere et al, 2010.

PanINs develop within the small ducts and ductiles of the exocrine pancreas, but due to their microscopic nature are difficult to recognise through CT and MRI (Koorstra et al, 2008; Su, 2003). These frequently observed precursors which are found in over 80% of neoplasms are localised mainly within the head of the pancreas and are graded from stages 1 to 3 (Hruban et al, 2008b). The different grades of PanIN (1A, 1B, 2 and 3) represent stages in tumour progression (Figure 1.5) (Bergmann et al, 2007). Development of low grade PanINs is common with increasing age. The presence of high grade PanINs and increased number is often detected in cases of advanced PC with metastatic disease. Over 80% of PDAC cases are thought to contain high grade PanINs, with approximately half being of PanIN-3 grade (Schwartz and Henson, 2007).

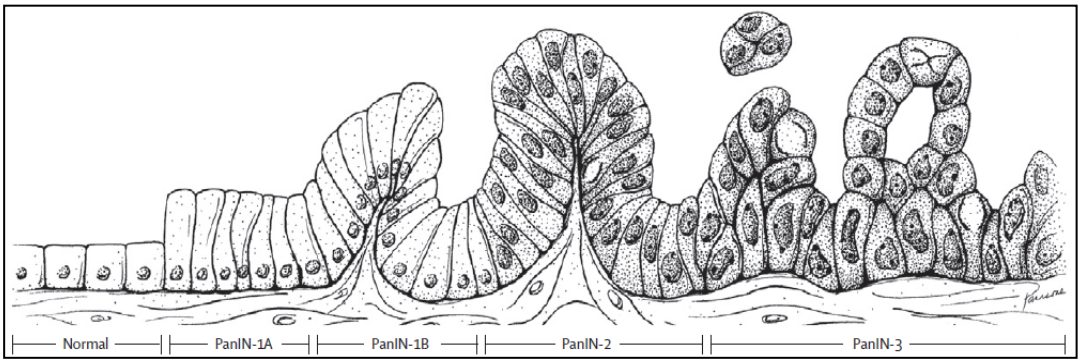

Figure 1.5: Pancreatic Intraepithelial Neoplasia (PanIN). PanINs develop in the smaller intercalated ducts of the exocrine pancreas and on average measure <5mm. They are graded based on their morphology and pathophysiology; PanIN-1 (A and B), PanIN-2 and PanIN-3. PanIN-1 lesions are made up of columnar epithelial cells with uniformly round nuclei found basally within the cell, similar to the morphology of a normal cell. They are separated into PanIN-1A where columnar epithelial cells remain flat, or PanIN-1B where the columnar cells form a protuberance. PanIN-2 lesions also have columnar epithelial cells, but nuclear polarity is lost resulting in non-uniform nuclei. The columnar shape of the epithelial cells is lost in the PanIN-3 lesions, and instead papillae and cribriform structures are formed. As well as lacking in polarity, nuclei appear enlarged and poorly orientated. Clusters of cells pertaining to the PanIN-3 lesions can be seen to bud off from the epithelium and travel into the lumen of the duct (Koorstra et al, 2008; Hruban et al, 2008b). Figure taken from (Maitra et al, 2003).

IPMN precursor lesions are observed as large papillae-like structures found most commonly in the head of the pancreas. They are macroscopic making them easier to observe by imaging when compared with PanINs (Hezel et al, 2006; Su, 2003). These cystic neoplasms are less frequently observed, but due to their greater size are more easily diagnosed (Vincent et al, 2011). Various other factors distinguish IPMNs from PanINs, with IPMNs producing excessive quantities of mucin and being characteristically found in ducts at least twice the diameter of those in which PanINs are discovered. IPMNs are described as having low-grade, moderate-grade, or high-grade dysplasia or associated invasive carcinoma (Table 1.4) (Su, 2003; Hruban et al, 2007). The malignant potential of IPMNs appears to be low in many cases, especially when these precursor lesions develop in the branches of the main pancreatic duct. The successful resection of IPMNs is generally associated with a high cure rate in cases that do not include invasive PC (Vincent et al, 2011).

Table 1.4: Grading of Intraductal Papillary Mucinous Neoplasms.

IPMN Grade	Description
Low-grade dysplasia	These lesions have only minimal architectural and cytologic dysplasia. The papillae have well-defined fibrovascular cores and the epithelial cells are oriented perpendicular to the papillae. The epithelial cells contain abundant mucin, the nuclei are small and uniform and nucleoli are not prominent. Mitoses are absent.
Moderate-grade dysplasia	These noninvasive neoplasms show moderate dysplasia. The papillae are not as well defined as they are for IPMN adenoma, and the nuclei show moderate nuclear pleomorphism and hyperchromasia. Occasional nuclei may contain a conspicuous nucleolus and mitoses can be seen.
High-grade dysplasia	These noninvasive neoplasms, also known as "carcinoma in situ," show significant nuclear dysplasia. True cribriforming of the papillae can be seen as can focal necrosis. Nuclei are irregularly shaped, nucleoli are prominent, and mitoses are frequent.
Associated invasive carcinoma	These lesions are defined by the presence of an invasive carcinoma arising in association with an IPMN. The invasive carcinoma is usually either a tubular (ductal) or colloid carcinoma.

IPMNs are principally found in the main pancreatic duct, but can also be found in branch ducts. A regular finding during endoscopy in patients with IPMN lesions is the identification of mucin being discharged from a patulous Ampulla of Vater (Hezel et al, 2006; Hruban et al, 2007). Table taken from (Su, 2003).

MCNs are mucin producing cystic epithelial neoplasms and are less frequently encountered than IPMNs and PanINs, affecting mostly women in their 40's and 50's. MCNs and IPMNs are structurally similar and exist as large papillary extrusions, measuring 1-3cm (Vincent et al, 2011; Su, 2003; Hruban et al, 2007). These lesions are mainly found within the body and tail of the pancreas, a feature which helps distinguish them from IPMNs (Su, 2003). The ductal system within the pancreas does not appear to be involved in MCN progression, another distinguishing feature (Vincent et al, 2011). About 30% of MCNs are associated with invasive disease, often in association with the pancreatic ducts. These advanced lesions have the potential to progress into metastatic disease**.** MCNs are graded in a similar manner to IPMNs (Table 1.5) (Su, 2003; Hruban et al, 2007).

Table 1.5: Grading of Mucinous Cystic Neoplasms.

MCN Grade	Description
Low-grade dysplasia	These noninvasive neoplasms are characterised by the formation of cystic spaces lined by a single row of columnar mucin-producing cells with uniform small nuclei. Nucleoli are inconspicuous and mitoses are absent.
Moderate-grade dysplasia	These noninvasive neoplasms show moderate dysplasia with nuclear crowding and pleomorphism. Mitoses may be seen as well as small nucleoli.
High-grade dysplasia	These noninvasive neoplasms show significant nuclear and architectural dysplasia. Architecturally, the papillae lack fibrovascular cores, and cribriforming and necrosis may be seen. Cytologically, significant nuclear pleomorphism, mitoses and prominent nucleoli are noted.
Associated invasive carcinoma	These are tissue invasive adenocarcinomas arising in association with a MCN. The invasive component usually resembles an invasive ductal carcinoma.

MCNs comprise of many small cavities which are filled with thick mucin or hemorrhagic fluid, and each cavity or cyst is lined by mucin-producing columnar epithelium. (Su, 2003; Hruban et al, 2007). Table taken from (Su, 2003).

1.1.4.8. Mutations in Pancreatic Cancer

Various somatic mutations occur in the pancreas which can drive tumourigenesis. Premalignant pancreatic precursor lesions show genetic changes that initiate, but do not transform these cells in regard to PC. With advancing grades these premalignant lesions obtain additional mutations which relate to their multistep progression to invasive neoplasm. The mutations observed support a relationship between precursor progression and the development of PC (Bardeesy and Depinho, 2002; Koorstra et al, 2008; Hruban et al, 2007). Hallmark genetic alterations, including losses and gains of genetic material which are known to drive the metastatic development of this disease, have been vigorously studied to determine how this disease develops. A better understanding of progression within these precursor lesions could enable the recognition of genetic and epigenetic changes occurring early in neoplastic development. This information could then be used to ascertain potential prognostic markers for use in diagnosis as well as for determining potential treatment targets (Hruban et al, 2008a).

1.1.4.8.1. Tumour Suppressor Genes

Various TSGs are mutated in PC, the most common include *CDKN2A*, *TP53* and *SMAD4* (Table 1.6). Both copies of these TSGs must undergo mutation for loss of function to occur. This is achieved through various mechanisms, including homozygous deletion or intragenic mutations, together with a loss of the second allele and silencing

of the gene promoter through hypermethylation (Gullo et al, 2001; 225 Hruban et al, 2008a).

The *CDKN2A* gene encodes the p16 protein, a member of the cyclin-dependent kinase inhibitor (CDKI) family which has a role in cell-cycle regulation. This CDKI prevents phosphorylation of the tumour supressor protein (TSP) Retinoblastoma-1 (Rb-1), which, in its hypophosphorylated form, prevents inappropriate G1/S phase transition (Bardeesy and Depinho, 2002; Koorstra et al, 2008). *CDKN2A* is inactivated in almost all cases of PC, as well as in increasing grades of PanIN, making it the most commonly mutated TSG in pancreatic tumourigenesis (Table1.6) (Hruban et al, 2008a). When this gene is lost it can no longer prevent the phosphorylation of Rb-1, allowing inappropriate progression of the cell cycle from G1 to S phase (Hruban et al, 2008b; Koorstra et al, 2008; Schutte et al, 1997).

Mutations of the *TP53* gene are the most commonly observed somatic alterations in human cancer and are found to occur in 50-75% of PCs. This gene encodes the p53 TSP which contributes to the control of both cell cycle arrest and programmed cell death in response to cytotoxic stress. When p53 activity is lost in PC, cell division and apoptosis are no longer regulated, leading to genetic instability (GIN), elevated cell survival and uncontrolled cell growth (Table 1.6) (Koorstra et al, 2008).

The *SMAD4* gene which encodes the TF Smad4, is inactivated in ~55% of PCs (Table 1.6). The Smad4 protein regulates the transforming growth factor- β (TGF- β) signalling pathway. It heterodimerises with active Smad proteins, leading to the transcription of specific target genes. When Smad4 is lost, the signalling cascade downstream of TGF- β is impeded often resulting in the loss of pro-apoptotic signalling and inappropriate transition from G1 to S phase (Hruban et al, 2008a; 297 Koorstra et al, 2008).

Mutations in both *TP53* and *SMAD4* occur late in PC pathogenesis, correlating with the detection of these mutations in late-stage PanIN-3 lesions (Bardeesy et al, 2002; Hruban et al, 2008a). Other TSGs which are targeted in less than 10% of PCs include *STK11*, MAPK kinase-4 (*MKK4*), *Rb-1* and TGF-β receptors I and II. Mutations within *STK11* are associated with Peutz-Jeghers syndrome, an inherited autosomal-dominant disease

which carries an increased risk of developing PC (Hamilton et al, 2000; Koorstra et al, 2008).

1.1.4.8.2. Oncogenes

Activating point mutations mainly within codon 12 of the *KRAS* gene are some of the early alterations in the multistep process to metastatic disease (Table 1.6) (Bardeesy et al, 2002; Hruban et al, 2008a). Such mutations are observed in over 90% of PDAC cases, with point mutations occurring less frequently in codons 13 and 61 (Koorstra et al, 2008). As pancreatic tumourigenesis progresses, so does the frequency with which *KRAS* point mutations occur, with the lowest levels observed in PanIN-1 lesions and in chronic pancreatitis (Hruban et al, 2008a; Koorstra et al, 2008; Hruban et al, 2007). The *KRAS* gene encodes a small guanosine triphosphate (GTP)-binding protein (K-Ras) which controls various effector pathways that modulate an array of cellular functions, including proliferation, cell survival and motility (Bardeesy et al, 2002; Koorstra et al, 2008). This gain of function mutation results in the constitutive activation of the K-Ras protein even when upstream growth factor signalling is absent. The constitutively active K-Ras has the capacity to activate various downstream effector pathways, in particular those involving RAF, phosphoinositide-3-kinase (PI3K) and Ral guanine nucleotide dissociation stimulator (RalGDS) (Koorstra et al, 2008).

Mutations in *KRAS* and *BRAF* are mutually exclusive in PC, with mutations in the *BRAF* gene observed in tumours containing only wild-type *KRAS*. *BRAF*, mutated in ~5% of pancreatic tumours, encodes a serine/threonine kinase which is a downstream effector of K-Ras involved in transcription and cell cycle progression (Table 1.6) (Hruban et al, 2008a; Koorstra et al, 2008).

K-Ras also regulates the PI3K downstream effector pathway which controls various cellular functions such as cell survival and proliferation. PI3K indirectly activates the *AKT* gene which encodes Ak mouse strain thymoma (Akt), also known as protein kinase B (PKB), an important component of this pathway which undergoes amplification in 10-20% of PCs (Hamilton et al, 2000; Koorstra et al, 2008). Mutations in *PIK3CA*, the gene which encodes PI3K, have been discovered in IPMNs, leading to increased PI3K activity and enhanced Akt signaling (Schonleben et al, 2006). Constitutive activation of this effector pathway is observed in most cases of PC even

when the *PIK3CA* gene is not mutated. This may occur following abnormal expression of the PI3K antagonist *PTEN* (Koorstra et al, 2008; Asano et al, 2004; Reichert et al, 2007).

Ral-GDS is a guanine-nucleotide exchange factor (GEF) which acts on downstream GTPases RalA and RalB, enabling their activation. The Ral-GDS pathway is also regulated by K-Ras signalling, with activation of RalA observed in various cases of PC. Other oncogenes which are also amplified in PC include the *AIB1* (60% cases) and *MYB* (10% cases) genes (Koorstra et al, 2008).

1.1.4.8.3. DNA Repair Genes

Mutations in various genome maintenance genes also play a role in pancreatic tumourigenesis, with DNA damage repair (DDR) gene mutations observed in >5% cases. Most DDR gene mutations occur in the germline which is commonly linked with familial forms of PC (Hruban et al, 2008a). GIN is often observed in PC due to various DDR gene defects, with the inactivation of *MLH1* and *MSH2* leading to microsatellite instability (MIN)(Table 1.6) (Hamilton et al, 2000; Koorstra et al, 2008). MIN occurs in ~4% of PCs as a result of DDR gene mutations. These cancers have a characteristic 'medullary' histology and much lower mutation rates in *TP53* and *KRAS* genes (Hamilton et al, 2000; Koorstra et al, 2008; Bardeesy et al, 2002). Fanconi anemia is a cancer susceptibility disorder which results through the inherited mutation of the genes *FANCC* and *FANCG*. These aid in the repair of interstrand cross-linking, however when genetically altered they are known to play a role in the progression of PC **(**Koorstra et al, 2008; Van Der Heijden et al, 2005). The TSG *BRCA2* is classed in PC as a DDR gene, and aids in the repair of DNA-strand and interstrand crosslinking. Inactivation of *BRCA2* occurs in ~7% of PDACs chiefly as an inherited mutation and its loss is observed as a late event in pancreatic tumourigenesis (Bardeesy et al, 2002; Hamilton et al, 2000; Koorstra et al, 2008). It has been observed in PC that mutations in *FANCC*, *FANCG* and *BRCA2* genes increase the sensitivity of these neoplasms to the DNA crosslinking agent Mitomycin C. This is due to the inability of these genes to repair the DNA-strand or interstrand crosslinks resulting in cell death (Abraham et al, 2001). This highlights the potential opportunity of using a PC patient's genetic profile to determine more efficient personalised clinical therapies.

Table 1.6: Summary of Hallmark Genes Mutated in Pancreatic Cancer.

Gene	Action	Chromosomal location	Activated/ Inactivated	% of cases	Causes of mutation	PanIN Stage
CDKN2A	TSG	9p	Inactivated	>95%	40% Homozygous deletion (both alleles) 40% Intragenic mutation one allele, loss second allele. 15% Hypermethylated gene promoter.	PanIN-1 <30% PanIN-2 55% PanIN-3 70%
TP53	TSG	17p	Inactivated	50-75%	Intragenic mutation one allele, loss second allele.	PanIN-3
SMAD4	TSG	18q	Inactivated	55%	30% Homozygous deletion 25% Intragenic mutation one allele, loss second allele.	PanIN-3
KRAS	Oncogene	12p	Activated	>90%	Point mutation	PanIN-1
BRAF	Oncogene	7q	Activated	~5%	(only in KRAS wt tumours)	-
AKT2	Oncogene	19q	Activated	10-20%	-	-
MLH1	DNA repair gene	3p	Inactivated	3-15%	-	-
BRCA2	DNA repair gene	13q	Inactivated	7%	Intragenic inherited mutation in one allele, loss of second allele (LOH).	-
FANCC	DNA repair gene	9q	Inactivated	<5%	-	-

LOH = loss of heterozygosity, TSG = tumour suppressor gene, wt = wild type (Hruban et al, 2008a; Koorstra et al, 2008; Schutte et al, 1997; Caldas et al, 1994).

1.1.4.8.4. Growth Factors

Overexpression of growth factors (GF) and their receptors is frequently observed in PC. GFs are important in the regulation of cellular differentiation and proliferation. However, deregulation of GFs and their receptor activation is often observed in cancer cells, and confers considerable growth advantage. The epidermal growth factor receptor

(EGFR), which is overexpressed in PC, acts upsteam of the PI3K signalling pathway. The EGFR receptor Her-2/neu is prominently overexpressed in ~70% of well differentiated PDACs and in early precursor lesions (Bardeesy et al, 2002; Hamilton et al, 2000). Increased expression of various other GFs and their receptors is also observed, including fibroblast growth factor , insulin-like growth factor I, nerve growth factor and vascular endothelial growth factor (VEGF) (Bardeesy et al, 2002; Koorstra et al, 2008; Korc, 1998).

1.1.4.8.5. Telomere Shortening

Telomeres are the protective "cap" like structures found at the end of linear chromosomes generated from short DNA repeats and associated proteins. They protect the terminal sequence of the chromosome, and when shortened enable the aberrant fusion of chromosome ends which can contribute to chromosome instability (CIN). Abnormal chromosomal fusion produces anaphase bridges which recurrently break during cellular replication leading to aberrant fusion events and chromosomal rearrangement (breakage-fusion-bridge cycles). Defective telomeres are commonly observed in both early PanIN lesions and PDAC and are attributed in part to the underlying loss and gain of function observed in TSG and oncogenes respectively. The TSP p53 typically acts to eliminate cells with high levels of CIN. However, in p53 mutant cells chromosomal rearrangement continues, leading to augmented CIN. Further mutations leading to the loss of p53 collaborate with the dysfunctional telomeres to help drive pancreatic carcinogenesis (Koorstra et al, 2008; Van Heek et al, 2002).

1.1.4.8.6. Mouse Models of Pancreatic Cancer

Mouse models of PC have been used over the last few decades not only to help understand disease pathogenesis and to discover which mutations are involved in driving the initiation and progression of pancreatic tumourigenesis, but also as a system to test novel therapeutic approaches. There are a variety of models available, including genetically engineered mouse models (GEMM) and patient-derived xenograft models.

Over three decades ago the first attempts at producing GEMMs of the exocrine pancreas were carried out. These early models used either the elastase or rat insulin promoter to enable the expression of SV40 large T antigen, a viral oncogene. Transgenic expression of this gene in acinar cells and β-cells resulted in the development of acinar cell

carcinomas and insulinomas respectively. However, no PanIN lesions or PDAC development were observed (Hezel et al, 2006; Colvin and Scarlett, 2014).

Activating mutations of *KRAS* are seen in the initial stages of PC progression and are commonly observed in early pancreatic lesions (PanIN-1). It therefore makes sense for GEMMs containing overexpressed mutant *KRAS* to exhibit tubular complex formations in younger mice and progressive PanIN lesions within older mice. This model emphasised the importance of mutant *KRAS* in the development and progression of PDAC precursors and the need for additional genetic mutations in order for this disease to progress (Grippo et al, 2003).

The LSL-*KRAS*^{G12D} mouse contains a conditional LoxP-STOP-LoxP cassette upstream of the *KRAS* gene which prevents its uncontrolled expression. A bi-transgenic mouse was produced with a 'knock-in' *KRAS*^{G12D} allele which was targeted to pancreatic epithelium through its combination with tissue specific Cre recombinase. Cre-induced expression of *KRAS*^{G12D} resulted in the excision of the STOP cassette which is located within the pancreas/duodenum homeobox protein 1 (Pdx1) promoter and the expression of the constitutively active *KRAS* mutant gene. Pdx1 is a TF found in the developing pancreas, so by situating the STOP cassette within this promoter, mutant *KRAS* can only be expressed in the pancreas (Koorstra et al, 2008; Hingorani et al, 2003). These mice developed the murine equivalent of human PanIN lesions, with a subset also developing invasive pancreatic carcinomas.

In order to produce a GEMM with the capacity to develop metastatic disease, further mutations which cooperate with *KRAS*^{G12D} are necessary. TSG inactivation is an event commonly observed later in PDAC progression following the activating mutation of *KRAS*. It was observed that when TSGs such as *CDKN2A* and *TP53* were inactivated alone no phenotype was observed. They needed to be combined with mutant *KRAS* in order to develop an advancing PDAC phenotype (Colvin and Scarlett, 2014). Subsequent models combined mutant *KRAS* with cooperating mutations in various TSGs, including *CDKN2A* and *TP53*. These transgenic mice which developed metastatic disease in most cases were considered a biologically relevant model for studying advanced human PC (Hingorani et al, 2005; Aguirre et al, 2003; Bardeesy et al, 2006).

Many other genes, some of which have been identified, are mutated at various stages of PDAC development and involved in progression of this disease. Understanding the genetic alterations which occur throughout the various phases of PDAC development could provide stage specific prognostic markers and the possibility of gene-specific therapies (Hruban et al, 2008a). With limited therapeutic advancement to date for PC, the prognosis remains bleak. The development of novel treatments and the ability to diagnose PDAC in the earlier stages are necessary developments in order to improve survival.

1.2. MicroRNAs

A group of >1000 small non-coding ribonucleic acids (RNAs) known as microRNAs (miRNAs), are involved in many important biological processes by controlling gene expression at the post-transcriptional level. They are single stranded and ~22 nucleotides in length, with ~50% of all mammalian miRNA loci located within close proximity to one another. Although some miRNAs are transcribed from independent loci, most miRNAs are clustered and are transcribed as part of a single polycistronic unit. Around 80% of miRNAs are encoded for by intergenic regions of DNA. The remaining miRNAs are encoded for in exonic regions, which are distributed equally between protein-coding and non-coding transcripts. Their ability to alter gene regulation following transcription means miRNAs have a strong influence on many biological processes, including proliferation, differentiation, apoptosis and metabolism (Dykxhoorn, 2010; Sassen et al, 2008; Li et al, 2010; Karius et al, 2012; Kim et al, 2009).

The first miRNA was discovered in 1993 following a genetic screen in *Caenorhabditis elegans*. Various genes involved in larval development were identified including *lin-4* which did not encode a protein, but did, however, encode a novel small non-coding RNA (Lee et al, 1993). This non-coding RNA was seen to inhibit translation of target genes, including *lin-14*, suggesting a new mechanism for gene regulation (He and Hannon, 2004). In 2000, whilst also working on *Caenorhabditis elegans,* Reinhart et al. encountered another gene involved in larval development. This gene, *let-7*, was also found to be a small non-coding RNA, and was later observed to be highly conserved across various different species (Reinhart et al, 2000; Pasquinelli et al, 2000). The extensive conservation of *let-7* within diverse species suggested an important role for

miRNAs in post-transcriptional regulation and this discovery was followed by the identification of hundreds of additional miRNAs (Sassen et al, 2008).

1.2.1. The Biogenesis of miRNAs

The biogenesis of miRNAs is a multi-step process spanning both the nucleus and cytoplasm of a cell (Figure 1.6). Initially transcription of a miRNA gene to produce primary miRNA (pri-miRNA) is carried out by either RNA polymerase II or RNA polymerase III. The RNase III (Drosha) and cofactor DiGeorge Critical Region 8 (DGCR8) protein act as the nuclear microprocessor complex to cleave pri-miRNA in order to produce precursor miRNA (pre-miRNA). DGCR8 is thought to help Drosha in the recognition of pri-miRNA through the use of its two double-stranded RNA-binding domains (dsRBDs). The nuclear exportin factor, Exportin 5 then recognises and binds the 'minihelix motif' of pre-miRNA to assist in its transfer into the cytoplasm from the nucleus in a Ran-GTP-dependent manner. Once pre-miRNA is successfully transferred to the cytoplasm, it undergoes further cleavage by the RNase III (Dicer) acting in complex with TAR RNA-binding protein (TRBP), a dsRBD containing protein, in order to produce an imperfect miRNA double stranded RNA (dsRNA) duplex with a two-nucleotide overhang at the 3' ends. The two strands of the RNA duplex then dissociate, a process arbitrated by one of four Argonaute (Ago) proteins (Ago1-Ago4). A functional guide strand and a passenger strand are then produced, followed by degradation of the passenger strand. The guide strand, known as the mature miRNA, becomes integrated into the RNA induced silencing complex (RISC) through stable association with the Ago protein, and goes on to guide the RISC complex in the targeting and repression of complementary messenger RNA (mRNA). Other core components of the RISC complex include Dicer, protein activator of the interferon induced protein kinase (PACT) and TRBP (Dykxhoorn, 2010; Li et al, 2010; Kim and Nam, 2006; Macfarlane and Murphy, 2010; Blahna and Hata, 2013).

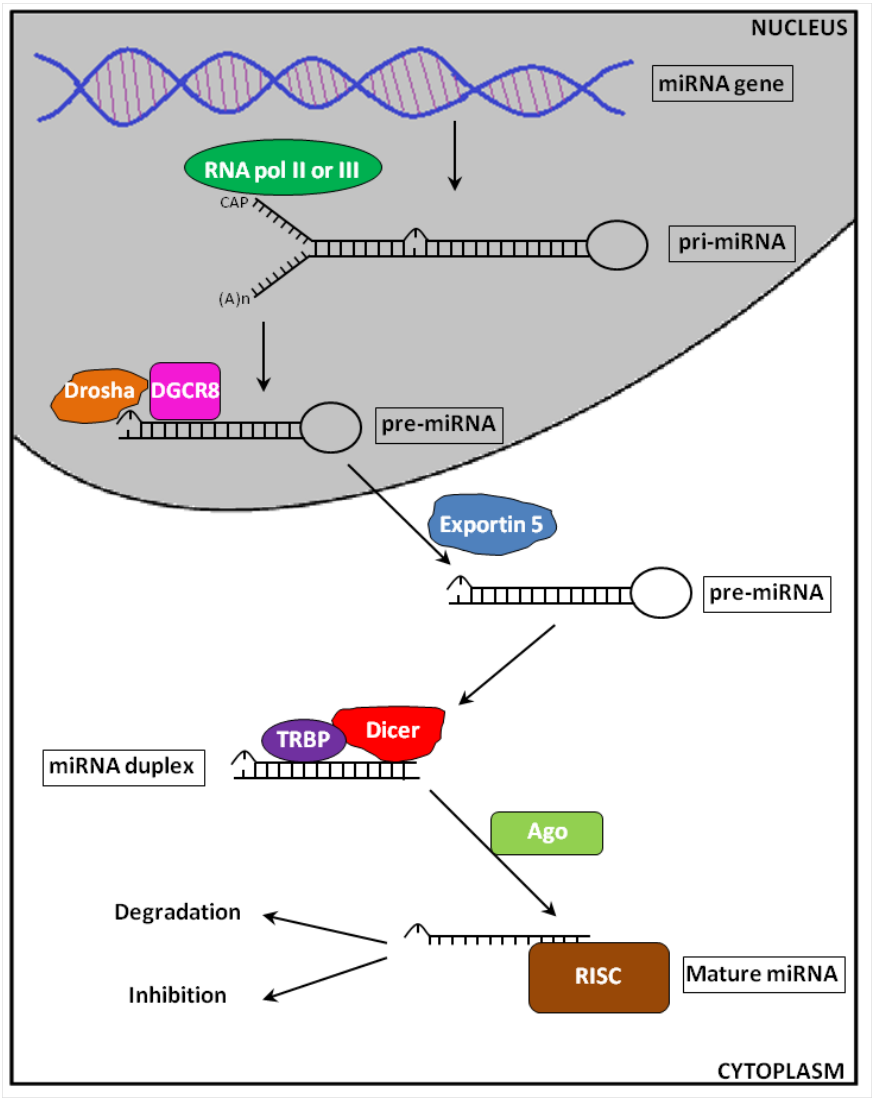

Figure 1.6: miRNA Biogenesis and its Effect on Gene Expression. Initially a transcript of around 100-1000 nucleotides known as pri-miRNA is produced compiled of a hairpin stem (~33bp), a terminal loop and two single-stranded regions adjacent to the hairpin. This transcript also possesses a 7-methyguanosine (m^7G) cap and poly-adenylated (poly(A)) tail. It is the stable hairpin stem loop structure which encodes the mature miRNA that goes on to regulate gene expression. The pri-miRNA is cleaved to produce pre-miRNA, a stem-loop structure composed of approximately 70 nucleotides, after which further cleavage and modification to remove the terminal loop results in the production of a ~22 nucleotide RNA duplex, which, when dissociated, goes on to produce mature miRNA. The mature miRNA is able to work in combination with the RISC complex to degrade or inhibit target mRNA. (Dykxhoorn, 2010; Sassen et al, 2008; Kim and Nam, 2006; Blahna and Hata, 2013). Figure adapted from (Li et al, 2010).

Each Ago protein has the capacity to mediate the manner in which a miRNA regulates gene expression; all promote translational inhibition, however Ago2 also acts to enable the degradation of a miRNA target mRNA (Blahna and Hata, 2013).

The RISC complex can also associate with small interfering RNA (siRNA) in order to initiate RNA interference (RNAi) leading to degradation of target mRNA (He and Hannon, 2004; Yang et al, 2009). This ability of small RNAs was discovered just prior to the identification of *let-7* (Fire et al, 1998). Even though miRNA and siRNA have numerous shared components, including the ability to silence gene function, they have divergent origins and biogenesis which are used to distinguish between them. They also differ in that siRNA exclusively instigates target mRNA cleavage as a result of perfect base pairing. In mammals base-pairing is predominantly imperfect resulting in mRNA target inhibition, unlike in plants where near perfect complementarity results in target mRNA degradation through an RNAi-like mechanism (Sassen et al, 2008; He and Hannon, 2004; Jackson and Standart, 2007; Filipowicz et al, 2008).

1.2.2. The Regulation of Protein Expression by miRNAs

miRNAs act by binding at the 3' untranslated region (UTR) of a target mRNA in combination with RISC, resulting in the inhibition of protein expression or accelerated mRNA decay (Bartel, 2004). The degree of base-pairing observed between the mature miRNA 'seed sequence' (nucleotides 2-8 at 5') and the mRNA target sequence 3'UTR determines how mRNAs are regulated (Figure 1.7) (Park et al, 2011a; Filipowicz et al, 2008).

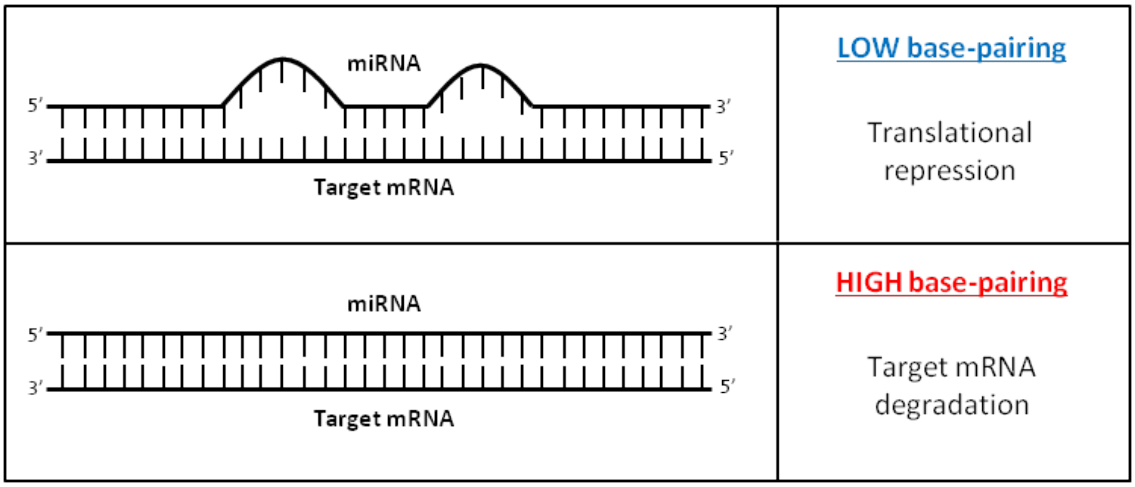

Figure 1.7: Perfect and Imperfect Base-pairing. When low base-pairing is observed between a miRNA and its target mRNA this results is translational repression, which is the mechanism by which miRNAs predominantly regulate mRNAs in humans. The high degree of base pairing between miRNAs and their target mRNAs, which is commonly observed in plants, results in target mRNA degradation (He and Hannon, 2004; Bartel and Bartel, 2003).

The perfect base-pairing of siRNA with target mRNA in combination with Ago2 as part of the RISC complex allows for cleavage and degradation. All Ago proteins contain a ribonuclease H (RNaseH)-like P-element induced wimpy testis domain. However, only Ago2 can use this domain to centrally cleave the phosphodiester bond within target mRNA opposite siRNA residues 10-11. This endonucleolytic cleavage is mainly observed during RNAi in conjunction with siRNA. However, it is also known to occur with certain miRNAs when perfect base pairing is present at the seed sequence and bases 10-11. Once cleaved the remaining fragments undergo normal mRNA decay pathway mediated degradation (Macfarlane and Murphy, 2010; Jackson and Standart, 2007; Filipowicz et al, 2008). Ago2 mediated mRNA cleavage requires a central A-form helix within the miRNA-mRNA duplex. However, due to imperfect binding most human RNA duplexes contain central bulges as a result of nucleotide mismatches which prevent RNAi dependent mRNA degradation (Pillai et al, 2007).

Eukaryotic translation is predominantly carried out through a cap-dependent mechanism consisting of three steps; initiation, elongation and termination (Figure 1.8). Various models of miRNA instigated translational repression have been suggested, including models of inhibition at both the initiation and post-initiation levels of translation (Filipowicz et al, 2008; Pillai et al, 2007).

Sucrose gradients used for polysome analysis identified repressed mRNAs within the lighter portion of sedimentation with peak levels pertaining to the 40S ribosomal subunit to disome fraction. When mRNAs shift in their location across the gradient this denotes a perturbation in translation at the initiation stage which appeared to occur only when an m^7G cap was present. It was postulated that miRNAs were capable of mediating translational inhibition through the cap-binding initiation factor eIF4E in the presence of an m^7G cap (Jackson and Standart, 2007; Pillai et al, 2007).

When combined, eIF4A, eIF4G and eIF4E make the translational initiation complex eIF4F, which enables the circularisation of target mRNA and thus its translation. The PABP binds at the 3' poly(A) tail of target mRNA and eIF4E identifies and binds at the 5'cap. Both PABP and eIF4E interact with the scaffolding protein eIF4G, a requirement for the circularisation of target mRNA (Figure 1.8) (Jackson and Standart, 2007; Pillai et al, 2007).

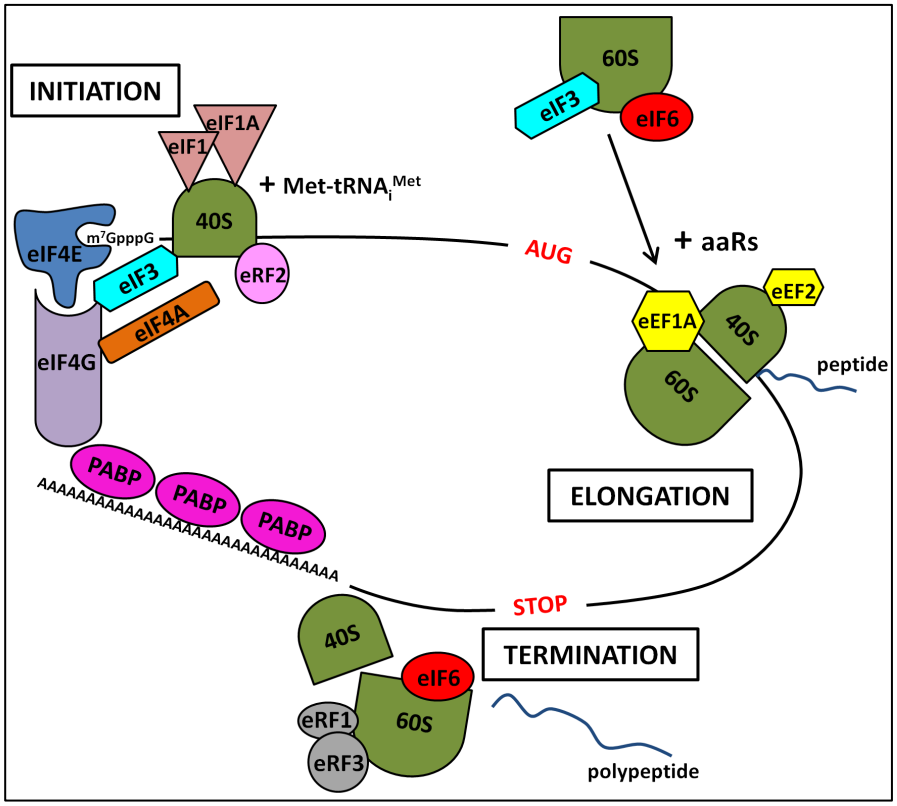

Figure 1.8: Eukaryotic Translation. During m^{7}G cap-dependent translational initiation eukaryotic translation initiation factor 4E (eIF4E) (which in combination with eIF4G and eIF4A makes up the eIF4F complex) recognises the 5' cap structure present on target mRNA. A 40S ribosome in combination with eIF3, eIF1, eIF1A, initiator Met-tRNA$_i^{Met}$, eIF2 and GTP makes up the 43S pre-initiation complex. Binding of this complex to the eIF4F-mRNA complex enables the 40S ribosome to scan target mRNAs 5'UTR in order to discover the start codon (AUG). Binding of the poly(A)-binding protein (PABP) with both the poly(A) tail and eIF4G enables mRNA circularisation, whilst eIF6 and eIF3 assist in stabilising the as yet unattached 60S ribosomal subunit. Once both the 40S and 60S ribosomal subunits are present elongation can commence assisted by eEF1A and eEF2 (elongation factors), with the binding of amino acids to cognate tRNAs catalysed by aminoacyl-tRNA synthetases (aaRs). The release factors eRF1 and eRF3 facilitate translational termination once a termination codon (STOP) is identified by the ribosomes A-site, after which finished polypeptides are released (Hernández, 2012). Figure adapted from (Bartel, 2004; Hernández, 2012).

The importance of the m^{7}G cap for successful translational inhibition was further supported by the lack of repression observed for mRNAs which lacked this cap but contained an internal ribosome entry site (IRES). IRES-mediated translational initiation does not require eIF4E. The lack of miRNA mediated translational repression observed in IRES controlled mRNAs strongly indicated the importance of both the m^{7}G cap and eIF4E initiation factor in the mechanism of repression at translational initiation (Jackson and Standart, 2007; Pestova et al, 1996). It was also proposed that disruption of the closed mRNA loop at translational initiation could occur either from the interference of

protein-protein or protein-mRNA interactions necessary to maintain the circularised mRNA or through the promotion of mRNA 3' poly(A) tail deadenylation (Jackson and Standar, 2007).

Polysome gradient analysis also showed, in some cases, unchanged patterns of sedimentation following miRNA-mediated mRNA inhibition, indicating the potential for post-initiation repression. Various models as to how translation post-initiation may have been perturbed have been suggested. These included a reduction in the rate of translational elongation, whereby target mRNA was assumed to maintain polysome association, the premature removal of ribosomes during translation and the subsequent degradation of newly synthesised protein either following or during translation (Jackson and Standart, 2007; Pillai et al, 2007).

Following miRNA mediated translational repression, target mRNAs are believed to accumulate in cytoplasmic processing bodies (p-bodies). Along with untranslated mRNAs and mRNA decay intermediates, p-bodies are also thought to contain various components of the translational repression machinery, including Ago proteins and miRNAs (Yang et al, 2009; Jackson and Standart, 2007; Liu et al, 2005). It is believed that p-bodies require mRNA to maintain their integrity and appear to function not only to sequester miRNA-targeted mRNA from translation machinery, but also to enable the degradation of mRNAs targets cleaved by either Ago2 dependent or independent mechanisms (Macfarlane and Murphy, 2010; Jackson and Standart, 2007; Pillai et al, 2007).

When translational initiation is blocked and reduced ribosomal occupancy occurs, repressed mRNA is thought to enter into p-bodies, increasing both the size and number of these protein aggregates (Pillai et al, 2007). However, when translation is repressed post-initiation and ribosomes are still present upon target mRNA, these cytoplasmic foci appear to reduce in both size and number, indicating the inability of ribosomes to enter these foci. This supports the belief that ribosomes, along with most translation initiation machinery, are unable to enter into p-bodies, and that without mRNA, p-bodies cannot exist (Jackson and Standart, 2007).

Following Ago2 mediated endonucleolytic cleavage, the remaining mRNA fragments undergo normal mRNA decay pathway-mediated degradation which is thought to begin with the deadenylation of the 3' poly(A) tail catalysed by the deadenylase Ccr4:Not1 complex. This is followed by the decapping and removal of the 5' m^7G cap mediated by the decapping complex containing enzymes Dcp1and Dcp2, followed by exonuclease Xrn1p mediated 5'-3' degradation of mRNA (Macfarlane and Murphy, 2010; Jackson and Standart, 2007; Pillai et al, 2007).

Transcriptionally repressed mRNAs targeted to p-bodies are believed to undergo either temporary reversible storage or mRNA degradation. Ago binding of miRNA has been shown to enable the interaction with GW182, a protein, that when present, plays a significant role in the localisation of Ago bound miRNA to p-bodies and the recruitment of various decay factors including RCK/p54, Dcp1 and Dcp2, pat1p and 4E-T (Jackson and Standart, 2007; Pillai et al, 2007; Liu et al, 2005).

GW182 is thought to indirectly promote mRNA deadenylation through the recruitment of PABP, thus interfering with its binding of eIF4G and leading to the association of PABP with the Ccr4:Not1 complex. This mechanism promotes translational repression through the inhibition of mRNA circularisation and accelerates degradation by recruiting the deadenylation complex. It is also believed that GW182 promotes the direct interaction of the Dcp1 and Dcp2 containing decapping complex with Ago, also leading to the acceleration of mRNA degradation (Jackson and Standart, 2007; Liu et al, 2005; Zekri et al, 2009; Behm-Ansmant et al, 2006).

Not all mRNAs entering into p-bodies will undergo decay. It is believed that translational repression and storage of miRNA target mRNAs within p-bodies could be both temporary and reversible. P-bodies contain various proteins known to have repressive capabilities, which when knocked down, can reduce the extent of miRNA mediated repression of target mRNA**.** The release of mRNA from p-bodies in response to various stimuli or as a result of general reactivation of protein synthesis can result in the re-entry of previously repressed mRNA into translation (Jackson and Standart, 2007; Pillai et al, 2007).

An example of this is the rapid increase in protein expression of the cationic amino acid transporter (CAT-1) following amino acid starvation. Endogenous miR-122 in Huh7 cells was found to decrease CAT-1 protein levels under fed conditions through the targeting of CAT-1 mRNA for translational repression, resulting in P-body localisation. Upon amino acid starvation CAT-1 protein expression was seen to rapidly increase, however there was no immediate increase in the amount of CAT-1 mRNA. Existing CAT-1 mRNA localised within the P-bodies was mobilised in order to form polysomes thus enabling protein expression (Jackson and Standart, 2007; Bhattacharyya et al, 2006).

Due to restricted complementarity in mammals, each miRNA has the ability to imperfectly bind a large number of mRNA 3'UTR's. This allows for each miRNA to have a multitude (>100) of gene targets and therefore act on a host of cellular processes (Dykxhoorn, 2010; Tili et al, 2010). It is estimated that more than 1% of human genes are able to encode miRNAs, and that around a third of all protein coding genes may be regulated by these miRNAs, making them one of the most abundant regulatory genes found in humans (Sassen et al, 2008; Chan et al, 2011). The expression patterns for many miRNAs appear to differ depending on tissue or developmental stage, with miRNA profiles often varying drastically for different diseases (Park et al, 2011a; Pillai et al, 2007).

1.2.3. Deregulation of miRNAs in Cancer Progression

The deregulation in expression of miRNAs has been associated with a variety of chronic diseases including cancer, with increased oncogenic miRNA expression and reduced tumour suppressor miRNA expression observed in a variety of cancer cells compared to non-transformed cells (Tili et al, 2010; Leung and Sharp, 2010). Extensive studies of a wide range of cancers have revealed that miRNA expression profiles can vary drastically between normal and neoplastic tissues (Negrini et al, 2007). The strong role of miRNAs in the regulation of many biological processes, in particular cellular proliferation and differentiation, highlights the huge impact their dysregulation would present (Macfarlane and Murphy, 2010).

More than 50% of miRNA genes in humans are located within regions of low genomic stability, including fragile sites known to undergo amplifications and deletions, as well

as genomic areas with LOH (Figure 1.9) (Chan et al, 2011; Calin et al, 2004). As a result many miRNAs are lost or elevated in expression due to the effects of GIN. Epigenetic forms of dysregulation include histone modification and CpG island methylation, which is believed to control 10% of miRNA expression (Figure 1.9) (Sassen et al, 2008; Han et al, 2007).

The first evidence of direct miRNA involvement in human cancer was observed in chronic lymphocytic leukaemia (CLL), when Calin et al. witnessed a decrease in expression of the tumour suppressors miR-15a and miR-16-1. These miRNAs were decreased in ~70% of cases, resulting from deletion or downregulation in expression and appeared to be in concurrence with a deletion within chromosome 13, an abnormality frequently witnessed in CLL (Park et al, 2011a; Sassen et al, 2008; 216 Yang et al, 2009; Calin et al, 2002**)**. The anti-apoptotic protein B cell lymphoma 2 (BCL2) is a target of miR-15a and miR-16-1; these miRNAs bind at the 3'UTR to inhibit its expression. In cases of malignancy, expression of miR-15a and miR-16-1 is reduced, thus impeding their ability to prevent BCL2 expression. The ensuing overexpression of BCL2 can promote tumourigenesis through evasion of apoptosis (Macfarlane and Murphy, 2010; Negrini et al, 2007).

Other tumour suppressor miRNAs downregulated in certain cancers include let-7, which acts to regulate the signal transducing GTPase, RAS. Decreased expression of let-7 has been detected in over 50% of lung cancer cases, as well as in numerous other cancer types (Sassen et al, 2008; Negrini et al, 2007). The ability of let-7 to prevent RAS overexpression is hindered in many malignancies, and several genes encoding this miRNA have been mapped to areas of the genome which are frequently lost or altered in cancer. It comes as no surprise that there is a strong correlation between reduced levels of let-7 and poor patient prognosis (Macfarlane and Murphy, 2010; Yang et al, 2009; Croce, 2009).

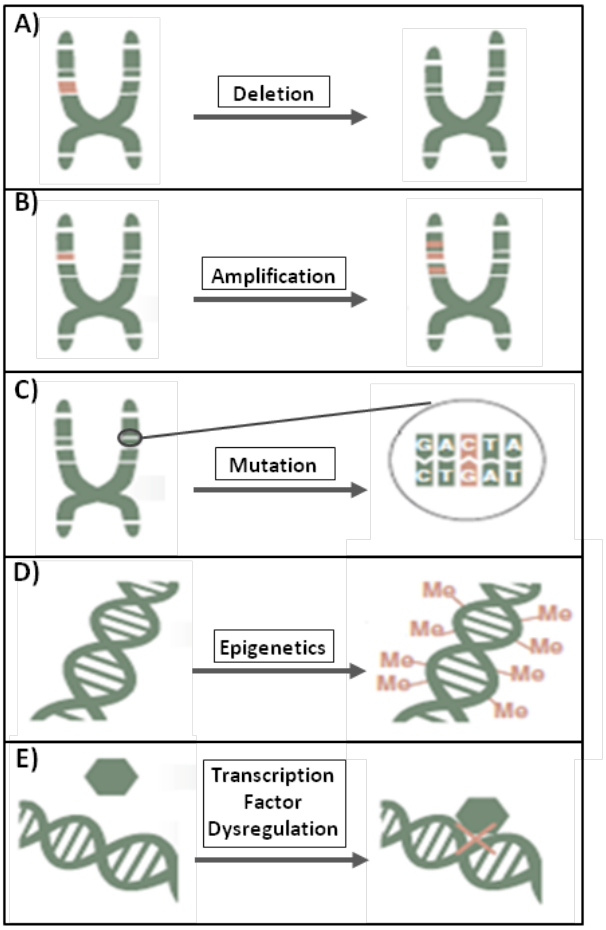

Figure 1.9: Causes of miRNA Dysregulation in Cancer. Various mechanisms are thought to contribute to dysregulated miRNA expression both as a result of and in order to contribute to cancer progression. These mechanisms include the **(A)** deletion or **(B)** amplification of chromosomal regions which encode miRNAs, and **(C)** the mutation of either a miRNA gene itself or the genetic sequence which encodes a miRNA target. Silencing of the miRNA promoter through **(D)** epigenetic regulation and **(E)** the deregulation of proteins upstream of miRNA signalling (e.g. transcription factors) also influences cancer development (Chan et al, 2011). Figure adapted from (Chan et al, 2011).

Tumour suppressor and oncogenic miRNAs both have the capacity to initiate and accelerate tumourigenesis. The miR-17-92 cluster and miR-155 were some of the first miRNAs thought to have oncogenic potential, resulting from the amplification of their coding genes in a number of B-cell lymphomas (Croce, 2009). The miR-17-92 cluster generates six mature miRNAs which are encoded for on a region of chromosome 13 which is frequently amplified in cases of B-cell lymphoma. A mouse model of B-cell lymphoma, which overexpressed the Myc oncogene, was used to highlight the capacity of the miRNA cluster in accelerating tumourigenesis stimulated by Myc. It was later observed that the miR-17-92 cluster itself appeared to be controlled to an extent by the Myc oncogene (Sassen et al, 2008; Macfarlane and Murphy, 2010; Negrini et al, 2007).

The gene encoding miR-155 lies in a conserved non-protein coding region known as B cell integration cluster. The mechanisms by which miR-155 is amplified are not well understood, however, a correlation between its increased expression and reduced survival was observed in a study of PC (Croce, 2009; Greither et al, 2010). This miRNA is overexpressed in Hodgkin lymphoma, paediatric Burkitt lymphoma, CLL and diffuse large B-cell lymphoma, amongst others (Negrini et al, 2007).

Many miRNAs have been established as either oncogenic or tumour suppressing, but this classification may be somewhat one-dimensional. Different patterns of miRNA expression have been observed between diverse cancer sub-types, as well as specific expression patterns correlating with the presence of certain cancer phenotypes. Depending on tissue type or stage of development, miRNA expression levels can vary. It is also observed that target mRNAs for specific miRNAs vary depending on tissue type. A single miRNA also has the capacity to affect a large number of different targets and therefore may control gene regulation by acting as both an oncogene and tumour suppressor in different contexts (Sassen et al, 2008; Croce, 2009). An example of this is miR-181 which becomes overexpressed in thyroid and prostate cancer, but is seen to decrease in expression in glioblastomas and pituitary adenomas (Negrini et al, 2007).

Understanding the correct cellular location of a miRNA is also extremely important, especially so that downstream studies can be conducted appropriately. It is sometimes the case that a miRNA's cellular location can be overlooked (Kent et al, 2014). Studies observing downregulated expression of miR-143 and miR-145 in colorectal cancer (CRC) believed that these miRNAs were expressed within colonic epithelial cells. It was understood that reduced expression of these miRNAs encouraged proliferation and tumourigenesis in CRC (Akao et al, 2006). Recent studies however, have discovered that miRs-143/145 are expressed at high levels in mesenchymal cells such as fibroblasts and smooth muscle cells and not in epithelial cells as previously stated (Chivukula et al, 2014). In the initial study the expression pattern for these miRNAs was determined from tissue level data, however many different cell types contribute to the composition of a tissue and each cell type has a unique capacity to express different miRNAs. It is therefore possible that misinterpreting the context in which a miRNA is expressed will cast doubt on any findings regarding the miRNA in question and its actions (Kent et al, 2014).

It is known that genetic and epigenetic aberrations, as highlighted in Figure 1.7, strongly contribute to the changed miRNA expression in many cancers when compared to normal tissues. It is also understood that miRNAs can contribute to carcinogenesis through their direct control by upstream tumour suppressor and oncogenic pathways such as downregulation in expression of the miR-17-92 cluster by oncogenic Myc (Negrini et al, 2007; Lotterman et al, 2008). Another example of miRNAs as downstream effectors is the activation of the miR-34 family by the TF p53, a protein involved in stress signalling. Together with the p53 tumour suppressor network, miR-34 acts to prevent inappropriate proliferation associated with cancer progression (Sassen et al, 2008; Negrini et al, 2007). It has also been suggested that dysregulated miRNA expression in cancer could be related to changes in tumour microenvironment. Kulshreshtha et al. observed a correlation between a hypoxic microenvironment and the elevated expression of a number of miRNAs which were also commonly upregulated in cancer (Negrini et al, 2007; Kulshreshtha et al, 2007).

Studies have also shown that aberrant miRNA expression is involved in the regulation of the metastatic cascade, EMT and CSCs, and is strongly associated with drug resistance in tumour cells. Chemotherapy is in many cases unable to completely eliminate all tumour cells. Those remaining often possess both EMT and CSC properties, which are believed to contribute to drug resistance, frequently leading to disease recurrence. Although the causes of drug resistance are not completely understood, it is believed that miRNAs have the capacity to regulate both EMT and CSC properties, making them key therapeutic targets when fighting drug resistance in cancer (Wang et al, 2010a; Sarkar et al, 2010; Hurst et al, 2009).

The miR-200 family helps to maintain an epithelial character by its ability to target and therefore silence expression of the Zeb family. As previously mentioned, Zeb1 and Zeb2, amongst other EMT TFs, have the capacity to repress the expression of E-box element containing genes, which include the cell adhesion protein E-cadherin (Dykxhoorn, 2010; 392 Hurteau et al, 2006; Hurteau et al, 2009). Using a cell line originating from a mouse model of metastatic lung adenocarinoma, it was observed that levels of the miR-200 family were decreased during EMT. However, forced expression of this miRNA family was shown to prevent EMT and reduce the capacity for invasion and metastasis (Gibbons et al, 2009). Zeb1 was found to directly suppress transcription

of various miR-200 family members which contribute to epithelial differentiation in colorectal and breast cancer cells. Zeb1 and miR-200 family members were seen to act through a feed-forward mechanism in order to regulate EMT, with Zeb1 promoting EMT by inhibiting the miR-200 family. Increased expression of the miR-200 family acted to prevent Zeb1 expression and induce epithelial differentiation, therefore slowing the metastatic potential of the cell (Burk et al, 2008).

Both EMT and CSC properties are essential for disease metastasis; it has been observed that both processes are linked with overlapping molecular signatures observed in secondary lung metastasis derived from breast cancer (DiMeo et al, 2009). This is further supported by the joint regulation of both EMT and CSC processes by numerous miRNAs in the metastatic development of different cancers. A sub-population of cells thought to have CSC properties was found to be regulated by miR-888 in the human breast cancer cell line MCF-7. This miRNA, which acts as an oncogene, is believed to target E-cadherin expression, and is understood to aid in the maintenance of CSCs and regulate EMT within MCF-7 cells (Huang and Chen, 2014). A significant downregulation in miR-132 expression was observed in CRC cell lines and patient tissue. Low expression levels of this tumour suppressor miRNA were shown to correlate with a reduced chance of disease free survival in CRC patients. It was also observed that Zeb2 was regulated by miR-132 and that increased expression of miR-132 was seen to inhibit cell invasion and EMT in CRC cell lines (Zheng et al, 2014). Within lung adenocarcinoma tissues miR-145 functions as a tumour suppressor through the targeting and inhibition of Oct-4, a TF involved in stem cell self-renewal. When expressed miR-145 is observed, both *in vitro* and *in vivo,* to downregulate lung CSCs and EMT processes by targeting Oct-4 (Hu et al, 2014).

In the two decades since the discovery of these small non-coding RNAs, huge advances have been made in understanding their targets and how they help regulate gene expression. However, the targets and biological functions of most miRNAs are still unknown, and their involvement in diseases such as cancer needs to be further elucidated (Macfarlane and Murphy, 2010). It is still not understood whether altered miRNA expression is the cause or consequence of this pathological process (Park et al, 2011a).

1.2.4. Techniques and Approaches for the Study of miRNAs

Since their initial discovery in the early nineties extensive work has gone into identifying novel miRNAs through the cloning and sequencing of endogenous short RNAs in various species including mammals and *Caenorhabditis elegans* (Lagos-Quintana et al, 2001; Lau et al, 2001; Lee and Ambros, 2001). To better understand these numerous miRNAs a public registry was created using both experimental approaches and bioinformatics, which is known as miRBase. This registry provides an up to date compilation of all identified miRNA genes from various species including *Caenorhabditis elegans* and *Homo sapiens* even prior to their publication (He and Hannon, 2004; Chan et al, 2011; Griffiths-Jones, 2004).

The examination of aberrant miRNA expression in cancerous tissues highlighted the possibility of using global miRNA profiling for the identification and classification of human cancers. It was found that miRNA expression patterns could be used to identify the developmental origin of a cancer and that the differentiation state of a tumour appeared to affect global miRNA expression levels (Chan et al, 2011; Gong et al, 2011; Lu et al, 2005).

Hierarchical clustering performed by Lu et al. found that cancers of epithelial and hematopoietic origin were associated with divergent miRNA expression profiles, and that profiles for numerous patients with ALL were separated into three groups according to their underlying genetic abnormalities (Sassen et al, 2008; Lu et al, 2005). Global miRNA expression decreased in cancer tissues; it was observed that within poorly differentiated cancers the expression level of miRNAs was much reduced in comparison to more-differentiated and non-cancerous samples. It was suggested that miRNA expression profiles could therefore be used to successfully indicate a tumour's developmental origin and state of differentiation (Chan et al, 2011; Lu et al, 2005).

Lu et al. attempted to diagnose 17 poorly differentiated tumours of unknown origin using expression profiles based on the differential expression of either 217 miRNAs or ~16,000 mRNAs. Successful diagnosis of 12 of these tumours was achieved using the miRNA based expression profile. However the mRNA expression profile only allowed the diagnosis of a single poorly differentiated tumour. These findings highlight the diversity of miRNA expression across all cancers and how information obtained from a

modest number of miRNAs (~200) in regard to tumour diagnosis seems to exceed that provided by existing gene expression profiles employing tens of thousands of mRNAs (Sassen et al, 2008; Chan et al, 2011; Lu et al, 2005).

Within plasma samples endogenous miRNAs appeared to resist RNase activity and were found to have high levels of overall stability (Lodes et al, 2009). It was hypothesised that a method by which miRNAs may be protected is by packaging within exosomes. These are endocytic cell-derived vesicles of approximately 50-90nm in size and are believed to be present within most human biological fluids (Mitchell et al, 2008). Exosome function is thought to include the mediation of various signalling events through their interaction with recipient cells. Studies using mouse (MC/9) and human (HMC-1) cell lines following microarray analysis have revealed that miRNAs, in addition to mRNAs, are present within exosomes. This RNA was transferable to other cells, and, following *in vitro* translation, it was determined that functionality of both mRNA and miRNA was maintained during this transfer (Valadi et al, 2007).

Alternative explanations for miRNA stability in plasma have also been discussed in the literature, and include the association of miRNAs with Ago proteins and the RISC complex and direct modifications of miRNAs providing resistance to RNase activity (Lodes et al, 2009; Mitchell et al, 2008).

It was observed that tumour-derived miRNAs in the blood could be detected in serum and plasma and used as circulating markers for cancer detection (Lodes et al, 2009; Mitchell et al, 2008; Jung et al, 2010). Furthermore miRNAs maintain a decent level of stability in formalin-fixed paraffin-embedded specimens and samples that have undergone various cycles of freeze-thawing (Mitchell et al, 2008; Xi et al, 2007).

There are various platforms on which miRNAs can be profiled, including northern blot analysis, miRNA microarray technology, high-throughput deep sequencing, bead-based flow cytometric miRNA analysis and RT-qPCR assays (Lu et al, 2005; Thomson et al, 2006; Liu et al, 2004; Thomson et al, 2004; Margulies et al, 2005; Jiang et al, 2005). These approaches have helped identify dysregulated miRNAs in various cancers and can be used, theoretically, to analyse all known human miRNAs (Li et al, 2010; Chan et al, 2011).

Bioinformatic approaches are commonly used to predict putative miRNA target genes following miRNA identification. These include miRWalk, TargetScan, DIANA-microT and mirTar (Dweep et al, 2011; Lewis et al, 2005; Maragkakis et al, 2009; Hsu et al, 2011). As previously discussed miRNAs have the potential to regulate numerous mRNA targets based on the extent of sequence complementarity. These bioinformatic approaches carry out predictive target recognition based on the requirement of exact base pairing of the seed sequence with its mRNA targets (Sassen et al, 2008). Following target prediction, experimental validation is recommended to confirm a genuine miRNA target (Croce, 2009).

1.2.5. The Use of miRNAs as Diagnostic/Prognostic Tools and Therapeutic Targets

The aberrant expression of miRNAs in malignant cells and their considerable influence on the development and progression of cancer highlights their potential use as biomarkers of disease and novel therapeutic targets (Chan et al, 2011; Negrini et al, 2007; Croce, 2009). The robust stability of miRNAs in serum and plasma accompanied by research which correlates plasma miRNA levels and patient outcome in various cancers renders the use of serum based miRNA detection as a viable option for cancer diagnosis and disease prognosis (Mitchell et al, 2008; Jung et al, 2010; Ayaz et al, 2014; Tang et al, 2013; Ye et al, 2014).

The use of anti-miRNA oligonucleotides (AMOs) as an effective therapy for cancer has been suggested following their ability to successfully inactivate miRNA function in diverse cancer cell lines. Glioblastoma cells over-express miR-21, which inhibits the expression of various apoptosis genes contributing to the cells malignant phenotype. Transfection of both 2'-O-methyl and locked nucleic acid (LNA) modified anti-miR-21 synthetic oligonucleotides into these cells resulted in caspase activation and subsequent apoptosis-mediated cell death (Negrini et al, 2007; Chan et al, 2005; Krutzfeldt et al, 2005).

AMOs containing either 2'-O-methyl residues or LNAs form duplexes of greater stability and potency when trying to knock-down expression of their target miRNAs, and have reduced toxicity to that previously observed with the use of AMOs *in vitro*. These features improve the feasibility of using modified AMOs for anti-cancer therapy, however successful and efficient target delivery is still an issue (Negrini et al, 2007;

Chan et al, 2005; Fluiter et al, 2003). Extensive work has been carried out into the use of siRNA in silencing single target genes, with various approaches for siRNA delivery having been investigated, including liposomes, viral vectors and nanoparticles. Due to numerous similarities between siRNA and miRNA, as previously discussed, the delivery systems already established for use with siRNA may be applicable for AMO delivery (Dykxhoorn, 2010; Negrini et al, 2007).

Most research into the potential of AMOs for use in cancer therapy has been carried out *in vitro* with few relevant animal models available for *in vivo* work (Li et al, 2010; Negrini et al, 2007). Recently a LNA-modified DNA phosphorothioate antisense oligonucleotide known as Miravirsen was assessed as part of a phase 2a clinical trial for the treatment of patients with chronic hepatitis C virus (HCV) genotype 1 infection. The miR-122, which is expressed in the liver, is understood to interact with the HCV genome, aiding in its stability and dissemination. Miravirsen appeared to reduce HCV RNA levels by sequestering miR-122 and inhibiting its role in HCV replication (Janssen et al, 2013). The success of Miravirsen in these patients provides strong support for the therapeutic potential of AMOs in the treatment of cancer.

Further work is still required to fully determine the potential of miRNAs as therapeutic targets (Lu et al, 2005). The ability of miRNAs, unlike siRNAs, to target numerous transcripts complicates the therapeutic application of AMOs. It is necessary to consider that the host of genes silenced by miRNAs often have opposing functions and the result of inhibiting miRNA expression may cause unanticipated/opposing effects (Dykxhoorn, 2010). Inconsistency in the differential expression of miRNAs observed in numerous independent studies is a further factor that needs to be contemplated. Before a miRNA can be considered as a clinical target, its role within cell signalling must be understood (Dykxhoorn, 2010; Chan et al, 2011; Gong et al, 2011).

1.2.6. The Involvement of miRNAs in Pancreatic Cancer Progression

Several studies have carried out expression profile analysis to determine a miRNA expression signature which could be used to aid in the diagnosis and prognosis of PC. To date the knowledge of differential miRNA expression in PC is fragmented, with much of the data lacking reproducibility.

Bloomston et al. endeavoured to differentiate cases of PDAC from normal pancreas and chronic pancreatitis with unique miRNA profiles. Following microarray analysis and RT-qPCR validation, miR-21, miR-221/222 and miR-155 were found to increase in PC when compared to normal pancreas and chronic pancreatitis. The miRNA miR-196a-2 was also associated with poor survival in PC patients (Bloomston et al, 2007).

Eun et al. also found increased expression of miR-21, miR-221/222 and miR-155 in human PDAC when compared to benign tissue. Aberrant expression of these miRNAs has been associated with various other cancers such as glioblastomas and diffuse large B-cell lymphomas (Chan et al, 2005; Ciafre et al, 2005; Eis et al, 2005; Lee et al, 2007). Deregulated expression of miR-376a and miR-301 was also observed in human PDAC. Dysregulation of these miRNAs has so far not been associated with any other cancers (Lee et al, 2007).

Using RT-qPCR, the differential expression of 95 miRNAs in PC was analysed. Following the analysis of 10 cell lines and 17 pairs of PC and normal tissues, a panel of eight miRNAs; miR-190, miR-186, miR-200b, miR-15b, miR-95, miR-196a, miR-221 and miR-222 was found to be significantly elevated in 70-100% of PC tissues and cell lines when compared to normal controls (Zhang et al, 2009).

Microarray analysis and RT-qPCR validation was carried out on surgically resected tissues from normal pancreas, chronic pancreatitis and PDAC to determine differential expression of 377 miRNAs. Dysregulated expression of miR-29c, miR-96, miR-143, miR-145, miR-148b and miR-150 was observed in both PDAC and chronic pancreatitis, however aberrant expression of miR-196a, miR-196b, miR-203, miR-210, miR-222, miR-216, miR-217 and miR375 was only observed in PDAC. It was determined that miR-217 and miR-196a alone were sufficient to differentiate a PDAC specimen from normal pancreas or chronic pancreatitis (Szafranska et al, 2007).

These and other studies have produced diverse expression profiles for PC whereby very few of the miRNAs recognised as differentially expressed are consistently identified in more than one study. Only a small number of miRNAs have been consistently reported as differentially expressed in PC and are thought to potentially aid in the diagnosis and prognosis of this disease (Table 1.7) (Sun et al, 2014).

In addition to these frequently encountered miRNAs, loss of the miR-34 family has also been associated with PC in studies researching CSCs and drug resistance. A reported reduction in expression of the miR-34 family has been linked with self-renewal of pancreatic CSCs and as a consequence, the development of drug resistance (Chang et al, 2007; Ji et al, 2009).

In order to use miRNAs as biomarkers for PC a reliable expression profile which is consistent throughout PC specimens must be elucidated (Koorstra et al, 2008). Consistent dysregulation of a few miRNAs (Table 1.7) which correlate with PC diagnosis and prognosis has been observed. Most PC expression profiles, however, are significantly diverse, an indication of how different cancers can be even within a subtype such as PC (Negrini et al, 2007; Zhang et al, 2009).

Previous research which used miRNA expression profiles to classify human cancers employed in the region of 200 miRNAs to aid in diagnosis (Lu et al, 2005). Realistically miRNA dysregulation in PC is unlikely to occur at this magnitude; however this study highlights the value of using a greater number of miRNAs to achieve a superior level of diagnostic or prognostic reliability. To achieve this, further work is necessary in order to identify additional miRNAs which become aberrantly expressed in PC in a consistent manner.

Table 1.7: miRNAs with Diagnostic and Prognostic Potential.

miRNA	Description	Reference
miR-221	Elevated expression often observed within PC, high plasma concentrations of this miRNA were found to correlate extensively with the development of distant metastasis and tumour unresectability.	(Kawaguchi et al, 2013)
miR-155	Expression levels of the TSG Sel-1-like (SEL1L) which is often down-regulated in PDAC were found to inversely correlate with the expression of miR-155. Increased expression suppressed SEL1L in PC cell lines, indicating potential as a therapeutic target.	(Liu et al, 2014a)
miR-21	Emerged as the single most predictive biomarker in relation to outcome for a patient following treatment. In patients with PDAC low expression of miR-21 following adjuvant treatments indicated the potential use of miR-21 as a target for treatment.	(Chan et al, 2011)
miR-200	Decreased levels in PC cell lines resistant to gemcitabine compared to a gemcitabine sensitive line, supporting the idea that for tumours to acquire EMT and undergo metastasis a change in miRNA expression profile within the tumour cells occurs. Re-expression of the miR-200 family within the gemcitabine resistant PC cell line MIA PaCa-2 led to an increase in E-cadherin and decreased expression of various mesenchymal markers suggesting reductions in this miRNA contribute to EMT.	(Ali et al, 2010; Li et al, 2009)
miR-196	Differential miRNA expression within PC or high-grade PanIN2/3 lesions was compared to healthy or low-grade PanIN1 lesions in the serum levels of both transgenic LSL-KrasG12D/+;LSL-Trp53R172H/+;Pdx1-Cre (KPC) mice and PC patients. Increased expression of miR-196a/b was observed highlighting the potential use of this miRNA in the early diagnosis. miR-196a/b expression was reduced following curative resection in some patients, and could therefore also be used to determine patient prognosis.	(Slater et al, 2014)

1.3. Phytochemicals

1.3.1. The Modern Diet

In 2002, the World Health Organisation (WHO) stated that throughout the globe each year a minimum of 2.7 million deaths occurred primarily as a result of insufficient consumption of both fruit and vegetables. The estimated average consumption was seen to vary throughout the world, with a two-fold difference in intake ranging from approximately 189g/day to 455g/day between regions (World Health Organisation, 2002).

There has been considerable emphasis over the last few years on the need to increase fruit and vegetable intake. A minimum consumption of 400g/day was recommended by the WHO in the early nineties following evidence for the protective capacity of fruit and vegetables against cardiovascular disease and cancer (World Health Organisation, 1990; Craig and Mindell, 2012). Data obtained from over 250 population-based studies noted

that individuals who consumed roughly five portions of fruit and vegetables each day had a 50% risk reduction in their chances of developing cancer compared to those consuming less than two portions (Surh, 2003; Winston, 1997).

In 1997 the World Cancer Research Fund (WCRF) and American Institute for Cancer Research (AICR) generated a report investigating the effects of nutrition, food, body composition and physical activity on moderating the risk of cancer. This report helped to highlight factors which most affected cancer development and became one of the most influential reports regarding lifestyle and cancer (AICR, 1997). A second updated report was produced in 2007 which contained eight general recommendations believed to aid in the prevention of most common cancers. One of these recommendations was to "eat mostly foods of plant origin" urging individuals to eat a minimum of five portions (~400g) of non-starchy fruit and vegetables each day (WCRF/AICR, 2007).

Six of these recommendations were applied in a study cohort of 57,841 men and women who prior to baseline had not been diagnosed with cancer. A 7.7 year follow-up concluded that adhering to the WCRF-AICR recommendations could considerably reduce cancer related mortality, and that recommendations related to plant foods in particular had a strong relationship with reduced cancer specific mortality (Hastert et al, 2014). Furthermore a recent health survey for England regarding the daily consumption of fruit and vegetables as recommended by governments worldwide also found that an intake of seven or more portions per day of fruit and vegetables was associated with reduced mortality in regard to various chronic diseases, including cancer (Oyebode et al, 2014).

Approximately 10% of morbidity and mortality in the UK could be attributed to food-related ill health, with most cases occurring as a result of an unhealthy diet, costing the National Health Service (NHS) around £6 billion per year (Rayner and Scarborough, 2005). It therefore seems logical that by consuming a minimum of 5-7 portions of fruit and vegetables each day, food related ill health could become less of a burden on our healthcare system. Various groups of fruit and vegetables are thought to possess potentially protective properties against disease through the actions of phytochemicals.

Phytochemicals are components obtained from plant based dietary intake which do not offer any form of nutrition, however they are biologically active. A large body of evidence indicates that numerous phytochemicals obtained via the consumption of certain fruits, vegetables, legumes, nuts, whole grains and herbs may have disease preventive properties and could be involved in cancer chemoprevention (Surh, 2003; Winston, 1997).

1.3.2. Phytochemicals, an Avenue for Cancer Treatment

It was during the mid-1970's that prevention of cancer progression was suggested by Michael Sporn, through the use of agents with the capacity to block or slow the development of neoplastic tumours (chemoprevention). The term cancer chemoprevention describes the consumption of either synthetic or natural agents such as phytochemicals in order to prevent, inhibit or reverse carcinogenesis either at the initiation phase or during neoplastic development (Priyadarsini and Nagini, 2012; Wattenberg, 1985).

The standard approach for dealing with cancer was to destroy and remove diseased cells; however it became apparent that carcinogenesis was a multi-step developmental process which provided numerous opportunities for agents to arrest or stabilise cancer progression before reaching end stage disease (Sporn, 1976).

The process of carcinogenesis is often oversimplified into three stages; initiation, promotion and progression (Greenwald et al, 1995; Landis-Piwowar and Iyer, 2014). Initiation is a rapid process whereby exposure of cell DNA to carcinogenic agents leads to genotoxic damage. Promotion occurs through the active proliferation and accumulation of preneoplastic cells, often a lengthy process which is reversible and progression is the final stage of neoplastic development where tumours develop invasive and metastatic properties (Figure 1.9) (Surh, 2003; Wattenberg, 1985; Gescher et al, 2001).

Chemoprevention is categorised into three levels; primary, secondary and tertiary. Primary chemoprevention is applied throughout the general population in particular those individuals who are at high-risk of developing cancer. Patients with pre-malignant lesions which may progress are targets for secondary chemoprevention and tertiary

chemoprevention is directed towards individuals who may develop secondary forms of cancer either in the form of metastasis or additional primary disease. All three levels of chemoprevention aim to reduce the chance of further disease progression (Priyadarsini and Nagini, 2012; Landis-Piwowar and Iyer, 2014; Gescher et al, 2001).

These agents are grouped into two main classes depending at which point during the carcinogenic process they are effective and are known as blocking agents and suppressing agents. Blocking agents act either to prevent the development of a carcinogen from its precursor or to stop carcinogens reaching and reacting with cellular targets in order to avoid DNA damage and mutations. These agents stop normal cells from becoming initiated cells and can act by preventing metabolic activation of carcinogens, boosting existing detoxification systems and also through confining reactive oxygen species (ROS) before they are able to cause damage. Suppressing agents inhibit already initiated cells from further neoplastic development either at the promotion or progression stage of carcinogenesis by controlling differentiation, proliferation, apoptosis and senescence (Figure 1.10) (Surh, 2003; Priyadarsini and Nagini, 2012; Greenwald et al, 1995).

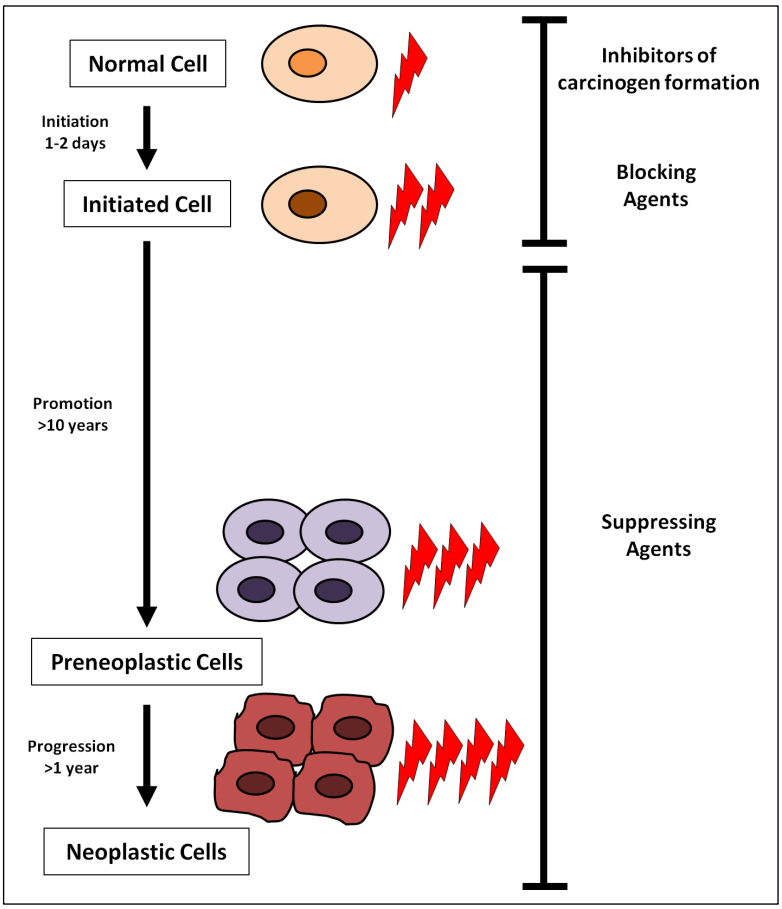

Figure 1.10: The Actions of Chemopreventive Agents on Multi-step Tumourigenesis. Multistep carcinogenesis is made up of closely linked stages; initiation, promotion and progression. There are agents which can act at these various stages in order to inhibit any further progression. There are two classes of agents known as blocking agents which either act to prevent initiation or suppressing agents which prevent promotion or progression. In addition to acting independently these agents have also been seen to augment the efficacy of existing chemotherapeutic agents (Priyadarsini and Nagini, 2012; Greenwald et al, 1995). Figure adapted from (Surh, 2003; Manson, 2003).

Even though many chemopreventive agents have been shown to assist in repressing carcinogenic progression, the mechanism of action for most of these agents is not fully elucidated (Surh, 2003; Wattenberg, 1985).

1.3.3. Phytochemicals as Chemopreventive Agents

It has been estimated that there are at least 35 different plant based foods including, cruciferous vegetables, green tea, turmeric, soybeans and allium vegetables which contain over 1000 structurally diverse phytochemicals of various classes, including flavonoids, polyphenols, terpenes, carotenoids and alkaloids with chemopreventive and therapeutic capacity (Surh, 2003; Aggarwal and Shishodia, 2006; Moiseeva and Manson, 2009; Milner et al, 2001). Phytochemical consumption has been associated

with risk reduction in a diverse range of cancer subtypes, making the use of these agents appealing in the attempt to control the progression of cancers (World Health Organisation, 2002; WCRF/AICR, 2007). With the acquisition of these agents being both relatively inexpensive and easily accessible, the use of phytochemicals globally could benefit cancer therapies (Surh, 2003). There are, however a variety of factors, including bioavailability and genetic polymorphisms, thought to impinge on the efficacy of these phytochemicals as therapeutic agents (Moiseeva and Manson, 2009; Wiencke, 2004).

The ability of an individual to metabolise phytochemicals affects the circulating concentrations of these agents. Gene polymorphisms result in an altered genotype, with polymorphisms in one or more genes related to potential increases or decreases in phytochemical metabolism, absorption and availability of metabolites (Milner, 2006). As a result, phytochemicals could be more or less effective in those populations with specific genetic polymorphisms. The allele and genotype frequencies for numerous metabolic genes within the global human population have been studied and significant differences in these frequencies between Caucasians, Asians and Africans/African Americans observed. Further heterogeneity in allele and genotype frequencies was detected when comparing Caucasian populations from diverse countries (Garte et al, 2001). A cancer prevention study assessing an array of polymorphic susceptibility genes in a cohort of Finnish male smokers observed similar polymorphic frequencies for most genes assessed when compared to other Caucasian populations. However, the prevalence of polymorphisms in the androgen receptor-CAG repeat (AR-CAG) and vitamin D receptor (VDR) was significantly different. High risk alleles for both AR-CAG and VDR have been associated with prostate cancer: however levels of these alleles in the Finnish cohort were underrepresented and may to some extent account for reduced prostate cancer incidence in Finland when compared to the United States (Milner et al, 2001; Woodson et al, 1999).

International diversity in patient diet and lifestyle will obviously occur with distinct food types being cultivated and consumed at different levels depending on geographical location. An example is the phytochemical isoflavone which is most commonly found in soybeans; it is consumed at a rate of 33.5 mg/day in China and 46.5 mg/day in Japan, in comparison to the diminutive level of ~0.44 mg/day in Europe (Wiencke, 2004;

Grace et al, 2004; Link et al, 2010). The consumption of a Mediterranean diet (olive oil, raw vegetables, and lean meats) has also been inversely associated with mortality (Masala et al, 2007; Tavani and La Vecchia, 1995).

Some agents with observed chemopreventive properties for certain cancers augment disease progression in other cancer sub-types. The flavonoid, isoflavone, when examined in the urine and serum of British women, was found to correlate with breast cancer incidence, possibly as a result of its estrogenic activity (Grace et al, 2004). However, when analysed in various cohort studies assessing both men and women from numerous countries, exposure to flavonoids was associated with reduced risk of lung cancer development (Neuhouser, 2004). It was also suggested that consuming flavonoids in the form of soy based foods could be a contributing factor to the comparatively low rates of colon, prostate and breast cancer in the Chinese and Japanese populations (Messina et al, 1994).

Many studies have been carried out to ascertain the therapeutic potential of phytochemicals on a variety of cancer subtypes. The downside of most existing chemotherapeutic agents is their damaging side effects. One of the major benefits of phytochemicals is their specificity against tumour cells which are often more susceptible to these agents in comparison to non-transformed cells. The chemical diversity and inherent biologic activity of phytochemicals in conjunction with their affordability, availability and lack of significant toxic effects makes them an increasingly attractive prospect for the treatment and prevention of cancer. However, factors such as lack of bioavailability and resulting inability to obtain sufficiently high physiological concentrations have hindered their use as cancer therapeutics. On the other hand it has been observed that many phytochemicals are efficacious even at low levels in certain cancer subtypes (Moiseeva and Manson, 2009; Priyadarsini and Nagini, 2012).

1.3.4. The Effects of Phytochemicals on Signalling Pathways in Cancer

Numerous molecular targets and signalling pathways have been associated with the mechanisms by which phytochemicals reduce cancer progression. It is understood that due to their chemical and biological diversity each phytochemical can act independently on a range of different molecular targets. This vastly enhances the number of potentially

chemopreventive interactions, and goes some way in explaining why phytochemical-mediated cancer treatment and chemoprevention is so complex (Aggarwal et al, 2006; Milner et al, 2001).

In their capacity as blocking agents, phytochemicals are believed to modulate redox signalling through the control of cellular metabolism, including processes such as carcinogen inactivation, scavenging of free radicals and the induction of anti-oxidative enzyme activity. As suppressing agents, they have been implicated in the modulation of various oncogenes and TSGs in order to influence proliferation, differentiation or apoptosis. Altered signalling through the modulation of mitogen-activated protein kinases (MAPKs), PI3K and protein kinase C (PKC), as well as modified TF activity e.g. nuclear factor kappa-light-chain-enhancer of activated B cells (NF-κB) and activator protein-1 (AP-1) are possible ways by which phytochemicals may exert their effects. These dietary agents are also known to regulate the cell cycle, DNA repair, hormonal and growth factor activity and epigenetic signalling, as well as angiogenesis and metastasis, at least *in vitro* (Surh, 2003; Landis-Piwowar and Iyer, 2014; Manson, 2003; Neergheen et al, 2010).

In order to prevent cancer occurrence, ROS and carcinogen induced DNA-damage which lead to the development of initiated cells must be avoided. Realistically, continual exposure to agents which encourage DNA-damage is unavoidable and therefore cancer-initiating events are inevitable. There are, however, ways to prevent DNA-damage, including the modulation of cytoprotective enzymes involved in directly scavenging ROS and preventing the conversion of a pro-carcinogen into a carcinogen (Landis-Piwowar and Iyer, 2014; Manson, 2003).

Phase I drug metabolising enzymes such as cytochromes P450 (CYP) are involved in carcinogen activation and phase II conjugating enzymes, which include glutathione-S-transferases (GST), assist in detoxification by removal of carcinogenic agents from within a cell. The balance maintained between phase I and phase II enzymes can greatly affect the amount of DNA-damage which occurs. Carcinogen activation of the aryl hydrocarbon receptor (AhR) leads to induction of the CYP enzymes and contributes to cancer cell initiation. Dietary agents, including epigallocatechin gallate (EGCG), resveratrol and curcumin can impair AhR activity, thus decreasing the activity of phase

I carcinogen activating enzymes (Priyadarsini and Nagini, 2012; Ciolino et al, 1998; Ciolino and Yeh, 1999; Muto et al, 2001).

Normal cells will inevitably generate ROS during cellular metabolism. However, through the implementation of low MW antioxidants such as glutathione and enzymes such as superoxide dismutase, cells maintain their redox potential. When the balance is perturbed, cells mount an oxidative stress response, which involves the altered expression of numerous genes including those which encode regulatory TFs (Dalton et al, 1999).

The nuclear-factor-(erythroid-derived 2)-related factor 2 (Nrf2) is a well documented basic region leucine zipper TF responsible in part for the expression of various phase II cytoprotective enzymes and is induced as a result not only of oxidative stress, but also in the presence of numerous phytochemicals, including *Curcuma longa* (turmeric) and *Camellia sinensis* (green tea) (Reuland et al, 2013; Hayes and McMahon, 2001). Under normal conditions Nrf2 is sequestered within the cytoplasm through an interaction with the Kelch-like ECH-associating protein 1 (Keap1). When a cell experiences stressful conditions Nrf2 is released from Keap1 and translocated to the nucleus to activate antioxidant responsive element (ARE) regulated genes which act to normalise the cell's redox potential and prevent DNA-damage (Figure 1.11) (Landis-Piwowar and Iyer, 2014; Reuland et al, 2013). Various dietary agents, including catechins, quercetin and isothiocyanates, have been associated with the induction of ARE-dependent cytoprotective genes (Khan, et al 1992; Valerio et al, 2001; Zhang, 2004). There have also been numerous signalling molecules and pathways implicated in the transcriptional activation of ARE, including MAPKs, (extracellular-signal-regulated kinase (ERK), JUN N-terminal kinase (JNK) and p38), PKC and PI3K (Huang et al, 2000; Yu et al, 2000a; Yu et al, 2000b; Lee et al, 2001). Activation of MAPKs by the phenolic antioxidant, butylated hydroxyanisol and the isothiocyanate, sulforaphane, was seen to support the transcription of ARE regulated cytoprotective genes (Kong et al, 2001). However, the exact mechanism by which Nrf2 is released from Keap1 within the cytoplasm has not yet been fully defined (Figure 1.11) (Manson, 2003).

ROS, often produced as a result of drug metabolism, can cause DNA-damage; however antioxidants through various mechanisms can scavenge ROS to prevent carcinogenesis occurring. Many dietary agents are believed to have antioxidant properties and act to inhibit pro-inflammatory mediators such as cyclooxygenase-2 (COX-2) and lipooxygenase (LOX) through the inhibition of various TFs, including AP-1 and NF-κB (Priyadarsini and Nagini, 2012; Neergheen et al, 2010; Oyagbemi et al, 2009). Reduced expression/inactivation of NF-κB and COX-2 following treatment with curcumin and 3,3-diindolylmethane (DIM) has been observed in pancreatic and liver cancer cell lines amongst others (Ali et al, 2010; Azmi et al, 2008).

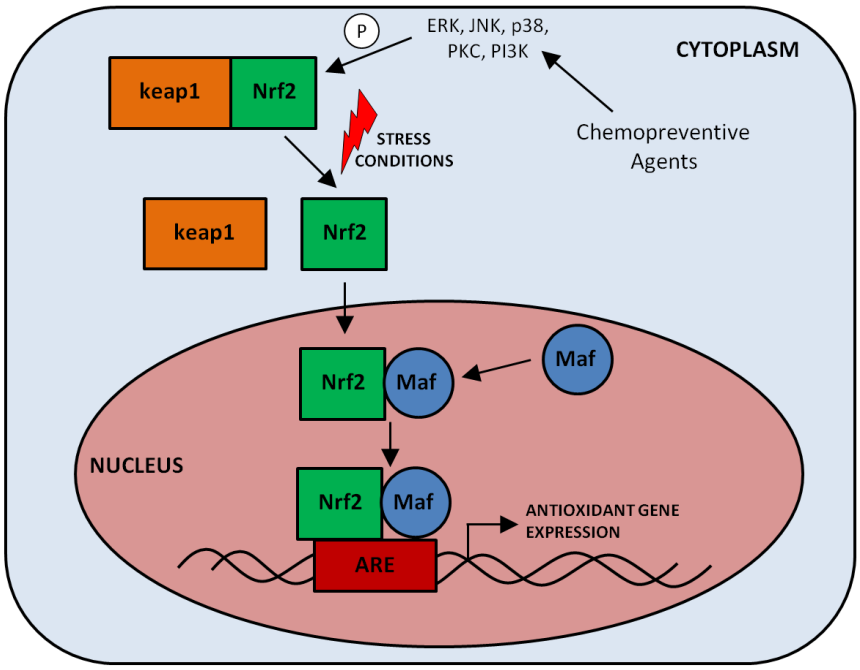

Figure 1.11: Regulation of the Transcription Factor Nrf2. When experiencing stress conditions (e.g. oxidants and electrophiles), Nrf2 is released from its interaction with Keap1 and is translocated to the nucleus to form a heterodimer with Maf proteins. It is believed that chemopreventive agents may act through signalling proteins, including MAPKs, PKC or PI3K which phosphorylate (P) the TF Nrf2 enabling its release from Keap1 and departure from the cytoplasm. The Nrf2:Maf heterodimer then binds the ARE which is 5' flanking of the promoter region for various drug-metabolising and antioxidant genes, for example GST, NAD(P)H:quinine oxidoreductase, oxidoreductase and aldo keto reductases (Landis-Piwowar and Iyer, 2014; Manson, 2003; Hayes and McMahon, 2001). Figure adapted from **(**Landis-Piwowar and Iyer, 2014; Manson, 2003).

It is not always possible to prevent cancer initiating events. However, the progression of cancer as a multistep process is usually slow, and provides the opportunity to decelerate or even arrest disease progression. Imbalanced signalling pathways associated with

proliferative and apoptotic processes often contain molecular alterations which contribute to cancer development and progression. There are numerous proteins that make up these complex signalling networks, of which the MAPKs are a central component. Their improper activation has been associated with uncontrolled proliferation and cancer progression. However, MAPKs, as well as other important cell-signalling kinases which are aberrantly expressed in cancer, such as PI3K, PKC and downstream TFs, NF-κB and AP-1, are known targets of various phytochemicals (Figure 1.12) (Surh, 2003; Kong et al, 2001). These dietary agents have been shown *in vitro* to suppress numerous signalling proteins highlighting their potential use in inducing cell cycle arrest and apoptosis (Surh, 2003; Manson, 2003; Sarkar et al, 2009).

Phytochemicals believed to modulate both NF-κB and AP-1 mediated gene expression include resveratrol, genistein, EGCG, lycopene and curcumin. Curcumin-mediated prevention of NF-κB translocation and activation was observed as a result of IKK inhibition and prevention of IκB degradation (Plummer et al, 1999; Han et al, 2002). The inhibition of the upstream PI3K/AKT signalling pathway was also observed following curcumin treatment (Qiao et al, 2013)**.** Resveratrol, present in red grapes, also prevents NF-κB activation and translocation into the nucleus through the inhibition of MAPKK and JNK signalling (Manna et al, 2000). Both curcumin and [6]-gingerol are able to inhibit COX-2 expression which is dependent on NF-κB (Plummer et al, 1999; Kim et al, 2005). [6]-Gingerol is seen to suppress the (P) and degradation of IκB through the inhibition of p38 MAPK and PKC signalling, preventing DNA binding and nuclear translocation of NF-κB (Kim et al, 2005;Lee et al, 2009). The abrogation of AKT kinase activity by soy derived genistein was seen to not only inhibit NF-κB activation, but also induce apoptosis (Li and Sarkar, 2002). EGCG found in green tea acts to reduce H_2O_2 mediated (P) of ERK1/2, p38 and JNK signalling through the inhibition of UVB, thus preventing the activation of downstream TFs such as NF-κB and AP-1 (Katiyar et al, 2001). Lycopene from tomatoes was found to inhibit the DNA binding abilities of the TFs NF-κB and specificity protein 1 (Sp1) and as a result inhibit the expression of the matrix metalloproteinase 9 (MMP-9) (Huang et al, 2007).

Although the identification of targets is incomplete many molecular alterations have been discovered which appear to be strongly regulated in phytochemical mediated cancer treatment (Surh, 2003). There is, however, uncertainty as to exactly how the

actions of these phytochemicals will affect a wide variety of cancer sub-types, and also how they elicit multi-targeted effects on numerous molecular targets specifically in tumour cells (Moiseeva and Manson, 2009; Link et al, 2010).

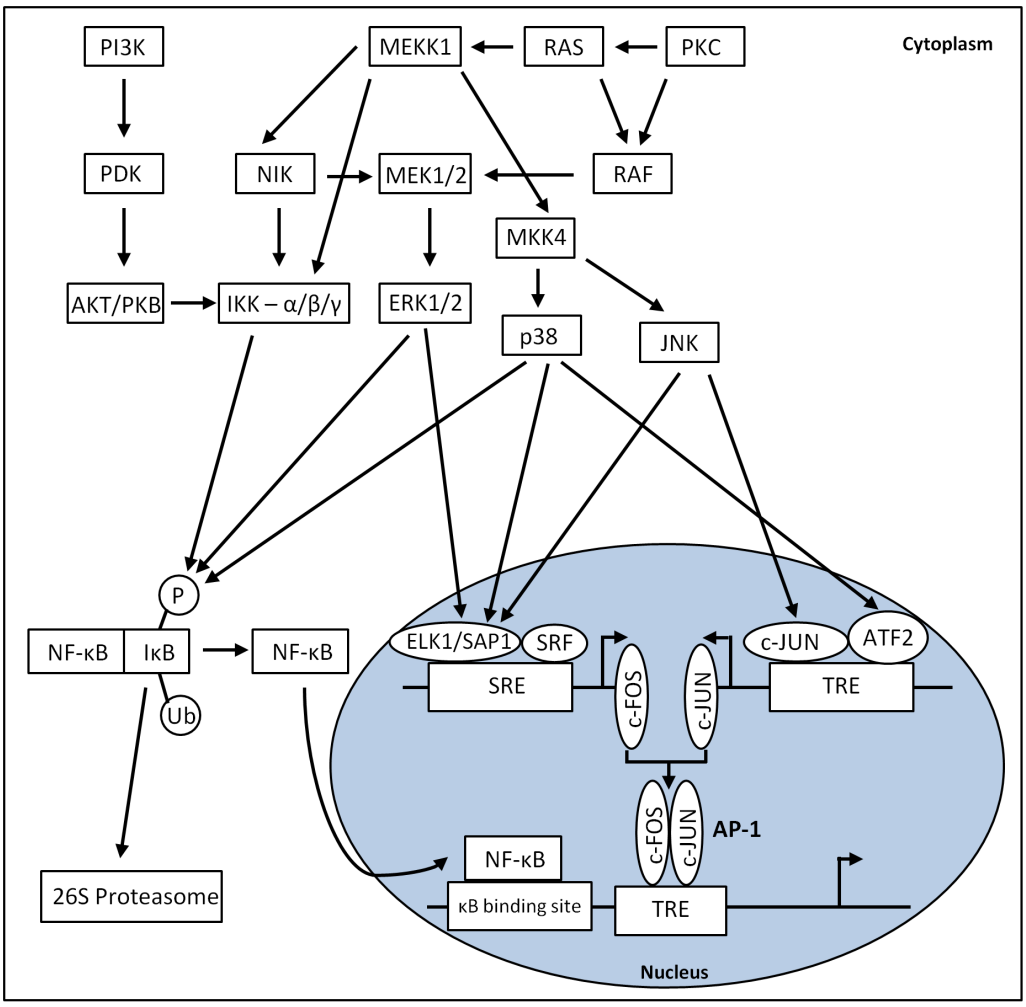

Figure 1.12: NF-κB and AP-1 Signalling via Protein Kinases. The MAPK family of proline-directed serine/threonine kinases is known to regulate gene expression through both NF-κB and AP-1. MAPK kinase kinase-1 (MEKK1), MAPK/ERK kinase (MEK1/2) and p38 pathways are believed to regulate NF-κB-inducing kinase (NIK) activity. NIK is involved in the translocation of NF-κB to the nucleus through its ability to activate the IκB kinase (IKK) signalsome. Signalling pathways which help modulate NF-κB activity converge on the multiprotein IKK signalsome complex. Whilst inactive NF-κB is bound to the inhibitory protein IκB within the cytoplasm, the IKK signalsome (P) and ubiquitylates (Ub) IκB, allowing for its 26S proteasome mediated degradation. Once NF-κB is released it translocates to the nucleus where it binds gene promoters enabling expression. PI3K activation of AKT/PKB via the (P) of 3-phosphoinositide-dependent protein kinase-1(PDK1) has also been associated with NF-κB activation. The three parallel MAPKs (ERK, JNK and p38) are all capable of regulating AP-1, a heterogeneous dimer consisting of members of the c-JUN, c-FOS and activating TF (ATF) families. Activation of PKC via external stimuli (e.g. UV radiation) enables ERK signalling via stimulation of the RAS pathway (through RAF and MEK1/2) and MEKK1 via MKK4 enables p38 and JNK activation. ERK1/2, JNK and p38 (P) ELK1, c-JUN and ELK1/ATF2 respectively leading to AP-1 activation and transcriptional activation of target genes (Kong et al, 2001; Surh, 2003**)**. Figure adapted from (Surh, 2003).

1.3.5. The Modulation of miRNAs by Phytochemicals

Even though it is understood that numerous mutations are responsible for driving tumourigenesis, existing cancer therapies tend to target a single molecule resulting in unsuccessful treatment (Li et al, 2010; Parasramka et al, 2012). Due to their ability to control multiple targets, miRNAs have a high regulatory potential and are important in many biological processes. As a result when miRNAs are altered in cancer they are believed to have a significant role in promoting disease progression (Karius et al, 2012). Their supposed involvement in cancer progression, formation of CSCs and acquisition of EMT phenotype, also makes them a reasonable target for the control and treatment of cancer (Dykxhoorn, 2010).

Studies have shown that through manipulating miRNA expression it is possible to inhibit proliferation and suppress metastasis, as well as induce drug sensitivity. Numerous phytochemicals have been characterised with the capacity to target multiple signalling molecules involved in various pathways acting within cancer cells. Such natural agents could modulate gene expression through the regulation of miRNAs indicating a potentially novel therapeutic approach (Table 1.8). The effects of dietary agents on miRNA expression could increase sensitivity of cancer cells to existing chemotherapeutics and inhibit cancer progression, resulting in improved patient outcome (Dykxhoorn, 2010; Li et al, 2010; Karius et al, 2012; Parasramka et al, 2012).

There are limits to the efficacy of these dietary agents as cancer therapeutics due to their poor water solubility, bioavailability and pharmacokinetic profiles. As a result of this many synthetic analogues or encapsulated phytochemicals have been produced and of the ~175 FDA approved drugs developed since the 1940's approximately 48.6% are either natural agents or directly derived there from (Li et al, 2010; Newman and Cragg, 2012).

Table 1.8: Selected Phytochemicals and miRNAs They Modify.

Agent (source)	Micro RNA altered expression/activity
Curcumin (turmeric)	Upregulated: miR-21; -22 ; -24; -27a; -34a; 181a; 181b; Downregulated: miR-7; -15b; -21; -98; -195; -196a; -199a; -374; -510; -186
Resveratrol (red grapes, wine)	Downregulated: miR146a; miR155
EGCG (green tea)	Upregulated: Let7; miR-16; -18b; -20a; -25; -92; -93; -221; -320; Downregulated: miR-10a; -18a; -19a; -26b; -29b; -34b; -98; -129; -181d;
I3C (cruciferous vegetables)	Upregulated: Let-7b; -c; -d; -e; miR122; -149; -200b; -200c; -638; -663; Downregulated: miR-20b; -21,- 31, -34c; -130a, -146b, -377; -654;
DIM (cruciferous vegetables)	Upregulated: Let-7b; -c; -d; -e; miR122; -149; -200b; -200c; -638; -663; Downregulated: miR-20b; -21,- 31, -34c; -130a, -146b, -377; -654;

Data obtained from a variety of publications, chiefly (Li et al, 2010). Table produced by Prof. M .Manson. UOL

Alterations in miRNA expression to more normal levels have been observed following curcumin, isoflavone and 3,3' DIM treatment in pancreatic cancer cell lines, (e.g. increased miR-200, decreased miR-21), reversal of the EMT phenotype with inhibition and, in some cases reversal of metastatic capability (Ali et al, 2010; Li et al, 2010). Alterations of miRNA profiles could therefore lead to inhibition of further cancer progression and potentially reverse various phenotypes typical of aggressive cancers e.g. EMT. Also, deregulated expression of miRNAs in cancer cells compared to non-cancerous cells could be used in order to characterise specific cancer phenotypes (Link et al, 2010).

1.4. Curcumin as a Therapeutic Agent

The polyphenol curcumin is an active component of the dietary spice (Figure 1.13) and is one of the most widely investigated chemopreventive agents (Hatcher et al, 2008). Turmeric powder which is yellow in colour is obtained from the dried, ground rhizome of *Curcuma longa* and has been used as a colorant in cookery and medicinally throughout Asia for many centuries (Ammon and Wahl, 1991; Sharma et al, 2005). Turmeric has been most commonly used in Asian medicine for the treatment of skin, pulmonary and gastrointestinal conditions, including ailments such as psoriasis, burns, arthritis, allergies, coughs, colic, diabetes and digestive disorders. Research within the

last few decades has gone on to show how many of the actions associated with turmeric are most likely due to the effects of curcumin (Hatcher et al, 2008; Aggarwal et al, 2007; Tilak et al, 2004). This dietary agent is understood to possess putative anti-inflammatory, antioxidant and anti-tumorigenic abilities which could go some way in explaining its apparent medical efficacy (Hatcher et al, 2008).

Figure 1.13: Turmeric from *Curcuma longa*. *Curcuma longa* is a perennial plant belonging to the monocotyledonous family Zingiberaceae which contains rhizomes which are dried and ground to obtain the spice turmeric (Brouk, 1975). Image produced by Prof. M. Manson, UOL.

The earliest record of turmeric is from Assyria in around 600B.C. However, it was not until 1815 that curcumin itself was first isolated from this spice (Brouk, 1975; Roughley and Whiting, 1973). Following its crystallisation in the early 1900's, the chemical structure of curcumin was established by Roughley and Whiting in 1973 (Roughley and Whiting, 1973; Padhye et al, 2010). Turmeric contains over 300 different components in addition to curcumin, including phenolics and terpenoids, with curcumin only accounting for an estimated 2-5% of turmeric's composition (Shishodia et al, 2007; Gupta et al, 2013a). In its chemically pure form curcumin is known as diferuloylmethane (1,7-bis (4-hydroxy-3-methoxyphenol)-heptadiene-3,5-dione) which consists of two ferulic acid residues connected by a methylene bridge (Figure 1.14) (Gupta et al, 2013a).

Curcumin is made up of two isomers which exist together in equilibrium; its bis-α,β-unsaturated β-diketone (bis-keto) form predominates under acidic and neutral pH and the enolate form dominates in >pH8 (Figure 1.14) (Sharma et al, 2005; Padhye et al, 2010). There are three main components (curcuminoids) in commercially available curcumin; diferuloylmethane (77%) demethoxycurcumin (18%) and bisdemethoxycurcumin (5%). (Aggarwal and Shishodia, 2007; Padhye et al, 2010). Following the breakdown of curcumin trans-6-(4′-hydroxy-3′-methoxyphenyl) 2,4-dioxo-5-hexenal was shown to be the major metabolic product, with vanillin, ferulic acid and feruloylmethane recognised as minor degradation products (Hatcher et al, 2008; Padhye et al, 2010;Wang et al, 1997).

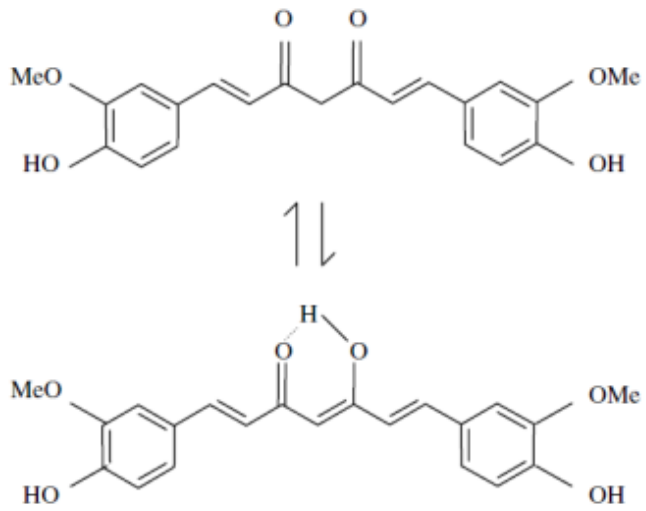

Figure 1.14: Curcumin Tautomerism. The phytochemical curcumin ($C_{21}H_{20}O_6$) has a MW of 368.37 g/mol and is polyphenolic in structure. In neutral and acidic conditions curcumin in its bis-keto form (top) can act as a potent H-atom donor exhibiting antioxidant capabilities. However in its enol-tautomer form (bottom) at a basic pH it acts as an electron donor a characteristic more typical of phenolic antioxidants (Sharma et al, 2005; Padhye et al, 2010; 234 Shureiqi and Baron, 2011). Diagram taken from (Sharma et al, 2005).

Animal and human studies have shown that as a result of oral administration and intestinal metabolism, curcumin can undergo glucuronidation and sulfation. It was also observed that the majority of the oral dose was excreted in the faeces (Ravindranath and Chandrasekhara,V. 1981b; Sharma et al, 2001; Garcea et al, 2005a). The intraperitoneal and intravenous administration of this agent results in its metabolism into mainly tetrahydrocurcumin and hexahydrocurcumin, but also hexahydrocurcuminol. Large quantities of curcumin and its metabolites were found to be excreted in the bile

following systemic administration (Sharma et al, 2005; Aggarwal et al, 2007; Holder et al, 1978; 534 Ravindranath and Chandrasekhara, 1981a).

Due to its hydrophobic nature curcumin displays limited solubility in water. However, it exhibits improved solubility in ethanol, DMSO or acetone (Padhye et al, 2010). Curcumin is also considerably unstable, and at basic pH has been shown to undergo 90% decomposition within 30 minutes, resulting in the production of decomposition products such as trans-6-(4′-hydroxy-3′-methoxyphenyl) 2,4-dioxo-5-hexenal. Stability could be improved with increasingly acidic conditions or in cell culture media containing 10% FCS, where only 20% decomposition within one hour was observed (Sharma et al, 2005; Wang et al, 1997). The limited stability and solubility of curcumin are believed to contribute considerably to this agent's reduced systemic bioavailability, with rapid metabolism and decomposition resulting in the accumulation of both metabolites and decomposition products (Hatcher et al, 2008). As a consequence of these processes, a number of studies into the biological activity of its decomposition products have been conducted with contradictory results (Ireson et al, 2001; Kang et al, 2014; Pal et al, 2014).

In an attempt to address the issues of limited bioavailability, various analogues of curcumin including the fluorocurcumin CDF, and novel methods of drug delivery, such as liposomes and nanoparticles have been investigated (Hatcher et al, 2008; Padhye et al, 2010; Li et al, 2005; Padhye et al, 2009b; Kanwar et al, 2011; Padhye et al, 2009a; Dandawate et al, 2012). Piperine an alkaloid in black pepper, was also administered in combination with curcumin and was shown to increase the serum concentrations of this phytochemical through its inhibition of hepatic and intestinal sulfation and glucuronidation, thus slowing down curcumin metabolism (Padhye et al, 2010; Shoba et al, 1998). It is possible, however, that increasing the bioavailability of curcumin may result in toxicity problems that previously have not been observed.

Curcumin is believed to exhibit its anti-tumorigenic activity through targeting a wide range of signalling pathways (Table1.9) (Padhye et al, 2009b). COX-2, NF-κB and tumour necrosis factor alpha (TNF-α) are just some of the molecules commonly seen to be modulated following exposure to curcumin (Shureiqi and Baron, 2011). This phytochemical has been seen to influence cellular metabolism, proliferation, and

apoptosis as well as regulation of the cell cycle, DNA repair, epigenetic signalling, angiogenesis and metastasis: however, its precise mechanism of action is as yet not fully elucidated (Padhye et al, 2010; Arbiser et al, 1998; Surh and Chun, 2007).

Table 1.9: Molecular Targets Modified by Curcumin.

14-3-3ε; p21; p23; p27; p38; p53; p70S6K; p300; c-abl; AIF; pAkt; AMPKalpha; AP-1; AR; ARNT; ATM; Bad; Bax; Bak; Bcl-2; Bcl-XL; BCRP/ABCG2; Bid; Bim; BTG2; Ca2+ influx; Ca2+-ATPase; E-cadherin; cadherin-11; calreticulin; caspase 3, 4, 7,8, 9, 10, 12; β-catenin; cdc25B; cdc25C; cdk1; cdk2; cdk4; cdk6; CHK1; CHK2; cyclin A/B1/D1/E; cyt c; COX-2; CXCR4; CXCL12; DR4/5; EGFR; EIF2α; ELK1; ENPP2; Erg1; ERK1/2; EZH2; fibronectin; fas; c-fos; GADD153/CHOP; GADD45; Gli1; GRP78; GRP94; GSK3β; HAT; HDAC; Her2; HES1; HIF-1; HLJ1(HSP40 family); HO-1; HSF-1; HSP70; HSP90; IAP1/2; IGF-1R; IκBα; IKK; IL1β; IL6; IL8; iNOS; β4-integrin; Jab-1/CSN assoc kinase; JAK1/2/3; JNK; c-jun; junD; LOX; MAPKAP-K1β; Mcl-1; MDM2; MICA/B; MMP1/2/3/9/13; MT1-MMP; mTOR; MUC5AC; myc; Nag-1(PLAB); NF-κB; NKX3.1; eNOS; Notch 1/3/4; Noxa; NPC1L1; Nrf2; ODC; PARP; PCNA; PERK; PGE; PGE2 synthase; Pgp; phase1/2 enzymes; PHK; PI3K; PIAS-3; PKC; PLCγ; PLK1; PPARδ: PPARγ; Puma; RANKL; pRb; RON; SDF-1alpha; smac; Sp1/3/4; src; STAT1 /3 /5; survivin; SYK; hTERT; TGFβ; TLR2; TNFα; TNFR1; topoisomerase II; Trail R1/2; α/β- tubulin; TxnRd1(thioredoxin reductase-1); uPA; VCAM-1; VEGF; wee1; WT1; XIAP

Molecular targets found to be altered in expression or activity (*in vitro)* following treatment with varying concentrations of curcumin in a number of different cancer cell types. (Data obtained from a variety of publications based on (Howells et al, 2007) Table produced by Prof. M. Manson)

Having demonstrated the therapeutic potential of curcumin through its ability to elicit changes in cancer signalling, both in cultured cells and animal models, numerous clinical trials have been carried out in order to ascertain the efficacy of this agent. To date over 100 clinical trials have been carried out, of which approximately a third are still in progress (Hatcher et al, 2008; Gupta et al, 2013b).

Many of the earlier clinical trials were used to ascertain the safety, toxicity and overall tolerability of elevated doses of curcumin (Gupta et al, 2013b). High risk individuals and patients with pre-malignant lesions were found to tolerate curcumin at a maximum dose of 8000mg/day for 3 months with no treatment related toxicity (Cheng et al, 2001). Various phase I studies in CRC patients found orally administered curcumin was tolerated up to a maximum dose of 2200mg/day and that the consumption of 3600mg/day for up to 4 months did not result in dose-limiting toxicity (Sharma et al, 2001; Sharma et al, 2004). Further assessment in healthy volunteers, where escalating doses of curcumin from 500 to 12,000mg were administered, also showed minimal toxicity and good tolerance to the agent (Lao et al, 2006). These phase I trials confirmed that the administration of curcumin for continuous periods of up to 4 months was

deemed safe and that although the maximum tolerated dose was not reached, the highest dose administered (12,000mg) was well tolerated with few side effects (Hsu and Cheng, 2007).

The tumour cell specific properties of curcumin were highlighted in these Phase 1 trials; with increased attention based upon the lack of curcumin bioavailability, which, following oral administration was relatively low. However, curcumin and its metabolites were detected within patient urine and plasma following the administration of doses between 3600mg and 12,000mg, which demonstrates that absorption of this agent and its metabolism must occur to some extent (Sharma et al, 2001; Sharma et al, 2004; Lao et al, 2006). Consumption of 3600mg daily resulted in the detection of curcumin (11.1-0.6nmol/L) at one hour post dose within the plasma, and detection of the glucuronide (15.8-0.9nmol/L) and sulphate (8.9-0.7nmol/L) metabolites at all time points (0.5, 1, 2, 3, 6 and 8 hours post dose). In addition urinary (1.3-0.1mol/L) and faecal (116-25nmol/g) levels of curcumin were also observed following consumption of 3600mg curcumin, as well as urinary levels of curcumin sulphate (45-19nmol/L) and curcumin glucuronide (510-210nmol/L). Detection of curcumin at later time points was infrequent and for patients consuming lower doses of curcumin detection within the plasma was not possible (Sharma et al, 2004).

A number of phase II trials have also been carried out in order to determine the biological effect of curcumin in various cancers, in particular pancreatic and colorectal. The administration of 8000mg/day of curcumin for 2 months in patients suffering from PC was tolerated without toxicity. Low levels of circulating curcumin were detected with biological activity observed in two patients, one of whom maintained stable disease for over 18 months. Levels of curcumin glucuronide and sulphate metabolites were more easily detected with steady-state levels of 22-41ng/ml observed in plasma by day 3 post dose. Biological activity was evident as detected by the reduced expression of COX-2, NF-κB and phosphorylated signal transducer and activator of transcription 3 (pSTAT3) in patient blood samples (Dhillon et al, 2008).

Studies in patients with CRC treated with either 2000mg or 4000mg/day for 30 days looked at the expression levels of prostaglandin E_2 (PGE_2) and 5-hydroxyeicosatetraenoic acid (5-HETE) pre and post-operatively in a group of smokers.

Patients were also screened for aberrant crypt foci (ACF) number and proliferation determined by Ki-67. No reductions in either proliferation or expression of PGE2 and 5-HETE were observed with either dose of curcumin administered. However the higher dose (4000mg) resulted in a significant reduction (40%) in ACF number (Carroll et al, 2011). Mean post-intervention levels of curcumin (3.8-1.3ng/mL) and its conjugates (78.5-84.3ng/mL) were observed in the plasma of patients in the 4000mg cohort. The anti-tumorigenic effects of curcumin against cancer as observed in these studies appear promising and with further trials being conducted, the biological activity and mechanism of action for curcumin when targeting human disease could be further elucidated.

Various *in vitro* studies have previously shown that in combination with other phytochemicals or in addition to chemotherapeutic agents curcumin can act in synergy to inhibit tumourigenesis and potentiate the effects of current therapeutic agents (Ali et al, 2010; Padhye et al, 2009b; Verma et al, 1997; Hour et al, 2002; Kunnumakkara et al, 2007). A number of clinical trials, some of which are still ongoing, have looked at the use of curcumin in combination with chemotherapeutic agents. Two studies both using a maximum dose of 8000mg/day were carried out to determine safety, toxicity and tolerability in PC patients treated in combination with gemcitabine, with the oral administration of these agents together determined to be safe and well tolerated (Kanai et al, 2011). However, Epelbaum et al. found that this dose resulted in side effects, including abdominal fullness and pain, with patients unable to complete the study, leading to a reduction in the curcumin dose administered (Epelbaum et al, 2010). Ongoing clinical trials, including those using curcumin in combination with FOLFOX (CUFOX) to treat inoperable CRC (University of Leicester) and in combination with gemcitabine and celebrex to treat PC patients with advanced or inoperable disease (Tel-Aviv Sourasky Medical Center) will hopefully provide more conclusive safety and tolerability information, in addition to further understanding the efficacy of combination treatments in these cancers (University of Leicester, 2014; Tel-Aviv Sourasky Medical Center, 2007).

1.4.2. The Effects of Curcumin on miRNA Expression in Cancer

It is known that curcumin possesses anti-tumorigenic properties and has been shown to have *in vitro* and *in vivo* inhibitory effects on cancer. With this in mind, there is a

growing interest in the regulation of miRNA expression by curcumin as the capacity of this agent to regulate a diverse range of molecular targets in various cancers may be in part through the control of these non-coding RNAs (Li et al, 2010; Karius et al, 2012; Gupta et al, 2013a).

Over the last few years modulation of various miRNAs in a variety of cancer types has been observed *in vitro* following curcumin treatment. A miRNA profile analysis of PC cells identified a number of miRNAs believed to be regulated by curcumin, including the upregulation of miR-22 and downregulation of miR-199a* (Sun et al, 2008). An array profile of A549/DDP multidrug-resistant lung adenocarcinoma cells found that curcumin altered the expression of various miRNAs, in particular downregulating the expression of miR-186*, a miRNA believed to inhibit apoptosis (Zhang et al, 2010). Treatment of the breast adenocarcinoma cell line MCF-7 resulted in the upregulation of miR-15a and miR-16 and downregulation of the anti-apoptotic BCL2 which is involved in oncogenesis (Yang et al, 2010).

The accumulation of numerous mutations over time is necessary for the progression of tumourigenesis, but many current cancer therapies only target a single aberrant molecule and as a result are often inefficient (Parasramka et al, 2012). The global deregulation in miRNA expression within cancer is understood to aid in promoting the progression of this disease, and as a result makes miRNAs a reasonable therapeutic target (Karius et al, 2012). By further investigating the capacity of curcumin to modulate miRNA expression its potential as a therapeutic agent may be better understood.

1.5. Aims and Objectives

Research into cancer regulation through the modulation of dysregulated miRNAs has taken off over the last few years with miRNA profile analysis highlighting altered expression when comparing normal and diseased states. The phytochemical curcumin has been implicated in both the modulation of miRNA expression and regulation of signalling in cancer. Some recent studies imply that the effects of curcumin on cancer signalling could be through the modulation of these dysregulated miRNAs. Curcumin is also under consideration as a potential therapeutic agent for PC, for which current disease markers lack both sensitivity and specificity. Therefore the identification of

miRNAs dysregulated in PC could provide an alternative method for disease diagnosis and ascertaining the capacity of curcumin to modulate these miRNAs could explain to some extent how this phytochemical is able to affect multiple signalling pathways in cancer.

Project Aims:

1. To discover novel miRNA targets for modulation by curcumin and to ascertain if any aberrantly expressed miRNAs in PC can be positively regulated by curcumin in cancer cell lines.
2. To examine the mechanism/s by which curcumin may modulate the expression of key miRNAs in tumour cells when compared to non-transformed cells.
3. To assess miRNA expression levels across PC cell lines to establish a panel of miRNAs which could be used as prognostic markers.

Project Objectives:

A key objective of this project is to establish a curcumin treatment which would most effectively modulate changes in relevant miRNAs and proteins, either independently or in combination with other treatments.

1. The effects of varying curcumin treatments on cell viability, apoptosis and the cell cycle will be used to validate efficacy.
2. Various miRNA and protein targets relevant to PC and reported to be modulated by curcumin, either from the literature or previous experiments will be evaluated using qPCR following treatment.

Another key objective will be to identify novel miRNAs modulated by curcumin in PC cells.

1. miRNA microarrays will be carried out using various PC cells lines following treatment with curcumin.
2. Potential miRNA targets found to be modulated will undergo validation via qPCR.

A further objective will be to ascertain if any miRNAs which may be aberrantly expressed in PC could have any diagnostic potential.

1. miRNA expression will be compared between untreated PC cell lines following miRNA microarray analysis.

Chapter 2. Materials and Methods:

2.1. Materials

2.1.1. General Chemicals and Reagents

All chemicals and reagents used were purchased from Sigma (Poole, UK) unless stated otherwise. ProtoGel, (30% Solution at 37.5:1 Ratio), 10X Running Buffer (TRIS/Glycine/SDS) (Cat#B9-0032) used for Sodium Dodecyl Sulphate Polyacrylamide gels (SDS-PAGE) and 10X Transfer Buffer (TRIS/Glycine)(Cat#B9-0056) used for western blotting were purchased from Geneflow (Fradley, UK). Enhanced Chemiluminescence (ECL™) Western Blotting Detection reagents (Cat#RPN2109) were purchased from GE Healthcare (Buckinghamshire) and Pierce Bicinchoninic acid (BCA) protein assay kit (Cat#23225) was purchased from Thermo Scientific. Prestained pageruler protein ladder (SM0671) (10-170 kilo Daltons (kDa)) was purchased from Fermentas (York, UK) and Acid Phenol-chloroform 125:24:1 (v/v) pH 4.3-4.7 (Cat#9720) was purchased from Ambion. TRI Reagent® (Cat # T8424) used for RNA extraction was purchased from Sigma. Agilent RNA 6000 Nano Reagents Part 1 and RNA Nanochips (Cat#5067-1511) used in the quantification of total RNA were obtained from Agilent Technologies. FirstChoice® Human Pancreas Total RNA (Cat#AM7954) used as a control in real-time reverse transcription quantitative polymerase chain reaction (RT-qPCR) validation was purchased from Ambion by Life Technologies. The RQ1 RNase-Free DNase (Cat #M6101) and GoScript™ Reverse Transcription System (Cat#A5000) were purchased from Promega. The qScript™ cDNA Supermix (Cat#95048) and SensiMix™ SYBR Hi-ROX kit (Cat#QT605) were purchased from Quanta Bioscience and Bioline respectively. MiScript SYBR® Green polymerase chain reaction (PCR) Kit (Cat#218073), miScript II RT Kit (Cat#218161) and miScript primer assays for Hs_RNU6-2_1 (Cat#MS00033740) for use in RT-qPCR were purchased from QIAGEN (Crawley, UK). TaqMan® MicroRNA Reverse Transcription Kit (Cat#4366597), TaqMan® Fast Universal PCR Master Mix (2X), No AmpErase® UNG (Cat#4352042) and MicroAmp® Optical 96-Well Reaction Plate (Cat#N8010560) were purchased from Applied Biosystems. 3DNA FlashTag RNA Labelling Kits for microRNA Arrays; Oyster®-550 (KR8850) and Oyster®-650 (KR8860) were purchased from Genisphere. MicroRNA microarray slides using miRBase release v.16.0 for use with Genisphere labelling reagents were provided by Dr Tim Gant (MRC, Leicester). SurePrint G3 Human v16 microRNA Array Kit, 8x60K (Release 16.0)(Cat#G4870A), microRNA Complete Labelling and Hyb Kit (p/n 5190-

0456), microRNA Spike-In kit (p/n 5190-1934), Microarray Hybridization Chamber kit (G2534A) and Gene Expression Wash Buffer Kit (p/n 5188-5327) were all purchased from Agilent Technologies. Micro Bio-Spin 6 chromatography columns (Cat#732-6222) were purchased from Bio-Rad. ATPlite™ Luminescence Assay System for cell viability analysis was purchased from Perkin Elmer. Annexin V-FITC Apoptosis Detection Kit used for analysis of cell death was purchased from Affymetrix eBioscience. ISOTON® II Diluent (Cat#8448011) purchased from Beckman Coulter was used for counting of cell number.

2.1.2. Buffers and Solutions

Table 2.1: Buffers and Solutions.

Buffer/Solution	Reagents
Antibody Lysis (ABL) Buffer	Tris pH7.5 (10mM), NaCl (50mM), NP40 (0.5%), Sodium Deoxycholate (0.5%), SDS (0.5%), Iodoacetamide (10mM). Stored at 4°C, covered in foil.
1x Lysis Buffer	Tris pH7.5 (20mM), NaCl (150mM), EDTA (1mM), Triton x-100 (1%), Sodium Pyrophosphate (2.5mM), Sodium Orthovanadate (1mM). Stored at 4°C, for up to 6 months.
4x SDS-PAGE Sample Buffer	Tris-HCl pH6.8 (0.25M), Glycerol (40%), SDS (8%), Bromophenol Blue (0.02%), DTT (0.2M).
10x Phosphate Buffer Saline (PBS)	50 PBS Tablets, 1000ml dH_2O.
10x Phosphate Buffer Saline Tween-20 (PBST)	50 PBS Tablets, 990ml dH_2O, 10ml Tween-20.
SDS-PAGE Running Buffer	Tris (25mM), Glycine (192mM), SDS (0.1%).
Western Transfer Buffer	Tris (25mM), Glycine (192mM), Methanol (20%).
Stripping Buffer	Glycine (0.2M), dissolve in water pH2.5 (HCl). SDS (0.4%).
Blocking Buffer (BB)	1x PBST, Milk (5%).
1xTris-EDTA(TE) Buffer	Tris (10mM), EDTA (1mM), pH7.5.
20x Saline-Sodium Citrate (SSC)	NaCl (3M), Sodium Citrate (300mM).

2.1.3. Antibodies

Table 2.2: Antibodies for Western Blotting.

Antibody	Supplier	Host	Dilution	Conditions	Expected MW band	Observed MW band
Anti-Actin I-19: SC-1616	Santa Cruz Biotechnology inc.	Rabbit (polyclonal)	1:4000	in BB O/N at 4°C	43kDa	43kDa
Anti-c-Myc clone 9E10 (Cat# M5546)	SIGMA	Mouse (monoclonal)	1:1000	in BB/LBB O/N at 4°C	62kDa	36kDa (main band) ~62kDa
PRAK=MAPKAPK5 (13H5) (LF-MA0195)	AbFRONTIER	Mouse (monoclonal)	1:2000	in BB O/N at 4°C	52kDa	52kDa
Anti-Dicer antibody [13D6]	AbCAM	Mouse (monoclonal)	1:2000	in BB O/N at 4°C	225kDa	225kDa
Anti-Drosha (D28B1) (#3364)	Cell Signaling Technology	Rabbit (monoclonal)	1:1000	in BB O/N at 4°C	160kDa	160kDa
Anti- Rabbit Horse-radish peroxidise (HRP) conjugated (A8275)	SIGMA	anti-rabbit (Goat)	1:2000	in BB 1hr RT	-	-
Anti-Mouse Horse-radish peroxidise (HRP) conjugated (A8924)	SIGMA	anti-mouse (Goat)	1:2000	in BB 1hr RT	-	-

Key: Overnight (O/N), hour (hr), Molecular Weight (MW), Blocking Buffer (BB) Room Temperature (RT).

2.1.4. Cell Culture

Roswell Park Memorial Institute medium (RPMI-1640)(Cat#R8758), Dulbecco's Modified Eagle Medium (DMEM)(Cat#D6429) and 10x trypsin/EDTA (5g/2g)(Cat#T4174) were purchased from SIGMA (Poole, UK), with Fetal Calf Serum (FCS)(Cat#A15-104) purchased from PAA: The Cell Culture Company.

2.1.5. Primers

Primers for use with the SensiMix™ SYBR Hi-ROX kit and miScript SYBR® Green PCR Kit (Biomers.net, Germany) (Table 2.3 and 2.4) were made up to a stock concentration of 5μM using 0.1x TE buffer. TaqMan® MicroRNA Assays were purchased from Life Technologies™ (Cat#4427975) (Table 2.5).

Table 2.3: Gene Primers for use with SensiMix™ SYBR Hi-ROX Kit.

Primer Name	Sequence (5´-3´)
DICER3 F	ACTGACAGAAGTGGGCTTTA
DICER3 R	GTCCCAGAACTACCAATACG
DROSHA3 F	CCTGACCAATATTCCACTGT
DROSHA3 R	GCTGTCTTCAAACAAAGGAC
EZH2 F	ACATAGATGGACCAAATGCT
EZH2 R	GTCCACAAGGTTTGTTGTCT
NOTCH2 F	GGAAGGCAGGTCTCCTGTGTC
NOTCH2 R	TGCTATTGGCCATGGCACA
NOTCH3 F	GGCAAGACTGGCCTCCTGTG
NOTCH3 R	GGTTGGCGCCGATAGAGC
RN18S F	AAACTGCGAATGGCTCATTA
RN18S R	GAATTACCACAGTTATCCAAGTAGG
RREB1 F	ATGCACATTCGCCAGCACA
RREB1 R	GTCCTTCTCATGGATCTTCATATGTC
MYC F	CACCGAGTCGTAGTCGAGGT
MYC R	TTTCGGGTAGTGGAAAACCA

Table 2.4: miRNA Primers for use with MiScript SYBR® Green PCR Kit.

Primer Name	Sequence (5´-3´)
miR-10b F	ATCCTGTAGAACCGAATTTGTG
miR-143 F	TGAGATGAAGCACTGTAGCTC
miR-145 F	CCAGTTTTCCCAGGAATC
miR-148a F	TCTCAGTGCACTACAGAACTTTGT
miR-155 F	TAATGCTAATCGTGATAGGGGTA
miR-196a F	GCTAGGTAGTTTCATGTTGTTGG
miR-200b F	CTTAATACTGCCTGGTAATGATGA
miR-200c F	TAATACTGCCGGGTAATGATG
miR-206 F	AGGAATGTAAGGAAGTGTGTGG
miR-21 F	GCTAGCTTATCAGACTGATGTTGA
miR-34a F	GGCAGTGTCTTAGCTGGTTG
miR-34b F	CAATCACTAACTCCACTGCCA
miR-375 F	TTGTTCGTTCGGCTCG
miR-503 F	TAGCAGCGGGAACAGTTCT
miR-518da-3p F	SAAAGCGCTTCCCTTTG
miR-518f-5p F	CCTCTAGAGGGAAGCACTTTCT

Table 2.5: TaqMan® miRNA Assays.

Primer Name	miRBase Accession	Target Sequence	Assay ID
miR-21	MIMAT0000076	UAGCUUAUCAGACUGAUGUUGA	000397
miR-145	MIMAT0000437	GUCCAGUUUUCCCAGGAAUCCCU	002278
miR-370	MIMAT0000722	GCCUGCUGGGGUGGAACCUGGU	002275
miR-380	MIMAT0000735	UAUGUAAUAUGGUCCACAUCUU	000569
miR-223	MIMAT0000280	UGUCAGUUUGUCAAAUACCCCA	002295
miR-132	MIMAT0000426	UAACAGUCUACAGCCAUGGUCG	000457
miR-128	MIMAT0001824	UCACAGUGAACCGGUCUCUUUU	000453
miR-34b-5p	MIMAT0000685	UAGGCAGUGUCAUUAGCUGAUUG	000427
miR-19a-3p	MIMAT0000073	UGUGCAAAUCUAUGCAAAACUGA	000395
miR-29b-3p	MIMAT0000100	UAGCACCAUUUGAAAUCAGUGUU	000413
miR-30c-5p	MIMAT0000244	UGUAAACAUCCUACACUCUCAGC	000419
miR-30b-5p	MIMAT0000420	UGUAAACAUCCUACACUCAGCU	000602
RNU6B	NR_002752	CGCAAGGAUGACACGCAAAUUCGUGAAGCGUU CCAUAUUUUU	001093

2.2. Methods:

2.2.1. Routine Maintenance and Treatment of Cells

2.2.1.1. Cell Culture: Routine Maintenance.

Three epithelial PC cell lines were used for this study (MIA PaCa-2, AsPC-1 and BxPC-3) along with HCT116 a (p53 +/+ wt) colorectal carcinoma cell line and HeLa a cervical carcinoma cell line. A table containing the mutational status for the PC cell lines can be found in Appendix 1. All cell lines were purchased from the American Type Culture Collection (ATCC, USA). AsPC-1 and BxPC-3 cell lines were cultured and treated in RPMI-1640 supplemented with 10% FCS. MIA PaCa-2, HCT116 and HeLa cell lines were cultured and treated in DMEM also supplemented with 10% FCS. To enable cell growth all cultured cell lines were incubated at 37ºC under humidified 95% air 5% CO_2. Once cells achieved a confluency of 70-90% they were passaged. The cell monolayer was initially washed twice using ~5ml 1xPBS. Once removed the cell monolayer underwent trypsinisation using 5ml trypsin/EDTA at 37ºC. Cell lines HCT116, HeLa and MIAPaCa-2 were incubated for approximately 5 minutes and BxPC-3 and AsPC-1 were incubated for around 15 minutes. Appropriate medium (5ml) was added to inactivate trypsinisation. Centrifugation for 5 minutes at 600g was used to form a cell pellet, which was resuspended at the appropriate dilution in culture medium. Cells were used up to passage 35-40 for experiments.

2.2.1.2. Cell Storage.

Cells were grown as a monolayer in a flask to a confluency of approximately 50-70%. They were then trypsinised (section 2.2.1.1) after which they were collected by centrifugation at 600g. The cell pellet was resuspended in 1ml of freezing medium (10% dimethyl sulfoxide (DMSO), 90% FCS), and transferred to a freezing vial. Cells were placed into a NALGENE™ Cryo 1°C freezing container (Thermo Fisher) and stored at -80°C overnight to achieve a -1°C/minute rate of cooling. Cells were then transferred to a liquid nitrogen storage container.

2.2.1.3. Plating Out Cells

Following trypsinisation a single cell suspension was produced, these cells were then counted using a haemocytometer. Cells were then plated out at the required density and incubated at 37ºC under humidified 95% air 5% CO_2 overnight to allow cells to adhere before they were treated.

2.2.1.4. Cell Treatment

The phytochemical curcumin was prepared by dissolving in DMSO to produce a stock concentration of 100μM. Further stock concentrations of 5, 10, 15, 25 and 50μM were produced using the initial 100μM curcumin stock and DMSO. Black opaque eppendorfs were used to store the curcumin stock to prevent light mediated degradation (Tonnesen et al, 1986). Cell lines were seeded at the required density and left between 3 hours and overnight at 37ºC under humidified 95% air 5% CO_2 for cells to attach. Following attachment culture medium was completely aspirated and replaced with fresh medium containing the final concentration of curcumin (1-20μM), DMSO (0.1%) or no treatment (NT) control. Plates were incubated at 37°C for the required time. Cells were treated with fresh curcumin-containing medium every 72 hours when treatment time exceeded this.

2.2.2. Annexin V/Propidium Iodide Staining for Apoptosis

Annexin V is a phospholipid binding protein and can be used to identify early stages of apoptosis by binding to exposed phosphotidylserine (PS) a component of the phospholipid bilayer. In healthy cells, Annexin V is unable to interact with PS due to its position along the cytosolic side of the plasma membrane. When a cell undergoes apoptosis the asymmetric distribution of PS within the phospholipid bilayer is lost, this enables PS to move from the inner to the outer leaflet of the membrane bilayer where it can be detected by FITC conjugated Annexin V. This change in PS distribution occurs in the early stages of apoptosis. It is not until late-stage apoptosis when membrane integrity is lost that the viability dye propidium iodide (Pi) is taken up into the nucleus of necrotic cells. Live cells do not have the capacity to bind Annexin V or take up Pi. Flow cytometry is used to detect both fluorescently conjugated Annexin V and Pi, allowing the ability to distinguish between live, apoptotic and necrotic cells.

Annexin V/Pi staining for apoptosis was carried out using 1, 2.5 and 5μM curcumin and DMSO (control) for 72, 120, 168 and 240 hours. Cells were seeded onto 6 well plates at between $1.9x10^3$ and $1.25x10^5$cells/well depending on the duration of the treatment. Cells were left for approximately 3 hours to adhere before they were treated. The medium containing floating cells from each well was retained and combined with the associated adherent cells following trypsinisation. The cells were pelleted at 350g for 5 minutes and resuspended in 4ml of fresh medium (containing 10% FCS) followed by

incubation at 37ºC for 30 minutes. Following this the cells were pelleted again and the pellet was resuspended in 1ml Annexin Binding Buffer. The cell suspension was combined with Annexin V FITC conjugate (4µl) and vortexed followed by incubation at room temperature (RT) for 10 minutes. Pi was then added to a final concentration of 1.5µg/ml, the sample was vortexed and incubated at RT for 1 minute. Samples were kept on ice and analysed on the FACscan (Becton Dickinson), using the Cell Quest software. Annexin V FITC conjugate and Pi are both light sensitive, so samples were kept in the dark when possible.

2.2.3. ATPlite™ Luminescence Assay System for Cell Viability

ATP is found in cells which are metabolically active and levels become drastically reduced in samples which undergo apoptosis or necrosis, for example in response to drug exposure. The system works by producing light as a result of ATP's reaction with $_D$-Luciferin and Luciferase, which is illustrated in the schematic below (PerkinElmer, 2013).

$$\mathbf{ATP + {}_{D}\text{-}Luciferin + O_2} \xrightarrow[\mathbf{Mg^{2+}}]{\mathbf{LUCIFERASE}} \mathbf{Oxyluciferin + AMP + PP_i + CO_2 + Light}$$

The amount of light emitted is relative to the concentration of ATP available, therefore the more ATP present the greater the light intensity. The decline in light emitted following curcumin treatment when compared to control treated cells represents percent reduction in cell viability.

ATPlite experiments were carried out using 1, 2.5 and 5µM curcumin and DMSO (control) for 24, 48, 72 and 120 hours. Cells were seeded onto a 96 well plate at between $7.82x10^2$ and $1.5x10^4$cells/well (in a volume of 50µl) depending on the duration of the treatment, and left for approximately 3 hours to adhere before cells were treated. A 2x concentration of curcumin was added to 50µl of appropriate medium, this was then added to the 50µl of cells/well to obtain a final 1x concentration of curcumin in a final volume of 100µl. Once treatment was complete analysis of cell viability was carried out as per the manufacturer's protocol (Perkin Elmer Cat# 6016943). Luminescence was measured in relative light units using a FLUOstar OPTIMA plate reader (BMG Labtech).

2.2.4. Growth Curves

Cells were seeded into a 24 well plate at $2.5x10^3$cells/well. Each well contained 1ml of appropriate medium and was left overnight at 37ºC for cells to adhere. Experiments were carried out using 1, 2.5 and 5μM curcumin and DMSO (control) treatment with three replicates of each treatment per day for up to 10 days. Cells were trypsinised and appropriate medium added to a final volume of 1ml to inactivate trypsinisation. The cell suspension was then combined with 9ml of ISOTON® II Diluent (Beckman Coulter) giving each sample a dilution factor of 10. The diluted cell suspension was then passed through a Z2 Coulter Particle Count and Size Analyzer (Beckman Coulter) to determine cell number for each sample.

2.2.5. Gel Electrophoresis and Western Blotting

2.2.5.1. Lysate/Sample Preparation for SDS Gel Electrophoresis

2.2.5.1.1. Preparation of Whole Cell Lysates

Dose response experiments were carried out for 5, 24, 48 and 96 hours with varying curcumin concentrations (0.5, 1, 1.5, 5 and 10μM) as well as NT and DMSO controls. Time course experiments were carried out using 1, 5 or 10μM curcumin also with NT and DMSO controls at 1, 5, 12, 24 and 48 hour time points. Once treatment was complete the medium was removed and cells were washed twice with 3ml 4°C 1xPBS whilst incubated on ice. This was followed by exposure to 200μl ABL buffer for MK5 and c-MYC protein identification and 200μl 1x Lysis Buffer for all other protein identification. Protease inhibitor cocktail of 100x concentration was added to both buffers prior to use for a 1x final concentration. After 10 minutes of incubation each dish was scraped and cells were harvested. For cells obtained using ABL Buffer, lysates were passed through a 23G needle 20 times. With cells obtained using 1x Lysis Buffer lysates were centrifuged at 16,000g at 4°C for 5 minutes, the supernatant obtained was then transferred to a fresh eppendorf. All lysates were stored at -20°C

2.2.5.1.2. Pierce BCA Assay

Protein concentrations for all samples were measured using a BCA protein assay (Pierce) kit (as per manufacturer's protocol). Absorbance readings were determined using a FLUOstar OPTIMA plate reader (BMG Labtech). A standard curve was produced using bovine serum albumin (0-2000μg/ml), against which samples were

compared in order to determine their protein concentration. All samples were diluted to a concentration of between 0.25-1μg/μl.

2.2.5.2. SDS-PAGE Gel Electrophoresis

Samples were combined with an appropriate volume of 4x SDS-PAGE Sample Buffer to obtain 1x SDS-PAGE Sample Buffer and heated at 100°C for 5 minutes. Samples were briefly centrifuged after which 10-40μg of each sample were loaded onto a polyacrylamide gel along with the prestained pageruler protein ladder (Fermentas). A resolving gel of either 10% or 12% (depending on the molecular weight of the protein of interest) was topped with a 5% stacking gel made up the polyacrylamide gel (Appendix 1). Separation of the proteins within the samples was carried out by electrophoresis at 80-120 Volts for 90-120 minutes using the Bio-Rad gel system in the presence of SDS-PAGE Running Buffer.

2.2.5.3. Protein Transfer and Western Blotting

2.2.5.3.1. Protein Transfer

Following electrophoresis SDS-PAGE gels were placed in combination with blotting paper and a nitrocellulose membrane (Whatman) into a wet transfer cell (BioRad) containing 1x transfer buffer. Protein samples were transferred onto the nitrocellulose membranes via electroblotting for 60 minutes at 100V for small transfer cells and at 0.7Amps for large transfer cells.

2.2.5.3.2. Western Blotting with ECL Detection

Once the transfer was complete, the nitrocellulose membrane was incubated with BB to prevent non-specific binding of the primary antibody, by gently rocking for 1 hour at RT. Then the membrane was incubated with primary antibody in BB overnight at 4°C whilst rocking. The membrane was washed three times (duration 10 minutes) using 1xPBST; then incubated with the secondary antibody for 1 hour at RT whilst rocking. The membrane was washed a further four times (duration 12 minutes) with 1xPBST, and incubated for 60 seconds in ECL Working Solution (Detection Reagent 1 and Detection Reagent 2 in 1:1 ratio) and exposed to x-ray film (GE Healthcare) for the required period of time. The film was then developed in the dark (with a red-safety light) using a Xograph imaging system Compact X4 developer. Analysis of band density was then determined using Quantity One 1-D analysis software (Bio-Rad).

2.2.5.3.3. Stripping a Membrane for Re-probing

Western blots were stripped and re-probed for house-keeping proteins to be used as loading controls. Nitrocellulose membranes containing the transferred proteins were incubated in Stripping Buffer at RT whilst rocking for 20 minutes. The stripped membrane was then washed once (duration 10minutes) with 1x PBST, after which the membrane was blocked and western blotting carried out as outlined in section 2.2.5.3.2.

2.2.6. RNA Production and Quantification

2.2.6.1. TRI reagent® RNA Extraction for miRNA Microarrays

TRI Reagent® was utilised for the isolation of microRNAs for their use in microarrays. AsPC-1, BxPC-3 and MIAPaCa-2 cell lines were treated as indicated in Table 2.6.

Table 2.6: Treatment with Curcumin and Exposure Times.

		Treatment		
		1.5µM	**5µM**	**DMSO**
Treatment Time	**24 hours**		AsPC-1, MIA PaCa-2	AsPC-1, MIA PaCa-2
	96 hours	AsPC-1, BxPC-3, MIA PaCa-2		AsPC-1, BxPC-3, MIA PaCa-2

The TRI Reagent® method for RNA extraction was adapted following its initial use; the original protocol is defined by option **A)** and the modified protocol is defined by option **B)** below.

Homogenisation

Once treated, cells were washed with 1xPBS, which was then aspirated from each plate/well. Treated cells were lysed by the addition of **A)** 1.5ml of TRI Reagent® per 10cm dish or **B)** 1ml of TRI Reagent® per well (6 well plate) (for BxPC-3 cells volume of TRI Reagent® used was increased to 1.5ml) and 4ml when using a 10cm dish; this was followed by incubation for 5 minutes at RT whilst gently tilting the plate/dish. The cell lysate was then passed through a pipette several times and incubated again for 5 minutes at RT.

Phase Separation

The homogenised cells were combined with 0.2ml of chloroform per 1ml of TRI Reagent® used, followed by 10 seconds of mixing using a vortex and finally incubation at RT for 3 minutes. Samples were then centrifuged at 12,000g for 15 minutes at 4°C, producing a lower red phenol-chloroform phase, an interphase and a colourless upper aqueous phase.

RNA Precipitation

The RNA containing aqueous phase (approx. 60% volume of TRI Reagent® used) was placed into a fresh tube and **A)** nothing further was added or **B)** 1.5µl of glycogen was added to each sample to act as a carrier for RNA precipitation. **A)** 750µl of isopropanol or **B)** 750µl of Ethanol:Isopropanol (2:1) mix per 1ml of TRI Reagent® initially used was added to each tube to aid in the precipitation of small microRNAs and samples were incubated **A)** at RT for 10 minutes or **B)** at -80°C overnight. Following incubation samples were centrifuged at 12,000g for a further 10 minutes at 4°C to form a gel like pellet followed by removal of the supernatant.

RNA Wash

The RNA pellet was washed using 1ml of **A)** 80% ethanol or **B)** 75% ethanol per 1ml of TRI Reagent® initially used; samples were mixed by vortexing and were then centrifuged at 7500g for 5 minutes at 4°C.

Redissolving the RNA

After centrifugation the supernatant was aspirated and the RNA pellet was left to air dry (but not to dry out completely) after which it was resuspended in 100µl of RNase free water by passing the solution through a pipette tip several times.

DNase Treatment (only used in protocol A)

To remove any possible traces of DNA from the preparation, RQ1 RNase-Free DNase was added to the resuspended RNA pellet, along with 20µl of 10x buffer. To each 200µl of resuspended pellet, 5µl of DNase was added, followed by incubation for 45 minutes at 37°C in a water bath. After this initial incubation 21µl of stop solution (1/10 the volume) was added to the resuspended RNA and incubated at 65°C in a block heater for

10 minutes. Glycogen (23µl) at a stock concentration of 2µg/µl was then added as 1/10 the initial volume producing a final volume of 250µl.

Acid-Phenol/Chloroform Protocol

An Acid-Phenol/Chloroform protocol was carried out to remove any remaining DNase, as this may interfere with subsequent PCR. Following the addition of **A)** 250µl or **B)** 100µl of Acid-phenol/chloroform 1:1 to the RNA, all samples were vortexed and centrifuged at 12,000g for **A)** 2 minutes or **B)** 15 minutes at 4°C to produce an upper aqueous phase which was placed into a fresh tube. A further **A)** 250µl or **B)** 100µl of RNase free water was added to the remaining phenol:chloroform mixture, all samples were then vortexed and centrifuged at 12,000g for 15 minutes at 4°C. A second upper aqueous phase was obtained and combined with the first, **A)** nothing or **B)** 1µl of glycogen was then added to each sample. To the upper aqueous phase 10% volume of sodium acetate 3M pH5.2 was added, followed by the addition of 2.5x the volume of **A)** Isopropanol or **B)** Ethanol:Isopropanol (2:1) after which samples were incubated at -80°C for **A)** 5 minutes or **B)** overnight. Samples were centrifuged at 12,000g for 15 minutes at 4°C, after which the supernatant was aspirated. The RNA pellet was then washed **A)** twice with 80% or **B)** once with 75% ethanol and vortexed. Samples were then **A)** incubated at RT or **B)** incubated on ice for 5 minutes prior to centrifugation at 7500g for 5 minutes followed by aspiration of the supernatant. The RNA pellet was then left to dry at RT for approximately 10 minutes (until completely dry), after which the pellet was resuspended in RNase free water and stored at -80°C.

2.2.6.2. RNA Quantification and Quality

2.2.6.2.1. Nanodrop

A Nanodrop spectrophotometer (Thermo Scientific) was used to ascertain RNA concentration. Nucleic acid samples are on occasion contaminated with other molecules including; proteins, phenol and EDTA hence the ratio of absorbance at 260/280nm and 260/230nm are used to determine purity. Ratio values of >2 for absorbance at 260/280nm and 260/230nm were required for all RNA samples produced.

2.2.6.2.2. Agilent RNA 6000 Nano Kit and 2100 Bioanalyser

The Agilent RNA 6000 Nano kit and 2100 Bioanalyser (Agilent Technologies) were used to determine RNA quality. RNA was assessed as per the manufacturer's protocol,

and an RNA integrity number (RIN) was produced for each sample (Table 2.1). The RIN number is determined not only by comparing the ratios of the 18s and 28s ribosomal bands, but also considers other factors like the presence of degradation products. Samples were given a RIN value of 1-10, with 10 indicating RNA of extremely high quality. A RIN value of >7 was preferred for all RNA samples.

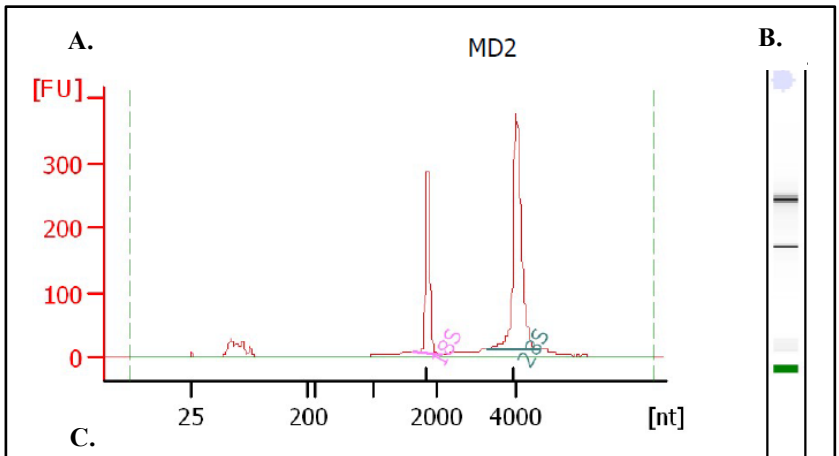

C.

Overall Results for sample 6 : MD2

RNA Area:	1,298.5
RNA Concentration:	660 ng/µl
rRNA Ratio [28s / 18s]:	2.2
RNA Integrity Number (RIN):	10 (B.02.07)
Result Flagging Color:	
Result Flagging Label:	RIN:10

Fragment table for sample 6 : MD2

Name	Start Size [nt]	End Size [nt]	Area	% of total Area
18S	1,611	2,158	264.3	20.4
28S	3,238	4,599	594.4	45.8

Figure 2.1: Bioanalyser Output Analysis for RNA Integrity using the Agilent RNA 6000 Nano Kit. (**A**) An electropherogram and (**B**) a Bioanalyser gel image from a non-degraded RNA sample. Peaks representing the 18s and 28s ribosomal subunits are observed on the electropherogram and two bands corresponding to these peaks are observed in the gel image. (**C**) RNA data obtained from the RNA sample gel image and electropherogram including the RIN value and concentration.

2.2.7. miRNA Microarrays

2.2.7.1. In House miRNA Microarrays using Genisphere Kits

RNA from AsPC-1 and MIA PaCa-2 cells treated with either 5µM curcumin or DMSO (control) for 24 hours was produced using TRI Reagent® extraction (section 2.2.6.1). Total RNA was labelled for use in microRNA microarrays using both Oyster-550 (Cy3) and Oyster-650 (Cy5) Flashtag RNA Labelling Kits from Genisphere. Curcumin treated cells were labelled with Oyster-650 and DMSO treated cells were labelled with Oyster-

550. Microarray slides containing probes providing coverage against all microRNAs in human, mouse and rat (and their related viruses) as annotated in miRBase Release v.16.0. (prepared in house by Dr Tim Gant) were washed prior to hybridisation with 2x 2 minute washes in 0.2% SDS followed by a further 2x 2 minute wash in dH_2O; slides were then centrifuged for 4 minutes at 250g (Beckman Coulter Allegra 6KR centrifuge) to dry. The FlashTag RNA labelling procedure was carried out as per the manufacturer's protocol, using only half the volumes indicated in the Genisphere kit for the labelling of 500ng of RNA per sample. Several alterations were incorporated into the Genisphere protocol, with the poly(A) tail reaction mix being combined with the appropriate dye solution and ligase at 16°C instead of RT for 30 minutes. The hybridisation buffer used following the addition of the stop FLASH solution was enhanced hybridisation buffer, not SDS buffer. Washing of the arrays following hybridisation was also modified in order to optimise the outcome of the experiment. Initially all array slides were washed in solutions of increasing stringency, twice in 2X SSC/0.1%SDS wash buffer which was pre-warmed to 52°C, with coverslips being removed from arrays during the first wash. Arrays were then washed in 1XSSC buffer twice for 2 minutes followed by a further two washes in 0.2xSSC buffer, all washes were carried out whilst rocking (40 oscillations/minutes). Slides were then centrifuged at 250g for 4 minutes after which all arrays were analysed using an Axon GenePix® 4200 scanner. The data obtained were then analysed using both R and Limma software.

2.2.7.2. Agilent Sureprint G3 Human v16 miRNA Microarrays

TRI Reagent® extraction (section 2.2.6.1) was used to obtain RNA from AsPC-1, BxPC-3 and MIA PaCa-2 cells treated with 1.5μM curcumin for 96 hours. The Agilent microRNA Spike-In kit (p/n 5190-1934) was used as per the manufacturer's protocol, as controls for the processes of RNA labelling and hybridisation. Agilent's microRNA Complete Labelling and Hyb Kit (p/n 5190-0456) was used to fluorescently label 245ng of total RNA as per the manufacturer's protocol. This entailed the ligation of a single Cyanine-3-pCp molecule to the 3 prime end of a single RNA molecule. Several alterations were incorporated into the Agilent protocol. The protocol specified to dilute total RNA samples in step 1 to 50ng/μl in order to pipette 100ng in a 2μl volume; however RNA was diluted to 122.5ng/μl in order to pipette 245ng of total RNA in a volume of 2μl. The optional step 2 (Purify the labelled RNA) using Micro Bio-Spin 6 Chromatography Columns (Cat#732-6221 Bio-Rad) was incorporated into the protocol

in order to remove DMSO and free Cyanine3-pCp from samples as well as to reduce drying time. Samples were kept in the dark in step 3 to prevent excitation of the light sensitive Cyanine-3-pCp molecule, and were dried using a vacuum concentrator for 1 hour. All other steps through to step 6 (Prepare the Hybridization assembly) using the Agilent Microarray Hybridization Chamber kit (Cat#G2534A) and Agilent SurePrint G3 Human v16 microRNA Arrays (Cat#G4870A) were carried out as stated in the manufacturer's protocol. Following hybridisation, arrays were washed using the Agilent Gene Expression Wash Buffer Kit (p/n 5188-5327) as per the manufacturer's protocol, after which they were scanned using the Agilent G2565 scanner. The array data were then analysed using either GeneSpring (Agilent) software, Partek (Partek) software or manually.

2.2.8. miRNA Microarray Target Validation through RT-qPCR

2.2.8.1. TaqMan® Reverse Transcription and qPCR

Initially 200ng of total RNA obtained from AsPC-1, BxPC-3 and MIA PaCa-2 cells using TRI Reagent® extraction (section 2.2.6.1) was reverse transcribed using the TaqMan® MicroRNA Reverse Transcription kit as per the manufacturer's protocol (Applied Biosystems Cat#4366597). The cDNA produced was then diluted in a 1:1 ratio with nuclease free water. An initial mastermix was also produced as outlined in Table 2.7.

Table 2.7: Mastermix for TaqMan® qPCR.

Component	1x Reaction
TaqMan® Universal PCR Master Mix II (2x), no UNG	10µl
TaqMan® Small RNA Assay (20x)	1µl
Nuclease Free Water	4µl
TOTAL	15µl

Reactions were made up in MicroAmp® Optical 96-Well Reaction plates combining 15µl of mastermix per sample with 5µl of the diluted (1:1) cDNA (5µl of nuclease-free water was added for no template controls). Samples were then mixed by gentle pipetting to avoid producing bubbles and centrifuged at 1000g for 1 minute to remove any bubbles. A 7500 Fast Real-Time PCR System (Applied Biosystems) was then used for

qPCR. The fast run mode consisted of 20 seconds at 95°C in order to activate the enzyme followed by 40 cycles of 3 seconds at 95°C and 30 seconds at 60°C.

2.2.8.2. miScript Reverse Transcription and SYBR® Green qPCR

RNA obtained from AsPC-1, BxPC-3 and MIA PaCa-2 cells using TRI Reagent® extraction (section 2.2.6.1) was reverse transcribed using the miScript II RT Kit. Nuclease-free water was combined with 500ng of total RNA to make a final volume of 12µl, this reaction mix was then incubated at 65°C for 10 minutes after which samples were placed directly on ice. This reaction mix was then combined with 8µl of mastermix, the components of which are outlined in Table 2.8. Each sample was mixed by gentle pipetting, briefly centrifuged and kept on ice.

Table 2.8: Mastermix for miScript Reverse Transcription.

Component	1x Reaction
5x miScript HiSpec Buffer	4µl
10x miScript Nucleics Mix	2µl
miScript Reverse Transcriptase Mix	2µl
TOTAL	8µl

Samples were then incubated at 37°C for 60 minutes followed by incubation for 5 minutes at 95°C to inactivate the miScript Reverse Transcriptase Mix.

The miScript SYBR® Green PCR Kit was used to perform qPCR on the recently transcribed cDNA which was diluted as required using nuclease-free water. A miScript mastermix was generated as outlined in Table 2.9, which was combined with 3µl of diluted cDNA (or water control) making a final volume of 16µl.

Samples were prepared in 96-well reaction plates and gently mixed. The plates were centrifuged at 1000g for 1 minute and analysed using a 7300 Real Time PCR System (Applied Biosystems), cycling conditions used are shown in Table 2.10.

Table 2.9: Mastermix for miScript qPCR.

Component	1x Reaction
2x QuantiTect SYBR Green PCR Master Mix	8µl
10x miScript Universal Primer (0.5µM)	2.4µl
10x miScript Primer Assay (Hs_RNU6-2_1)/microRNA Primer (0.5µM)	2.4µl
RNase-Free Water	0.2µl
TOTAL	13µl

Table 2.10: Cycling Conditions for miScript qPCR.

Analysis Mode	Cycles	Segment	Target Temp.	Time
Pre-Incubation				
None	1	-	50°C	2 min
		HotStarTaq DNA pol activation	95°C	15 min
Amplification				
Quantification	44	Denaturation	94°C	15 sec
		Annealing	55°C	30 sec
		Extension	70°C	30 sec
Melting Curve Analysis				
Melting Curves for Colour Compensation	1	Denaturation	95°C	15 sec
		Annealing	60°C	30 sec
		Extension	95°C	15 sec
Cooling				
None	1	-	4°C	∞

2.2.8.3. GoScript Reverse Transcription and SensiMix SYBR® Green qPCR

The GoScript™ Reverse Transcription System was used on 1µg of total RNA obtained from AsPC-1, BxPC-3 and MIA PaCa-2 cells following TRI Reagent® extraction (section 2.2.6.1). The RNA was reverse transcribed as per the manufacturer's protocol (Promega Cat#A5000); choosing the options of using the Random Primer (0.5µg/reaction) and 1.2µl of $MgCl_2$ (1.5µM final concentration). The SensiMix SYBR Hi-ROX kit (Bioline) was then used to carry out qPCR on the cDNA samples obtained using the GoScript™ Reverse Transcription System. The qPCR reaction mix was prepared as shown in Table 2.11 using the cDNA produced which had been diluted with nuclease-free water.

Using the SensiMix system to carry out qPCR meant that conditions for each set of primers (forward and reverse) had to be optimised for successful quantification. The cDNA dilution (8x-128x), primer concentrations (0.2-0.5µM) and annealing temperatures (55-57°C) varied and touchdown qPCR (57→61°C) was used for certain primers.

Table 2.11: Reagents for SensiMix qPCR Mastermix.

Component	1x Reaction
2x SensiMix™ SYBR	8µl
Forward Primer (5µM)	0.64-1.6 µl
Reverse Primer (5µM)	0.64-1.6 µl
Template cDNA	3µl
dH_2O	Make up to 16µl
TOTAL	16µl

Prepared samples were aliquoted into the 96-well reaction plates, gently mixed and centrifuged at 1000g for 1 minute. The 7300 Real Time PCR System was used for qPCR and the cycling conditions are highlighted in Table 2.12.

Table 2.12: Cycling Conditions for Sensimix qPCR.

Analysis Mode	Cycles	Segment	Target Temp.	Time
Pre-Incubation				
None	1	-	50°C	2 min
		Polymerase Activation	95°C	15 min
Amplification				
Quantification	44	Denaturation	94°C	15 sec
		Annealing	55-60°C	30 sec
		Extension	72°C	30 sec
Melting Curve Analysis				
Melting Curves for Colour Compensation	1	Denaturation	95°C	15 sec
		Annealing	60°C	30 sec
		Extension	95°C	15 sec
Cooling				
None	1	-	4°C	∞

All RT-qPCR data was analysed using the ΔΔCt method of analysis (Livak and Schmittgen, 2002).

Chapter 3. The Diagnostic Potential of miRNAs in Pancreatic Cancer and their Modulation by Curcumin.

3.1. Introduction

Pancreatic tumourigenesis is a furtive disease characterised by its lack of palpable symptoms and the inconsistency in expression of its various diagnostic markers. Consequently detection of PC is challenging, and is often unattainable until the occurrence of aggressive local invasion and metastatic disease. The inability to accurately diagnose early stage pancreatic tumourigenesis presents a barrier against using existing therapies, as they appear to be potentially curative only when applied earlier in this disease. Therefore, in order to improve patient outcome a more accurate and specific panel of markers for PC is necessary, in addition to therapeutic agents with the capacity to treat advanced disease.

It comes as no surprise that at advanced-stage presentation existing treatments for PC are ineffective, disease recurrence is frequent and overall prognosis is dismal with only 5% of patients diagnosed with PC surviving for >5 years (Warshaw and Fernandez-Del Castillo, 1992; Hanbidge, 2002). A study looking at the clinical and histopathological features of patients who had survived for 5 years following resection with curative intent did so in order to ascertain what contributed to their positive outcome. It was determined that patients diagnosed with less advanced disease, and therefore, in the earlier stages of PC development prior to resection, had a better chance of long term survival (Cleary et al, 2004).

Imaging modalities, FNA and tumour markers detected within the blood are all characteristically used in order to identify and stage PC. These modalities often struggle with early disease detection, in part, due to the presentation of pancreatic tumourigenesis with distant metastases (Russo et al, 2011). They also tend to lack sensitivity when determining the presence of microscopic metastasis, which are regularly the culprit for patient relapse, and are often unable to differentiate between cancer and inflammatory diseases such as chronic pancreatitis (Hanbidge, 2002; Ansari et al, 2011; Cleary et al, 2004**)**.

A considerable number of hormones, enzymes and tumour-associated antigens have been identified as potential biomarkers for PC; however few have been successfully validated with most exhibiting low sensitivity and lack of specificity (Ballehaninna and Chamberlain, 2013). The most extensively studied of these markers, CA19-9, becomes elevated in the serum of individuals with PC. However, it lacks both sensitivity and specificity and is elevated in patients with various other cancers and inflammatory diseases, highlighting the need for novel biomarkers for pancreatic tumourigenesis (Jazieh et al, 2014; Jiang et al, 2004; Ni et al, 2005; Goggins, 2011).

Various microarray profiling studies have shown that miRNA expression is often deregulated in PC (Gong et al, 2011; Lee et al, 2007; Wang et al, 2009a; Jamieson et al, 2012; Kent et al, 2009; Szafranska et al, 2007). Due to their ability to control multiple targets, miRNAs have a high regulatory potential and are important in numerous biological processes. Therefore, those miRNAs aberrantly expressed in PC are believed to play a significant role in promoting disease progression (Dykxhoorn, 2010; Karius et al, 2012). *In vitro* studies show that by manipulating miRNA expression, it is possible to inhibit proliferation, suppress metastasis and induce drug sensitivity in PC cells (Bera et al, 2014; Zhao et al, 2014; Bao et al, 2011b).

Due to its chemical and biological diversity, curcumin has also been shown to regulate multiple molecular targets and signalling pathways involved in cancer progression (Kunnumakkara et al, 2007**)**. One way in which this natural agent and its more bioavailable analogues have been shown to modulate gene expression is through the regulation of miRNAs (Yang et al, 2010; Ali et al, 2012; Gandhy et al, 2012; Yang et al, 2013). *In vitro* studies of PC have shown how curcumin can increase cancer cell sensitivity to current chemotherapeutics, and inhibit proliferation and metastasis through the modulation of differentially expressed miRNAs (Ali et al, 2010; Iwagami et al, 2013; Zhao et al, 2013; Hamada et al, 2012).

Existing research investigating the use of miRNAs as diagnostic markers and therapeutic targets has shown promise, with many studies highlighting select miRNAs for their suitability as predictive markers for PC (Lee et al, 2007; Wang et al, 2009a; Jamieson et al, 2012; Szafranska et al, 2007; Wang et al, 2013; Setoyama et al, 2011) This research shows the feasibility of using miRNAs as biomarkers; however with no

uniform pattern of deregulation and a unique miRNA profile for PC yet unidentified, more needs to be done (Kent et al, 2009). The aim of this work, based on the current knowledge of miRNAs and their clinical capacity in PC, was to identify miRNAs aberrantly expressed in PC which could be targets for modulation by curcumin.

3.2. Results

3.2.1. RNA Production and Quality Control

Microarray slides produced in house by Dr Tim Gant (MRC, Leicester) were used in combination with Genisphere labelling reagents to assess miRNA expression within the PC cell lines AsPC1 and MiaPaCa-2 following treatment for 24 hours with either 5μM curcumin or DMSO (control). In part these cell lines were chosen because of their differences in both differentiation status and origin. It was thought that the moderately differentiated AsPC-1 cells originating from ascites and the poorly differentiated MIA PaCa-2 cells found in a primary tumour (details can be found in Appendix 1) may respond differently to curcumin treatment. The TRI-reagent® RNA extraction method A (section 2.2.6.1) was utilised for total RNA isolation after which sample quality control (QC) was performed. RNA concentration and ratio of absorbance at 260/280nm and 260/230nm were determined through the use of a Nanodrop spectrophotometer, with RIN values obtained using an Agilent 2100 Bioanalyser (Table 3.1). An outline of the experimental setup used for assessing curcumin treatment of both PC cell lines is outlined in Figure 3.1.

3.2.2. Data Processing, Quality Assessment and Normalisation

Total RNA obtained from MIA PaCa-2 and AsPC-1 cells was labelled using a Flashtag RNA Labelling Kit from Genisphere (section 2.2.7.1). RNA obtained from curcumin and DMSO treated cells was labelled with Oyster-650 (Cy5) and Oyster-550 (Cy3) respectively and hybridised to in house microarray slides (section 2.2.7.1). Linear regression analysis was used as a form of QC in order to determine if both the Cy3 (DMSO) and Cy5 (curcumin) labelled RNA samples were hybridised to the microarray slides equally (data in Appendix 2). The raw Cy3 and Cy5 fluorescence values were plotted against one another for each individual miRNA to produce a line of best fit (linear regression) (Figure 3.2). The value attributed to the slope of the linear regression was an estimation of how both samples had hybridised to the microarray, with values

closer to 1 (on a scale of 1 to 0) indicating equal hybridisation of Cy3 and Cy5 labelled samples. Microarray slides were also visually assessed to determine any irregularities such as smears and smudges obtained post-hybridisation and if the hybridisation itself had been successful (Figure 3.3).

Table 3.1: Quality Control Data Following RNA Extraction.

Sample ID	Conc. (ng/µl)	A260/280	A260/230	RIN
M1	1475	2.10	2.09	6.6
M2	1173	2.14	2.12	6.8
M3	1383	2.11	2.10	6.6
M4	1002	2.14	2.10	5.2
M5	1100	2.10	2.06	4.9
M6	927	2.12	2.08	6.3
M7	805	2.14	2.08	5.7
M8	781	2.15	2.07	4.8
M9	1586	2.09	2.06	5.6
M10	2007	2.09	2.07	7.1
A1	494	2.04	1.98	6.7
A2	458	2.03	1.98	4.6
A3	701	2.07	1.99	6.7
A4	451	2.05	1.98	5.9
A5	407	2.06	1.96	5.4
A6	387	2.05	1.96	5.8
A7	358	2.06	1.92	3.9
A8	235	2.03	1.86	5.3
A9	371	2.06	1.91	3.7
A10	295	2.10	1.92	5.7

Measurements obtained following TRI-reagent® extraction A of 5 pairs of independent biological repeats acquired from MIA PaCa-2 and AsPC-1 cell lines treated with either 5µM curcumin or DMSO (control) for 24 hours. (Key: M = MIA PaCa-2, A= AsPC-1)

Microarray slides were initially processed using GenePix® Pro 6.0 software for the acquisition of gpr files containing raw miRNA expression data as outlined in Figure 3.1. Using the Limma software package which is implemented in the R software environment, average values of the four replicate probe sets present for each miRNA were determined, following background subtraction, and subsequent intra and inter array normalisation. Intra-array normalisation consists of normalising the data within each individual microarray slide, whereas inter-array normalisation consists of array

normalisation of the data between all microarray slides within an experiment. The commands used within this software are shown in Appendix 3.

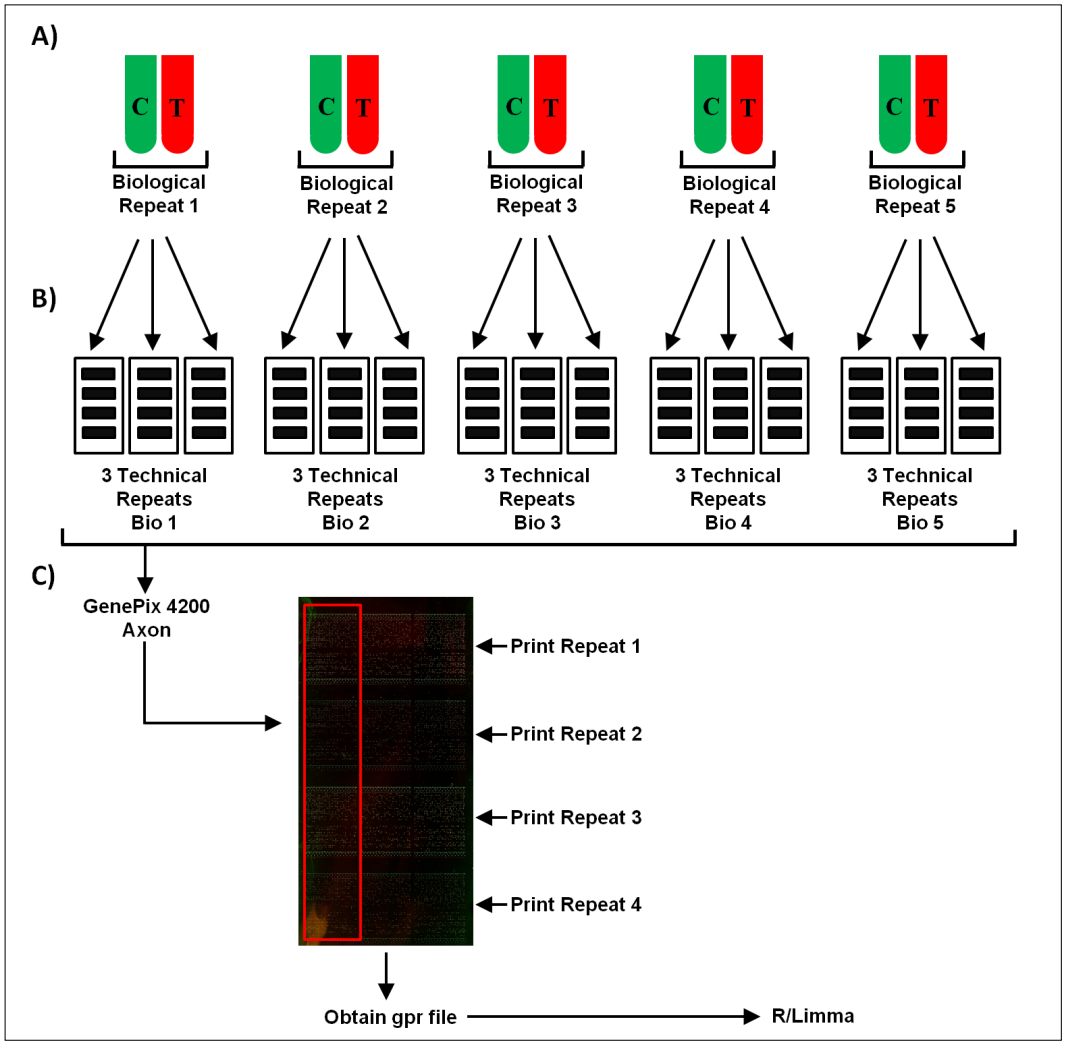

Figure 3.1: Experimental Design for miRNA Microarray Analysis. A) Five paired biological repeats consisting of a curcumin (5μM) treated sample and a DMSO (control) treated sample were produced following 24 hours exposure. The in house microarrays produced were two-colour microarrays, whereby curcumin treated RNA was labelled with Cy5 dye producing a red fluorescence and DMSO treated RNA was labelled with Cy3 dye producing a green fluorescence (Genisphere), these samples were then combined for each biological repeat. **B)** Each biological repeat was hybridised to three independent microarray slides (technical repeats) which were all printed with the same probe set. **C)** The microarray slides were then scanned using a GenePix® 4200 Axon scanner to obtain a TIFF file. Each microarray slide comprised of four probe set repeats (red box). Therefore within each slide there were four print repeats for each miRNA. Each microarray slide was further processed using GenePix® Pro 6.0 software to obtain a gpr file, and all files per cell line were further processed and normalised through R (Integrated suite of software facilities for data manipulation, calculation and graphical display) using the programme Limma (differential expression analysis of data from microarray experiments). (Key: C = control, T= treated (curcumin) Bio = biological repeat)

Visual representations of the two channel microarray miRNA expression data, before and after normalisation, were shown by producing MA and density plots. These images were used to evaluate the quality of the microarray data prior to analysis. An MA plot can be used to study the relationship between the log ratio (M) of two sets of data and the mean average (A) signal intensity of the same two sets of data. In the context of microarray analysis, an MA plot can be employed to compare two channels of intensity measurements (in this case Cy5 (red fluorescence) and Cy3 (green fluorescence)).

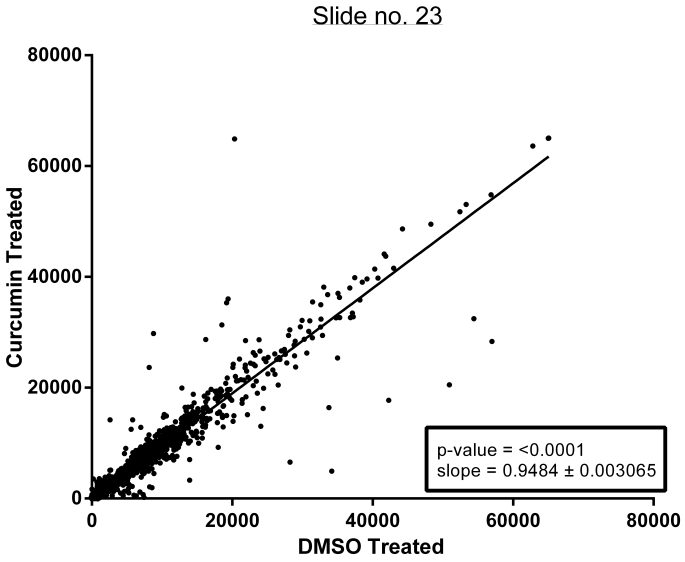

Figure 3.2: Linear Regression Analysis. An example plot for linear regression analysis. The linear regression had a slope of 0.9484±0.003065, indicating the equal hybridisation of both Cy3 and Cy5 labelled samples (t-test, $p<0.0001$).

It is understood that for most large arrays the majority of targets will not differ in expression across the treatments used. Data following normalisation are therefore mostly expected to fall along a straight horizontal line which equates with zero on the y-axis (M) of the MA plot (Figure 3.4B and C). Prior to normalisation some samples may cluster away from this horizontal line reflecting a probable bias of miRNAs towards a specific dye (Figure 3.4A). The normalisation of dual channel microarrays in part aims to re-align any data which cluster away from this horizontal line thus reducing this bias. Independent MA plots for each experimental repeat were observed within the Limma software both before and after normalisation (Appendix 4). These MA plots showed the successful normalisation of the microarray data prior to analysis (Appendix 4).

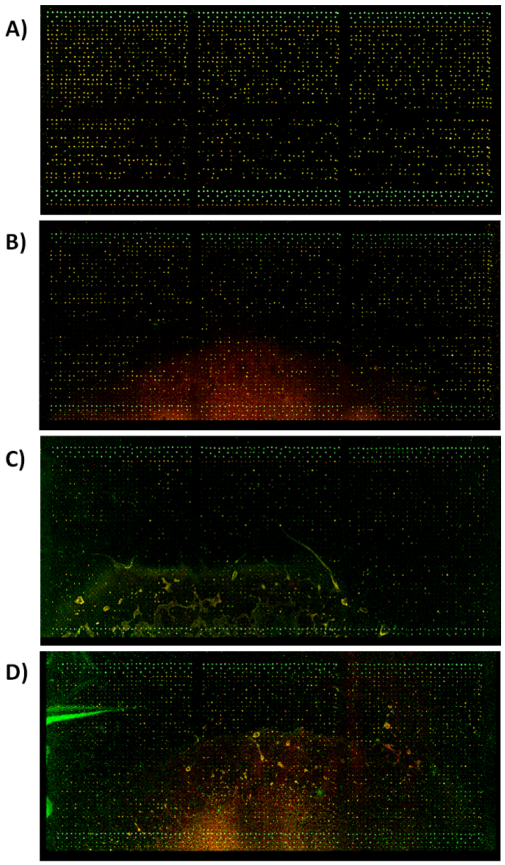

Figure 3.3: RNA Sample Hybridisation. The images produced post-hybridisation were visualised as a form of qualitative QC for each microarray slide. **(A)** An example of a microarray slide to which fluorescently labelled samples appear to have hybridised both equally and successfully. **(B)(C)** and **(D)** examples of unsuccessful hybridisation, the presence of irregularities such as smears and smudges or a mixture of both.

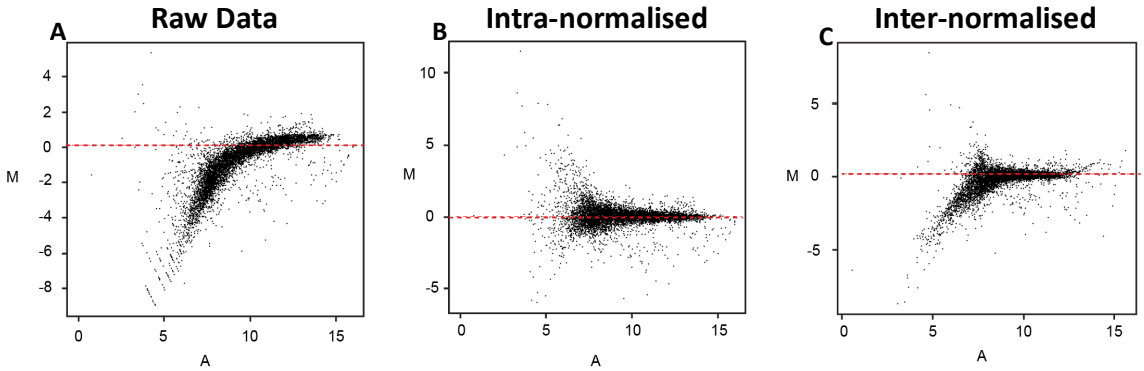

Figure 3.4: MA Plots for Microarray Normalisation. MA plots for a microarray slide containing Cy3 and Cy5 labelled samples from a single technical repeat for the **A)** raw data prior to normalisation and following **B)** intra and **C)** inter-array normalisation.

The distribution of red and green fluorescence signals for all microarray slides within an experiment can be displayed using a density plot (Figure 3.5). The signals for both dyes within each sample are expected to show a fairly similar pattern of distribution even prior to normalisation. If the fluorescence distribution of a sample varies considerably from the others within an experiment, this may indicate the bias of the microarray slide towards either dye. Further assessment of these data is then required before a decision can be made either for or against their inclusion within the final analysis. MA plots and density plots are used to determine if the microarray data obtained are of sufficiently high quality for use in later analysis.

Once normalised the fold change and standard error were estimated for each microarray experiment. MA and volcano plots were used in order to show the distribution of data following normalisation (Figure 3.6). Most data points within the MA plot would be expected to fall along a straight horizontal line which equates to zero on the y-axis (M), as most miRNA targets would not be expected to differ in expression following treatment with curcumin (zero fold change). This is the case for both cell lines, with most data points clustered around the zero value of the y-axis (Figure 3.6 A and B). For the miRNAs which are regulated by curcumin, those with a positive M-value are more highly expressed and those with a negative M-value have a decreased expression following treatment.

A volcano plot was used to visually identify if any meaningful changes in miRNA expression were present following curcumin treatment. By plotting the negative log10 of the significance/odds (y-axis) against the log fold change (x-axis) as calculated by the Limma software, a 'volcano like' distribution of the data is observed. Most of the data points show a log fold change of around zero, indicating no effect in regard to curcumin (Figure 3.6 C and D). The further away a data point is from zero on the x-axis the bigger the fold change and the more positive the value on the y-axis the greater the significance of the fold change observed. Any miRNAs which may be significantly differentially expressed would be expected to have fold change values of >1 or <-1 on the x-axis and significance values of >1.3 (equates to $p<0.05$) on the y-axis. MA and volcano plots for both PC cell lines following microarray analysis indicate the presence of a number of miRNAs that are significantly differentially expressed following curcumin treatment (Figure 3.6).

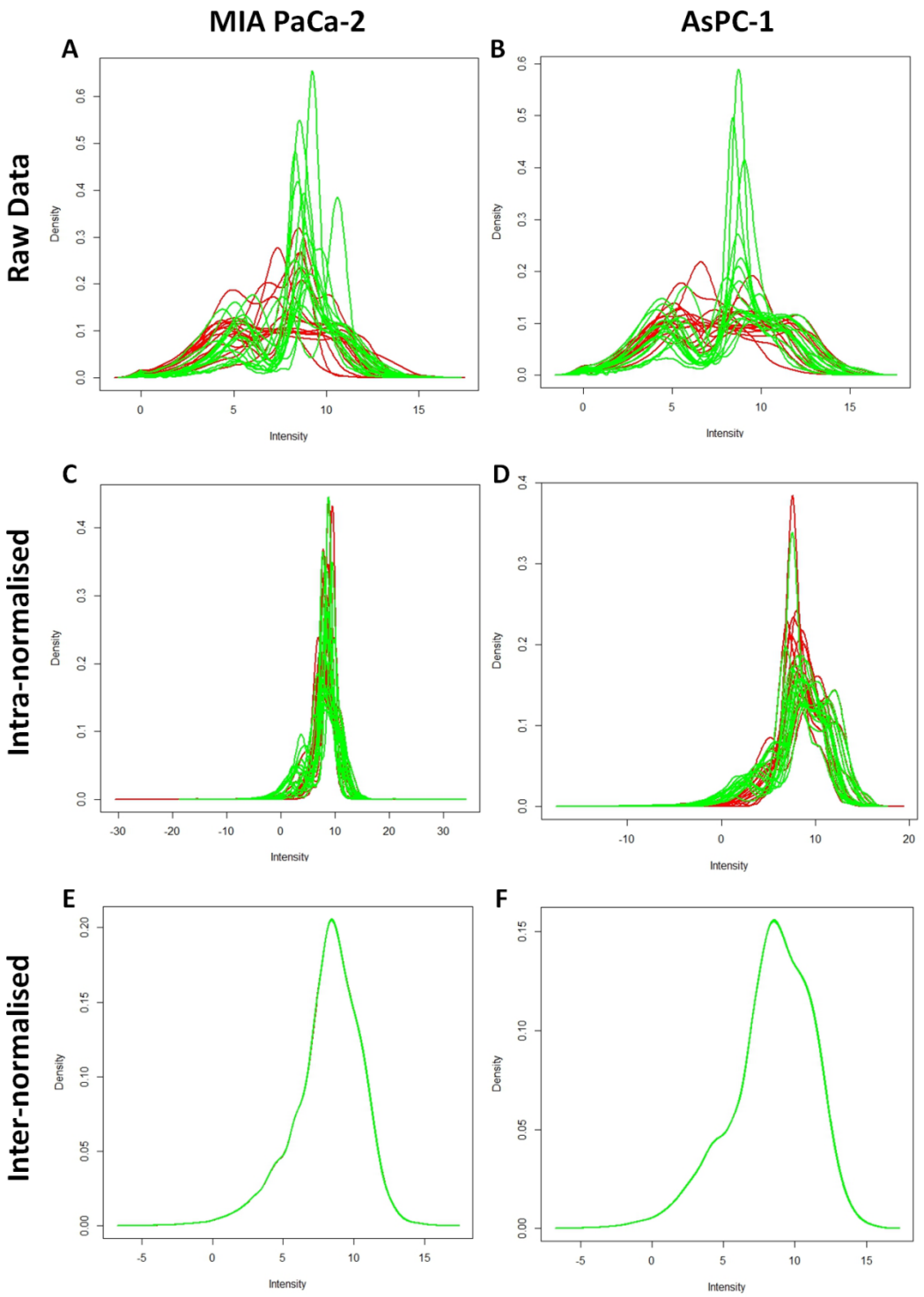

Figure 3.5: Density Plots for MIA PaCa-2 and AsPC-1 Samples. Density plots are used to show individual green and red channels for each microarray slide within an experiment. **(A, B)** Prior to normalisation considerable variation is observed not only between the red and green channels within a microarray but also between microarrays. **(C, D)** Following intra-array normalisation the distribution of red and green channels becomes similar for each microarray slide however variation is still present between microarrays. **(E, F)** The application of inter-array normalisation makes the distribution of green and red channels the same across all microarray slides within an experiment. This results in the similar distribution of green and red channels across all microarray slides as well as within each microarray slide, resulting visually in the overlap of red and green signals on a density plot.

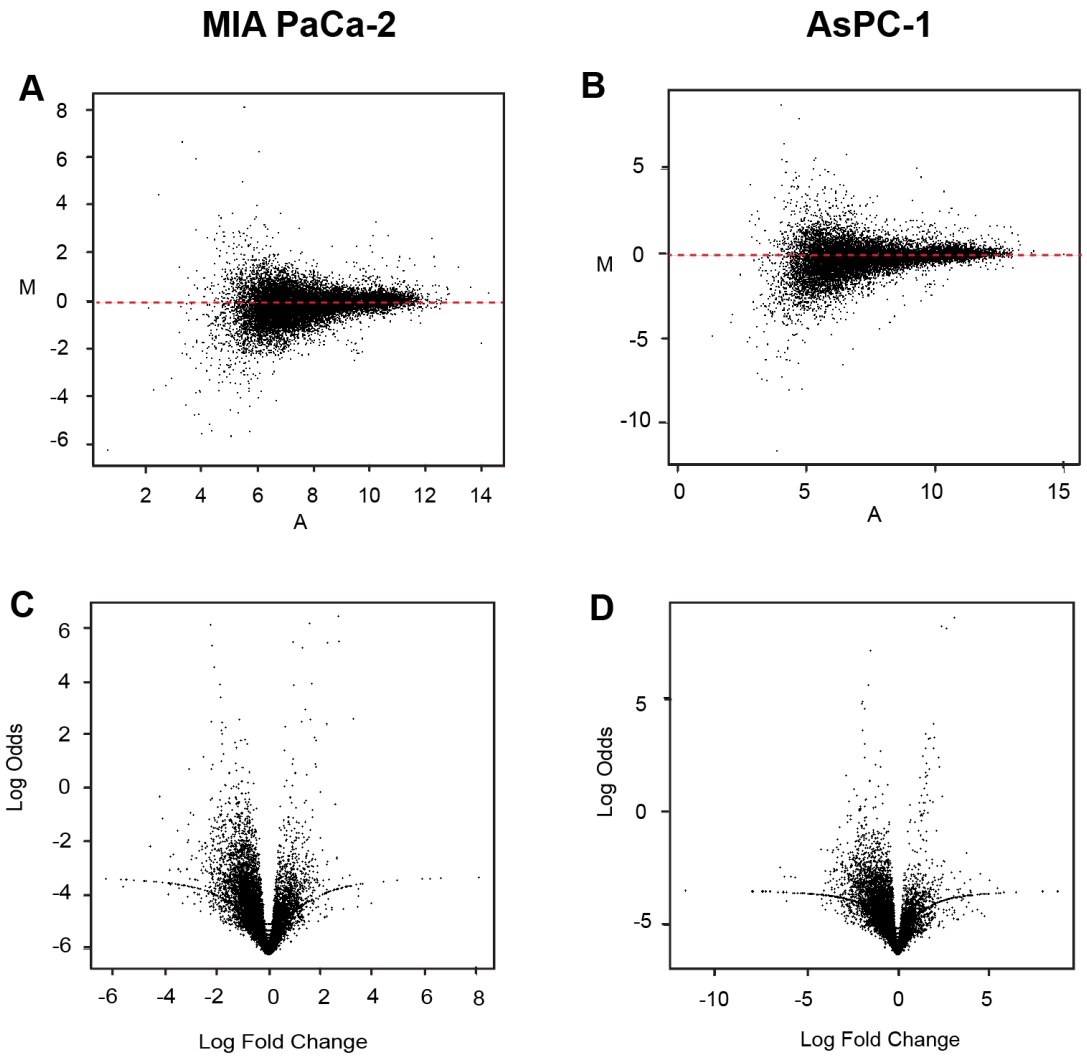

Figure 3.6: MA Plots and Volcano Plots for Normalised MIA PaCa-2 and AsPC-1 Samples. Following normalisation of microarray data, the average values for each miRNA were fitted to a linear model in order to estimate the fold change and standard error for the data which was then represented as either an MA plot **(A)** MIA PaCa-2 and **(B)** AsPC-1 or a volcano plot **(C)** MIA PaCa-2 and **(D)** AsPC-1.

3.2.3. Analysis of miRNA Microarray Data

Following processing and normalisation of the raw microarray data, differentially expressed miRNAs were determined using R and Limma software. The criteria used to produce a list of miRNAs believed to be differentially expressed following curcumin treatment consisted of targets with a fold change either >2 or <0.5 in combination with a p-value of <0.5. Tables for the top differentially expressed miRNAs found to meet these criteria were produced for both MIA PaCa-2 and AsPC-1 treated cells (Table 3.2 and Table 3.3) with an additional table produced highlighting the 34 miRNAs found to be differentially expressed in both cell lines (Table 3.4).

Table 3.2: MIA PaCa-2 miRNA Microarray Top Table.

Name	Avg FC	Log2 FC	St.Dev	Median P-value
hsa-miR-454*	4.451	2.154	0.828	0.000
hsa-miR-361-5p	0.406	-1.300	0.064	0.000
hsa-miR-4258	0.267	-1.906	0.061	0.001
hsa-miR-518f*	0.283	-1.821	0.131	0.002
hsa-miR-432*	0.385	-1.376	0.075	0.006
hsa-miR-301b	0.374	-1.419	0.133	0.006
hsa-miR-223	0.423	-1.241	0.158	0.007
hsa-miR-539	0.413	-1.276	0.173	0.007
hsa-miR-656	0.418	-1.257	0.069	0.008
hsa-miR-136*	0.482	-1.051	0.135	0.008
hsa-miR-518d-3p	0.217	-2.206	0.185	0.012
hsa-miR-148b	0.451	-1.149	0.114	0.013
hsa-miR-132	0.463	-1.111	0.074	0.014
hsa-miR-588	0.340	-1.558	0.221	0.015
hsa-miR-876-3p	0.185	-2.432	0.308	0.017
hsa-miR-744	0.415	-1.267	0.128	0.018
hsa-miR-448	0.463	-1.110	0.087	0.019
hsa-miR-4315	0.340	-1.556	0.431	0.019
hsa-miR-126	0.466	-1.102	0.100	0.020
hsa-miR-561	0.500	-0.999	0.248	0.021
hsa-miR-129-3p	0.469	-1.092	0.177	0.021
hsa-miR-562	0.445	-1.169	0.342	0.022
hsa-miR-582-3p	0.399	-1.326	0.107	0.024
hsa-miR-486-5p	0.468	-1.097	0.153	0.025
hsa-miR-637	4.725	2.240	29.161	0.025
hsa-miR-188-5p	0.206	-2.281	0.101	0.026
hsa-miR-1249	0.344	-1.538	0.186	0.028
hsa-miR-943	0.414	-1.274	0.169	0.030
hsa-miR-548j	0.466	-1.103	0.055	0.031
hsa-miR-1229	0.463	-1.112	0.242	0.031
hsa-miR-10b*	0.453	-1.141	0.121	0.033
hsa-miR-20a*	0.424	-1.239	0.147	0.033
hsa-miR-302c*	0.429	-1.219	0.176	0.034
hsa-miR-518a-3p	0.501	-0.998	0.089	0.034
hsa-miR-1279	0.497	-1.008	0.262	0.034
hsa-miR-302a*	0.322	-1.634	0.194	0.036
hsa-miR-380	0.493	-1.021	0.198	0.037
hsa-miR-519e	0.459	-1.125	0.153	0.037
hsa-miR-148a	0.372	-1.428	0.273	0.038
hsa-miR-19b-1*	0.425	-1.236	0.131	0.039
hsa-miR-643	0.433	-1.208	0.183	0.040
hsa-miR-145*	0.509	-0.974	0.126	0.047
hsa-miR-370	0.386	-1.373	0.139	0.049

high	4.725
NC	1.000
low	0.185

hsa-miR-101*	0.493	-1.021	0.159	0.051
hsa-miR-1228*	0.488	-1.034	0.281	0.052
hsa-miR-133b	0.327	-1.614	0.201	0.052
hsa-miR-519d	0.447	-1.162	0.209	0.053
hsa-miR-367	0.503	-0.992	0.134	0.054
hsa-miR-3156	0.369	-1.438	0.155	0.055
hsa-miR-410	0.488	-1.035	0.115	0.063
hsa-miR-708*	0.372	-1.425	0.250	0.064
hsa-let-7f-2*	0.472	-1.083	0.099	0.066
hsa-miR-770-5p	0.445	-1.169	0.321	0.069
hsa-miR-425	0.383	-1.385	0.067	0.069
hsa-miR-455-5p	0.490	-1.029	0.245	0.075
hsa-miR-1247	0.377	-1.407	0.379	0.076
hsa-miR-1237	0.419	-1.255	0.163	0.080
hsa-miR-1207-3p	0.373	-1.421	0.287	0.081
hsa-miR-524-5p	0.507	-0.981	0.165	0.089
hsa-miR-651	0.495	-1.015	0.256	0.092
hsa-miR-660	0.509	-0.973	0.233	0.094
hsa-miR-145	0.471	-1.088	0.185	0.102
hsa-miR-507	0.470	-1.090	0.175	0.105
hsa-miR-663	0.428	-1.223	0.173	0.109
hsa-miR-181c*	0.375	-1.415	0.442	0.109
hsa-miR-1271	0.464	-1.107	0.267	0.111
hsa-miR-210	0.498	-1.007	0.091	0.113
hsa-miR-142-3p	0.470	-1.090	0.266	0.123
hsa-miR-3159	0.507	-0.980	0.370	0.123
hsa-miR-369-5p	0.491	-1.025	0.260	0.134
hsa-miR-100	0.497	-1.008	0.204	0.137
hsa-miR-590-3p	0.480	-1.059	0.234	0.139
hsa-miR-450b-3p	0.450	-1.151	0.176	0.145
hsa-miR-516a-3p/hsa-miR-516b*	0.333	-1.588	0.347	0.146
hsa-miR-1225-5p	0.405	-1.305	0.272	0.166
hsa-miR-23a	0.493	-1.019	0.201	0.168
hsa-miR-122*	2.114	1.080	2.481	0.188
hsa-miR-596	0.475	-1.074	0.199	0.188
hsa-miR-99a*	0.488	-1.034	0.209	0.220
hsa-miR-139-5p	0.445	-1.169	0.258	0.225
hsa-miR-3943	0.445	-1.168	0.447	0.232
hsa-miR-133a	0.499	-1.004	0.525	0.233
hsa-miR-605	0.440	-1.184	0.713	0.240
hsa-miR-196b	0.429	-1.221	0.317	0.247
hsa-miR-548w	0.481	-1.057	0.233	0.252
hsa-let-7i*	0.411	-1.283	0.281	0.261

hsa-miR-192*	0.340	-1.555	0.220	0.262
hsa-miR-1193	0.417	-1.261	0.643	0.321
hsa-miR-579	0.474	-1.077	0.186	0.362
hsa-miR-144*	0.505	-0.984	0.359	0.474

A table of all miRNAs demonstrating an average fold change (Avg FC) of > 2 (red) or < 0.5 (blue) and a p-value of <0.4 (Med P-value) following treatment for 24 hours with 5μM curcumin in MIA PaCa-2 cells. The log2 of the avg FC (Log2 FC) and the standard deviation (SD) between the values used to calculate the avg FC are also given. The miRNAs with a p-value of ≤0.05 can be observed in the first part of the table. (Key: NC= no change, High = increased fold change, Low = decreased fold change)

Table 3.3: AsPC-1 miRNA Microarray Top Table.

Name	Avg FC	Log2 FC	St.Dev	Median P-value
hsa-miR-4258	0.340	-1.558	0.137	0.000
hsa-miR-423-3p	3.385	1.759	0.582	0.000
hsa-miR-454*	4.188	2.066	1.178	0.000
hsa-miR-125b-2*	2.422	1.276	0.055	0.001
hsa-miR-1281	0.315	-1.668	0.137	0.005
hsa-miR-1277	0.213	-2.229	0.073	0.007
hsa-miR-656	0.501	-0.998	0.224	0.007
hsa-miR-518f*	0.301	-1.734	0.540	0.010
hsa-miR-345	0.453	-1.143	0.135	0.011
hsa-miR-518a-3p	0.483	-1.051	0.202	0.011
hsa-miR-432*	0.446	-1.165	0.132	0.013
hsa-miR-3909	0.073	-3.784	0.842	0.015
hsa-miR-302c*	0.400	-1.321	0.120	0.016
hsa-miR-650	0.385	-1.379	0.151	0.016
hsa-miR-128	0.266	-1.909	0.137	0.018
hsa-miR-19b-1*	0.343	-1.543	0.164	0.018
hsa-miR-29c	0.479	-1.062	0.151	0.020
hsa-miR-653	0.340	-1.557	0.167	0.021
hsa-miR-1227	0.471	-1.086	0.148	0.023
hsa-miR-148b	0.303	-1.722	0.119	0.024
hsa-miR-136*	0.489	-1.032	0.366	0.024
hsa-miR-380	0.324	-1.624	0.258	0.025
hsa-miR-301b	0.363	-1.461	0.048	0.026
hsa-miR-193a-3p	0.473	-1.080	0.223	0.027
hsa-miR-891b	0.267	-1.903	0.080	0.027
hsa-miR-643	0.417	-1.262	0.240	0.027
hsa-miR-370	0.303	-1.724	0.163	0.032
hsa-miR-145	0.275	-1.863	0.210	0.032
hsa-miR-367	0.338	-1.563	0.135	0.033
hsa-miR-452*	0.461	-1.116	0.404	0.033
hsa-miR-132	0.401	-1.320	0.113	0.035
hsa-miR-619	0.322	-1.637	0.215	0.036

high	4.188
NC	1.000
low	0.073

hsa-miR-514	0.394	-1.344	0.064	0.037
hsa-miR-1247	2.920	1.546	144.039	0.039
hsa-miR-770-5p	0.239	-2.063	0.077	0.039
hsa-miR-196a	0.474	-1.078	0.157	0.039
hsa-miR-1470	0.459	-1.125	0.190	0.040
hsa-miR-548x	0.212	-2.239	0.525	0.041
hsa-miR-29a	0.474	-1.078	0.174	0.043
hsa-miR-578	0.293	-1.769	0.073	0.046
hsa-miR-507	0.144	-2.794	0.254	0.046
hsa-miR-19a	0.382	-1.388	0.157	0.047
hsa-miR-429	0.435	-1.202	0.328	0.049
hsa-miR-20a*	0.442	-1.178	0.136	0.049
hsa-miR-455-3p	0.280	-1.835	0.120	0.050
hsa-miR-558	0.296	-1.758	0.088	0.051
hsa-miR-450b-3p	0.335	-1.577	0.152	0.051
hsa-miR-3622a-5p	0.253	-1.981	0.210	0.052
hsa-miR-146a*	0.181	-2.469	0.084	0.053
hsa-miR-3935	2.635	1.398	4.184	0.054
hsa-miR-101*	0.214	-2.227	0.177	0.057
hsa-miR-182*	0.357	-1.486	0.230	0.058
hsa-miR-520d-3p	0.413	-1.275	0.136	0.060
hsa-miR-23a*	0.452	-1.145	0.156	0.061
hsa-miR-1537	0.272	-1.880	0.123	0.063
hsa-miR-223	0.391	-1.355	0.177	0.068
hsa-miR-1913	0.415	-1.268	0.135	0.069
hsa-miR-769-3p	0.351	-1.509	0.250	0.078
hsa-miR-188-3p	0.433	-1.206	0.096	0.079
hsa-miR-449c*	0.093	-3.429	0.145	0.079
hsa-miR-518e	0.295	-1.759	0.334	0.080
hsa-miR-19a*	0.281	-1.830	0.545	0.081
hsa-miR-512-5p	0.116	-3.104	0.383	0.082
hsa-miR-1228	0.348	-1.523	0.174	0.084
hsa-miR-4253	2.602	1.380	5.871	0.087
hsa-miR-548o	0.217	-2.206	0.183	0.088
hsa-miR-324-5p	0.311	-1.685	0.324	0.092
hsa-miR-1229	0.310	-1.689	0.161	0.092
hsa-miR-718	0.238	-2.069	0.485	0.093
hsa-miR-1237	0.247	-2.017	0.145	0.097
hsa-miR-582-3p	0.343	-1.545	0.163	0.097
hsa-miR-3680*	0.372	-1.426	0.176	0.107
hsa-miR-21-3p	0.337	-1.569	0.225	0.109
hsa-let-7a*	0.398	-1.330	0.259	0.109
hsa-miR-518d-3p	0.322	-1.633	0.447	0.111
hsa-miR-10b*	0.241	-2.051	0.088	0.111

hsa-miR-588	0.393	-1.348	0.118	0.112
hsa-miR-425	0.189	-2.405	0.166	0.116
hsa-miR-758	0.378	-1.403	0.228	0.118
hsa-miR-519d	0.392	-1.350	0.209	0.119
hsa-miR-191*	0.366	-1.449	0.141	0.122
hsa-miR-1274b	0.339	-1.562	0.268	0.130
hsa-miR-1268	0.337	-1.568	0.116	0.133
hsa-miR-9	0.227	-2.141	0.374	0.137
hsa-miR-3186-5p	3.121	1.642	0.368	0.138
hsa-miR-624*	0.350	-1.514	0.207	0.138
hsa-miR-137	0.337	-1.568	1.033	0.144
hsa-miR-4281	0.295	-1.762	0.230	0.148
hsa-miR-1231	0.159	-2.654	0.293	0.150
hsa-miR-517c	0.257	-1.963	0.146	0.152
hsa-miR-4304	2.232	1.158	0.556	0.156
hsa-miR-579	0.316	-1.660	0.196	0.160
hsa-miR-3692*	2.256	1.174	1.382	0.177
hsa-miR-3139	0.287	-1.802	0.429	0.181
hsa-miR-3714	2.032	1.023	0.399	0.213
hsa-miR-591	0.298	-1.744	0.251	0.230
hsa-let-7e*	0.246	-2.021	0.248	0.237
hsa-miR-449a	2.548	1.349	15.734	0.251
hsa-miR-548w	0.146	-2.776	0.516	0.355
hsa-miR-510	2.460	1.299	4.105	0.381

A table of the top 100 miRNAs demonstrating an average fold change (Avg FC) of > 2 (red) or < 0.5 (blue) and a p-value of <0.5 (Med P-value) following treatment for 24 hours with 5μM curcumin in AsPC-1 cells. The log2 of the avg FC (Log2 FC) and the standard deviation (SD) between the values used to calculate the avg FC are also given. The miRNAs with a p-value of ≤0.05 can be observed in the first part of the table. (Key: NC= no change, High = increased fold change, Low = decreased fold change)

Table 3.4: Differentially Expressed miRNAs Present in both MIA PaCa-2 and AsPC-1 Microarray Top Tables.

Name	Avg FC		Median P-value	
	AsPC-1	Mia Paca-2	AsPC-1	Mia Paca-2
hsa-miR-101*	0.214	0.493	0.057	0.051
hsa-miR-10b*	0.241	0.453	0.111	0.033
hsa-miR-1229	0.310	0.463	0.092	0.031
hsa-miR-1237	0.247	0.419	0.097	0.080
hsa-miR-1247	2.920	0.377	0.039	0.076
hsa-miR-132	0.401	0.463	0.035	0.014
hsa-miR-136*	0.489	0.482	0.024	0.008
hsa-miR-145	0.275	0.471	0.032	0.102
hsa-miR-148b	0.303	0.451	0.024	0.013
hsa-miR-19b-1*	0.343	0.425	0.018	0.039
hsa-miR-20a*	0.442	0.424	0.049	0.033
hsa-miR-223	0.391	0.423	0.068	0.007
hsa-miR-301b	0.363	0.374	0.026	0.006
hsa-miR-302c*	0.400	0.429	0.016	0.034
hsa-miR-367	0.338	0.503	0.033	0.054
hsa-miR-370	0.303	0.386	0.032	0.049
hsa-miR-380	0.324	0.493	0.025	0.037
hsa-miR-425	0.189	0.383	0.116	0.069
hsa-miR-4258	0.340	0.267	0.000	0.001
hsa-miR-432*	0.446	0.385	0.013	0.006
hsa-miR-450b-3p	0.335	0.450	0.051	0.145
hsa-miR-454*	4.188	4.451	0.000	0.000
hsa-miR-507	0.144	0.470	0.046	0.105
hsa-miR-518a-3p	0.483	0.501	0.011	0.034
hsa-miR-518d-3p	0.322	0.217	0.111	0.012
hsa-miR-518f*	0.301	0.283	0.010	0.002
hsa-miR-519d	0.392	0.447	0.119	0.053
hsa-miR-548w	0.146	0.481	0.355	0.252
hsa-miR-579	0.316	0.474	0.160	0.362
hsa-miR-582-3p	0.343	0.399	0.097	0.024
hsa-miR-588	0.393	0.340	0.112	0.015
hsa-miR-643	0.417	0.433	0.027	0.040
hsa-miR-656	0.501	0.418	0.007	0.008
hsa-miR-770-5p	0.239	0.445	0.039	0.069

A table of the 34 miRNAs demonstrating an average fold change (Avg FC) of > 2 (red) or < 0.5 (blue) and a p-value of <0.5 (Med P-value) following treatment for 24 hours with 5μM curcumin in both MIA PaCa-2 and AsPC-1 cells.

3.2.4. Global Decreases in miRNA Expression

Microarray profiling in both PC cell lines revealed ~80% of miRNAs showing a global decrease in expression following curcumin treatment. It was assumed that, in order for curcumin to regulate a large number of miRNAs, it must act within a pathway with the capacity to affect many of these non-coding RNAs. An inherent logical belief was that curcumin may be affecting the miRNA biogenesis machinery, in particular the RNase proteins drosha and dicer. To ascertain if this was the case, either at the mRNA or protein level, SensiMix SYBR® green RT-qPCR (section 2.2.8.3) and western blot analysis (section 2.2.5.3) were carried out following treatment of both PC cell lines for 24 hours with 5μM curcumin (Figure 3.7).

No statistically significant changes in either drosha or dicer mRNA abundance, when normalised against 18S rRNA expression, were observed for either cell line following curcumin treatment (Figure 3.7). Western blot data, when normalised against the DMSO control, showed a doubling in expression for drosha following treatment with curcumin in MIA PaCa-2 cell; however, no change was observed for AsPC-1 cells (Figure 3.7E). Protein expression for dicer appeared to be unchanged in both cell lines following curcumin treatment (Figure 3.7F). Interestingly, it was observed that when compared to normal pancreas (NP), drosha and dicer mRNA expression was elevated in both PC cell lines (Figure 3.8).

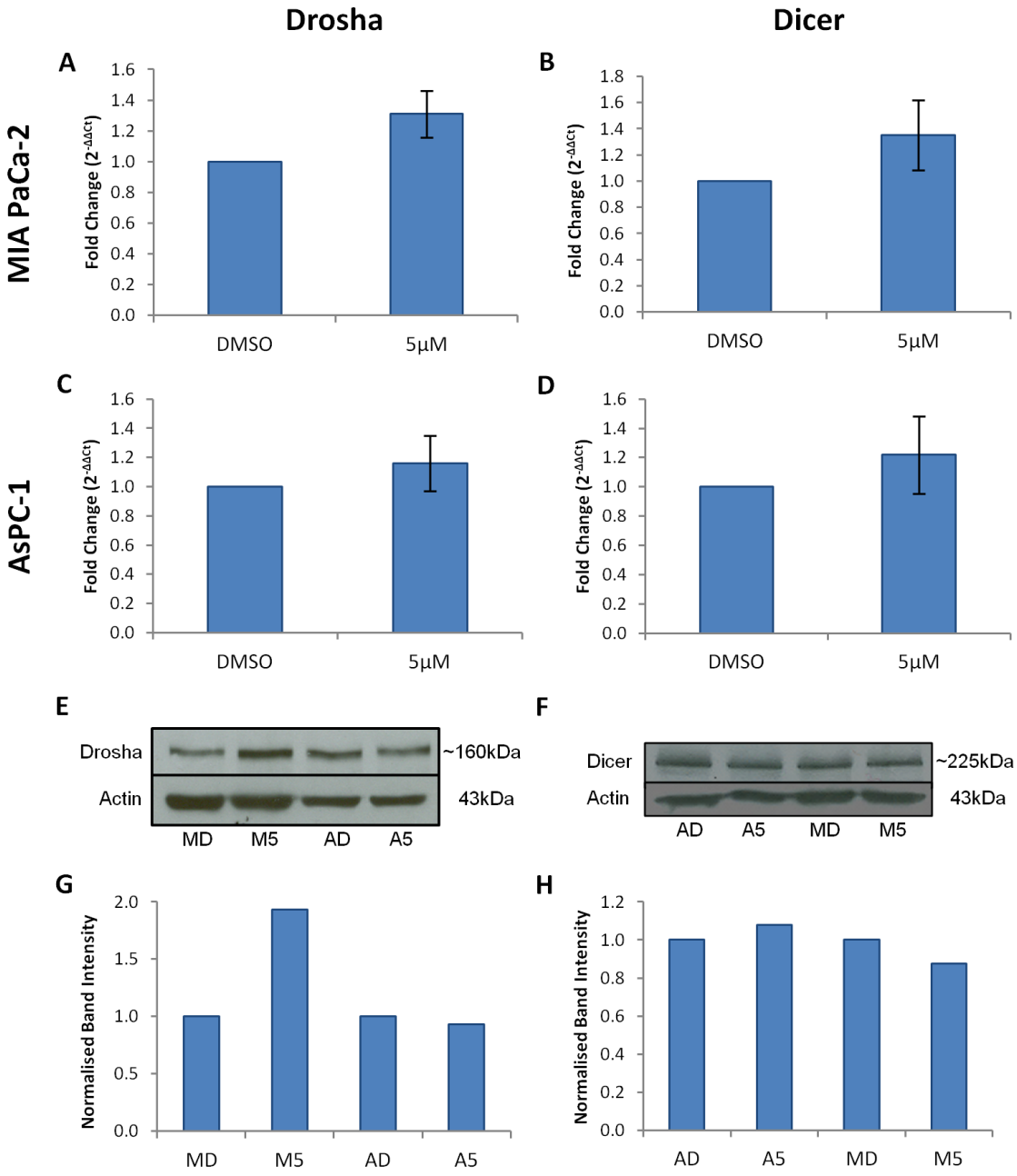

Figure 3.7: Effects of Curcumin on Drosha and Dicer mRNA and Protein Expression. MIA PaCa-2 and AsPC-1 cells were treated with 5µM curcumin or DMSO (control) for 24 hours and analysed for **(A, C)** drosha and **(B, D)** dicer mRNA expression. SensiMix SYBR Green RT-qPCR data were normalised against 18S rRNA and represent the mean ± SEM (n=4) (paired T-test). Representative ECL blots showing changes in amount of **(E)** drosha and **(F)** dicer following treatment with curcumin with actin as a loading control. Histograms representing changes in band intensity of **(G)** drosha (n=1) and (**H)** dicer (n=1) protein expression for curcumin treated cells when normalised against DMSO treated cells. (Key: MD = MIA PaCa-2 DMSO treated, M5= MIA PaCa-2 curcumin treated, AD = AsPC-1 DMSO treated, A5 = AsPC-1 curcumin treated.)

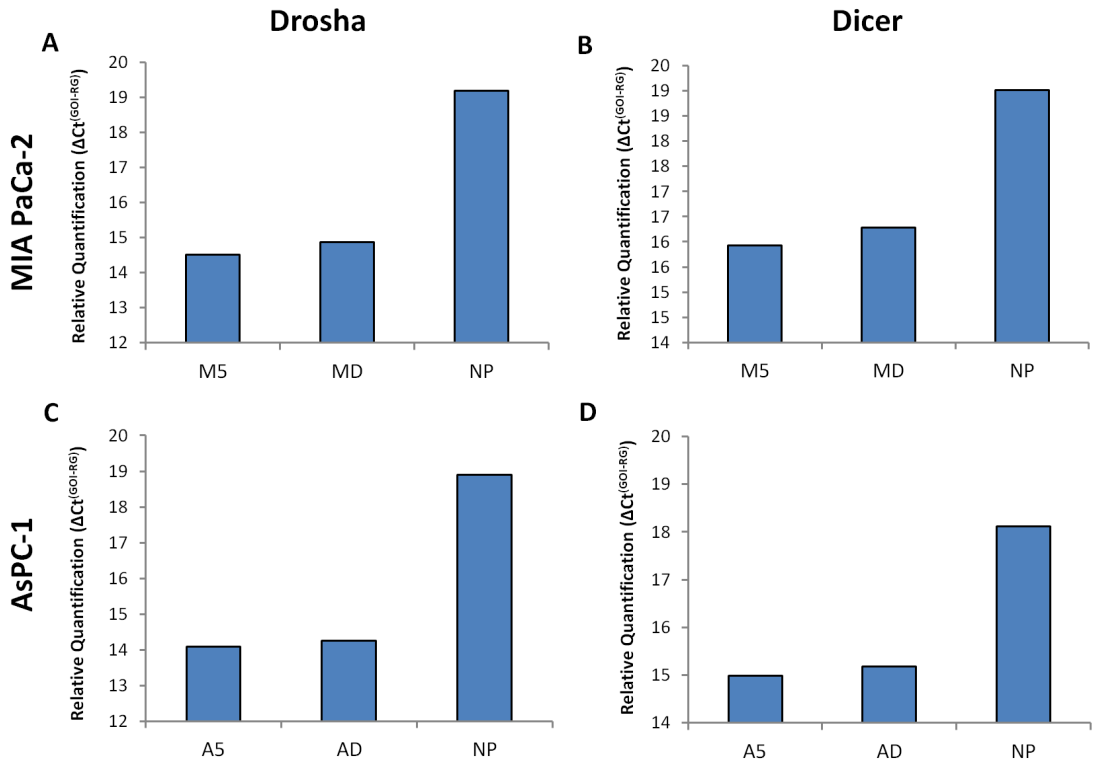

Figure 3.8: Drosha and Dicer mRNA Expression in MIA PaCa-2 and AsPC-1 Cells Compared With Normal Pancreas. RT-qPCR data were normalised against 18S rRNA and represent the $\Delta Ct^{(GOI-RG)}$ value for drosha and dicer in **(A, B)** MIA PaCa-2 and **(C, D)** AsPC-1 cells. (Key: MD = MIA PaCa-2 DMSO treated, M5= MIA PaCa-2 curcumin treated, AD = AsPC-1 DMSO treated, A5 = AsPC-1 curcumin treated, NP = normal pancreas, GOI = gene of interest, RG = reference gene.).

3.2.5. Canonical Pathway Analysis

To identify if the miRNAs differentially expressed following curcumin treatment were involved in common regulatory networks, 6 miRNAs (miR-223, miR-132, miR-370, miR-380, miR-145 and miR-143) were investigated. These miRNAs were entered into the miRWalk database and a list of target mRNAs containing validated binding sites was obtained and uploaded to Ingenuity IPA software for pathway analysis (IngenuityR Systems, www.ingenuity.com) to investigate any associations between them. The IPA software identified canonical pathways which contained a significant number of these mRNAs shown to be potential targets of the differentially expressed miRNAs (Table 3.5). These target mRNAs, which were potentially affected following curcumin treatment, were represented as either the ratio or number of genes. Interestingly within the top 5 significantly enriched canonical pathways for this miRNA combination was the pancreatic adenocarcinoma signalling pathway (Figure 3.9). This supports the idea that through its ability to modulate the expression of various miRNAs, curcumin may be able to regulate pancreatic tumourigenesis.

Table 3.5: Canonical Pathways Predicted by IPA Analysis as Significantly Altered as a Result of Curcumin Treatment.

Ingenuity Canonical Pathways	-log p-value	Ratio	Genes
Colorectal Cancer Metastasis Signalling	31.70	0.17	45/268
Molecular Mechanisms of Cancer	31.10	0.13	51/388
Role of Macrophages, Fibroblasts and Endothelial Cells in Rheumatoid Arthritis	28.30	0.14	46/342
Pancreatic Adenocarcinoma Signalling	28.20	0.24	31/128
Glucocorticoid Receptor Signalling	26.90	0.14	42/299
Glioblastoma Multiforme Signalling	26.10	0.20	33/168
Hepatic Fibrosis / Hepatic Stellate Cell Activation	25.70	0.21	32/155
Acute Myeloid Leukemia Signalling	22.80	0.29	24/84
IL-8 Signalling	21.40	0.14	32/225
Role of Tissue Factor in Cancer	21.10	0.20	26/130
PI3K/AKT Signalling	21.10	0.18	27/152
Prostate Cancer Signalling	20.50	0.22	23/103
ILK Signalling	20.30	0.15	31/205
Ovarian Cancer Signalling	20.10	0.18	27/152
IL-12 Signalling and Production in Macrophages	20.10	0.17	27/157
Glioma Signalling	19.10	0.20	23/113
TGF-β Signalling	18.70	0.23	22/94
Role of Osteoblasts, Osteoclasts and Chondrocytes in Rheumatoid Arthritis	18.20	0.12	31/250
HMGB1 Signalling	18.00	0.20	22/109
Chronic Myeloid Leukemia Signalling	17.90	0.21	22/106
PPARα/RXRα Activation	17.80	0.14	28/200
Thyroid Cancer Signalling	17.40	0.36	16/44
Aryl Hydrocarbon Receptor Signalling	17.30	0.15	25/171
Bladder Cancer Signalling	17.20	0.22	21/97
Cardiac Hypertrophy Signalling	16.90	0.12	30/250
PTEN Signalling	16.90	0.17	23/138
Renal Cell Carcinoma Signalling	16.90	0.24	19/79
IL-17 Signalling	16.60	0.25	19/75
Regulation of the Epithelial-Mesenchymal Transition Pathway	16.50	0.14	27/196
Ed	16.40	0.25	18/73
ErbB Signalling	16.40	0.22	20/90
ERK5 Signalling	16.30	0.27	18/68
p53 Signalling	16.30	0.19	21/113
NF-κB Signalling	16.00	0.14	26/181
B Cell Receptor Signalling	15.90	0.14	25/175
IL-6 Signalling	15.80	0.18	22/124
NGF Signalling	15.50	0.17	21/122
PEDF Signalling	15.40	0.23	18/79

Table 3.5 Continued:

Ingenuity Canonical Pathways	-log p-value	Ratio	Genes
LPS-stimulated MAPK Signalling	15.20	0.22	18/83
iNOS Signalling	15.10	0.28	15/53
Germ Cell-Sertoli Cell Junction Signalling	15.10	0.14	24/169
Neuregulin Signalling	14.80	0.18	19/104
GNRH Signalling	14.70	0.14	22/153
EGF Signalling	14.70	0.25	16/64
Regulation of IL-2 Expression in Activated and Anergic T Lymphocytes	14.50	0.20	18/89
Renin-Angiotensin Signalling	14.20	0.16	20/126
ERK/MAPK Signalling	14.10	0.12	25/211
Melanoma Signalling	14.00	0.28	14/50
STAT3 Pathway	13.90	0.21	17/80
Endometrial Cancer Signalling	13.90	0.25	15/60

Having obtained a list of target mRNAs for the miRNA combination miR-223, miR-132, miR-370, miR-380, miR-145 and miR-143 using miRWalk, these data were uploaded to the Ingenuity IPA software in order to identify any canonical pathways which may have been affected following treatment of PC cells with curcumin. Both the ratio and genes columns represent the number of mRNAs that could potentially be affected by curcumin within each canonical pathway. The significance for each canonical pathway is represented as the –log of the p-value (whereby a p-value of 0.001 is represented as a –log value of 3).

3.2.6. Validation of Differentially Expressed miRNAs using RT-qPCR

To confirm the microarray findings, Taqman® RT-qPCR (section 2.2.8.1) was used to initially validate a subset of five of the top differentially expressed miRNAs; miR-132, miR-380, miR-370, miR-223 and miR-145. These appeared to be regulated following treatment with 5μM curcumin for 24 hours in both PC cell lines (fold change < 0.5, p-value < 0.07) (Tables 3.2 and 3.3). The miR-21-3p, even though only differentially expressed in AsPC-1 cells following curcumin treatment (fold change <0.5, p-value <0.1), was also chosen for RT-qPCR validation based on its suggested oncogenic potential, having been extensively studied in numerous cancers including PC (Table 3.3) (Ye et al, 2014; Chan et al, 2005; Bhatti et al, 2011).

The identification of miR-132, miR-380 and miR-370 as significantly downregulated by microarray analysis in both PC cell lines following curcumin treatment could not be validated by Taqman® RT-qPCR when using a p-value <0.05 (Figure 3.10). Target miRNA expression appeared to increase for miR-132 (Figure 3.10A and B), miR-380 (Figure 3.10C and D) and miR-370 (Figure 3.10E and F) compared to DMSO treated samples in both cell lines, however these changes were not statistically significant.

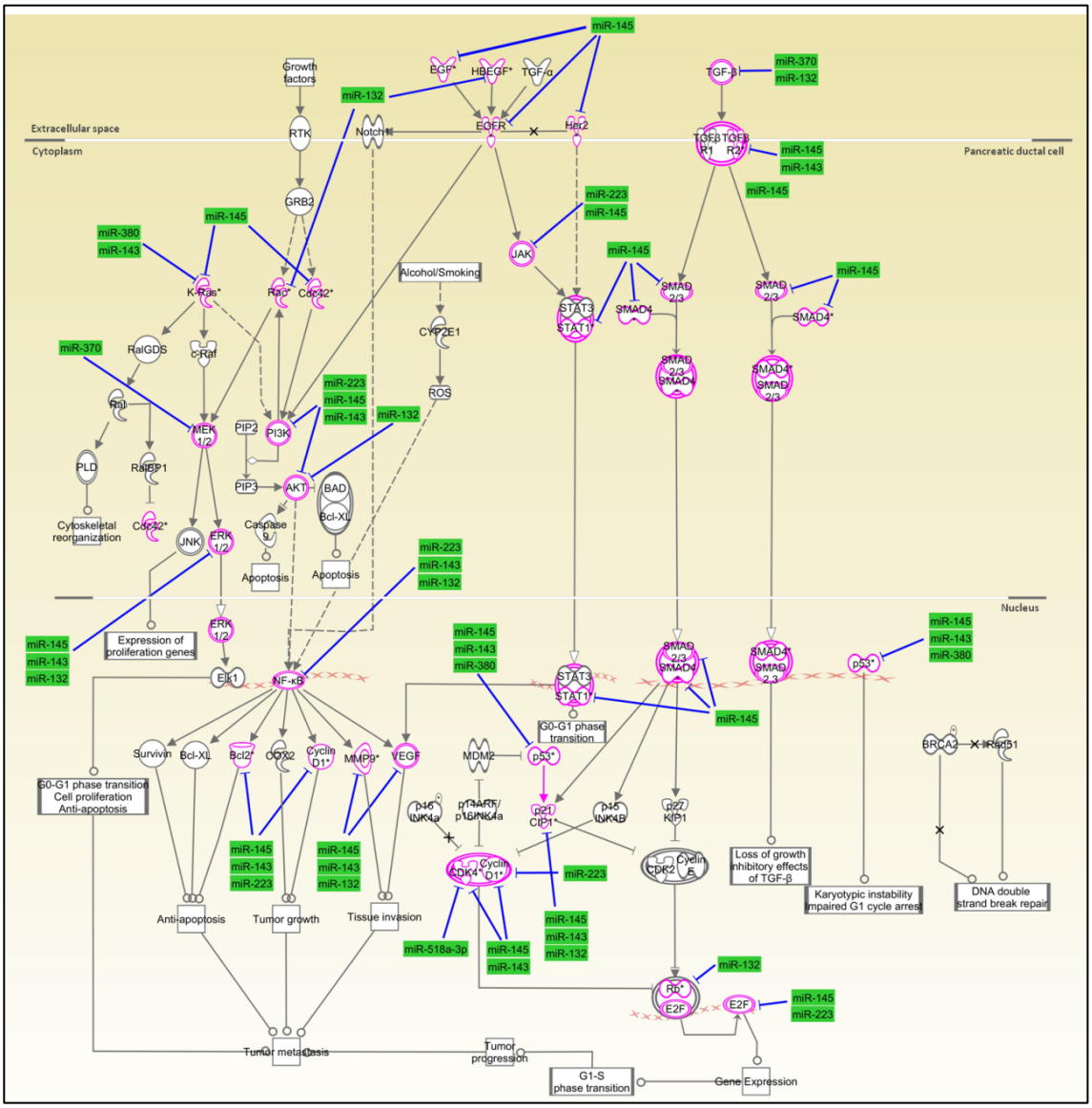

Figure 3.9: The Pancreatic Adenocarcinoma Signalling Pathway. The mRNA target list produced in miRWalk for the selected miRNAs was uploaded to Ingenuity IPA software and connections between these mRNAs were mapped. Of the 128 mRNA target encoding genes associated with the pancreatic adenocarcinoma signalling pathway, 31 were targeted by one or more of the assessed miRNAs and are highlighted in pink. Interactions between the molecules in this pathway are indicated by solid and dashed grey lines corresponding to direct and indirect interactions respectively. The miRNAs deregulated in curcumin treated PC cells are coloured green according to their decrease in expression and blue lines are used to indicate their validated mRNA targets (an enlarged version of this figure is available in Appendix 8).

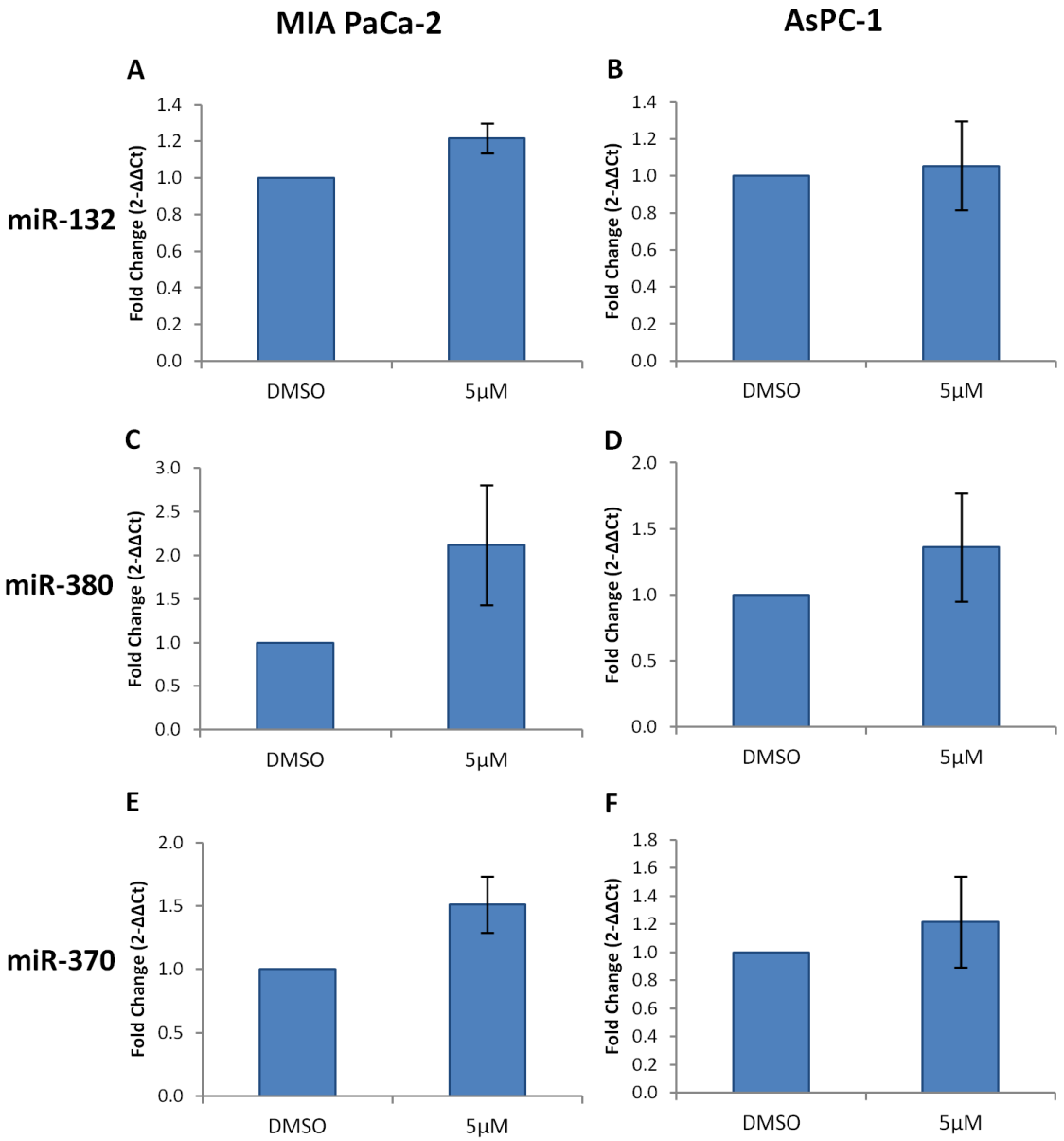

Figure 3.10: Taqman® RT-qPCR Analysis for Validation of Microarray Profiling Data. MIA PaCa-2 and AsPC-1 cells were treated with 5µM curcumin or DMSO (control) for 24 hours and analysed for **(A, B)** miR-132 **(C, D)** miR-380 and **(E, F)** miR-370. RT-qPCR data were normalised against RNU6B and represent the mean ± SEM (n=4) (paired T-test, no data with $p \leq 0.05$).

Similarly for miR-223, miR-145 and miR-21-3p RT-qPCR analysis could not validate the downregulation in target expression initially observed following microarray analysis (Figure 3.11). For miR-223 and miR-21-3p in both PC cell lines, treatment with curcumin resulted in either no effect or elevated expression of target miRNA (Figure 3.11A, B, E and F). Within MIA PaCa-2 cells curcumin treatment did not appear to affect miR-145 expression, but in AsPC-1 cells miR-145 was reduced in expression, although none of these changes were statistically significant (Figure 3.11C and D).

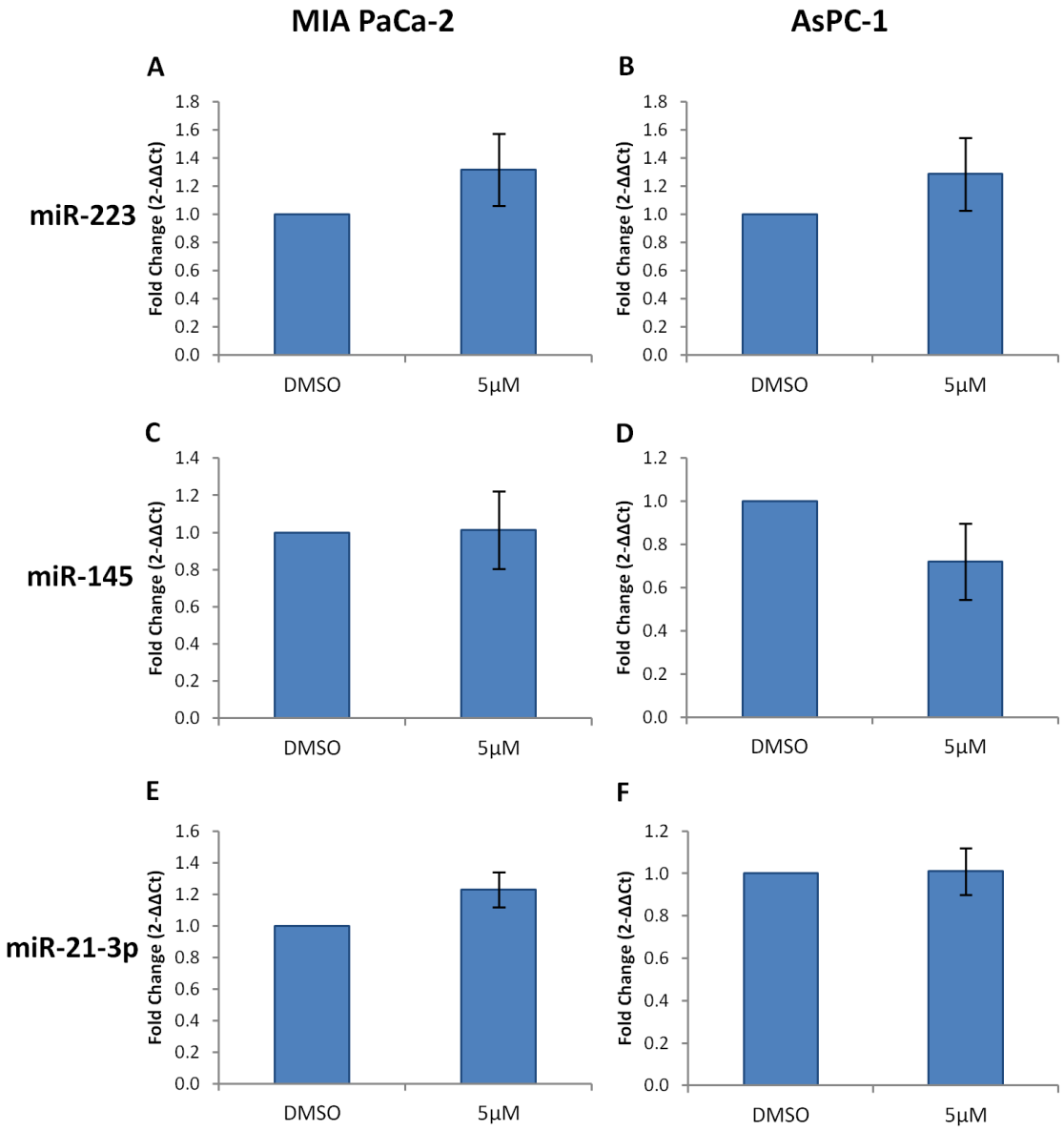

Figure 3.11: Taqman® RT-qPCR Analysis for Validation of Microarray Profiling Data. MIA PaCa-2 and AsPC-1 cells were treated with 5µM curcumin or DMSO (control) for 24 hours and analysed for **(A, B)** miR-223 **(C, D)** miR-145 and **(E, F)** miR-21-3p. RT-qPCR data were normalised against RNU6B and represent the mean ± SEM (n=4) (paired t-test).

The miR-145 is clustered and transcribed with miR-143, with repression of both miRNAs by Ras commonly observed in PC. K-Ras mutant cell lines, including MIA PaCa-2 and AsPC-1 have also been shown to contain negligible levels of both miRNAs. With the miR-143/145 cluster commonly downregulated in PC, and the identification of miR-145 as a differentially expressed target following treatment (Table 3.2 and 3.3), it was deemed logical to assess the effects of curcumin on miR-143 expression (Kent et al, 2009; Pramanik et al, 2011; Kent et al, 2010). MiScript SYBR® Green RT-qPCR (section 2.2.8.2) revealed increased miR-143 expression in MIA PaCa-2 cells following

curcumin treatment (Figure 3.12A), however this change in expression was not statistically significant. Curcumin treated AsPC-1 cells appeared to have no change in miR-143 expression (Figure 3.12B).

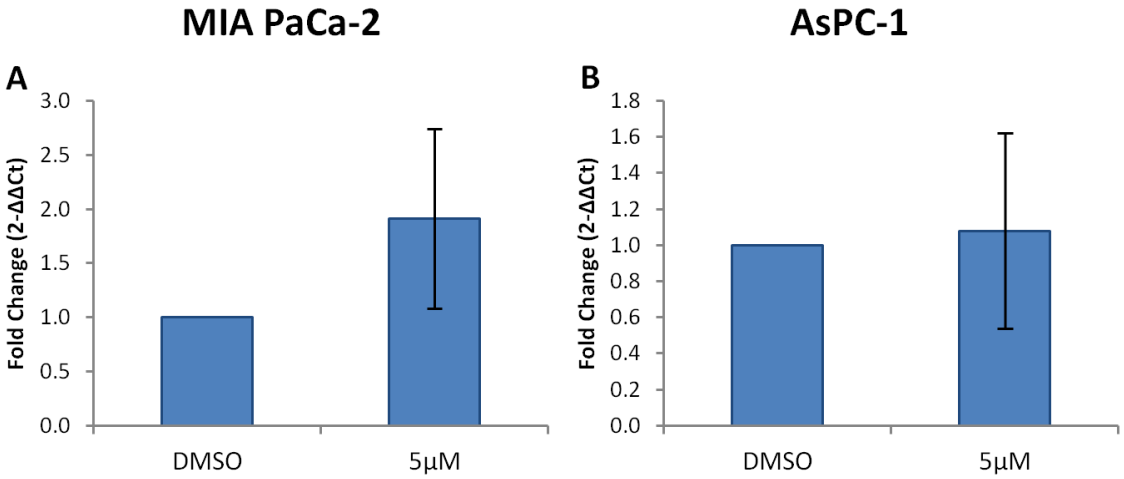

Figure 3.12: miScript SYBR® Green RT-qPCR Analysis of miR-143. Cells were treated for 24 hours. RT-qPCR data were normalised against miR-15a and represent the mean ± SEM for miR-143 expression (n=4) (paired T-test).

The inability to validate any of the differentially expressed miRNAs observed by microarray analysis using RT-qPCR raised concerns about the reliability of the microarrays and the data they produced. Each microarray slide contained four probe set repeats for each miRNA, with each probe repeat located in a different geographical location within the microarray (Figure 3.1). After normalisation the fold change for each of the four probe repeats was calculated by combining data from all the microarray slides within an experiment. The fold change values for each probe were then combined to calculate the average fold change, and this value was used (in addition to the p-value) to establish the top differentially expressed miRNAs following curcumin treatment in MIA PaCa-2 and AsPC-1 cells (Table 3.2 and 3.3). Any irregularities in fold change for the four probe set repeats for each miRNA could affect the average fold change used to identify any differentially expressed miRNAs, highlighting a change in expression that may not be genuine. When examined, the fold change values for each probe repeat, although not identical, were sufficiently similar with no anomalous elevation in fold change which could explain the RT-qPCR validation results (Table 3.6).

Table 3.6: Microarray Probe Repeat Fold Change Values.

Cell Line	microRNA	FC Probe Rep 1.	FC Probe Rep 2.	FC Probe Rep 3.	FC Probe Rep 4.	Avg FC	Median p-value
MIA PaCa-2	hsa-miR-132	0.409	0.440	0.443	0.576	0.463	0.014
MIA PaCa-2	hsa-miR-380	0.286	0.438	0.656	0.716	0.493	0.037
MIA PaCa-2	hsa-miR-370	0.214	0.419	0.457	0.542	0.386	0.049
MIA PaCa-2	hsa-miR-223	0.249	0.438	0.462	0.636	0.423	0.007
MIA PaCa-2	hsa-miR-145	0.298	0.389	0.609	0.694	0.471	0.102
MIA PaCa-2	hsa-miR-21-3p	0.421	0.614	0.705	0.735	0.604	0.123
AsPC-1	hsa-miR-132	0.263	0.392	0.497	0.503	0.401	0.035
AsPC-1	hsa-miR-380	0.174	0.175	0.527	0.688	0.324	0.025
AsPC-1	hsa-miR-370	0.193	0.234	0.334	0.558	0.303	0.032
AsPC-1	hsa-miR-223	0.277	0.338	0.371	0.673	0.391	0.068
AsPC-1	hsa-miR-145	0.056	0.429	0.465	0.515	0.275	0.032
AsPC-1	hsa-miR-21-3p	0.122	0.391	0.401	0.674	0.337	0.109

High	2
NC	1
Low	0

Each microarray slide contained four probe set repeats for each miRNA, with each probe repeat located in a different geographical location within the microarray. After normalisation the fold change for each of the four probe repeats was calculated by combining data from the 15 microarray slides which made up each experiment. The fold change values calculated for the four probe repeats (FC Probe Rep) belonging to each miRNA within a microarray slide were combined to determine the average FC (Avg FC) for each miRNA target. The significance for each Avg FC is represented as the median p-value. (Key: FC = fold change, Avg = Average)

Further validation of the microarray findings was attempted using miScript SYBR® Green RT-qPCR to confirm differential expression of four additional miRNAs (miR-518f*, miR-518d-3p, miR-518a-3p and miR-148a). Interestingly, in both PC cell lines miR-518f*, miR-518d-3p and miR-518a-3p were differentially expressed following microarray analysis when treated with curcumin (fold change < 0.5, p-value < 0.1). It is only recently that studies have highlighted the involvement of miR-518 family members in cancer, however at the outset of this research little was known about their actions (Zhang et al, 2012; Rubie et al, 2014; Kushwaha et al, 2014). The rationale, therefore, in choosing these miRNAs was that if curcumin could modulate a number of miRNAs from the same family, this family could potentially be of some importance in PC progression. To assess miR-518a-3p and miR-518d-3p expression a mix containing both primers was produced for RT-qPCR analysis, referred to as miR-518da-3p. The reduced expression of miR-148a has been associated with PC, with some studies suggesting that its expression, or lack thereof, could be of diagnostic relevance

(Bloomston et al, 2007; Szafranska et al, 2007). Therefore the apparent ability of curcumin to deregulate the expression of this miRNA in both PC cell lines (fold change < 0.5, p-value < 0.1) was chosen for validation by RT-qPCR.

The decreased expression of these miRNAs following curcumin treatment could not be successfully validated (Figure 3.13). In most cases curcumin appeared to increase target miRNA expression, as was the case for miR-518f*, miR-518da-3p and miR-148a, although these data were not found to be statistically significant (Figure 3.13 A-C, E and F). As with Table 3.6, fold change values of the four probe set repeats for the miR-518 family members and miR-148a were assessed (Table 3.7). Most fold change values were similar between the repeats, however the values relating to FC probe repeat four appeared elevated when compared to the other repeats, but not by enough to alter the average fold change calculated (Table 3.7).

3.2.7. Analysis of Curcumin Induced Changes in miRNAs Previously Associated with Pancreatic Cancer using RT-qPCR

In addition to discovering novel miRNA targets dysregulated in PC and modulated by curcumin, part of the objective was to identify miRNAs previously shown to be aberrantly expressed in PC which may also respond to curcumin. Both the miR-34 and miR-200 families have been frequently associated with PC, especially in regard to CSC, EMT and drug resistance, processes commonly linked to poor prognosis and advanced disease (Li et al, 2009; Chang et al, 2007; Kent et al, 2009; Bao et al, 2011b; Pramanik et al, 2011; Bao et al, 2011a; Bao et al, 2012; Ji et al, 2009).

Increased expression of miR-200b and miR-200c in both PC cell lines following treatment with 5μM curcumin for 24 hours was observed by miScript SYBR® Green RT-qPCR analysis (Figure 3.14), with a statistically significant ($p<0.05$) increase in miR-200c in MIA PaCa-2 cells (Figure 3.14C). Although not statistically significant, miR-34a and miR-34b were also seen to increase in expression following curcumin treatment (Figure 3.15). The potential of curcumin to increase the expression of these miRNAs, which are usually downregulated in PC, is a promising result.

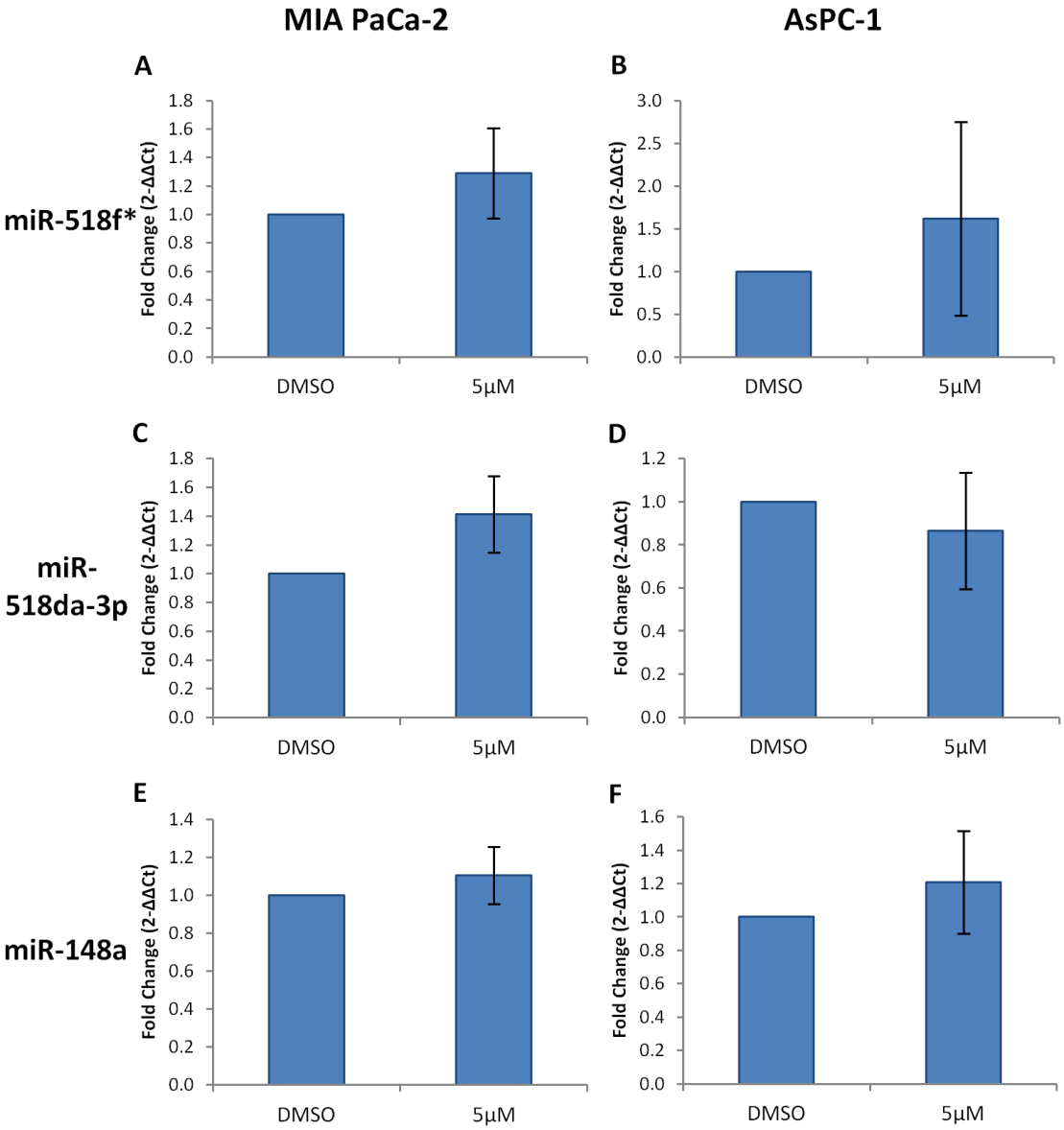

Figure 3.13: miScript SYBR® Green RT-qPCR Analysis used to Validate Microarray Profiling Data. MIA PaCa-2 and AsPC-1 cells were treated with 5µM curcumin or DMSO (control) for 24 hours and analysed for **(A, B)** miR-518f* **(C, D)** miR-518da-3p and **(E, F)** miR-148a. The miR-518da-3p experiment used a primer mix containing half miR-518a-3p and half miR-518d-3p. RT-qPCR data were normalised against miR-15a and represent the mean ± SEM (n=4) (paired T-test).

Table 3.7: Microarray Probe Repeat Fold Change Values.

Cell Line	miRNA	FC Probe Rep 1.	FC Probe Rep 2.	FC Probe Rep 3.	FC Probe Rep 4.	Avg FC	Median p-value
MIA PaCa-2	hsa-miR-518f*	0.120	0.342	0.390	0.400	0.283	0.002
MIA PaCa-2	hsa-miR-518d-3p	0.069	0.360	0.411		0.217	0.012
MIA PaCa-2	hsa-miR-518a-3p	0.421	0.443	0.558	0.604	0.501	0.034
MIA PaCa-2	hsa-miR-148a	0.152	0.372	0.416	0.809	0.372	0.038
AsPC-1	hsa-miR-518f*	0.101	0.194	0.327	1.271	0.301	0.010
AsPC-1	hsa-miR-518d-3p	0.139	0.259	0.271	1.109	0.322	0.111
AsPC-1	hsa-miR-518a-3p	0.261	0.464	0.615	0.728	0.483	0.011
AsPC-1	hsa-miR-148a	0.180	0.186	0.593	0.711	0.345	0.393

High	2
NC	1
Low	0

The fold change values calculated for the four probe repeats(FC Probe Rep) belonging to each miRNA within a microarray slide were combined to determine the average FC (Avg FC) for each miRNA target. The significance for each Avg FC is represented as the median p-value. (Key: FC = fold change, Avg = Average)

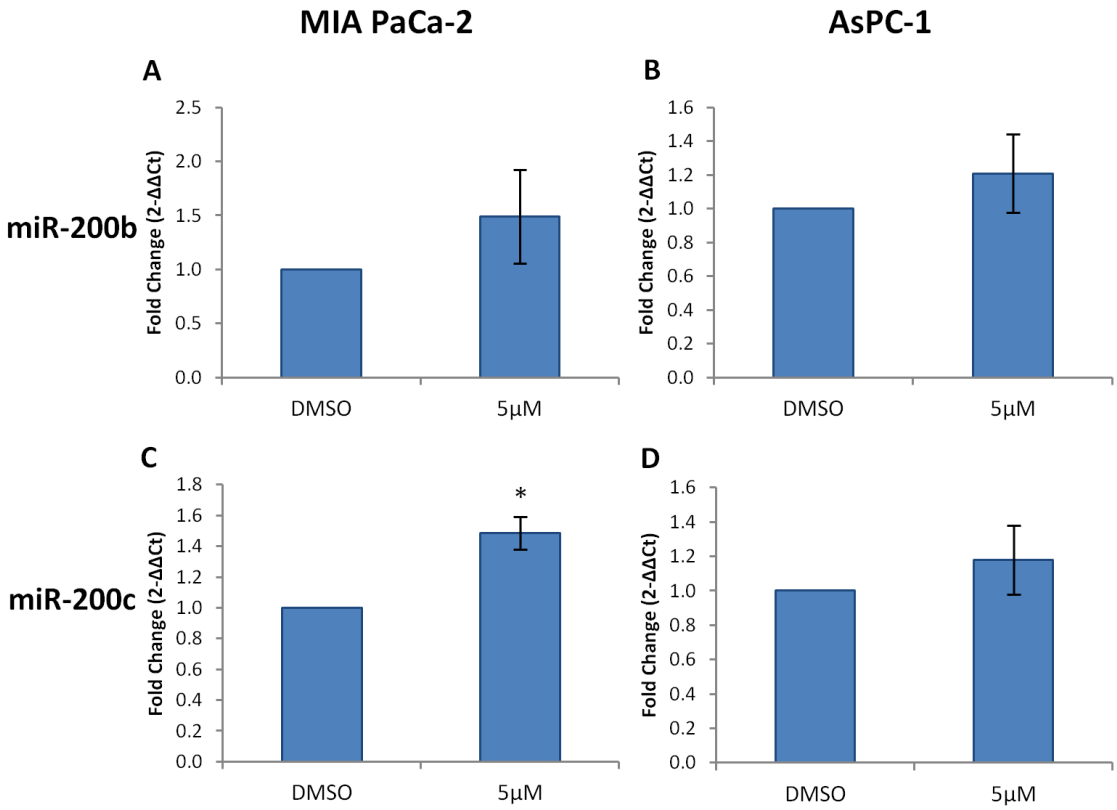

Figure 3.14: miScript SYBR® Green RT-qPCR Analysis of miR-200b/c. Cells were treated with curcumin or DMSO for 24 hours and analysed for **(A, B)** miR-200b or **(C, D)** miR-200c. RT-qPCR data were normalised against miR-15a and represent the mean ± SEM (n=4) (paired T-test * $p < 0.05$).

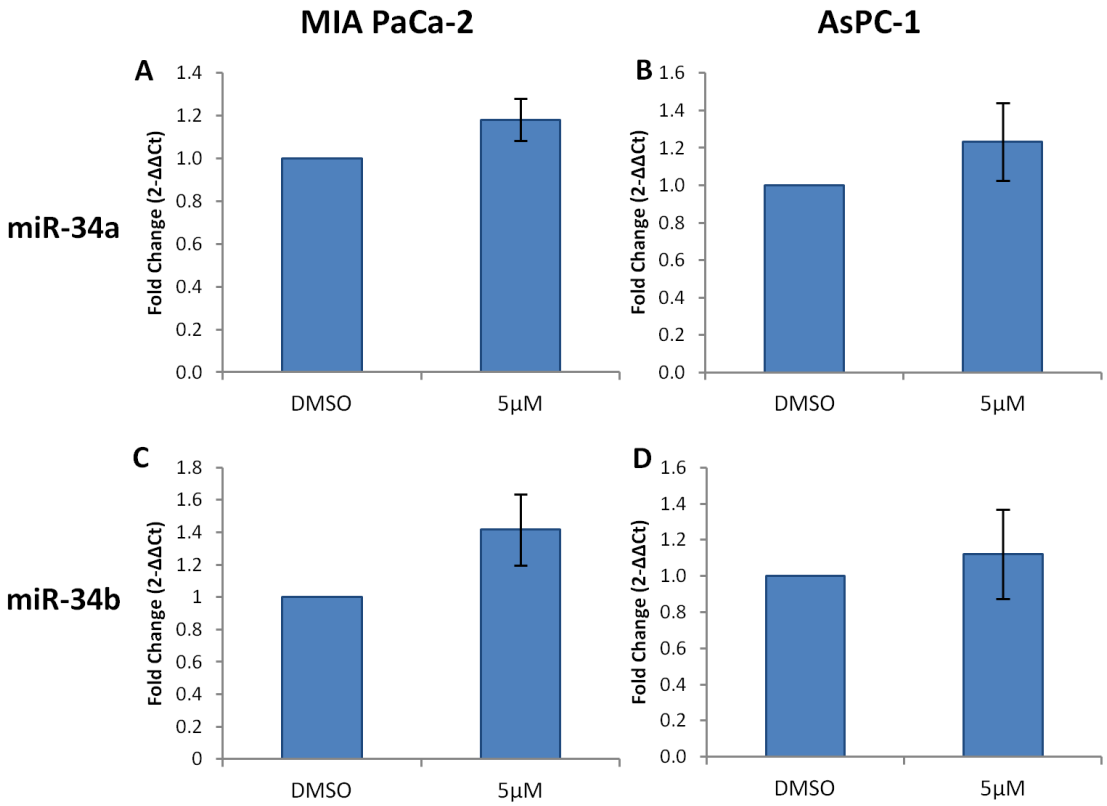

Figure 3.15: miScript SYBR® Green RT-qPCR Analysis of miR-34a/b. Cells were treated with curcumin or DMSO for 24 hours and analysed for **(A, B)** miR-34a or **(C, D)** miR-34b. RT-qPCR data were normalised against miR-15 and represent the mean ± SEM (n=4) (paired t-Test).

3.2.8. Target Gene Analysis by RT-qPCR

A key objective was to establish whether curcumin treatment could not only modulate the expression of relevant miRNAs, but also regulate key proteins involved in PC. Consequently Notch2, Notch3, Ras-responsive element-binding protein (RREB1), enhancer of zeste homologue 2 (EZH2) and c-Myc mRNA levels were assessed following treatment.

The activation and overexpression of Notch signalling proteins has been linked to increased chemoresistance in PC cells. Several *in vitro* and *in vivo* studies have shown how elevated Notch expression in PC has led to the development of EMT and accelerated disease progression (Wang et al, 2011; Wang et al, 2009b; Guengoer et al, 2011). Previous research within this laboratory has demonstrated the association of Notch signalling with aggressive disease and poor prognosis in PC, in particular Notch3, which was suggested as a potential biomarker for advanced disease (Mann et al, 2012; Doucas et al, 2008). Emerging evidence has suggested that miRNAs are able

to regulate Notch signalling in tumourigenesis, with members of both the miR-200 and miR-34 families shown to target Notch signalling in various cancers, including PC (Ji et al, 2009; Vallejo et al, 2011; Wang et al, 2010b; Radtke and Raj, 2003). Studies in both pancreatic and esophageal cancer cells have also demonstrated the ability of curcumin to downregulate Notch1 expression resulting in growth inhibition and apoptosis (Subramaniam et al, 2012; Wang et al, 2006). On this basis, expression levels of Notch2 and Notch3 were assessed by SensiMix SYBR Green RT-qPCR following treatment. Unfortunately, no significant changes in expression were observed for either target (Figure 3.16).

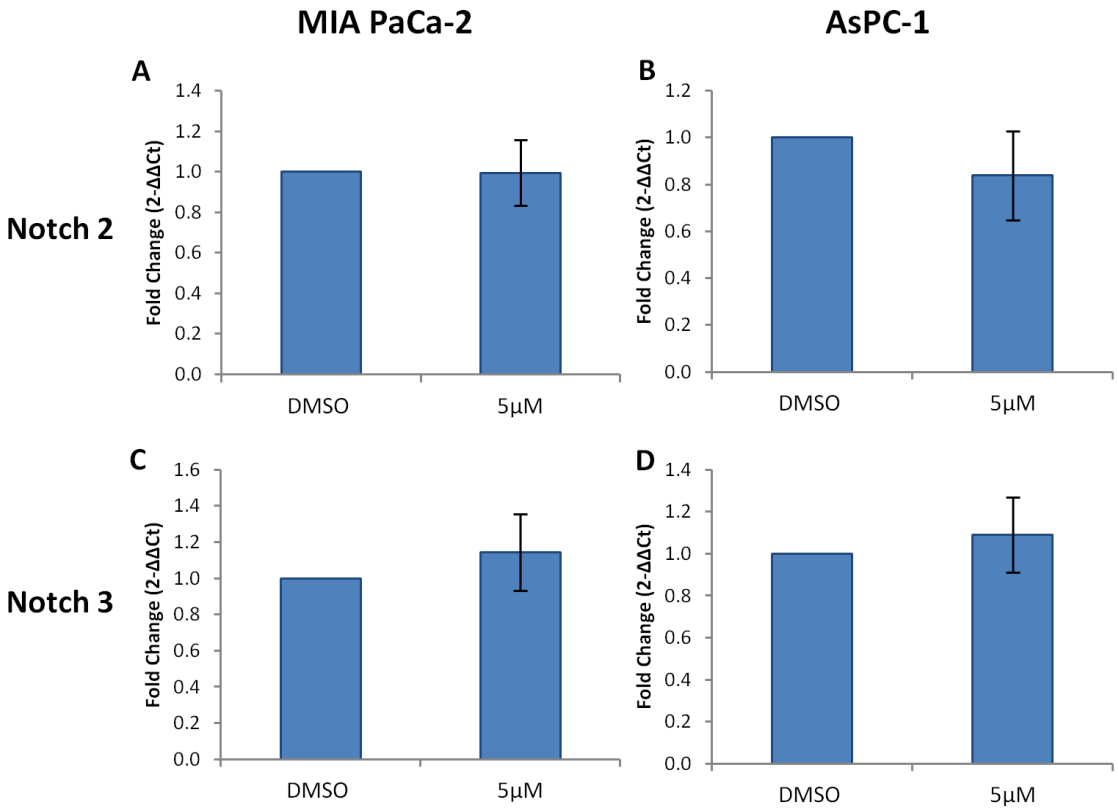

Figure 3.16: SensiMix SYBR Green RT-qPCR Analysis of Notch2/3. Cells were treated as shown for 24 hours and analysed for Notch 2 and Notch 3 mRNA expression. RT-qPCR data were normalised against 18S RNA and represent the mean ± SEM (n=4) (paired T-test).

As previously mentioned, the miR-143/145 cluster is often repressed in K-Ras mutant PC cells. This downregulation also requires RREB1, a downstream effector of Ras, which represses the miR-143/145 promoter, preventing target miRNA expression (Pramanik et al, 2011; Kent et al, 2010; Pham et al, 2013). EZH2 which is believed to be a CSC marker and the TF c-Myc are also overexpressed in PC. When treated with CDF the expression of EZH2 both *in vitro* and *in vivo* becomes reduced (Bao et al,

2011a; Bao et al, 2012; Li et al, 2013). It has also been shown that both miR-34 family members and miR-145 are able to negatively regulate c-Myc (Asano et al, 2004; Boominathan, 2010; Buchholz et al, 2006; Hermeking, 2010). SensiMix SYBR Green RT-qPCR analysis showed no change in RREB1, EZH2 or c-Myc expression following treatment with curcumin (Figure 3.17).

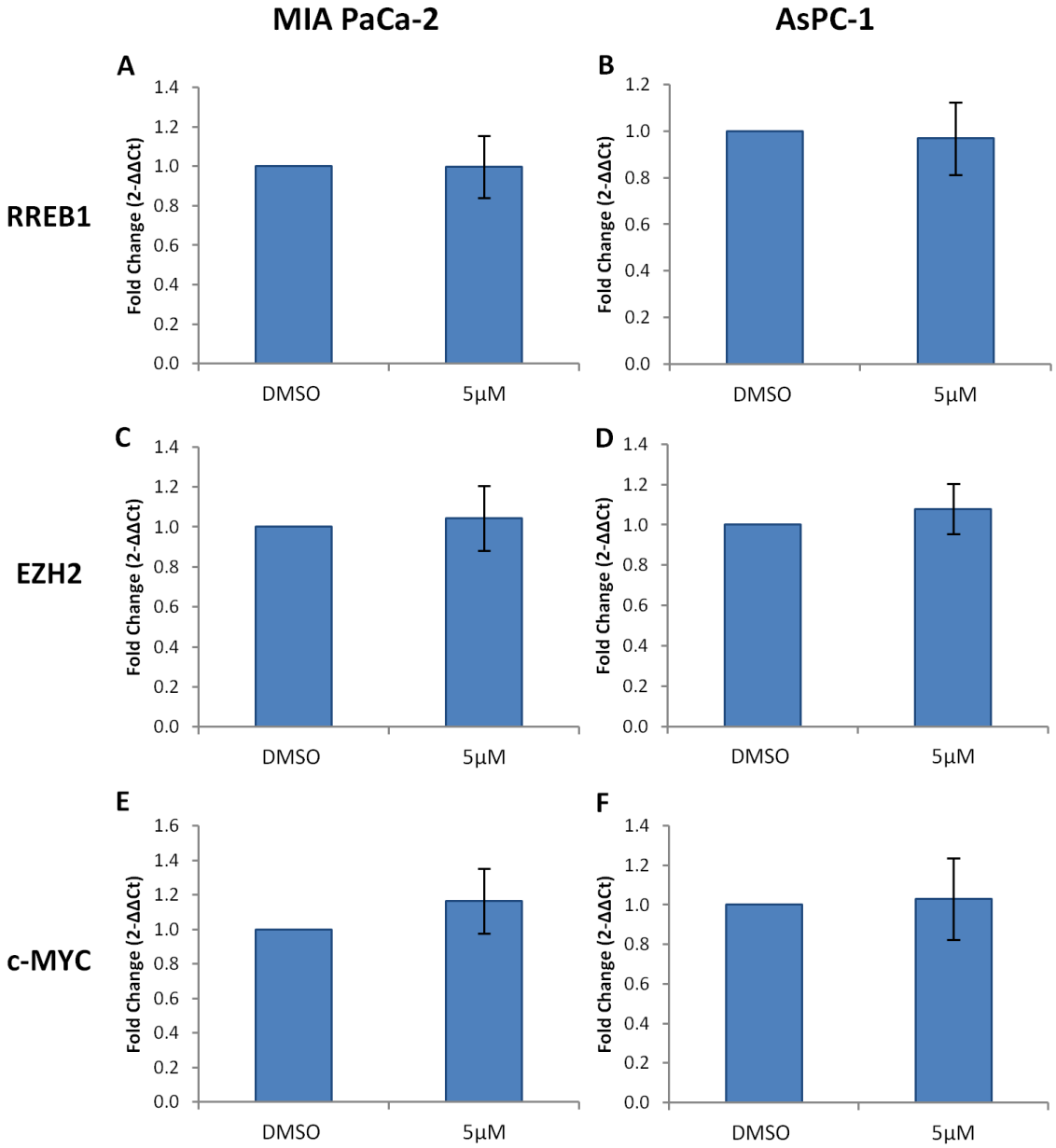

Figure 3.17: SensiMix SYBR Green RT-qPCR Analysis of RREB1, EZH2 and c-MYC. MIA PaCa-2 and AsPC-1 cells were treated with either 5µM curcumin or DMSO (control) for 24 hours **(A, B)** RREB1 **(C, D)** EZH2 **(E, F)** c-MYC. RT-qPCR data were normalised against 18S RNA and represent the mean ± SEM (n=4) (paired T-test).

3.3. Discussion

The central aim of this study was to identify miRNAs aberrantly expressed in PC which could be both targets for modulation by curcumin, as well as potential diagnostic biomarkers. Although the effects of curcumin on miRNAs are also being investigated by others, no uniform pattern of differential expression in PC has been established (Bloomston et al, 2007; Lee et al, 2007; Kent et al, 2009**)**. In this study differential miRNA expression following curcumin treatment was assessed using microarray analysis. Although other techniques such as qPCR and deep sequencing may be more accurate, the capacity for microarrays to measure numerous biological samples and screen a considerable number of potential miRNA targets made them the ideal platform for this research (Baker, 2010). Microarray analysis of MIA PaCa-2 and AsPC-1 cells did identify a number of differentially expressed miRNAs following treatment with curcumin. However, these changes in expression could not be successfully validated using RT-qPCR.

Many well established commercially available kits and protocols are available for RNA isolation of which TRI-reagent® is one of the most widely utilised. The TRI-reagent® method was chosen for its ability to extract total RNA which allows for the assessment of both miRNAs and mRNA from within the same sample (Lee et al, 2007; Kent et al, 2009; Pritchard et al, 2012; Mraz et al, 2009). With traditional methods of RNA isolation not tailored to recover small miRNAs, the TRI-reagent® RNA extraction protocol was adapted. It is recommended that RNA for use in microarray analysis have a ratio of absorbance at A260/280 and A260/230 of >2 and RIN values of ≥7 (Ibberson et al, 2009; Fleige et al, 2006). Most RNA samples obtained for microarray analysis achieved A260/280 and A260/230 values of >2, and RIN values of ≥4 (Table 3.1). Further RNA extractions were attempted to improve RNA quality, however RIN values of >7 could not be achieved. Although RIN values of >7 are recommended, some miRNA expression profile studies appear to have successfully used RNA with RIN values of ≥4 (Lee et al, 2007). It is also surprisingly common for microarray studies to insufficiently assess RNA quality prior to its use in miRNA profile analysis (Bloomston et al, 2007; Kent et al, 2009; Yu et al, 2012). Studies assessing miRNA stability in degraded RNA samples found that RIN values had little or no effect on miRNA results (Jung et al, 2010). With this in mind the RNA samples obtained were considered suitable for microarray analysis.

To assess the efficiency of RNA labelling and hybridisation for each microarray slide, linear regression plots were produced (Figure 3.2) (Appendix 2). Equal hybridisation of both Cy3 and Cy5 labelled RNA was shown when the slope of the regression line was 1. Values established by regression analysis can be used to compare labelling and hybridisation efficiency between microarray slides to determine reproducibility. Although many of the microarray slides in this experiment appeared to be reproducible there were a number which were not. Those which were not reproducible could result from either inefficient or unequal labelling of miRNAs, or a bias of the array platform towards one of the dyes. It is not uncommon to observe dye bias, with the labelling step having been previously suggested to account for much of the variability seen within microarray experiments (Baker, 2010; Pritchard et al, 2012). Microarrays which are not reproducible and do not fit the criteria required for their further assessment are often excluded from an experiment. However, as this form of quality analysis was performed in retrospect all microarray samples were included for further assessment.

Using the Limma and R software miRNA fold change values were calculated for curcumin treated cells following processing and normalisation of data. The aim of normalisation was to eliminate variation within and between arrays which was not directly related to the effects of treatment. MA (Figure 3.4)(Appendix 3) and density plots (Figure 3.5) produced by the Limma software were used to evaluate the quality of the microarray data before and after normalisation. Quantile normalisation applied to these data used the global measure for the miRNA expression against which to normalise the expression of each individual target miRNA (Pritchard et al, 2012). MA and volcano plots (Figure 3.6) were then used to show the equal distribution of data following normalisation.

Initially when analysing the normalised microarray data more stringent criteria were used to identify significant changes following curcumin treatment, however few were observed. Depending on the application of the technique being used and the experimental aim, the level of stringency applied to an experiment can afford to be altered. Microarray analysis is most commonly used as a screening technique, with the balance between the identification of significantly altered targets for further analysis and an elevated false discovery rate (FDR), often dependent on the aim of the

experiment. The purpose of this experiment was to screen a number of samples to identify miRNAs altered by curcumin treatment. As target identification was key, and further validation using RT-qPCR was also applied, less stringent criteria were used. Top tables were manually constructed based on fold change (>2 or <0.5) and p-values (<0.5), where both values were attributed equal weight (Table 3.2 and Table 3.3).

Interestingly, when assessing differential miRNA expression throughout the microarray experiments, a general decrease was observed following curcumin treatment. For curcumin to regulate such a large number of miRNAs in one direction, it must affect a pathway with the ability to modulate many of these non-coding RNAs. Drosha and dicer make up part of the machinery involved in miRNA biogenesis and were considered to be possible targets for the regulation of so many miRNAs. Studies investigating their involvement in cancer have shown that upregulation in many cancers is often associated with aggressive disease and poor prognosis (Vaksman et al, 2012; Han et al, 2013; Muralidhar et al, 2011; Ma et al, 2011). Interestingly, when compared to normal pancreatic mRNA, drosha and dicer expression was elevated in both PC cell lines (Figure 3.8). With this in mind it was hypothesised that curcumin may act by reducing drosha and/or dicer expression. However, RT-qPCR and western blot analysis showed no significant changes in expression (Figure 3.7). A doubling in protein expression for drosha after curcumin treatment was observed by western blot analysis, but only in MIA PaCa-2 cells (Figure 3.7 E and G). It was concluded from these data that in neither cell line does curcumin appear to significantly regulate drosha or dicer expression.

To determine if the differentially expressed miRNAs following curcumin treatment were involved in any common regulatory networks, six miRNAs; miR-223, miR-132, miR-370, miR-380, miR-145 and miR-143 chosen for validation were investigated. The miR-454* was also seen to be considerably upregulated in both AsPC-1 and MIA PaCa-2 cells following curcumin treatment (Table 3.2 and 3.3). Previous work with this array platform had identified an increase in miR-454* when carrying out control experiments using dH_2O, for this reason it was not included for further analysis. Using the miRWalk database, a list of target mRNAs which had been previously validated was produced for the six differentially expressed miRNAs (Dweep et al, 2011; Griffiths-Jones, 2004). This list was then uploaded to the Ingenuity IPA software and analysed in order to

identify pathways which may be affected by the treatment of PC cell lines with curcumin. Pancreatic Adenocarcinoma Signalling (Figure 3.9.) was one of the most significantly enriched pathways identified by the IPA software. Of the 128 mRNA target encoding genes associated with this pathway, 31 were targeted by at least one if not more of the differentially expressed miRNAs. Although differential expression of these miRNAs following curcumin treatment could not be validated, the fact that in combination they have the potential to modulate a quarter of the signalling molecules involved in pancreatic adenocarcinoma signalling supports the notion that curcumin could mediate a network of associated molecules involved in PC through the modulation of miRNAs.

Six of the top differentially expressed miRNAs; miR-132, miR-380, miR-370, miR-223, miR-145 and miR-21-3p following curcumin treatment were chosen for microarray validation by Taqman® RT-qPCR. Although the literature states that these miRNAs are involved in cancer progression, their downregulated expression, as observed following microarray analysis, could not be successfully validated (Figure 3.10 and Figure 3.11) (Zhang et al, 2011; Park et al, 2011b; Li et al, 2012; Gusscott et al, 2012; Lo et al, 2012; Ye et al, 2014; Chan et al, 2005; Kent et al, 2010). As previously mentioned miR-143 is clustered and transcribed with miR-145 and is commonly repressed in PC; with miScript SYBR® Green RT-qPCR of this miRNA there was no significant change in expression following curcumin treatment (Figure 3.12) (Kent et al, 2010).

Both Taqman® and miScript SYBR® Green RT-qPCR were used to validate the microarray findings. Taqman® RT-qPCR is a more specific method of quantifying mRNA expression, as it uses a fluorescently labelled probe which is specific for its target gene (Holland et al, 1991). SYBR® Green is a dye which binds to nucleic acids and therefore DNA, so this dye cannot differentiate between DNA sequences and therefore can label non-specific RT-qPCR products. However, a dissociation curve can be obtained after each RT-qPCR reaction to ascertain that only one product has been amplified (Zipper et al, 2004). Although Taqman® is often proffered as the more reliable method, SYBR® Green RT-qPCR can be just as accurate if correctly executed. Both RT-qPCR methods were used to validate miR-145 with near identical results.

In order to produce reliable qPCR data it is recommended that the Minimum Information for Publication of Quantitative Real-Time PCR Experiments (MIQE) guidelines be followed as closely as possible. It has been suggested that technical deficiencies such as; inadequate sample preparation and storage, low RNA quality, inefficient primers and probes and inappropriate statistical analysis could affect assay performance and lead to unreliable and inconsistent data (Bustin et al, 2009). Measures were taken throughout preparation and analysis of qPCR experiments such as the assessment of RNA quality and the optimisation of primers prior to use in order to produce as reliable and reproducible data as possible.

As mentioned when discussing normalisation of data and also within the MIQE guidelines, it is important to have reliable endogenous controls when profiling miRNAs (Bustin et al, 2009). When carrying out RT-qPCR, altered expression for a miRNA of interest is compared against a reference gene (RG) to ascertain that any changes in expression are a result of the biological criteria that are being assessed. A RG allows for the correction of variation as a result of technical error or biological variation between samples. Unlike mRNA expression analysis where various stably expressed and reproducible RGs exist (e.g. β-actin or α-tubulin), to date there are no standard RGs against which miRNA expression can be normalised. Currently small nuclear RNAs (snRNAs) or miRNAs with consistent expression across all samples are most commonly used as RGs for RT-qPCR (Benes and Castoldi, 2010; Peltier and Latham, 2008). The U6 snRNA, also known as RNU6B, was used as the endogenous control for Taqman® RT-qPCR validation. However, the miR-15a was found to be more consistently expressed when using miScript SYBR® Green RT-qPCR (Zhang et al, 2009).

A further four miRNAs; miR-518f*, miR-518a-3p, miR-518d-3p and miR-148a found to be downregulated by curcumin during microarray analysis were not successfully validated by miScript SYBR® Green RT-qPCR (Figure 3.13). The inability to validate the differentially expressed miRNAs observed in microarray analysis raised concerns about the reliability of the microarrays and the data they produced. The fold change values for the four probes used to calculate the average fold change for each miRNA were assessed to ascertain if any data were irregular. However the average fold change for each probe appeared to be fairly consistent (Table 3.6 and Table 3.7). These data however, do show that the hybridisation efficiency varies within the arrays depending

on geographic location as consistent patterns of fold change variation are observed depending on location of the probes.

Another aspect of the research was to examine miRNA and mRNA targets previously shown to be aberrantly expressed in PC which may also respond to curcumin. Deregulated expression of miR-200b, miR-200c, miR-34a and miR-34b has been associated with PC. When assessed using miScript SYBR® Green RT-qPCR, increased expression of all miRNAs was observed in both PC cell lines treated with curcumin when compared to DMSO treated cells. However, only the modulation in expression of miR-200c in MIA PaCa-2 cells was statistically significant ($p<0.05$) (Figure 3.14 and Figure 3.15). The signalling proteins Notch 2, Notch3, RREB1, EZH2 and c-Myc, which are often found deregulated in PC, were also assessed using miScript SYBR® Green RT-qPCR, but no significant changes were observed following curcumin treatment (Figure 3.16 and Figure 3.17).

Although microarray analysis appeared to demonstrate differentially expressed miRNAs as a result of curcumin treatment, when using RT-qPCR, which is often considered to be the gold standard for miRNA quantification, no alterations in target miRNA expression could be validated. The quality of a miRNA expression profile and the reproducibility of data are greatly dependent not only on the high quality of the RNA assessed, but also on the successful QC, processing and normalisation of data produced (579 Mraz,M. 2009). RNA degradation, as assessed by RIN value, has been shown to significantly impact on the outcome of miRNA profiling experiments (Ibberson et al, 2009; Podolska et al, 2011). Biases which develop during the labelling and hybridisation of the RNA samples can also negatively impact on the specificity of the microarray data. As a result, thorough QC prior to normalisation of microarray data must be applied for the data obtained to be worth assessing. It was difficult to establish whether this microarray analysis was unsuccessful due to ineffective curcumin treatment or shortcomings of the screen itself preventing successful assessment of the data. To address these difficulties, the biological effects of curcumin in PC cells need to be further validated and modifications to the microarray technique applied.

Chapter 4. The Effect of Curcumin on miR-34b/c and the Oncogenic Transcription Factor c-Myc.

4.1. Introduction

It is understood that deregulation of the TF Myc, and consequently the pathways by which it operates, appear to contribute to the tumourigenesis of many human cancers (Wolfer et al, 2010; Adhikary and Eilers, 2005). Myc has approximately 25,000 possible binding sites in the human genome, providing this TF with the potential to regulate a substantial number of genes (Adhikary and Eilers, 2005; Fernandez et al, 2003). Through the control of invasion and migration, oncogenic Myc is seen to influence cancer cell metastasis, a characteristic commonly associated with poor prognosis. High levels of Myc in advanced cancers have been observed in combination with an elevated potential of cancer cells to metastasise, making Myc a possible target for patients with progressive disease (Wolfer et al, 2010; Myant and Sansom, 2011). Research to date has highlighted the involvement of the miR-34a-c family in the regulation of Myc. Mechanisms involved are both dependent on p53, but also independent, working in combination with an MK5-FoxO3a negative feedback loop (Boominathan, 2010; Kress et al, 2011; He et al, 2007).

To activate the expression of its target genes, Myc must interact with its partner protein Max. Both are members of a family of carboxy-terminal basic helix-loop-helix-leucine zipper (bHLHZ) TFs which interact to form homo- or heterodimers. The bHLHZ structure is essential for all members of this family to dimerise (Adhikary and Eilers, 2005; Weinberg, 2013). Once in its dimeric form, Myc can bind specific DNA sequences within the promoter of its target genes such as the E-box (CACGTG) to promote transcription of proliferative genes (Fernandez et al, 2003; Pelengaris et al, 2002). When partnered with Max, Myc is able to promote transcription; however, Max is also able to interact with other members of the bHLHZ family like Mad and Mnt to repress transcription (Figure 4.1) (Adhikary and Eilers, 2005; Weinberg, 2013).

There are various genes in the Myc family, of which c-Myc, N-Myc and L-Myc have been implicated in tumourigenesis (Adhikary and Eilers, 2005). c-Myc can act as an oncoprotein when its expression becomes deregulated. This has been associated with poor prognosis in some cancers, including colorectal and pancreatic (Pelengaris et al,

2002; Cannell et al, 2010; Weinberg, 2013). Additionally to its role as a TF, c-Myc is involved in regulating cell cycle progression in response to DNA damage. Activation of various DNA damage response (DDR) proteins (ATR/ATM, Chk1/Chk2) results in the direct upregulation of miR-34b/c through activation of the tumour suppressor protein p53 (Myant and Sansom, 2011; He et al, 2007). Through the regulation of the signalling protein p38, DDR proteins enable MK5 activation. Once active, MK5 goes on to phosphorylate the TF FoxO3a, enabling its translocation into the nucleus and subsequent induction of miR-34b/c (Figure 4.2) (Kress et al, 2011; Cannell et al, 2010). It has been shown through mapping deletions of the c-Myc transcript that miR-34b/c targets this TF within its 3'UTR, thus inhibiting its expression (Kress et al, 2011).

As a result of DNA damage, increased miR-34b/c expression leads to decreased levels of c-Myc and inhibition of the cell cycle allowing successful DNA repair. However, if miR-34b/c levels become reduced, as is observed in colorectal and pancreatic tumourigenesis, either directly through p53 or indirectly in combination with MK5 and FoxO3a, levels of c-Myc would remain elevated. This would result in early departure from cell cycle arrest and the inability to repair damaged DNA, causing GIN and aggressive disease progression (Myant and Sansom, 2011; Cannell et al, 2010).

The ability to increase miR-34 expression in cancer cells, either lacking in this miRNA or with elevated c-Myc levels, could be of therapeutic value. p53 is commonly mutated in PC, and is a factor which often contributes to the rapid progression of this disease (Morton et al, 2010). Restoration of miR-34 using mimics or lentiviral infection appeared to restore to some extent the function of p53 in the PC cell lines MIA PaCa-2 and BxPC-3 which are deficient in this tumour suppressor activity (Ji et al, 2009). Many dietary agents have been seen to regulate miRNA expression, and recently curcumin has been shown in certain circumstances to increase expression of the miR-34 family and decrease expression of c-Myc (Li et al, 2010; Kunnumakkara et al, 2007; Boominathan,. 2010; Azmi et al, 2011; Roy et al, 2012; Wu et al, 2014). A study using CSCs found that, following treatment with curcumin, a variety of miRNAs became upregulated, including miR-34, possibly through p53 (Boominathan, 2010).

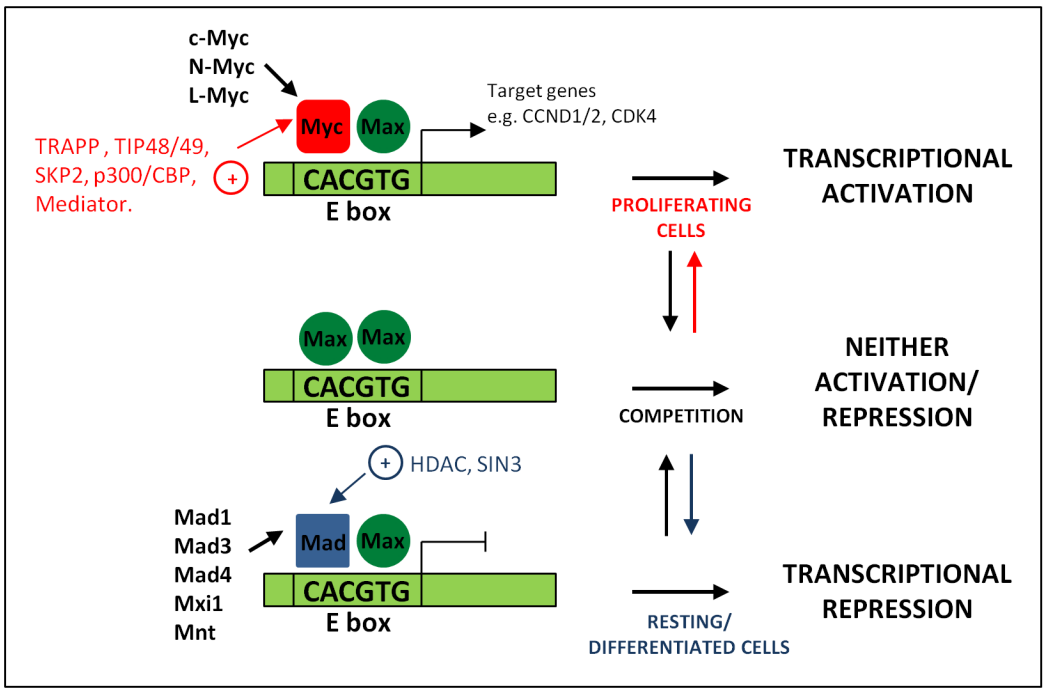

Figure 4.1: Transcriptional Regulation of the bHLHZ Family of Transcription Factors in Association with the E-box Consensus Sequence. Myc (c-Myc, N-Myc, L-Myc), along with Mad (Mad1/3/4, Mxi1, Mnt) and Max, belong to the bHLHZ family of transcription factors. When dimerised with Max, Myc is able to bind to the E-box consensus sequence and activate transcription. The Myc-Max heterodimer is found in proliferating cells and drives cell number by allowing the expression of a wide variety of genes (e.g. CCND1/2, CDK4). Myc also requires interactions with other protein complexes and coactivators which help to modulate transcriptional activation, including TRRAP, TIP48 and 49, SKP2, p300/CBP and Mediator complex. Max is capable of forming a homodimer which also binds the E-box consensus sequence. However, it neither activates nor represses transcription. The Max-Mad heterodimer is predominantly found in resting or differentiated cells and also binds the E-box consensus sequence causing transcriptional repression. Mad is thought to recruit HDAC and SIN3 to help in transcriptional repression by silencing proliferative genes that are activated by Myc (Wolfer et al, 2010; Adhikary and Eilers, 2005; Pelengaris et al, 2002).

As already highlighted, in PC cells miR-34 expression has been shown to decrease. Levels of c-Myc, in contrast, become elevated and have been associated with metastasis and cancer progression (Vogt et al, 2011; Roy et al, 2012; Wolfer et al, 2010; Lin et al, 2013). These alterations have so far only been associated with direct regulation by p53 (Chang et al, 2007; Ji et al, 2009; Vogt et al, 2011). Treatment of PC cells with curcumin or an analogue has resulted in re-expression of miR-34 and a decline in c-Myc (Boominathan, 2010; Roy et al, 2012; Chen and Huang, 1998). There is no defined research linking declining miR-34b/c expression and upregulated c-Myc in PC with regard to the p53 independent pathway involving MK5 and FoxO3a (Kress et al, 2011). However, based on published literature it could be possible that escalating c-Myc levels and reduced miR-34b/c expression may be linked, as has been shown in CRC (Myant

and Sansom, 2011; Kress et al, 2011; Cannell et al, 2010). It may also be possible that curcumin acts independently of p53 in order to target miR-34 and c-Myc. RT-qPCR analysis of miR-34a and miR-34b expression outlined in chapter 3 showed that, although not statistically significant, increased expression of both miRNAs was observed in MIA PaCa-2 and AsPC-1 cells following treatment with 5μM curcumin for 24 hours. With this in mind the aim of this chapter was to ascertain if there was any effect of curcumin on c-Myc protein expression in PC cells.

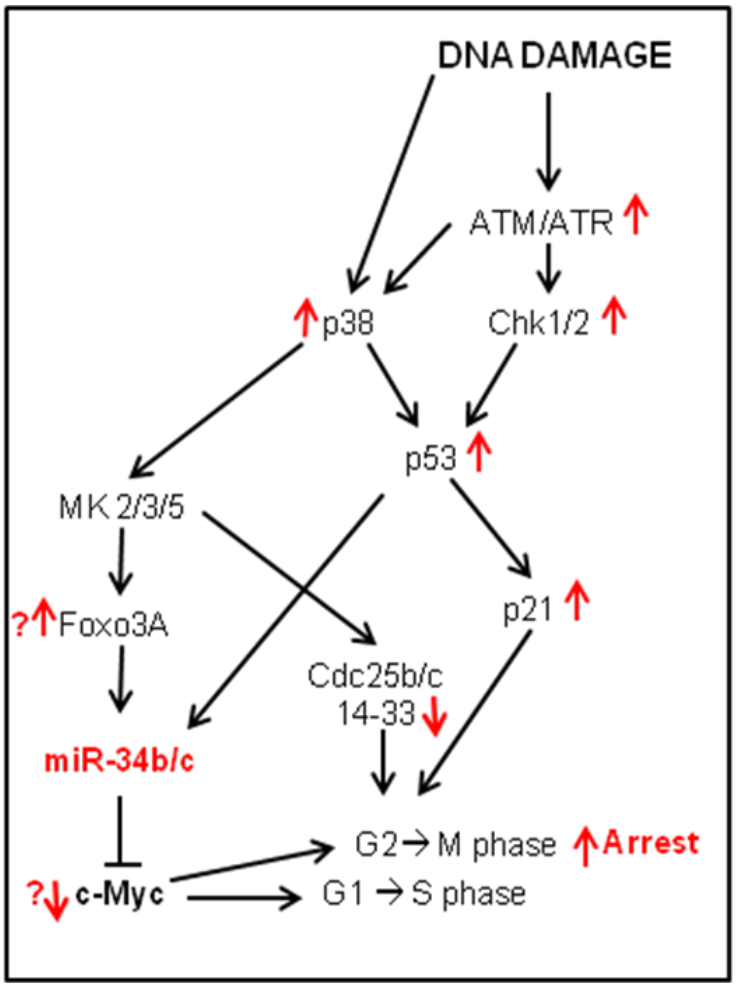

Figure 4.2: DNA Damage-induced Cell Cycle Arrest Modulated by c-Myc Inhibition. DNA damage during the cell cycle leads to the recruitment and activation of various DNA damage response proteins (ATR/ATM, Chk1/2). In response to these proteins activation of the tumour suppressor p53 and the signalling protein p38 occurs, leading to direct and indirect upregulation of miR34b/c respectively. Indirect upregulation occurs following phosphorylation of FoxO3a by MK5. Phosphorylated FoxO3a then translocates into the nucleus enabling induction of miR-34b/c. As a result of increased miR-34b/c, c -Myc becomes inhibited, preventing the expression of a variety of vital cell cycle proteins (e.g. CDK4, Cyclin D). Without the expression of many c-Myc targets the cell cycle cannot progress from G1 to S phase. This gives the cell time to fix any damaged DNA before recommencing the cell cycle. Potential curcumin effects are indicated by red arrows (Pelengaris et al, 2002; Cannell and Bushell, 2010). Figure adapted from (Myant and Sansom, 2011).

4.2. Results

4.2.1. Effects of Curcumin on c-Myc Expression in Pancreatic Cancer Cell Lines.

The two PC cell lines, MIA PaCa-2 and AsPC-1 used in the miRNA microarrays described in chapter 3 underwent various treatments with curcumin. Dose response experiments using 0.5, 1, 5 and 10μM for 24 or 48 hours and time course experiments with 1, 5 or 10μM for 1, 5, 12, 24 and 48 hours were carried out (section 2.2.1.4). Western blot analysis was used to determine any changes in c-Myc protein expression. Untreated HeLa cells were used as a positive control for c-Myc due to heightened expression levels in this cell type. Although mRNA expression levels for c-Myc were fairly high in MIA PaCa-2 and AsPC-1 cells (average Ct values ~19 chapter 3) protein expression, in both cell lines appeared to be relatively low. As a result, data for some time course and dose response experiments for both PC cell lines could not be successfully obtained, resulting in the inability to determine statistical significance for some datasets.

MIA PaCa-2 dose response experiments at 24 hours did not show any clear changes in c-Myc expression. However, at 48 hours, increases in c-Myc expression were observed with 0.5 and 1μM curcumin and a decrease was observed at 10μM when compared with the DMSO control (Figure 4.3). No consistent changes in c-Myc expression were observed in AsPC-1 cells following treatment with either 1μM or 5μM curcumin, however most time points showed a slight decrease in c-Myc levels in curcumin treated samples when compared to their DMSO controls (Figure 4.4A-D). Elevated c-Myc levels were observed after 1 hour with 1μM curcumin when compared to the DMSO control (Figure 4.4A-B). Treatment with 10μM curcumin, however appeared to show a time dependent decrease in c-Myc expression (Figure 4.4E-F). When cells were treated with curcumin for 48 hours in a dose-dependent manner no consistent changes in c-Myc expression was observed (Figure 4.4G-H). Due to the lack of replicates firm conclusions could not be drawn following treatment of MIA PaCa-2 and AsPC-1 cells with curcumin.

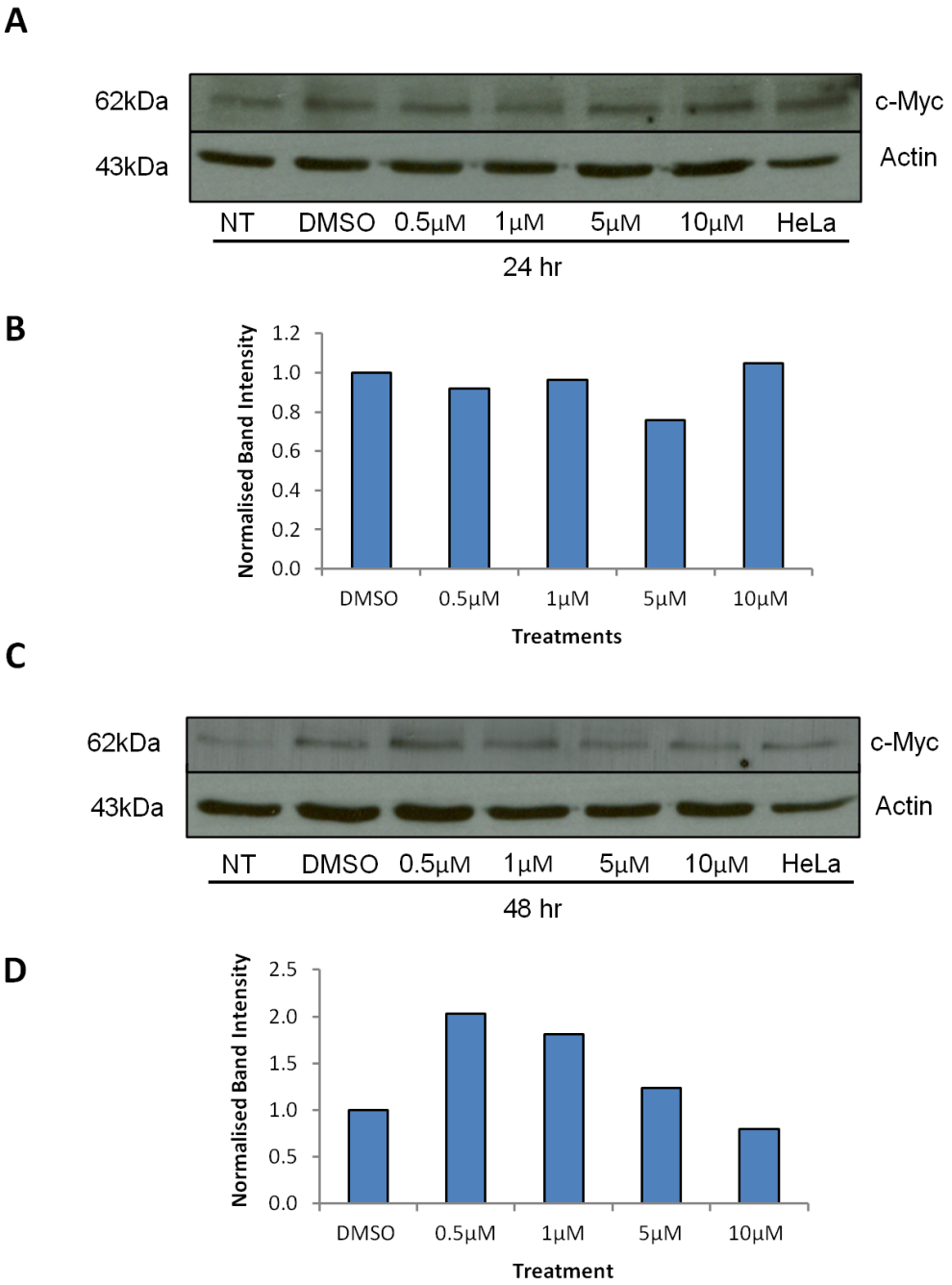

Figure 4.3: c-Myc Protein Levels in MIA PaCa-2 Cells Following Curcumin Treatment. MIA PaCa-2 cells were treated as shown **(A, B)** (n=2) **(C, D)** (n=1). **(A,C)** Representative ECL blots showing changes in c-Myc following treatment with curcumin with actin as the loading control. **(B,D)** Histograms representing normalised (against DMSO) changes in band intensity for c-Myc (NT= No Treatment).

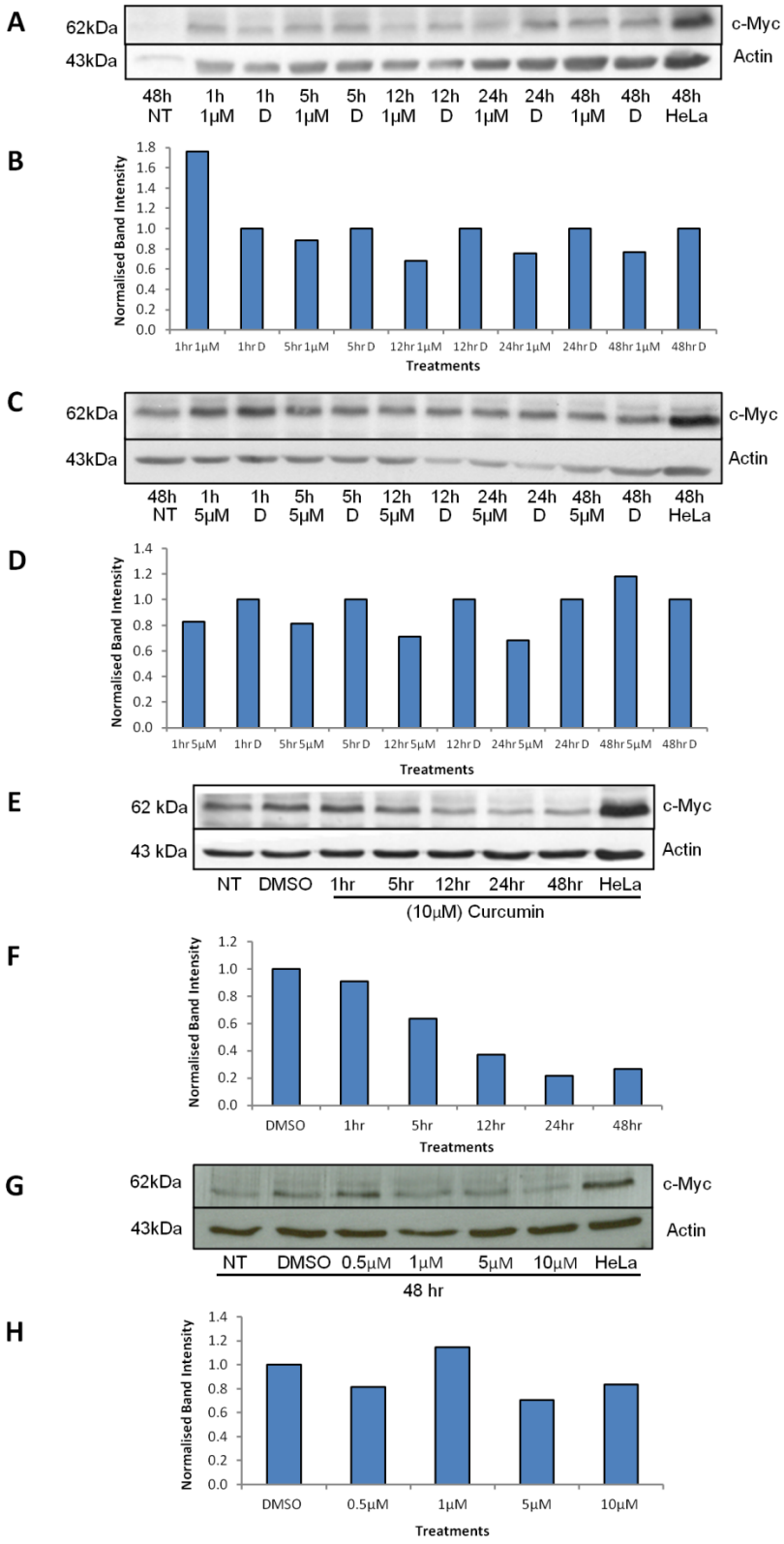

Figure 4.4: c-Myc Protein Expression in AsPC-1 Cells Following Curcumin Treatment. AsPC-1 cells were treated as shown, **(A, B)** (n=1), **(C, D)** (n=2), **(E, F)** (n=1), **(G, H)** (n=1). **(A,C,E,G)** Representative ECL blots showing changes in c-Myc following treatment with curcumin with actin as the loading control. **(B,D,F,H)** Histograms representing normalised (against DMSO) changes in band intensity for c-Myc (NT= No Treatment).

4.2.2. Effects of Curcumin on c-Myc Expression in Colorectal Cancer Cell Lines.

Treatment of human CRC tissue with the curcumin analogue, CDF, was shown to lead to the re-expression of various members of the miR-34 family. Renewed expression of this miRNA family led to growth inhibition, however no link was made between curcumin exposure and c-Myc expression (Roy et al, 2012). To determine if curcumin was able to modulate c-Myc in CRC, expression levels were assessed in the CRC cell line HCT116.

Due to the lack of replicates firm conclusions could not be drawn following treatment of HCT116 cells with 1μM or 5μM curcumin. Although no consistent changes were observed following curcumin treatment, following 48 hours incubation a decrease and an increase in c-Myc expression were identified at 1μM and 5μM respectively (Figure 4.5A-D). Following treatment with 10μM curcumin, a statistically significant ($p>0.05$) time dependent decrease in c-Myc expression was observed (Figure 4.5E-F). However, despite a decrease, when compared to DMSO treated samples, levels were still higher. A dose-dependent increase in c-Myc expression was observed following curcumin treatment for 24 and 48 hours (Figure 4.6). Although triplicate datasets were produced for both dose-response experiments, significant increases in c-Myc expression were only observed at 5μM ($p>0.05$) and 10μM ($p>0.01$) after 48 hours (Figure 4.6C-D). Since data were inconsistent between experiments and not all datasets were complete, it was not possible to draw any firm conclusions for c-Myc expression in HCT116 cells.

As mentioned miR-34b/c can be regulated directly by p53 and indirectly through MK5-FoxO3a, as is the case for CRC (Myant and Sansom, 2011; Kress et al, 2011). However, no link between MK5-FoxO3a and miR-34b/c has been made in PC. As highlighted in Figure 4.2, signalling proteins, including p38 and MK5, provide a different route for miR-34b/c regulation. It was proposed-that curcumin may act on one of these signalling proteins either directly or through the modulation of alternate miRNAs. Since curcumin failed to induce any changes in c-Myc expression in either PC or CRC cells, the effects of this agent on the expression of MK5 were examined.

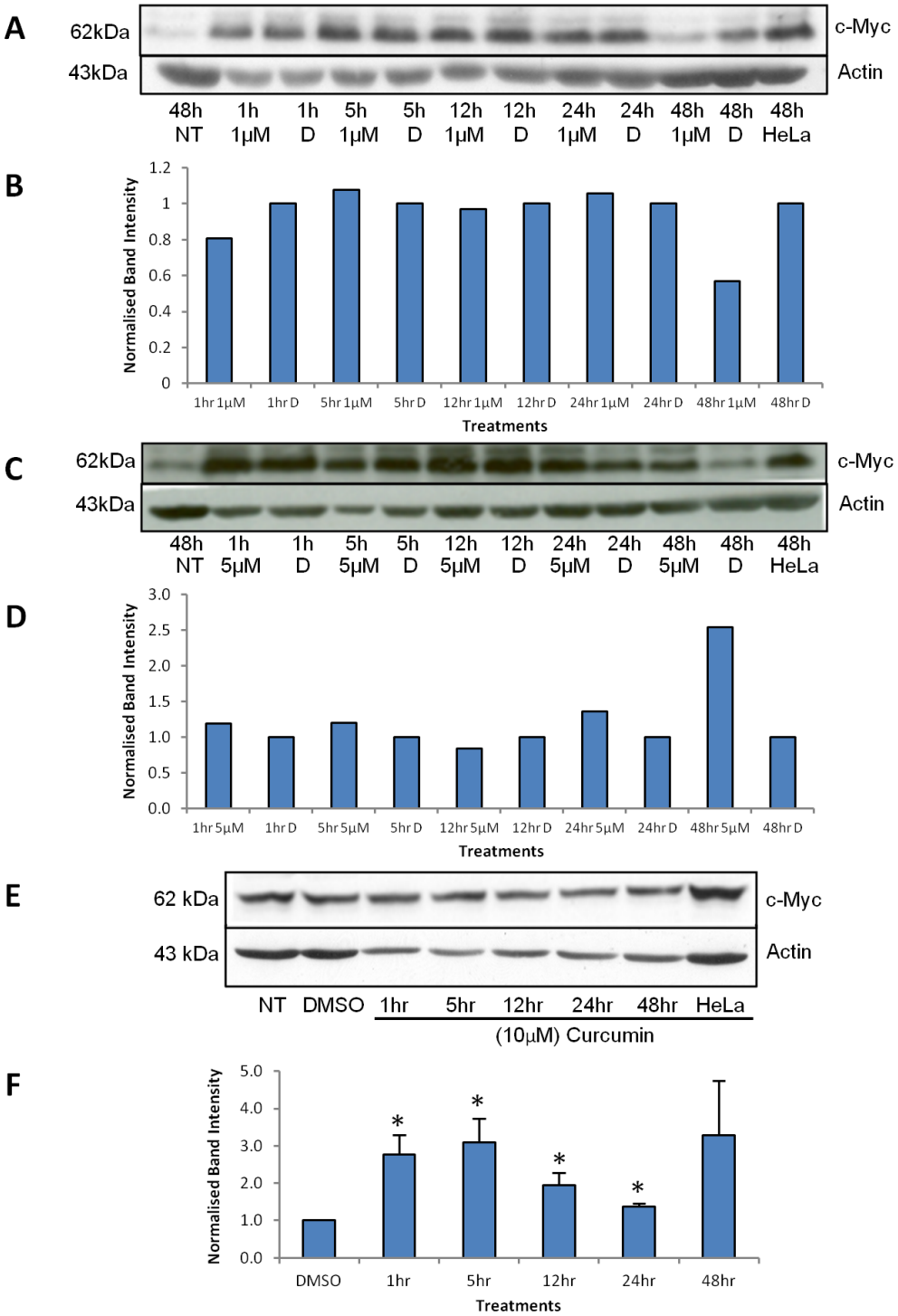

Figure 4.5: c-Myc Protein Expression in HCT116 Cells Following Curcumin Treatment. Colorectal cancer cells HCT116 were treated as shown. **(A, B)** (n=1), **(C, D)** (n=1) or **(E, F)** (n=3). **(A,C,E)** Representative ECL blots showing changes in c-Myc following treatment with curcumin with actin as the loading control **(B,D,F)** Histograms representing normalised (against DMSO) changes in band intensity for c-Myc ± SEM (T-test, *p>0.05). (NT= No Treatment, D = DMSO)

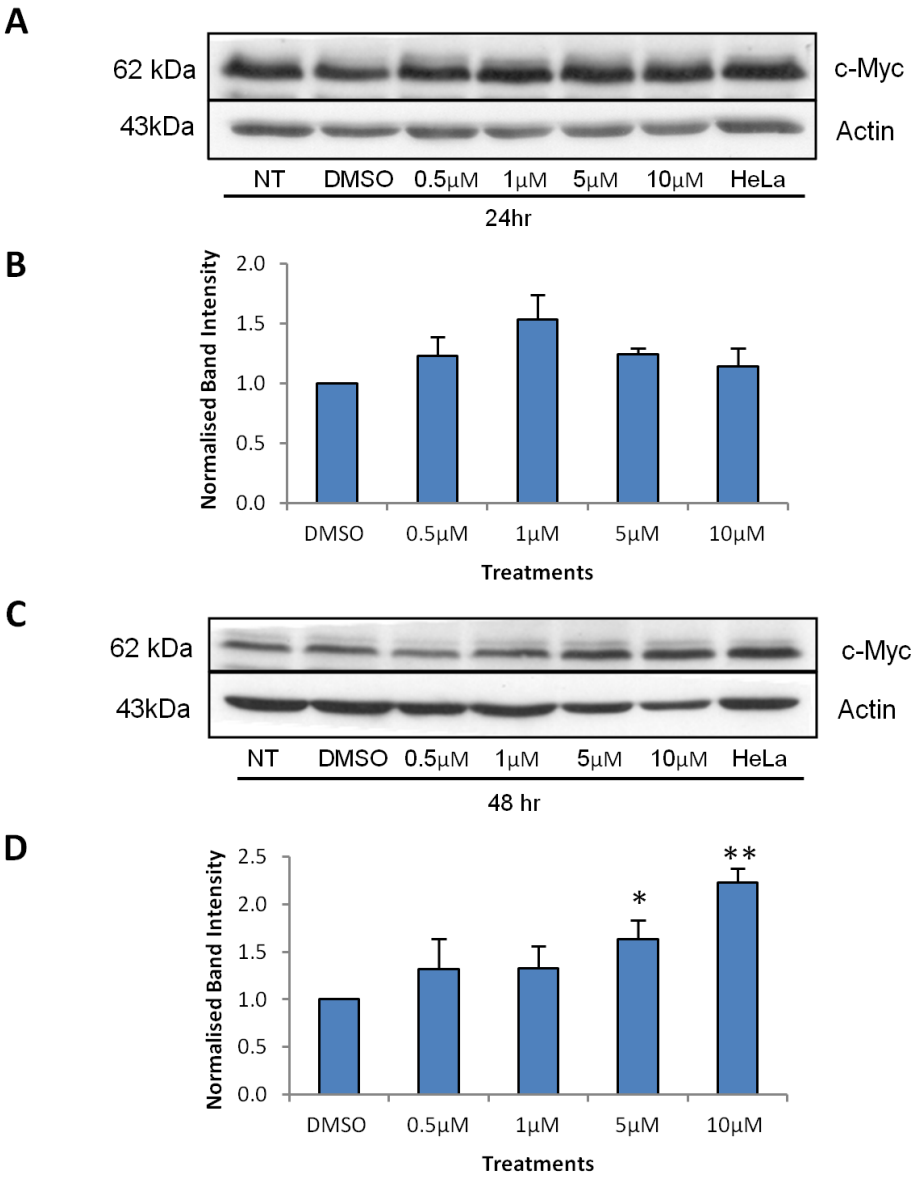

Figure 4.6: Dose Dependent Changes in c-Myc Protein Levels in HCT116 Cells Following Curcumin Treatment. HCT116 cells were treated as shown, **(A, B)** (n=3) or **(C, D)** (n=3). **(A,C)** Representative ECL blots showing changes in c-Myc following treatment with curcumin with actin as the loading control. **(B,D)** Histograms representing normalised (against DMSO) changes in band intensity for c-Myc ± SEM (T-test, *P < 0.05, **P < 0.01). (NT= No Treatment, D = DMSO)

4.2.3. Effects of Curcumin on MK5 Protein Expression in Pancreatic and Colorectal Cancer Cell Lines.

Protein levels of MK5 were assessed in MIA PaCa-2, AsPC-1 and HCT116 cells by western blot analysis following exposure to curcumin. Treatment of MIA PaCa-2 cells with 10μM curcumin appeared to have little effect on MK5 protein expression, with dose-dependent decreases in MK5 levels observed at 24 hours but not at 48 hours following treatment (Figure 4.7). MK5 levels remained largely unaffected by curcumin

treatment in the AsPC-1 cells (Figure 4.8 and 4.9), except when treated with 10μM curcumin for 24 or 48 hours (Figure 4.9).

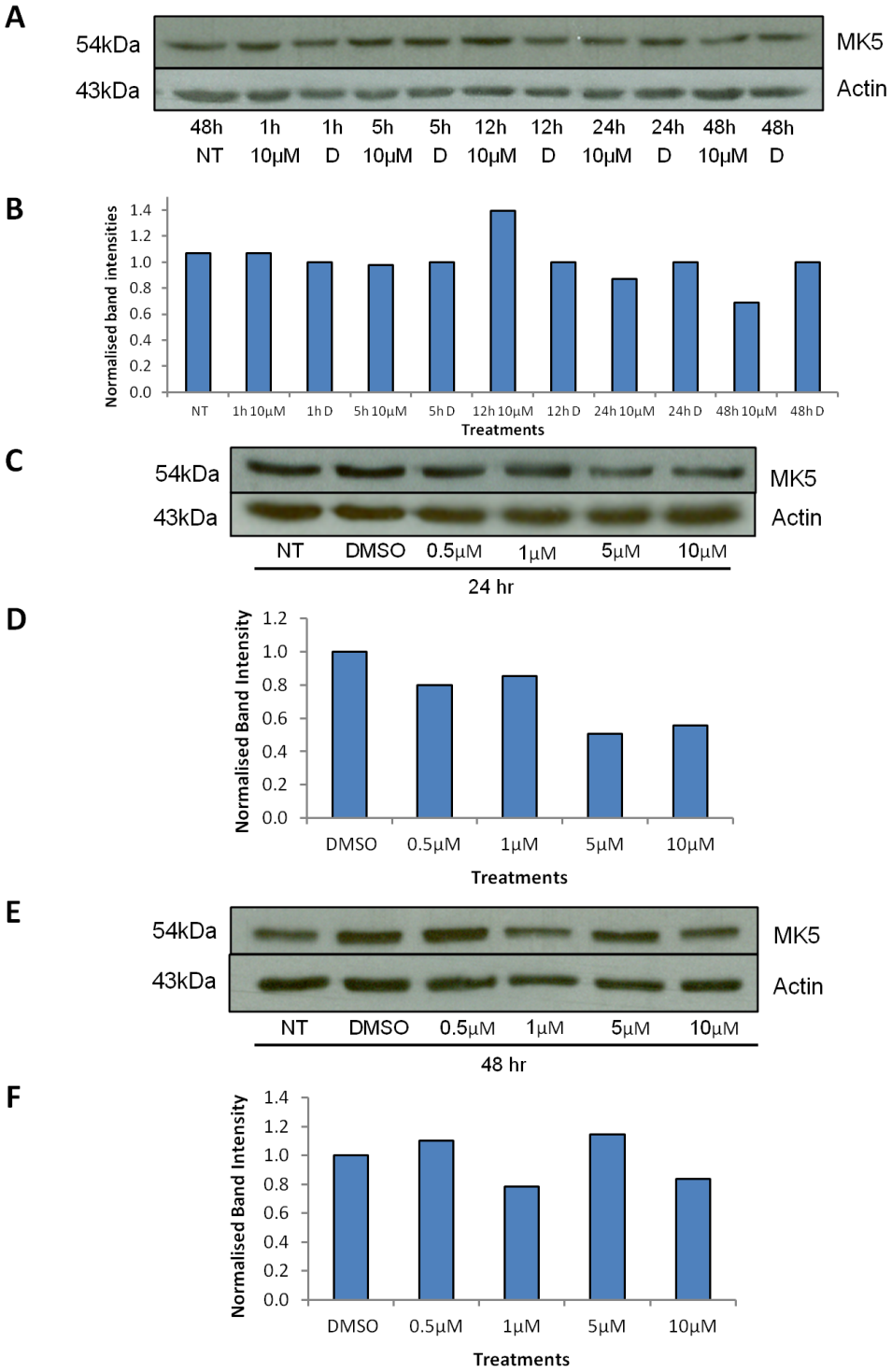

Figure 4.7: MK5 Protein Expression in MIA PaCa-2 Cells Following Curcumin Treatment. MIA PaCa-2 cells were treated as shown. **(A,C,E)** Representative ECL blots showing changes in MK5 following treatment with curcumin with actin as the loading control. **(B,D,F)** Histograms representing normalised (against DMSO) changes in band intensity for MK5 (n=1). (NT= No Treatment, D = DMSO)

As with the PC cell lines, HCT116 cells appeared to be largely unaffected by curcumin treatment (Figure 4.10 and 4.11). MK5 expression appeared to increase in a dose-dependent manner but only following 24 hours (Figure 4.11). Although some changes in MK5 expression were observed following curcumin treatment for both PC and CRC cells, due to the lack of replicates (n=1) firm conclusions could not be drawn.

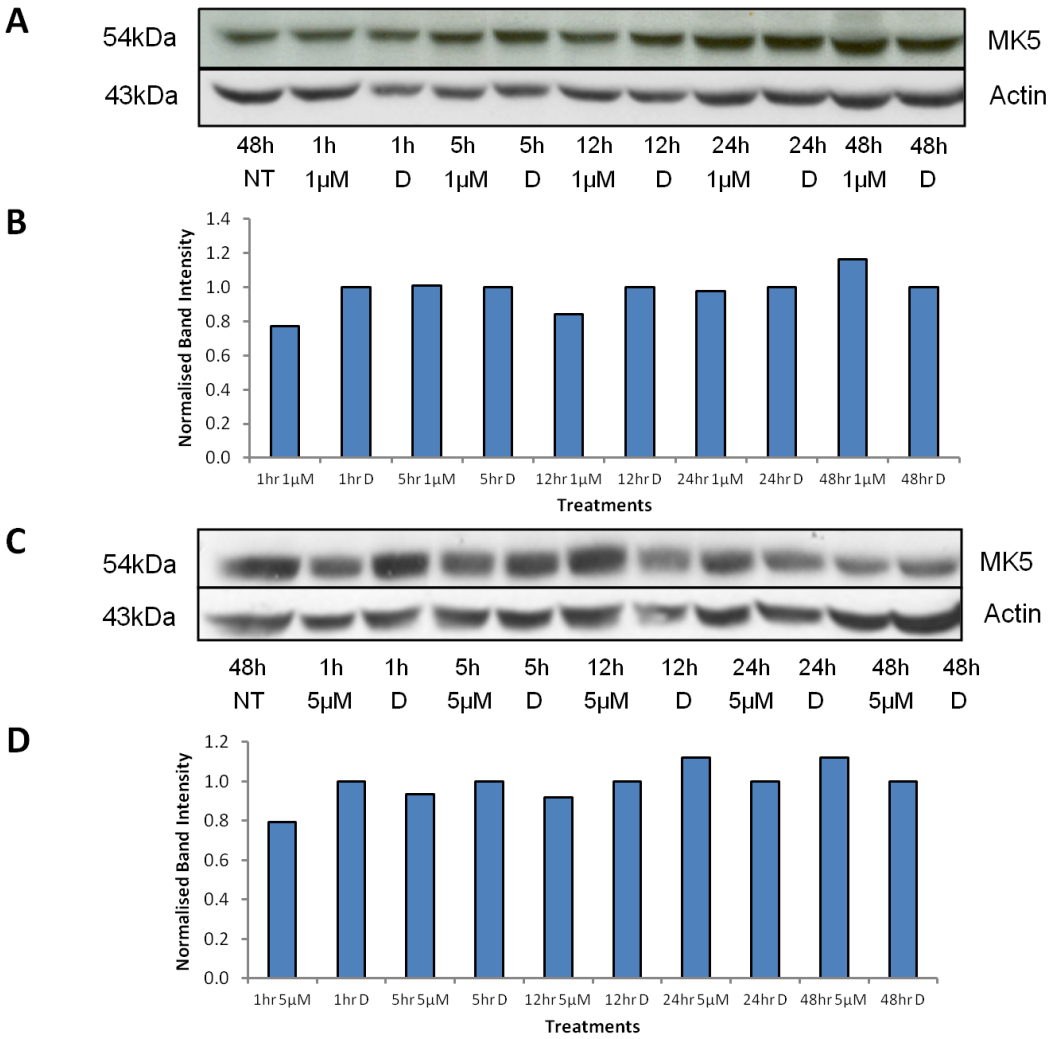

Figure 4.8: MK5 Protein Levels in AsPC-1 Cells Following Curcumin Treatment. AsPC-1 cells were treated as shown. **(A,C)** Representative ECL blots showing changes in MK5 following treatment with curcumin with actin as the loading control. **(B,D)** Histograms representing normalised (against DMSO) changes in band intensity for MK5 (n=1). (NT= No Treatment, D= DMSO)

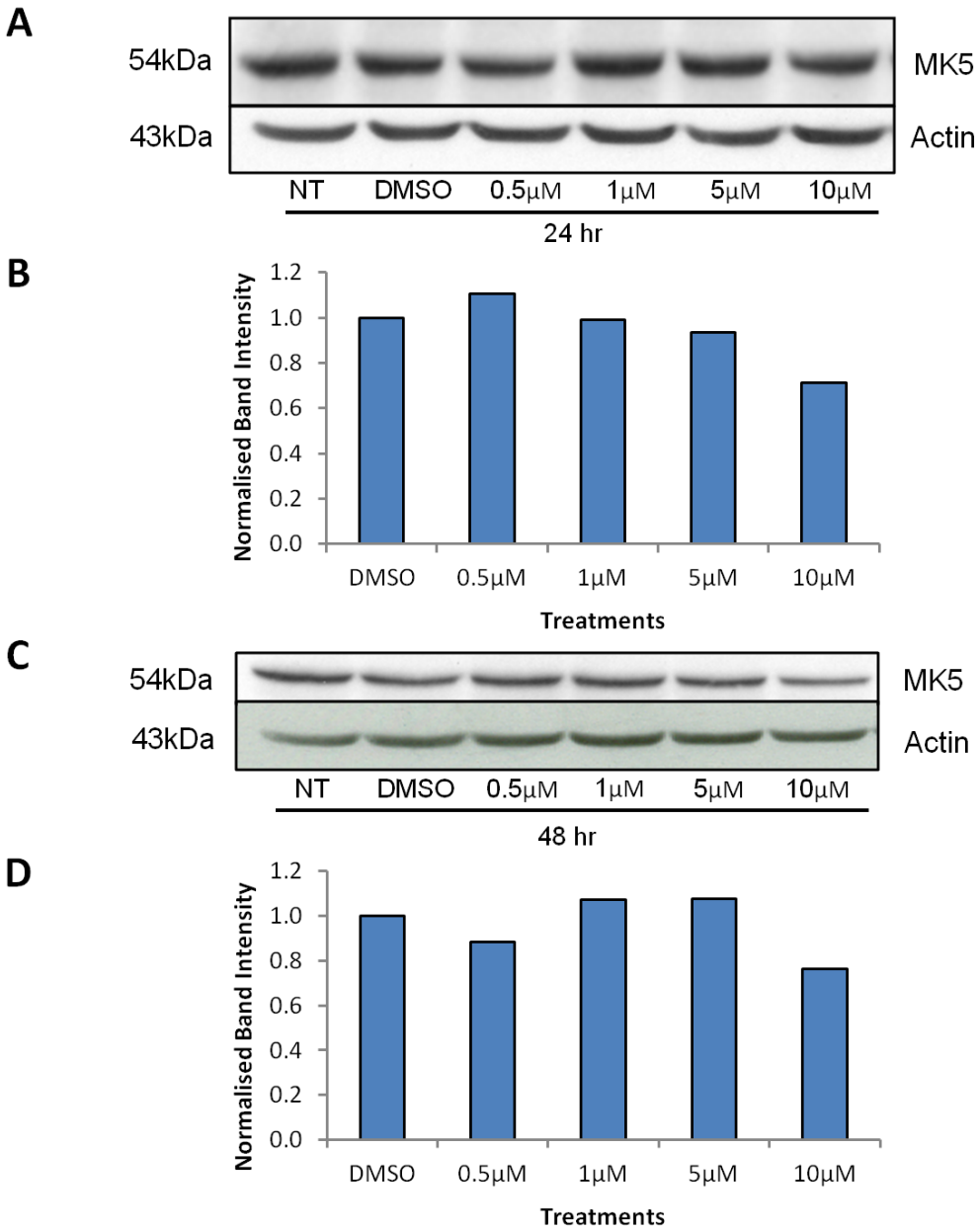

Figure 4.9: MK5 Protein Levels in AsPC-1 Cells Following Curcumin Treatment. AsPC-1 cells were treated as shown. **(A,C)** Representative ECL blots showing changes in MK5 following treatment with curcumin with actin as the loading control. **(B,D)** Histograms representing normalised (against DMSO) changes in band intensity for MK5 (n=1). (NT= No Treatment, D = DMSO).

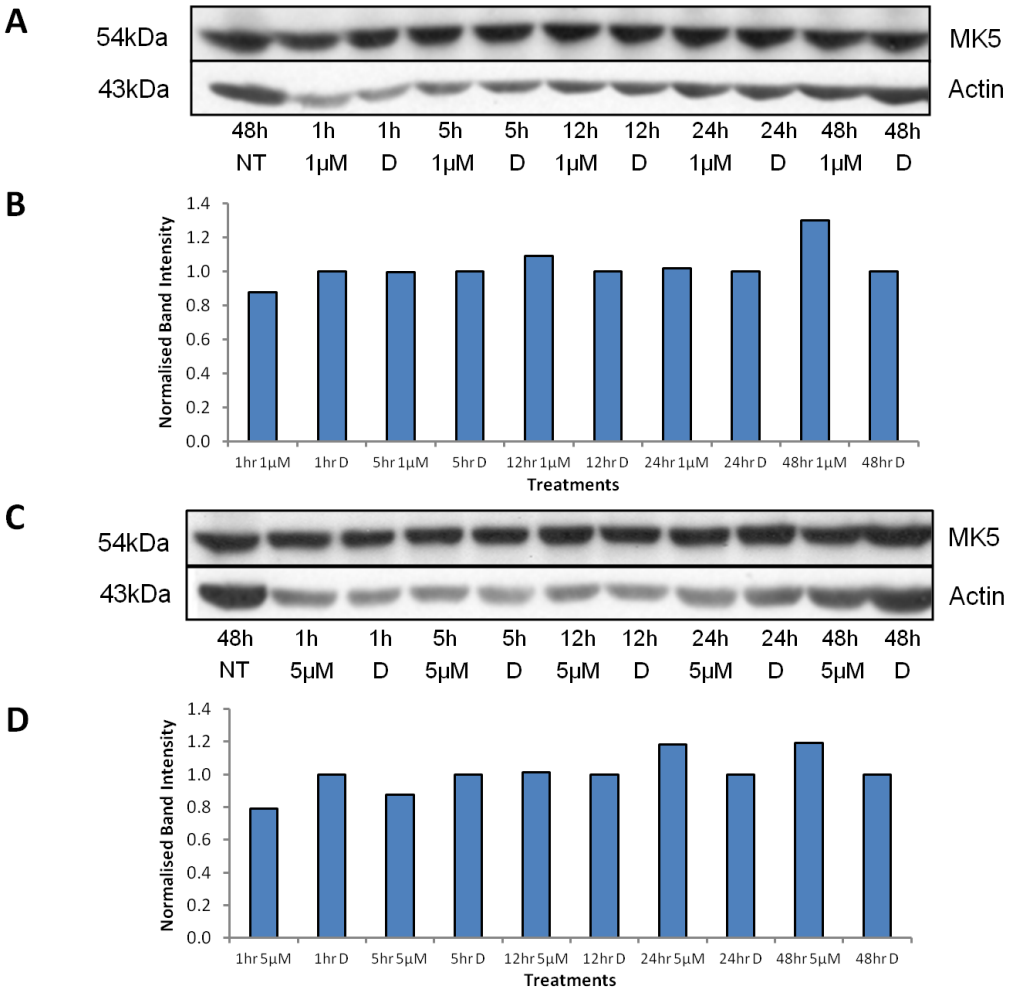

Figure 4.10: MK5 Protein Levels in HCT116 Cells Following Curcumin Treatment. HCT116 cells were treated as shown. **(A,C)** Representative ECL blots showing changes in MK5 following treatment with curcumin with actin as the loading control. **(B,D)** Histograms representing normalised (against DMSO) changes in band intensity for MK5 (n=1). (NT= No Treatment, D= DMSO)

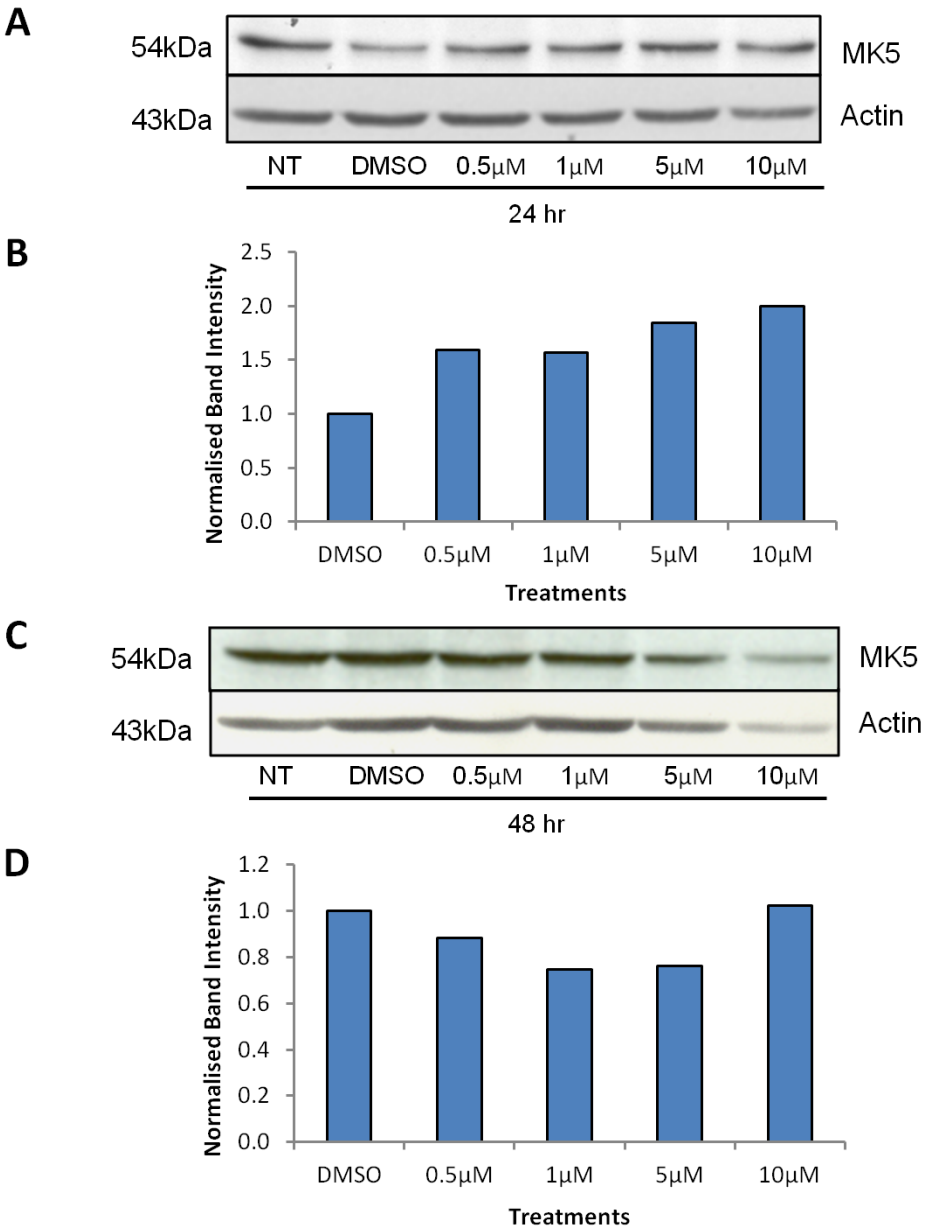

Figure 4.11: MK5 Protein Levels in HCT116 Cells Following Curcumin Treatment. HCT116 cells were treated as shown. **(A,C)** Representative ECL blots showing changes in MK5 following treatment with curcumin with actin as the loading control. **(B,D)** Histograms representing normalised (against DMSO) changes in band intensity for MK5 (n=1). (NT= No Treatment, D = DMSO).

Levels of c-Myc and MK5 in both PC and CRC cells remained largely unaffected following curcumin treatment, suggesting that curcumin was unable to significantly modulate their expression. The effect of curcumin on phosphorylation of p38, another signalling protein known to be involved in modulating c-Myc expression was previously examined in the lab (upublished data Manson lab) (Figure 4.2). However, no change was observed.

Based on the experiments in this chapter, treatment of both PC and CRC cell lines with 5μM curcumin over 24 hours did not appear to elicit any consistent changes in expression of protein targets. Previously obtained data for PC cell lines (Christopher Mann, Thesis) and evidence from the literature was used to determine an appropriate dose and treatment time for the initial microarray experiments (chapter 3). Bioavailability data have shown that the maximum physiological concentration achievable for curcumin in the human colon was in the range of 10μM/L (Garcea et al, 2005a; Gandhy et al, 2012; Howells et al, 2007; Huang et al, 1991). Reduced cell viability had also been observed in HCT116 cells following treatment with concentrations as low as 2.5μM, for 24 hours (Watson et al, 2010). It was therefore assumed that exposure to 5μM curcumin for 24 hours, would elicit a significant effect in PC cell lines. However, differential miRNA expression observed in the initial microarray analysis (Chapter 3) was not observed following validation by RT-qPCR. This could suggest that the dose of curcumin chosen for the initial microarray may not have had the desired effect in PC cell lines. Therefore, cell viability and cell growth were further assessed in various PC cell lines, following treatment with curcumin.

4.2.4. Effects of Curcumin on Pancreatic Cancer Cell Viability, Death and Growth.

4.2.4.1. Cell Viability

Cell viability was determined using the ATPlite™ Luminescence ATP detection system (section 2.2.3), which monitors the levels of adenosine triphosphate (ATP) present within a sample. Significant dose-dependent reductions in cell viability were apparent for BxPC-3, AsPC-1 and MIA PaCa-2 cells at 48, 72 and 120 hours (Figure 4.12 and 4.13). Reductions in cell viability were also observed at 24 hours in BxPC-3 and AsPC-1 cells following exposure to curcumin (Figure 4.12A and B). A greater effect on cell viability was observed in BxPC-3 and AsPC-1 cells in comparison to MIA PacA-2 cells (Figure 4.12 and 4.13).

4.2.4.2. Cell Death

The ability of curcumin to stimulate apoptosis in PC cell lines was assessed using fluorescently labelled (FITC) Annexin V and Pi (section 2.2.2). BxPC-3 cells were seen to have statistically significant increases in both apoptosis and necrosis following 72 hours treatment (Figure 4.14A). However, no effect of curcumin on either AsPC-1 or

MIA PaCa-2 cells was observed until 120 hours exposure (Figure 4.14B and C). Statistically significant increases in apoptotic and necrotic cells were observed in curcumin-treated AsPC-1 cells at both 168 and 240 hours (Figure 4.15B). Treatment of these cells with 5μM curcumin for 240 hours resulted in reduced cell number and the inability to assess levels of cell death. Significant increases in apoptosis and necrosis were not observed in MIA PaCa-2 cells until 240 hours exposure to 5μM curcumin (Figure 4.15C). Treatment of BxPC-3 cells for more than 168 hours resulted in severe reduction in cell number preventing analysis through flow cytometry (Figure 4.15A). These data indicated that BxPC-3 cells displayed heightened sensitivity to curcumin compared to both AsPC-1 and MIA PaCa-2 cells.

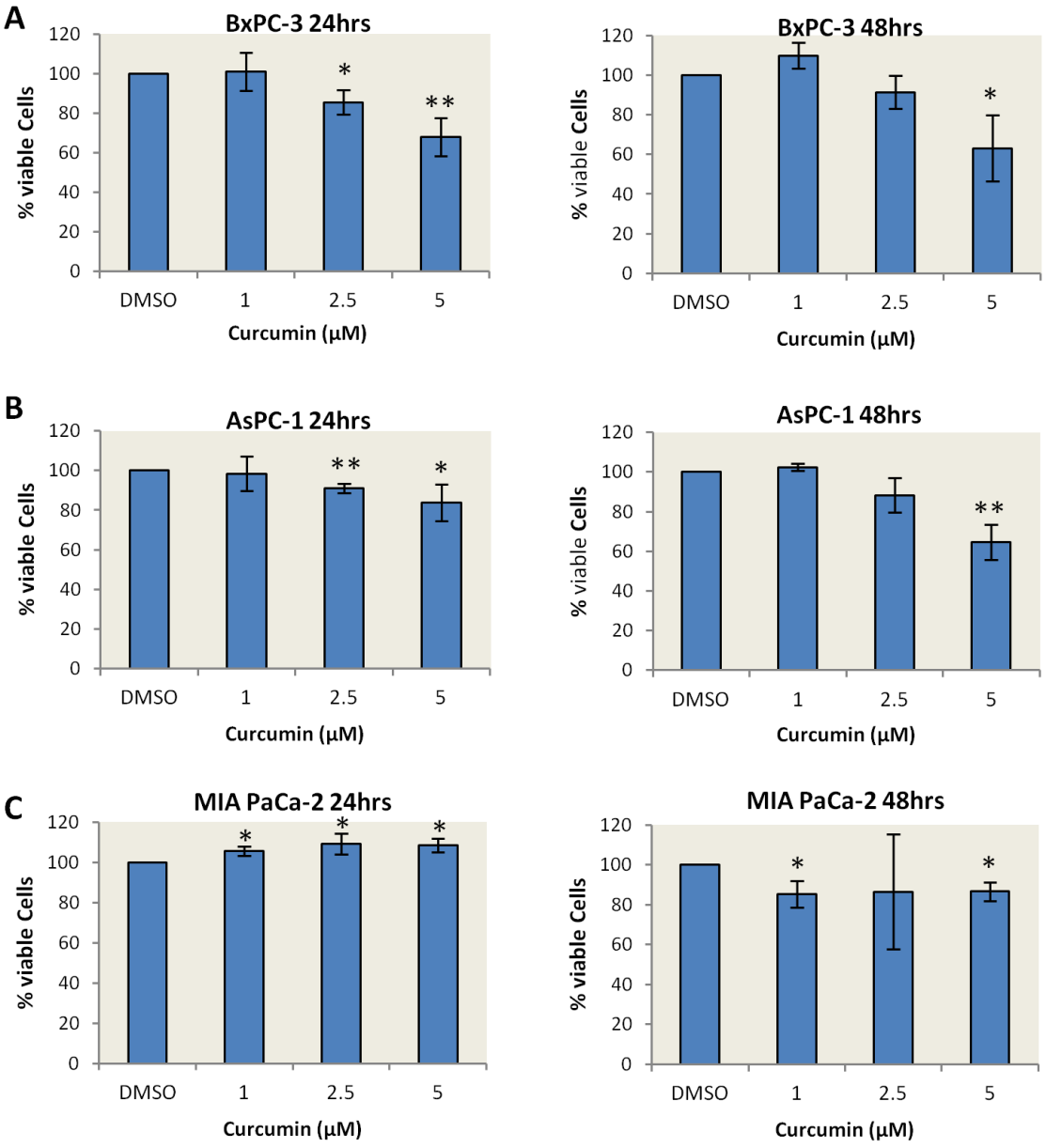

Figure 4.12: Percentage Cell Viability of Pancreatic Cancer Cell Lines Following Treatment with Curcumin for 24 and 48 Hours. Effect of varying concentrations of curcumin (1, 2.5 or 5µM) on cell viability as determined using an ATPlite™ Luminescence Assay System after 24 or 48 hours exposure in pancreatic cancer cell lines, **(A)** BxPC-3 **(B)** AsPC-1 and **(C)** MIA PaCa-2 as normalised against DMSO treated cells +SEM (n=3). (T-test; *P < 0.05, **P < 0.01).

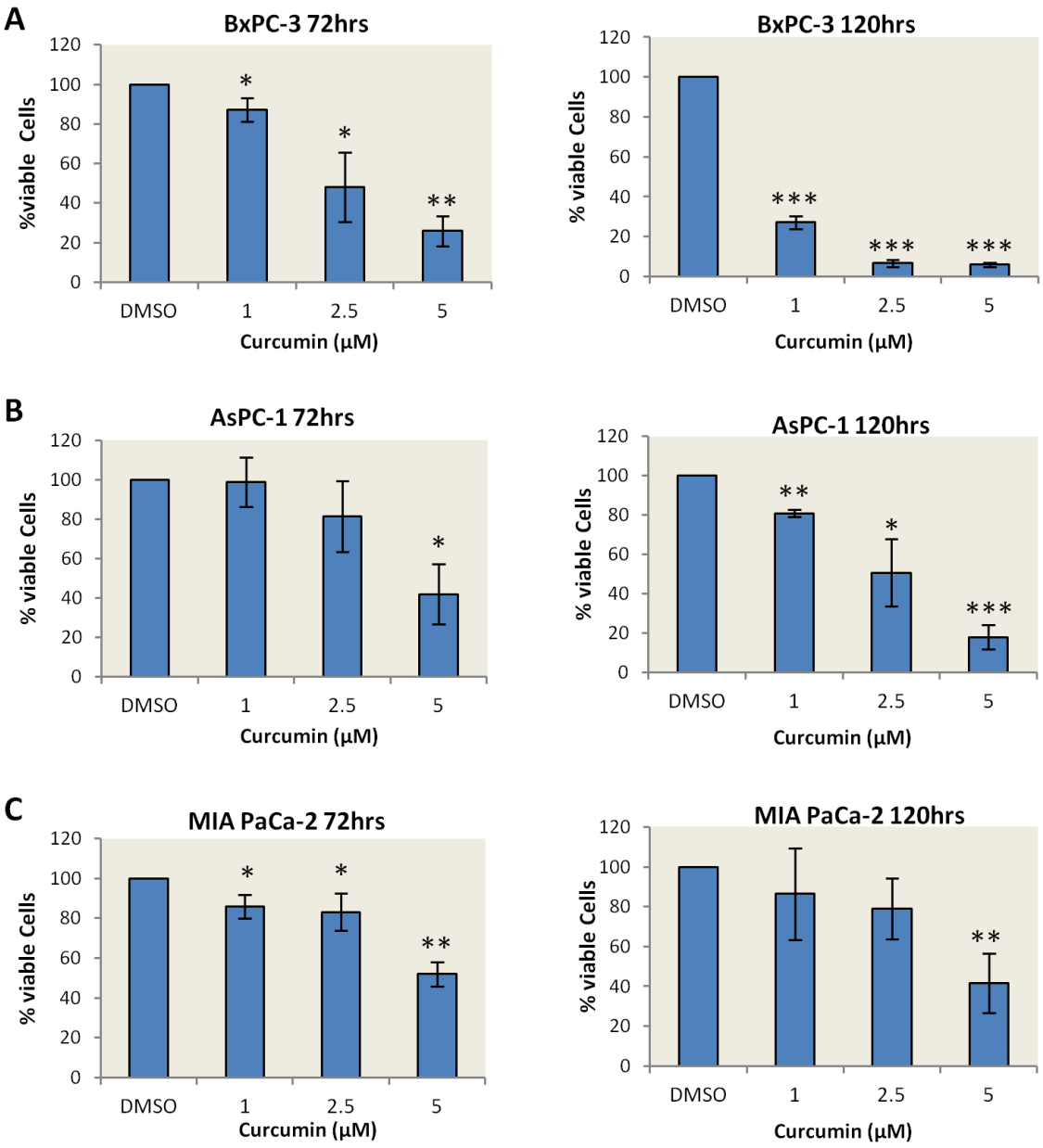

Figure 4.13: Percentage Cell Viability of Pancreatic Cancer Cell Lines Following Treatment with Curcumin for 72 and 120 Hours. Effect of varying concentrations of curcumin (1, 2.5 or 5µM) on cell viability as determined using an ATPlite™ Luminescence Assay System after 72 or 120 hours exposure in pancreatic cancer cell lines, **(A)** BxPC-3 **(B)** AsPC-1 and **(C)** MIA PaCa-2 as normalised against DMSO treated cells +SEM (n=3). (T-test; *P < 0.05, **P < 0.01, ***P < 0.001).

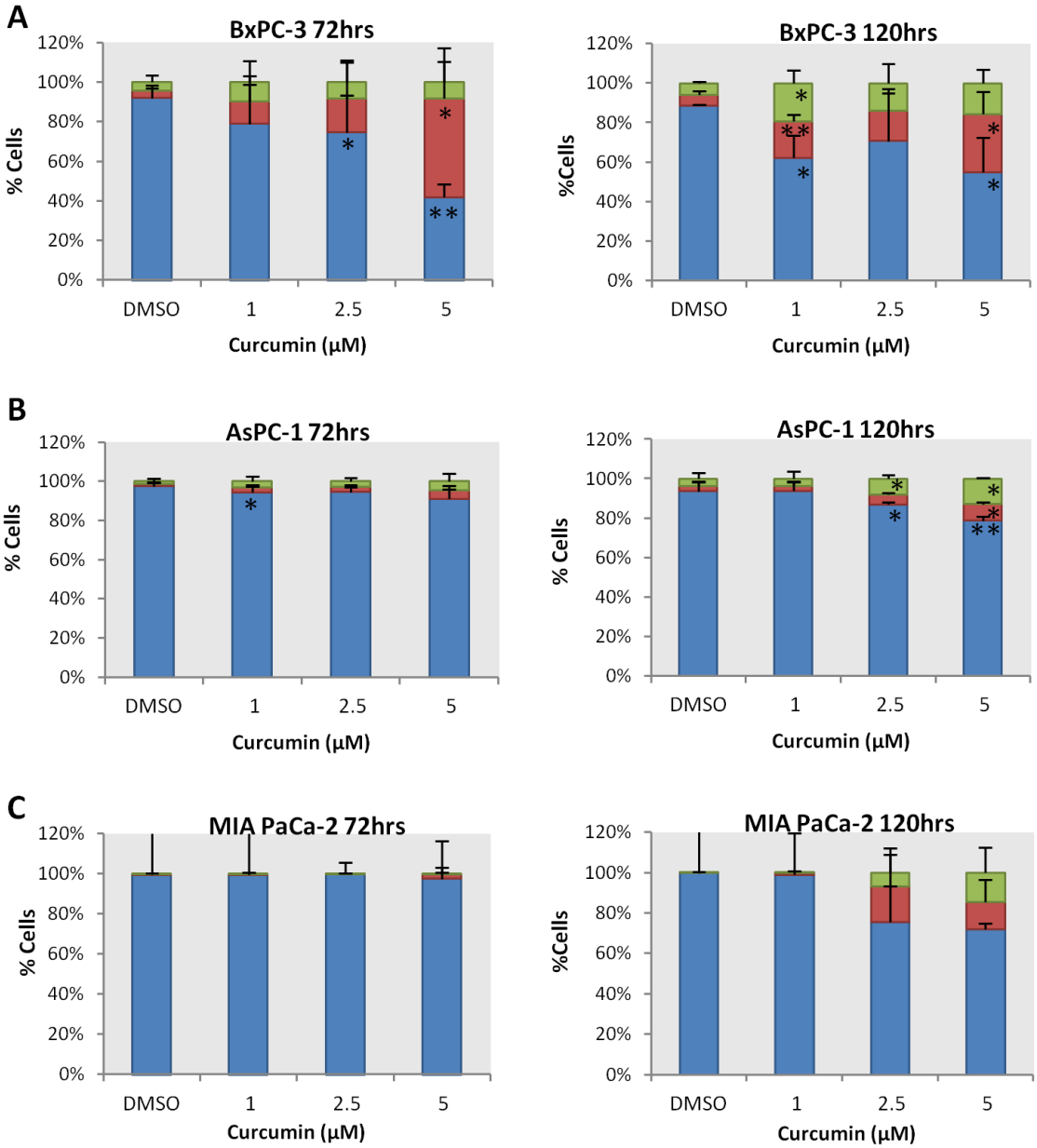

Figure 4.14: Cell Death as Observed Following Annexin V/Pi Assays in Pancreatic Cancer Cell Lines. Effect of varying concentrations of curcumin (1, 2.5 or 5µM) on cell death as measured following labelling of cells with Annexin V/Pi after either 72 or 120 hours exposure in pancreatic cancer cell lines **(A)** BxPC-3 **(B)** AsPC-1 and **(C)** MIA PaCa-2 normalised against DMSO treated cells +SEM (n=3). (T-test; *P < 0.05, **P < 0.01). Apoptotic (green), necrotic (red), live (blue).

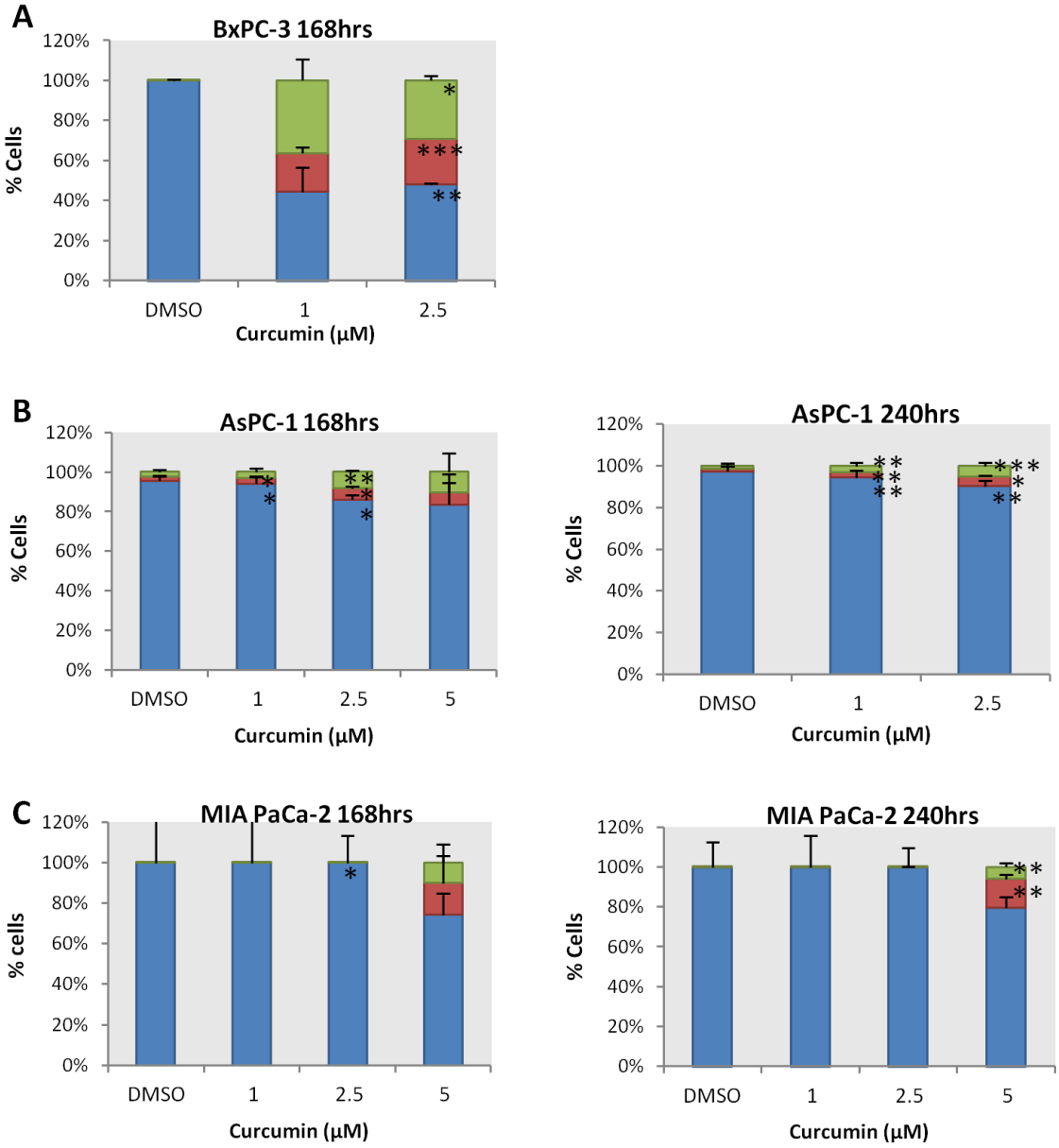

Figure 4.15: Cell Death as Observed Following Annexin V/Pi Assays in Pancreatic Cancer Cell Lines. Effect of varying concentrations of curcumin (1, 2.5 or 5µM) on cell death as measured following labelling of cells with Annexin V/Pi after either 168 or 240 hours exposure in pancreatic cancer cell lines **(A)** BxPC-3 **(B)** AsPC-1 and **(C)** MIA PaCa-2 normalised against DMSO treated cells +SEM (n=3). (T-test; *P < 0.05, **P < 0.01, ***P < 0.001). Apoptotic (green), necrotic (red), live (blue).

4.2.4.3. Growth Curves

To assess the effect of curcumin on the ability of MIA PaCa-2, AsPC-1 and BxPC-3 cells to proliferate, growth curves were determined daily following treatment with 1, 2.5 and 5μM curcumin using a Z2 Coulter Particle Count and Size Analyzer (section 2.2.4) over a period of 10 days. The ability of BxPC-3 cells to proliferate was greatly reduced following treatment with all curcumin concentrations (Figure 4.16A). Reduced cell proliferation for AsPC-1 was detected following treatment with 2.5 and 5μM curcumin (Figure 4.16B). However, MIA PaCa-2 cell proliferation was only mildly reduced when treated with 5μM curcumin (Figure 4.16C).

Results indicated an increased sensitivity of BxPC-3 and AsPC-1 cells to curcumin when compared to MIA PaCa-2 cells (Figure 4.12-4.16). This correlates with previous characterisation of various PC cell lines, which determined BxPC-3 and AsPC-1 cells to be moderately differentiated and MIA PaCa-2 cells to be poorly differentiated (Sipos et al, 2003). Effects of curcumin on growth, apoptosis and viability were only observed for MIA PaCa-2 cells when the highest doses of curcumin were used and at the longest time points. Even though both BxPC-3 and AsPC-1 cells are termed moderately differentiated, BxPC-3 cells appeared to be more sensitive to curcumin with greater reductions observed for cell viability and growth when compared with AsPC-1 cells (Figure 4.12, 4.13 and 4.16). BxPC-3 cells also appeared to undergo apoptosis at both lower doses of curcumin and shorter exposure times. Significant increases in apoptosis and necrosis occurred following 72 hours exposure in BxPC-3 cells, but not until 120 hours for AsPC-1 cells (Figure 4.14 and 4.15).

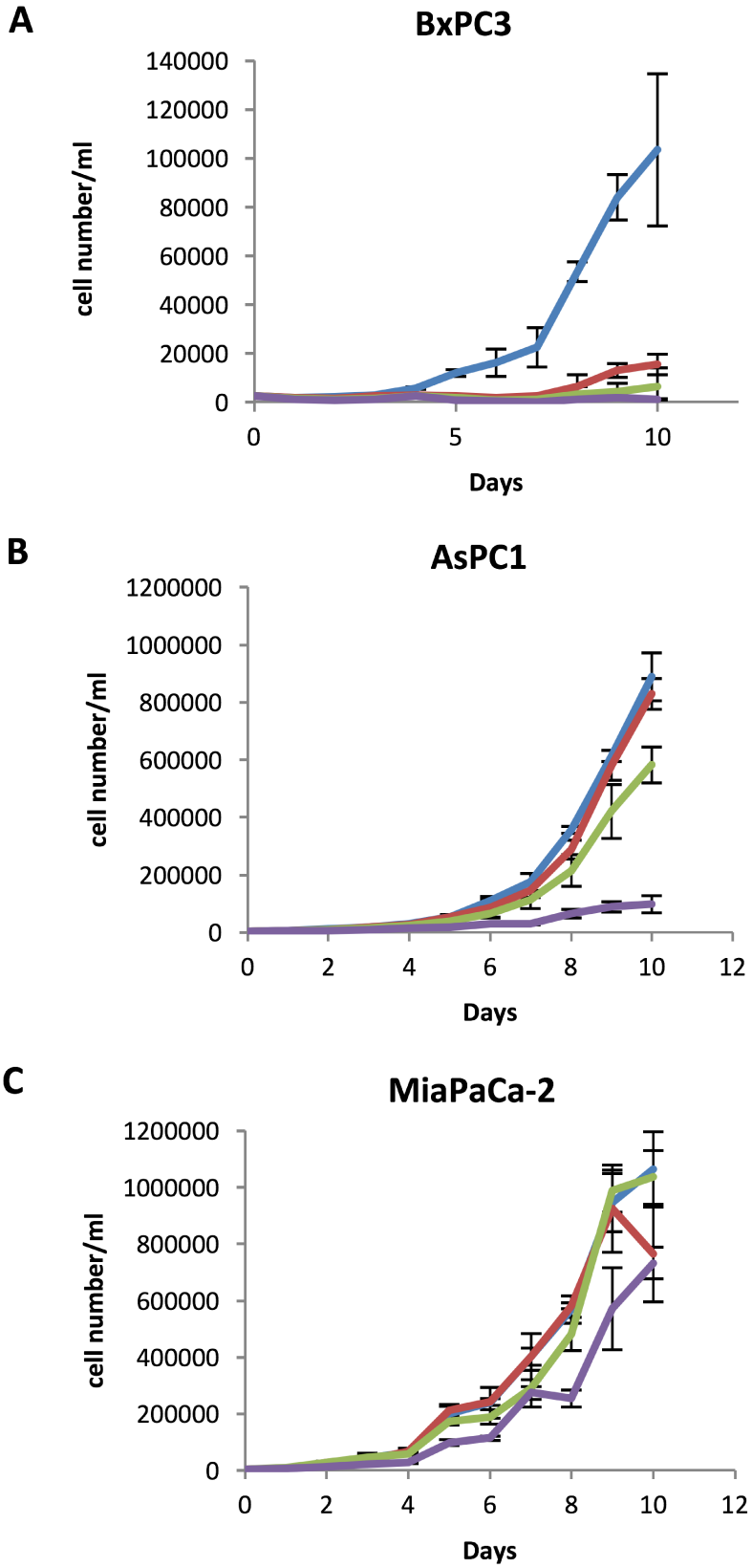

Figure 4.16: Growth Curves for Pancreatic Cancer Cell Lines Following Curcumin Treatment. Pancreatic cancer cells were seeded at $2.5x10^3$ cells/well on day zero and were treated with 1µM (red), 2.5µM (green) or 5µM curcumin (purple) along with DMSO (blue) for 10 days after which cell number (cell number/ml) per day was determined (n=1). Standard deviation between the three technical repeats produced at each time point can be observed on the graph.

4.3. Discussion

The aim of the experiments described in this chapter was to determine if increased miR-34 expression observed in PC cell lines following treatment with curcumin translated into the downregulation of c-Myc protein expression. To date, literature has been published in regard to the modulation of the miR-34 family through both p53 dependent and independent pathways in CRC and its downstream effects on c-Myc (Kress et al, 2011; Cannell et al, 2010). Downregulated miR-34 levels and elevated c-Myc expression have been observed in PC cells, but with no proof that miR-34 may regulate c-Myc as is seen in CRC (Ji et al, 2009; Boominathan, 2010; Pelengaris et al, 2002). No other study to date has looked to see whether the miR-34 family can regulate c-Myc expression in PC cells lines, or if curcumin has the potential to modulate components of this pathway to prevent up regulation of c-Myc. Data produced in this study suggested that c-Myc and MK5 expression in both PC and CRC cells appeared to be unaffected following curcumin treatment. This was in spite of the obvious effects of curcumin on cell viability, cell death and cell growth in the PC cell lines BxPC-3, AsPC-1 and MIA PaCa-2.

Several factors, including the intrinsic protein levels of c-Myc and potential technical difficulties related to the antibody prevented the successful production of complete datasets for the range of dose and time dependent experiments. Protein expression for c-Myc in both cell lines was low making it difficult to produce consistent and reliable western blots. In order to overcome this, various antibodies, protein extraction methods and detection techniques (ECL/odyssey) were employed. However, western blots for c-Myc expression remained problematic. In addition, no significant decreases in c-Myc protein expression were observed in the CRC cell line HCT116 following treatment with curcumin (Figure 4.5 and 4.6).

Although miR-34b/c has been shown to be indirectly regulated by MK5 in CRC, no link between these signalling molecules had been shown in PC (Figure4.2) (Myant and Sansom, 2011; Kress et al, 2011). When curcumin failed to induce any changes in c-Myc expression in either PC or CRC cells, the effects of this agent on the expression of MK5 were examined. Protein levels remained largely unaffected following treatment in MIA PaCa-2, AsPC-1 and HCT116 cells (Figure 4.7-4.11). The actin loading controls for some of the western blots were inconsistently expressed. The reason for this is

uncertain. Protein concentrations were calculated for all samples using a BCA assay (section 2.2.5.1.2), so that equal amounts of sample could be loaded onto each gel. Although it is possible that curcumin could affect levels of actin, on most of the western blots actin levels were consistent and unaffected by this agent. While the reduced expression of actin for certain western blots was disconcerting, overall, curcumin appeared to have no effect on c-Myc and MK5 protein expression irrespective of this issue.

The inability to validate the differentially expressed miRNAs obtained from microarrays treated for 24 hours with 5μM curcumin (chapter 3), in addition to lack of any changes in either MK5 or c-Myc protein expression, cast doubt on the capacity of curcumin to elicit a biological response. Therefore, cell viability and cell growth in response to curcumin were reassessed in various PC cell lines. Analysis of cell viability highlighted increased sensitivity of both BxPC-3 and AsPC-1 cells to curcumin when compared with MIA PaCa-2 cells (Figure 4.12 and 4.13). Treatment of BxPC-3 and AsPC-1 cells resulted in elevated levels of apoptosis and necrosis when compared with MIA PaCa-2 cells (Figure 4.14 and 4.15). Although both BxPC-3 and AsPC-1 cells are understood to be moderately differentiated, lower doses and shorter treatment times were sufficient to elicit apoptosis in BxPC-3 cells (Figure 4.14 and 4.15) (Sipos et al, 2003). Cell growth data also indicated that BxPC-3 cells appeared to be the most sensitive to curcumin with MIA PaCa-2 cells the least sensitive (Figure 4.16). These data also showed that longer exposure to lower doses of curcumin could potentially be equally as efficient at affecting growth and viability as higher doses for shorter periods of time.

It is possible that the dose of curcumin used (5μM, 24 hrs) for the microarray analysis in chapter 3 was not sufficient to obtain a significant cellular response from either AsPC-1 or MIA PaCa-2 cells. The data presented here have demonstrated that even with low doses of curcumin biological changes are observed in these cell lines, when treated over longer periods of time. Based on this evidence and to investigate this further a dose of 1.5μM curcumin was used to treat BxPC-3, AsPC-1 and MIA PaCa-2 for 96 hours for further miRNA microarray analysis.

Chapter 5. Agilent Microarray Analysis of Differentially miRNA Expression in Pancreatic Cancer Cell Lines Following Curcumin Treatment

5.1. Introduction

Initial attempts at microarray profiling following curcumin treatment (chapter 3), suggested a number of modulated target miRNAs. However, attempts to validate these changes using RT-qPCR analysis were not successful. It was difficult to determine whether this was because there was no genuine effect following curcumin treatment, or if deficiencies within the microarray experiment prevented successful assessment of the data.

In an attempt to address these difficulties and optimise curcumin treatment, the biological effect on PC cell lines was evaluated in chapter 4. The data generated indicated a lack of response from both AsPC-1 and MIA Paca-2 cells when treated with 5μM curcumin for 24 hours. Further assessment, however, demonstrated that longer exposure to lower doses of curcumin could potentially be equally as efficient as higher doses for shorter periods of time. As mentioned in section 3.2.1 the PC cell lines AsPC-1 and MIA PaCa-2 were chosen for their dissimilar differentiation status and origin. The response of the PC cell line BxPC-3 to curcumin was assessed in addition to AsPC-1 and MIA PaCa-2, with high, moderate and low sensitivity observed in each cell line respectively (detailed cell line information in Appendix 1). Due to the varied response of these PC cell lines to curcumin, BxPC-3 cells were chosen in addition for subsequent microarray analysis. With this evidence in mind further miRNA microarray analysis was carried out using a dose of 1.5μM curcumin to treat BxPC-3, AsPC-1 and MIA PaCa-2 cells for 96 hours.

5.2. Results

5.2.1. RNA Production and Microarray Quality Control

Agilent Sureprint miRNA microarrays were used in combination with spike-in and labelling reagents, also from Agilent, to observe differential miRNA expression (section 2.2.7.2). MIA PaCa-2, AsPC-1 and BxPC-3 cells were treated for 96 hours with 1.5μM curcumin or DMSO (control), after which TRI-reagent® RNA extraction method B (section 2.2.6.1) was utilised for total RNA isolation. QC was performed to ascertain

that all RNA samples achieved the recommended ratio of absorbance at 260/280nm and 260/230nm of ≥2 and RIN value of ≥7. All samples met or exceeded these criteria and were therefore used in the microarray profiling analysis (Table 5.1).

Table 5.1: Quality Control Data Following RNA Extraction.

Sample ID	Conc. (ng/µl)	A260/280	A260/230	RIN
M1	336	2.01	1.99	10.0
M2	421	2.05	2.00	10.0
M3	222	1.95	1.90	9.8
M4	444	1.99	2.05	10.0
M5	290	1.95	1.97	9.9
M6	352	2.06	1.98	10.0
M7	288	1.99	1.99	10.0
M8	392	2.04	2.04	10.0
A1	265	1.99	1.97	9.9
A2	187	2.03	1.83	9.9
A3	206	2.05	1.87	9.6
A4	179	2.03	1.85	10.0
A5	210	1.99	1.91	10.0
A6	198	2.01	1.88	8.3
A7	189	2.05	1.87	10.0
A8	128	2.02	1.89	10.0
B1	122	2.09	1.91	10.0
B2	296	2.10	2.02	9.8
B3	298	2.02	2.07	10.0
B4	354	2.09	2.01	10.0
B5	126	2.02	1.93	10.0
B6	188	2.08	1.96	10.0
B7	194	1.95	1.90	8.9
B8	284	2.09	1.93	9.4

Measurements obtained following TRI-reagent® extraction B of 4 pairs of independent biological repeats acquired from MIA PaCa-2, AsPC-1 and BxPC-3 cell lines treated with either 1.5µM curcumin or DMSO (control) for 96 hours. (Key: M = MIA PaCa-2, A= AsPC-1, B= BxPC-3)

The experimental setup consisted of four paired biological repeats with curcumin (1.5µM) and DMSO control treated samples following 96 hours exposure. Single colour microarrays were used, whereby 245ng of total RNA for each sample were combined with spike-in solutions, after which a single Cyanine-3-pCp molecule was ligated to the 3' end of each individual RNA molecule (section 2. 2.7.2). A single technical repeat

was carried out for each biological sample. Each microarray comprised of twenty repeats for each miRNA probe, with two different probes present for each miRNA assessed. Once labelled, RNA samples were hybridised to Agilent SurePrint G3 human v16 miRNA arrays (G2534A), scanned using an Agilent G2565 scanner and processed using Agilent feature extraction software. QC reports for each microarray sample were produced by this software in order to evaluate the reproducibility and reliability of the data (Figure 5.1).

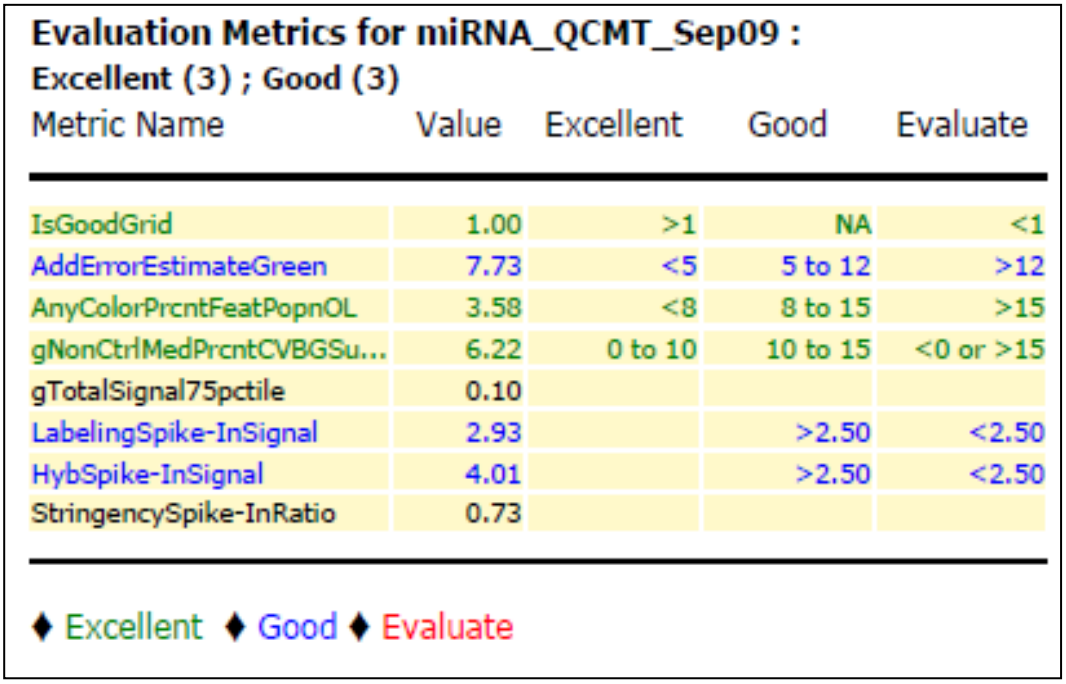

Evaluation Metrics for miRNA_QCMT_Sep09 :
Excellent (3) ; Good (3)

Metric Name	Value	Excellent	Good	Evaluate
IsGoodGrid	1.00	>1	NA	<1
AddErrorEstimateGreen	7.73	<5	5 to 12	>12
AnyColorPrcntFeatPopnOL	3.58	<8	8 to 15	>15
gNonCtrlMedPrcntCVBGSu...	6.22	0 to 10	10 to 15	<0 or >15
gTotalSignal75pctile	0.10			
LabelingSpike-InSignal	2.93		>2.50	<2.50
HybSpike-InSignal	4.01		>2.50	<2.50
StringencySpike-InRatio	0.73			

♦ Excellent ♦ Good ♦ Evaluate

Figure 5.1: Microarray Quality Control Report. Various criteria were assessed for the labelling and hybridisation of samples within each array in order to determine if data were both reproducible and reliable. A rating system for the assessment of the QC data allowed for the quick evaluation of each microarray. Values deemed good (blue) or excellent (green) indicated criteria had been reached or exceeded, and values which did not reach the criteria were flagged as evaluate (red). Microarrays attributed as good or excellent were incorporated for further analysis, with remaining microarrays evaluated to determine their suitability for further analysis.

5.2.2. Manual Analysis of Agilent miRNA Microarray Data

Once processed, raw microarray data can be normalised and analysed in order to identify differentially expressed miRNAs. Due to lack of software available at the time, manual analysis of the microarray data was initially attempted. The gMeanSignal (the mean green fluorescence signal) for each probe is the measure of fluorescence present for a specific miRNA, and therefore an indication of the level of expression for a particular miRNA in a sample. These values underwent background subtraction (to

exclude background fluorescence) followed by manual normalisation using the 75th percentile. Once normalised, the fold change and p-value (T-test) were calculated and miRNAs with negative expression levels removed. There are potentially 40 probes present on each microarray for each miRNA target, which consists of twenty repeats of two different probe sequences. When manually assessing the microarray data each probe value was processed, normalised and analysed independently. The fold change in expression for each independent miRNA probe was then evaluated to identify candidate miRNAs for differential expression following curcumin treatment. When assessed, no miRNAs stood out as having any large significant change in expression. It was decided therefore to look for miRNAs where multiple independent probes for the same miRNA were frequently observed with log2 fold changes >1 or <-1.

5.2.3. Global Increases in miRNA Expression

Microarray analysis of MIA PaCa-2 and AsPC-1 cells had previously shown that following curcumin treatment miRNA expression was globally decreased (chapter 3). Interestingly, manual analysis of the Agilent microarray data demonstrated the opposite, with ~90% of the miRNAs showing an increase in expression in the MIA PaCa-2 and AsPC-1 cells treated for 96 hours with 1.5μM curcumin. It was proposed that the biogenesis enzymes drosha and dicer may be regulated by curcumin, thus contributing to the observed increase in miRNA expression. It was important to know what was happening in regard to miRNA processing, as global effects on miRNA expression, as a result of curcumin treatment, could have altered how this data was analysed. Therefore, mRNA and protein expression levels for drosha and dicer were again assessed in all curcumin treated PC cell lines.

Using SensiMix SYBR® Green RT-qPCR (section 2.2.8.3) no statistically significant changes in mRNA expression for drosha or dicer were observed in either MIA PaCa-2 or AsPC-1 cells (Figure 5.2C-F). No change in mRNA expression was observed for dicer in BxPC-3 cells, however, a statistically significant decrease ($p<0.05$) was observed for drosha (Figure 5.2A and B). Western blot analysis showed no changes in protein expression in any of the cell lines following treatment when normalised against the DMSO control (Figure 5.2G-J). When compared to normal pancreas, drosha and dicer mRNA expression was elevated in all PC cell lines including BxPC-3 (unpublished data from Manson Lab).

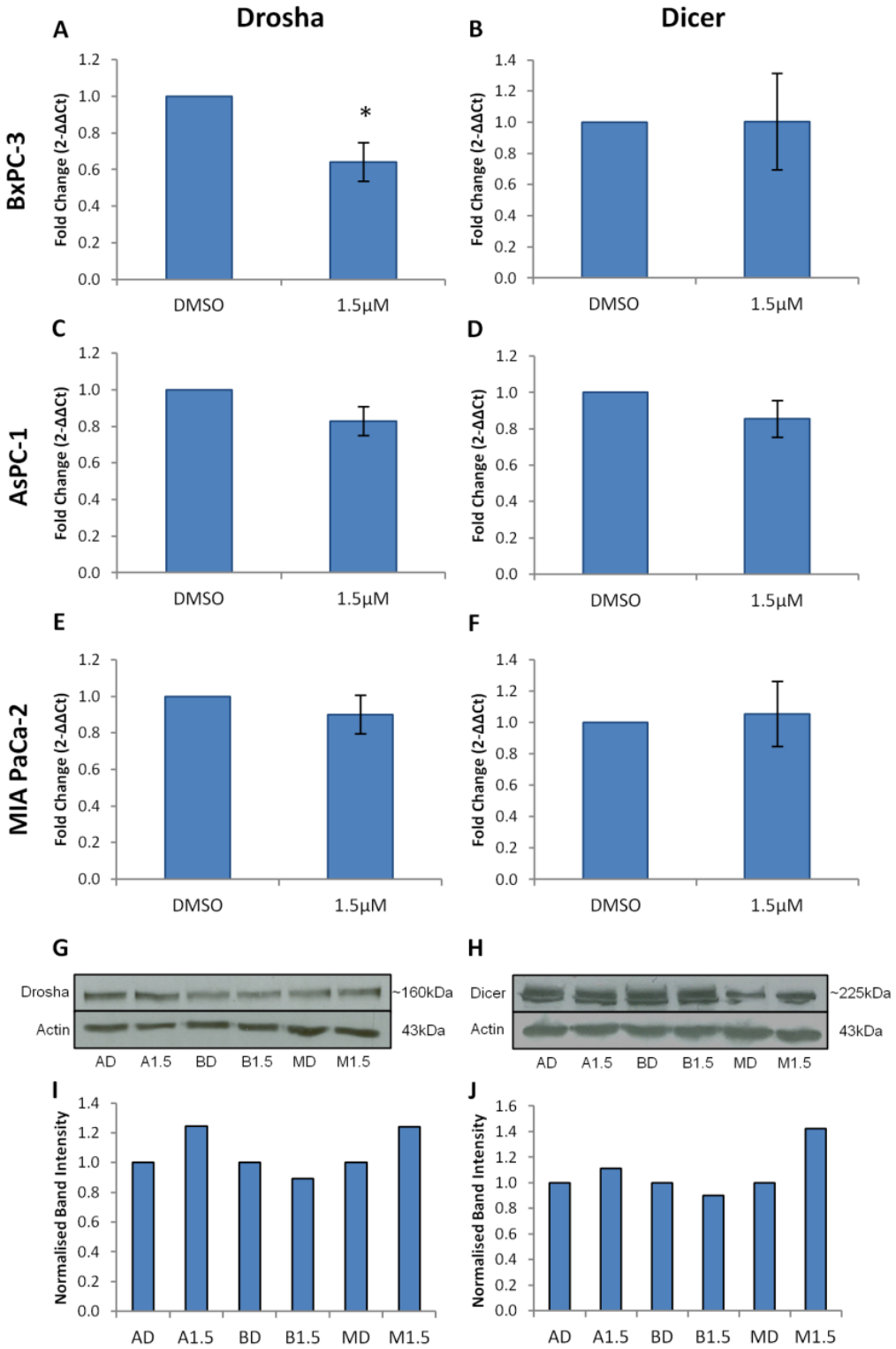

Figure 5.2: Effects of Curcumin on Drosha and Dicer mRNA and Protein Expression. BxPC-3, AsPC-1 and MIA PaCa-2 cells were treated with 1.5µM curcumin or DMSO (control) for 96 hours and analysed for **(A, C, E)** drosha and **(B, D, F)** dicer mRNA expression. SensiMix SYBR® Green RT-qPCR data were normalised against 18S rRNA and represent the mean ± SEM (n=4) (paired T-test). Representative ECL blots showing changes in amount of **(G)** drosha and **(H)** dicer following treatment with curcumin with actin as a loading control. Histograms representing changes in band intensity of **(I)** drosha (n=1) and **(J)** dicer (n=1) protein expression for curcumin treated cells when normalised against DMSO treated cells. (Key: MD = MIA PaCa-2 DMSO treated, M1.5= MIA PaCa-2 curcumin treated, AD = AsPC-1 DMSO treated, A1.5 = AsPC-1 curcumin treated, BD= BxPC-3 DMSO, B1.5= BxPC-3 curcumin treated.)

5.2.4. Canonical Pathway Analysis

The miRNAs miR-29b-3p, miR-34b-5p, miR-30b-5p, miR-30c-5p and miR-128a, identified as differentially expressed following curcumin treatment, were entered into the miRWalk database. A list of all target mRNAs containing validated binding sites for these miRNAs was then uploaded to Ingenuity IPA software for pathway analysis (IngenuityR Systems, www.ingenuity.com) and any associations investigated. The IPA software identified canonical pathways which contained a significant number of these mRNAs shown to be potential targets of the differentially expressed miRNAs (Table 5.2). The pancreatic adenocarcinoma signalling pathway was the second most significantly enriched canonical pathway for this miRNA combination (Figure 5.3).

Table 5.2: Canonical Pathways Predicted by IPA Analysis as Significantly Altered Following Treatment with Curcumin.

Ingenuity Canonical Pathways	-log (p-value)	Ratio	Genes
Molecular Mechanisms of Cancer	32.10	0.19	72/388
Pancreatic Adenocarcinoma Signaling	23.70	0.28	36/128
Cell Cycle: G1/S Checkpoint Regulation	19.30	0.36	26/72
Chronic Myeloid Leukemia Signaling	19.10	0.28	30/106
Hepatic Fibrosis / Hepatic Stellate Cell Activation	18.40	0.23	35/155
p53 Signaling	16.40	0.25	28/113
Small Cell Lung Cancer Signaling	14.90	0.25	23/94
Glioblastoma Multiforme Signaling	14.90	0.19	32/168
Role of Osteoblasts, Osteoclasts and Chondrocytes in Rheumatoid Arthritis	14.90	0.16	39/250
Cyclins and Cell Cycle Regulation	14.70	0.25	24/96
Glucocorticoid Receptor Signaling	14.40	0.14	42/299
Colorectal Cancer Metastasis Signaling	14.20	0.15	40/268
Aryl Hydrocarbon Receptor Signaling	13.80	0.18	30/171
PI3K/AKT Signaling	13.70	0.18	28/152
TGF-β Signaling	12.80	0.25	23/94
Wnt/β-catenin Signaling	12.20	0.18	31/175
Role of Macrophages, Fibroblasts and Endothelial Cells in Rheumatoid Arthritis	12.00	0.12	42/342
Factors Promoting Cardiogenesis in Vertebrates	11.60	0.22	22/99
Role of Tissue Factor in Cancer	11.30	0.19	24/130
ILK Signaling	11.10	0.15	31/205
Ovarian Cancer Signaling	11.10	0.17	26/152
Glioma Signaling	11.00	0.20	22/113
Human Embryonic Stem Cell Pluripotency	10.90	0.16	26/162
Regulation of the Epithelial-Mesenchymal Transition Pathway	10.80	0.15	30/196
PTEN Signaling	10.80	0.17	24/138
Estrogen-mediated S-phase Entry	10.70	0.43	12.28

Table 5.2: Continued.

Ingenuity Canonical Pathways	-log (p-value)	Ratio	Genes
IL-8 Signaling	10.40	0.13	30/225
Prostate Cancer Signaling	10.40	0.19	20/103
HER-2 Signaling in Breast Cancer	9.31	0.22	18/82
Melanoma Signaling	8.43	0.26	13/50
Agrin Interactions at Neuromuscular Junction	8.30	0.23	16/70
Macropinocytosis Signaling	8.30	0.21	16/77
PPARα/RXRα Activation	8.28	0.13	26/200
VDR/RXR Activation	8.23	0.19	17/88
Regulation of IL-2 Expression in Activated and Anergic T Lymphocytes	8.14	0.19	17/89
Bladder Cancer Signaling	8.13	0.19	18/97
Clathrin-mediated Endocytosis Signaling	7.87	0.13	26/198
STAT3 Pathway	7.82	0.20	16/80
Axonal Guidance Signaling	7.76	0.09	43/487
Antiproliferative Role of TOB in T Cell Signaling	7.66	0.39	10.26
Tec Kinase Signaling	7.43	0.13	23/184
Induction of Apoptosis by HIV1	7.39	0.21	14/67
Huntington's Disease Signaling	7.34	0.11	28/252
HGF Signaling	7.30	0.16	18/111
Renal Cell Carcinoma Signaling	7.23	0.19	15/79
iNOS Signaling	7.14	0.23	12.53
Hereditary Breast Cancer Signaling	6.98	0.14	19/134
IL-6 Signaling	6.98	0.15	19/124
Tight Junction Signaling	6.94	0.13	22/167
Germ Cell-Sertoli Cell Junction Signaling	6.78	0.13	22/169

Having obtained a list of target mRNAs for the miRNA combination miR-29b-3p, miR-34b-5p, miR-30b-5p, miR-30c-5p and miR-128a using miRWalk, these data were uploaded to the Ingenuity IPA software in order to identify any canonical pathways which may have been affected following treatment of PC cells with curcumin. Both the ratio and genes columns represent the number of mRNAs that could potentially be affected by curcumin within each canonical pathway. The significance for each canonical pathway is represented as the –log of the p-value (whereby a p-value of 0.001 is represented as a –log value of 3).

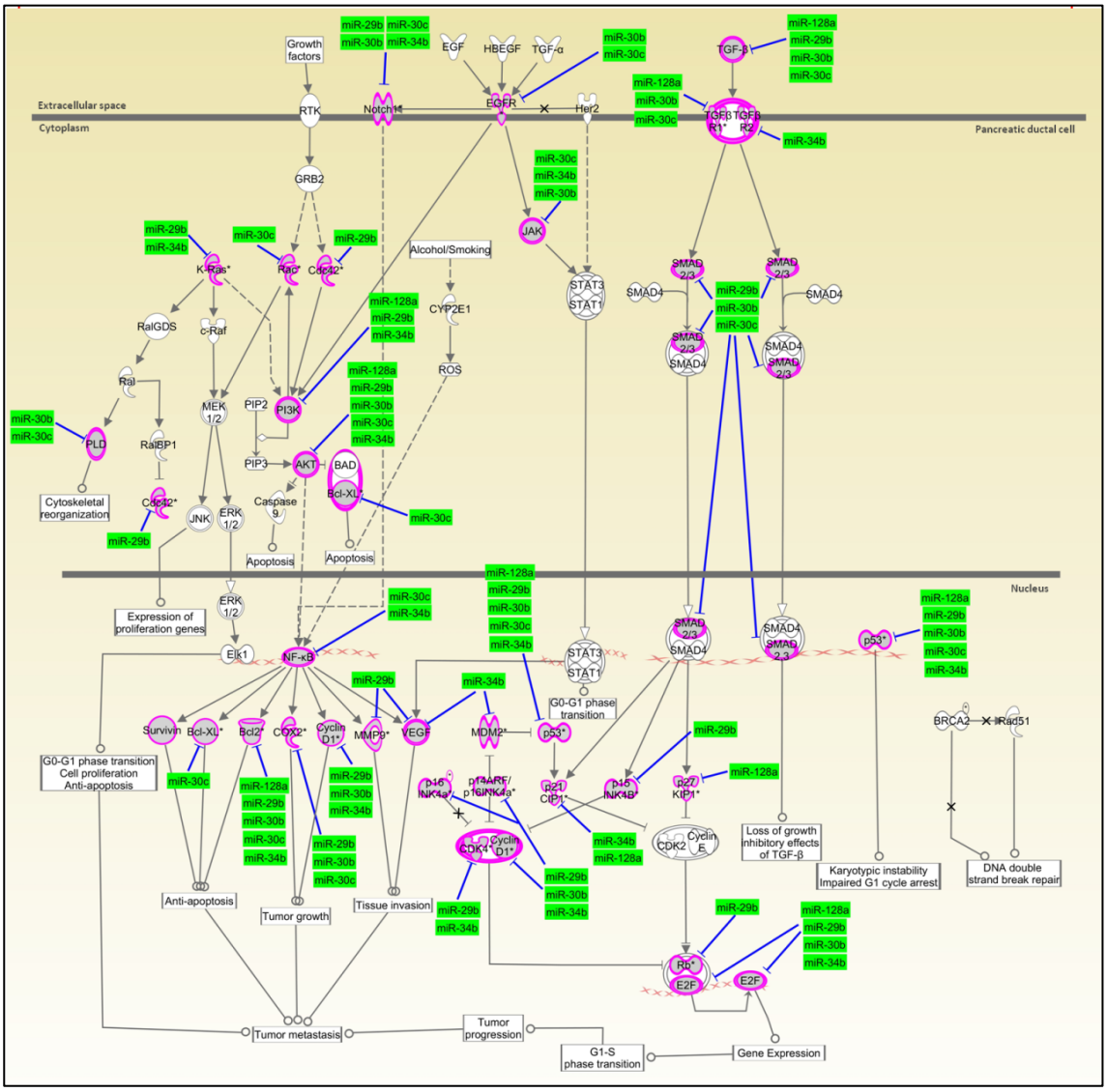

Figure 5.3: The Pancreatic Adenocarcinoma Signalling Pathway. The mRNA target list produced in miRWalk for the selected miRNAs was uploaded to Ingenuity IPA software and connections between these mRNAs were mapped. Of the 128 mRNA target encoding genes associated with the pancreatic adenocarcinoma signalling pathway, 36 were targeted by one or more of the assessed miRNAs and are highlighted in pink. Interactions between the molecules in this pathway are indicated by solid and dashed grey lines corresponding to direct and indirect interactions respectively. The miRNAs deregulated in curcumin treated PC cells are coloured green according to their decrease in expression and blue lines are used to indicate their validated mRNA targets (an enlarged version of this figure is available in Appendix 8).

5.2.5. Validation of Differentially Expressed miRNAs using RT-qPCR

Taqman® RT-qPCR (section 2.2.8.1) was used to confirm the differential expression of a subset of miRNAs; miR-29b-3p, miR-34b-5p, miR-30b-5p, miR-30c-5p and miR-128a, identified following manual analysis of the microarray data. Following treatment each of these miRNAs was found to be differentially expressed in at least two of the PC cell lines. In the AsPC-1 and BxPC-3 cell lines miR-30b-5p and miR-30c-5p were both downregulated, and in MIA PaCa-2 and AsPC-1 cells miR-34b-5p was upregulated. Interestingly, miR-128a and miR-29b-3p were both upregulated by curcumin in AsPC-1 cells and downregulated in BxPC-3 cells.

Taqman® RT-qPCR analysis of the altered expression in these five miRNAs was not successful, with no change in expression observed for any of the target miRNAs (Figure 5.4, 5.5 and 5.6). Although not statistically significant, an increase in expression of miR-34b-5p was observed in BxPC-3 treated cells (Figure 5.4B). Interestingly, this miRNA was not found to be differential expressed in this cell line when manually analysing the microarray data, with its elevated expression only being detected in curcumin treated MIA PaCa-2 and AsPC-1 cells.

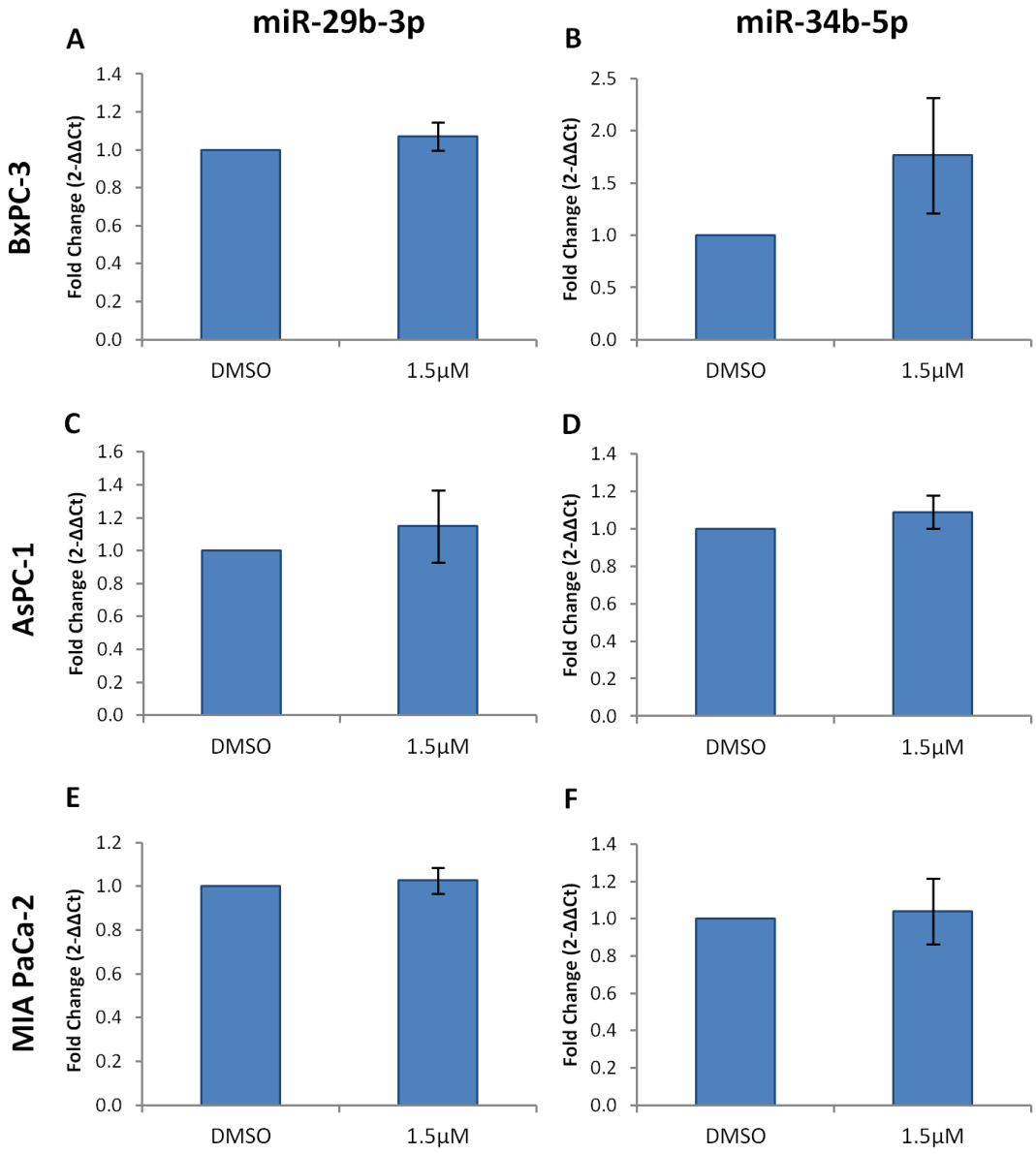

Figure 5.4: Taqman® RT-qPCR Analysis for Validation of Microarray Profiling Data. MIA PaCa-2, AsPC-1 and BxPC-3 cells were treated with 1.5µM curcumin or DMSO (control) for 96 hours and analysed for **(A, C, E)** miR-29b-3p and **(B, D, E)** miR-34b-5p. RT-qPCR data were normalised against RNU6B and represent the mean ± SEM (n=4) (paired T-test, no data with $p \leq 0.05$).

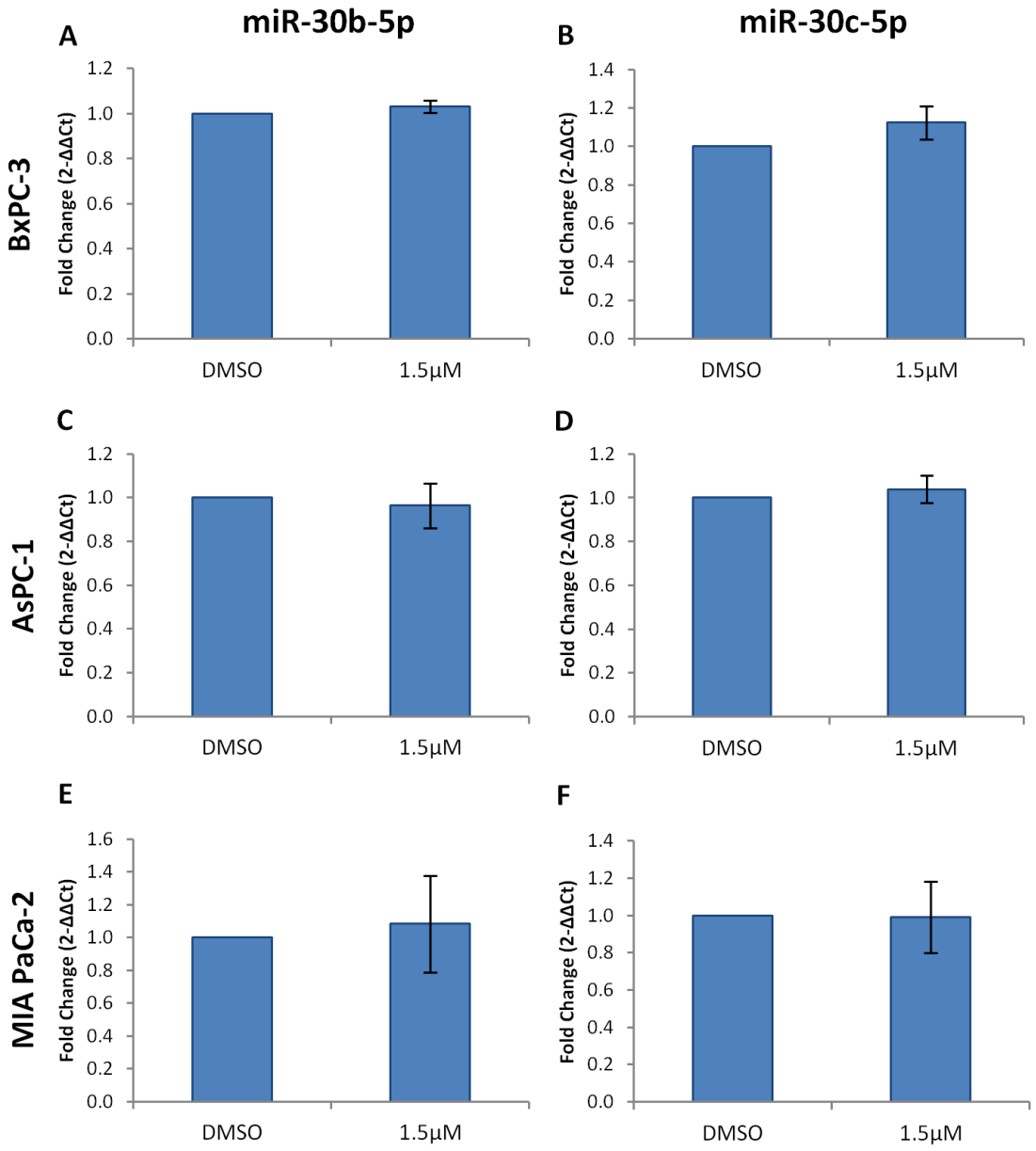

Figure 5.5: Taqman® RT-qPCR Analysis for Validation of Microarray Profiling Data. MIA PaCa-2, AsPC-1 and BxPC-3 cells were treated with 1.5µM curcumin or DMSO (control) for 96 hours and analysed for **(A, C, E)** miR-30b-5p and **(B, D, E)** miR-30c-5p. RT-qPCR data were normalised against RNU6B and represent the mean ± SEM (n=4) (paired T-test, no data with $p \leq 0.05$).

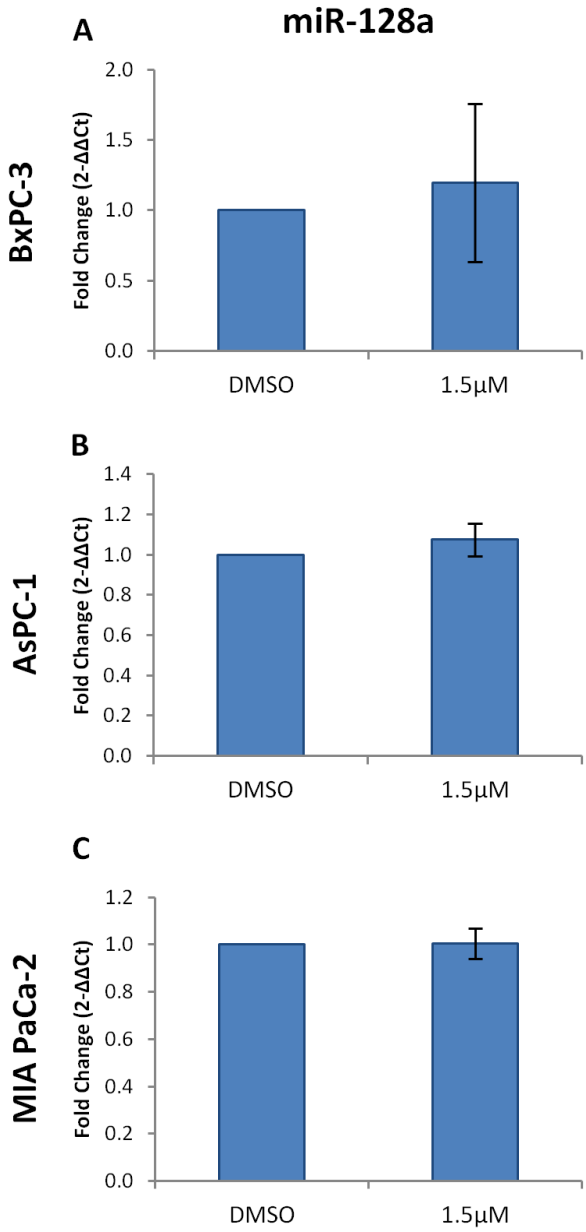

Figure 5.6: Taqman® RT-qPCR Analysis for Validation of Microarray Profiling Data. MIA PaCa-2, AsPC-1 and BxPC-3 cells were treated with 1.5µM curcumin or DMSO (control) for 96 hours and analysed for miR-128a. RT-qPCR data were normalised against RNU6B and represent the mean ± SEM (n=4) (paired T-test, no data with $p \leq 0.05$).

5.2.6. GeneSpring GX

The microarray data were also normalised (percentile shift normalisation: 90th) using Agilent Technologies GeneSpring GX software which became available during the project. Principle component analysis (PCA) plots were produced following normalisation to show data quality and expression variation between samples (Figure 5.7). A PCA plot is a method of statistical analysis which converts a set of potentially

correlative values into a set of linearly uncorrelated variables known as principal components, highlighting variability within a dataset.

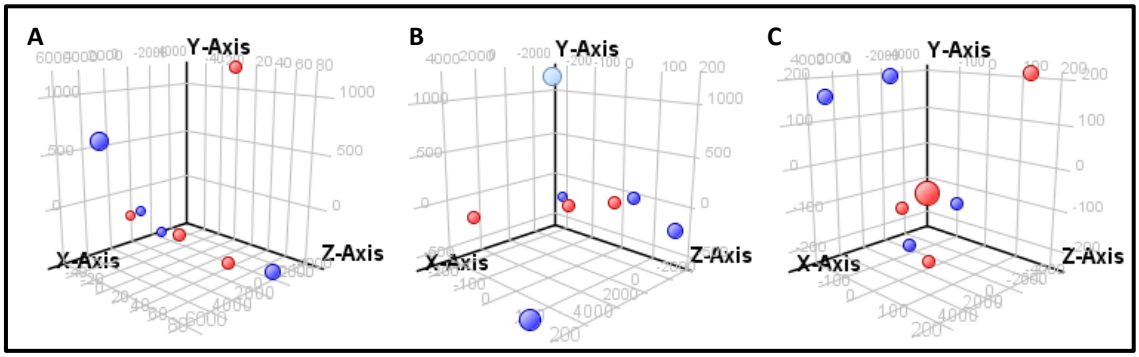

Figure 5.7: PCA Plots Following GeneSpring GX Normalisation. A PCA plot shows how data are separated in regard to expression variation and can be used in quality assessment to identify outliers and to observe grouping of samples. **(A)** MIA PaCa-2, **(B)** AsPC-1 and **(C)** BxPC-3. (Red= curcumin treated samples, blue= DMSO treated samples).

Statistical analysis of the normalised microarray data was also carried out using the GeneSpring software. Multiple testing correction (Benjamini Hochberg FDR) was applied to the data before producing a list of miRNAs believed to be differentially expressed following curcumin treatment. Tables were produced containing those miRNAs with a log2 fold change >1 or <-1 and a p-value of ≤0.5 (Appendix 5). Only two of the five miRNAs (miR-128a and miR-34b-5p) chosen from the manual analysis for validation of differential expression were also observed in the top tables produced using the GeneSpring software.

5.2.7. Analysis of Curcumin-Induced Changes in miRNAs Previously Associated with Pancreatic Cancer using RT-qPCR

Research by others has identified a number of miRNAs (miR-21, miR-200c, miR-34a, miR-148a, miR-145 and miR-143, see Chapter 3) shown to be aberrantly expressed in PC (Yu et al, 2012; Lee et al, 2007; Kent et al, 2009; Bloomston et al, 2007). It was therefore of interest to evaluate the ability of curcumin to modulate the expression of these miRNAs.

Elevated expression of miR-21 and miR-200c in BxPC-3 cells following treatment was detected using miScript SYBR® Green RT-qPCR analysis, however these changes were not found to be statistically significant (Figure 5.8A and B). Curcumin appeared to have no effect on miR-21 and miR-200c expression in MIA PaCa-2 and AsPC-1 cells (Figure

5.8C-F). Although not statistically significant, increased miR-34a expression was observed in the BxPC-3 cell line when compared to DMSO treated cells (Figure 5.9A). Expression levels of miR-34a in MIA PaCa-2 and AsPC-1 cells however, were unaltered by curcumin (Figure 5.9C and E). Surprisingly, following treatment, a statistically significant ($p<0.05$) decrease in miR-148a was seen only in the MIA PaCa-2 cells. (Figure 5.9B, D and F). No significant changes in miR-145 and miR-143 expression were observed in BxPC-3 and AsPC-1 cells (Figure 5.10A-D). Expression of miR-143 remained unaltered in MIA PaCa-2 cells, however a statistically significant ($p<0.01$) decrease in miR-145 expression was detected (Figure 5.10E and F).

An additional panel of six miRNAs (miR-503, miR-206, miR-155, miR-196a, miR-10b and miR-375), which were being investigated within our laboratory in relation to their expression in plasma samples of PC patients, were also examined. Studies have shown that, when compared to normal pancreas, elevated expression of miR-155, miR-196a and miR-10b and reduced levels of miR-375 are observed in PC (Yu et al, 2012; Bloomston et al, 2007; Setoyama et al, 2011; Szafranska et al, 2007; Bhatti et al, 2011). Decreased expression of miR-503 and miR-206, although not demonstrated in PC, have been observed in numerous cancers, including breast, gastric, hepatocellular and lung (Peng et al, 2014; Yang et al, 2014; Zhou et al, 2014; Elliman et al, 2014; Min et al, 2014; Liu et al, 2014b; Ren et al, 2014).

miScript SYBR Green RT-qPCR analysis showed that miR-503 expression although unaffected in MIA PaCa-2 and AsPC-1 cells, was upregulated in BxPC-3 cells following treatment with 1.5μM curcumin for 96 hours (Figure 5.11A, C and E). Increased expression of miR-206 was also detected in curcumin-treated BxPC-3 cells, however neither increase was statistically significant (Figure 5.11B). Surprisingly miR-206 expression was significantly ($p<0.01$) reduced, with no change in expression in curcumin treated MIA PaCa-2 cells (Figure 5.11D and F). In all PC cell lines miR-155 and miR196a expression became increased following curcumin treatment, however only the upregulation of 196a in AsPC-1 cells was statistically significant (Figure 5.12). The expression of miR-10b and miR-375 in all PC cell lines following curcumin treatment appeared to be unaltered (Figure 5.13). A non-significant increase in expression of miR-375 in curcumin treated BxPC-3 cells was observed (Figure 5.13B).

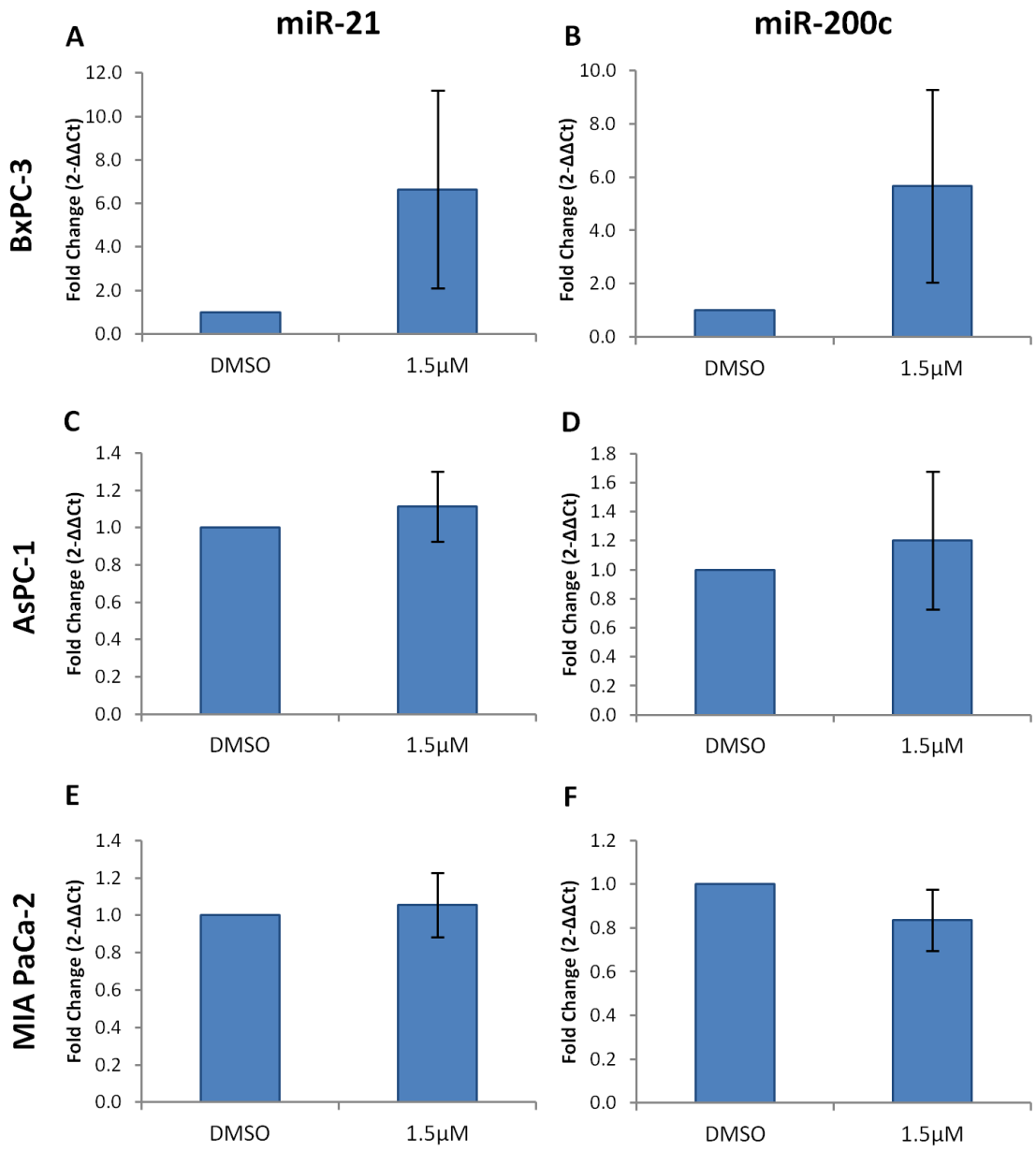

Figure 5.8: miScript SYBR® Green RT-qPCR Analysis used to Validate Microarray Profiling PC Associated Data. PC cells were treated with 1.5µM curcumin or DMSO (control) for 96 hours and analysed for **(A, C, E)** miR-21 and **(B, D, E)** miR-200c. RT-qPCR data were normalised against RNU6B for MIA PaCa-2 samples, miR-15a for BxPC-3 samples and an average of RNU6B and miR-15a for AsPC-1 cells and represent the mean ± SEM (n=4) (paired T-test).

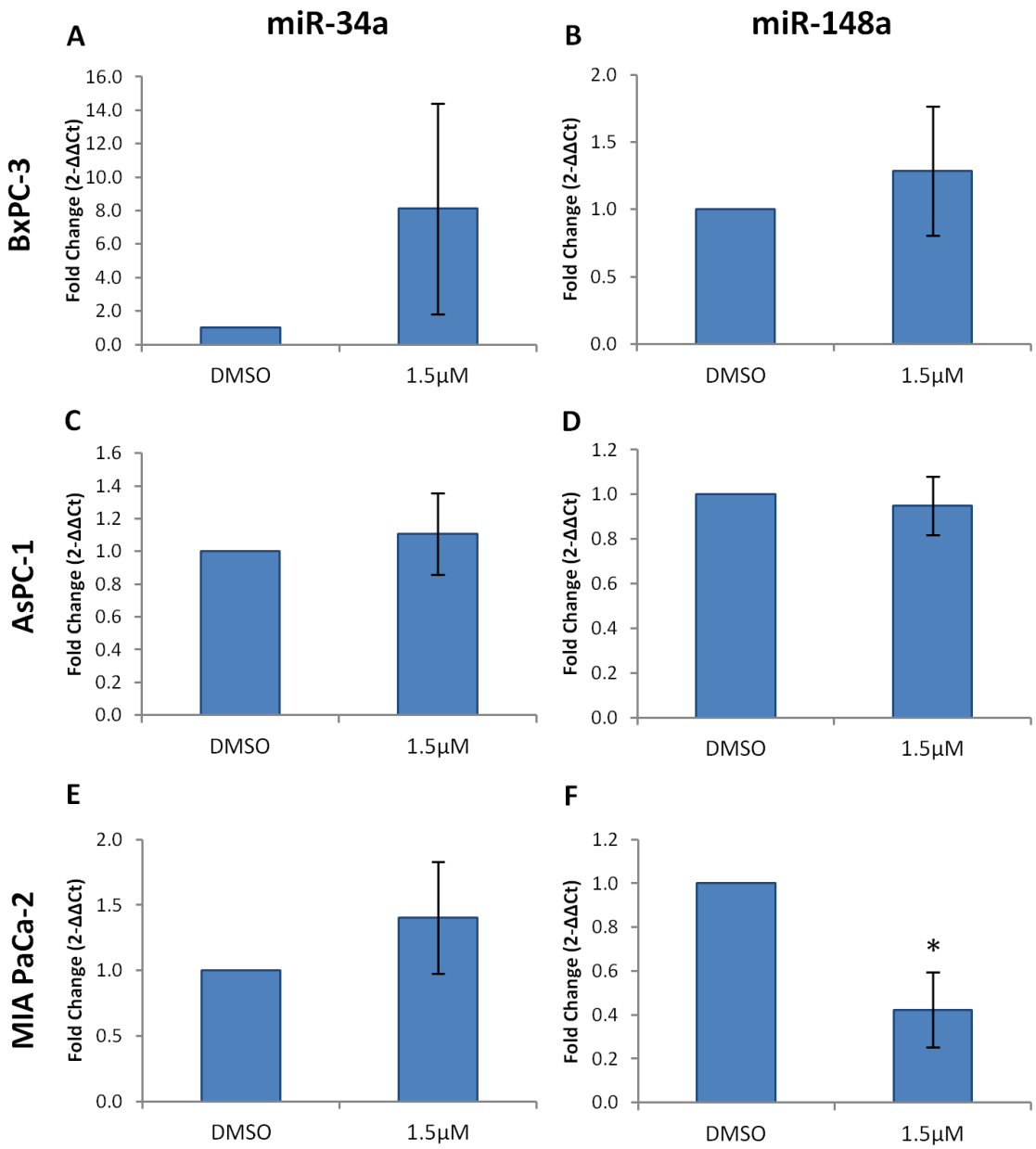

Figure 5.9: miScript SYBR® Green RT-qPCR Analysis used to Validate Microarray Profiling PC Associated Data. PC cells were treated with 1.5µM curcumin or DMSO (control) for 96 hours and analysed for **(A, C, E)** miR-34a and **(B, D, E)** miR-148a. RT-qPCR data were normalised against RNU6B for MIA PaCa-2 samples, miR-15a for BxPC-3 samples and an average of RNU6B and miR-15a for AsPC-1 cells and represent the mean ± SEM (n=4) (paired T-test, *$p<0.05$).

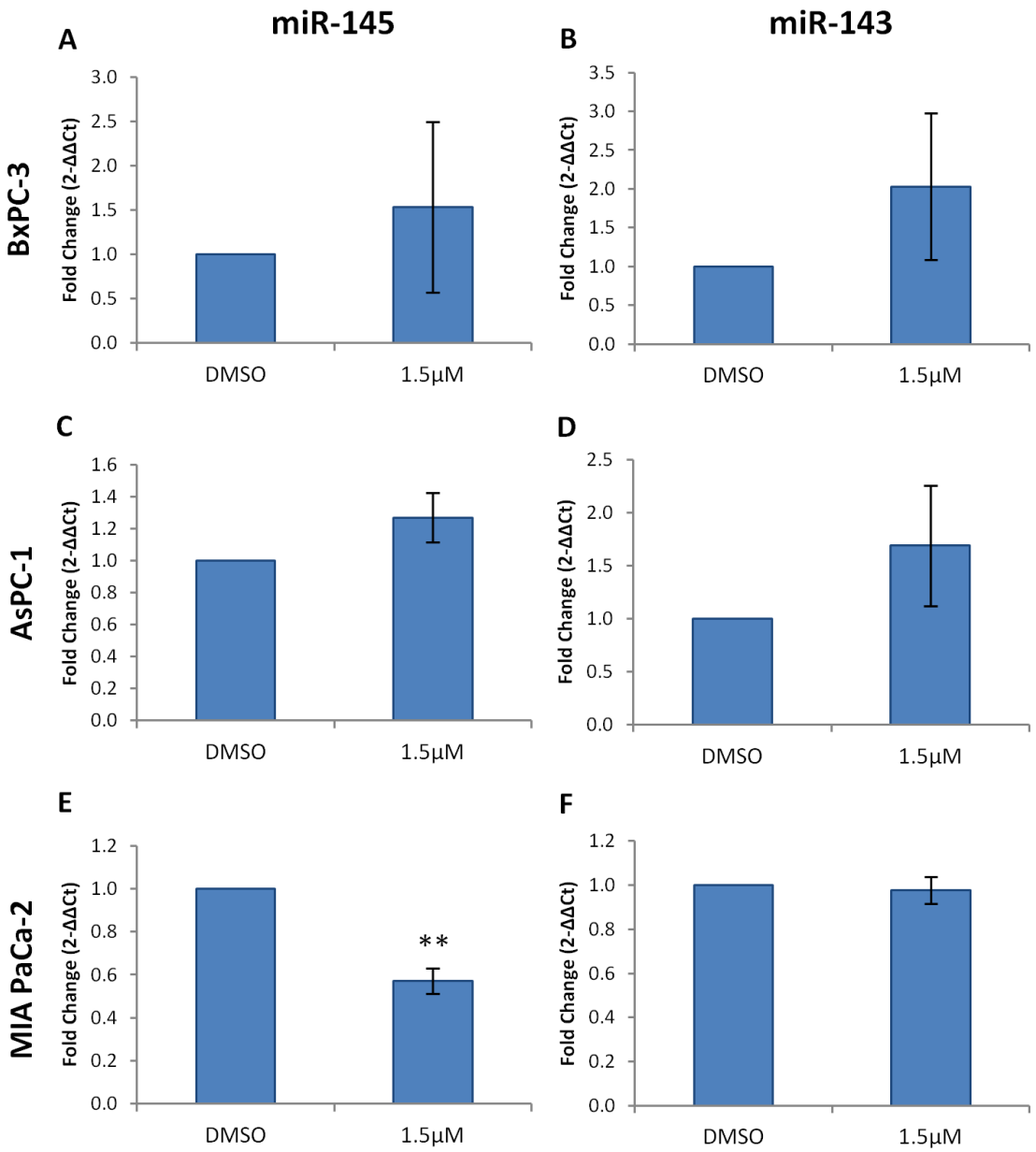

Figure 5.10: miScript SYBR® Green RT-qPCR Analysis used to Validate Microarray Profiling PC Associated Data. PC cells were treated with 1.5µM curcumin or DMSO (control) for 96 hours and analysed for **(A, C, E)** miR-145 and **(B, D, E)** miR-143. RT-qPCR data were normalised against RNU6B for MIA PaCa-2 samples, miR-15a for BxPC-3 samples and an average of RNU6B and miR-15a for AsPC-1 cells and represent the mean ± SEM (n=4) (paired T-test, **p<0.01).

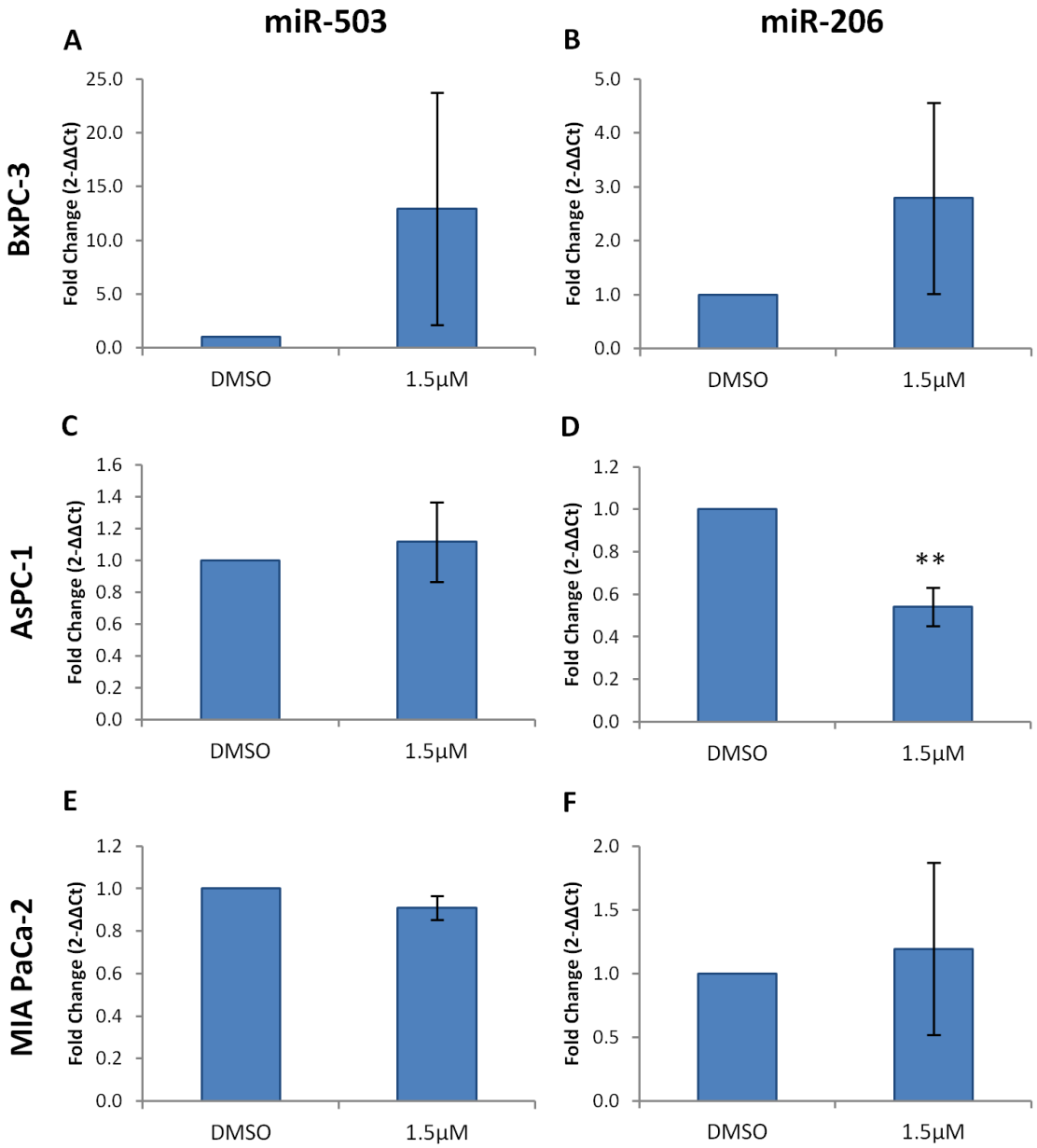

Figure 5.11: miScript SYBR® Green RT-qPCR Analysis used to Validate Microarray Profiling PC Associated Data. PC cells were treated with 1.5µM curcumin or DMSO (control) for 96 hours and analysed for **(A, C, E)** miR-503 and **(B, D, E)** miR-206. RT-qPCR data were normalised against RNU6B for MIA PaCa-2 samples, miR-15a for BxPC-3 samples and an average of RNU6B and miR-15a for AsPC-1 cells and represent the mean ± SEM (n=4) (paired T-test, **p<0.01).

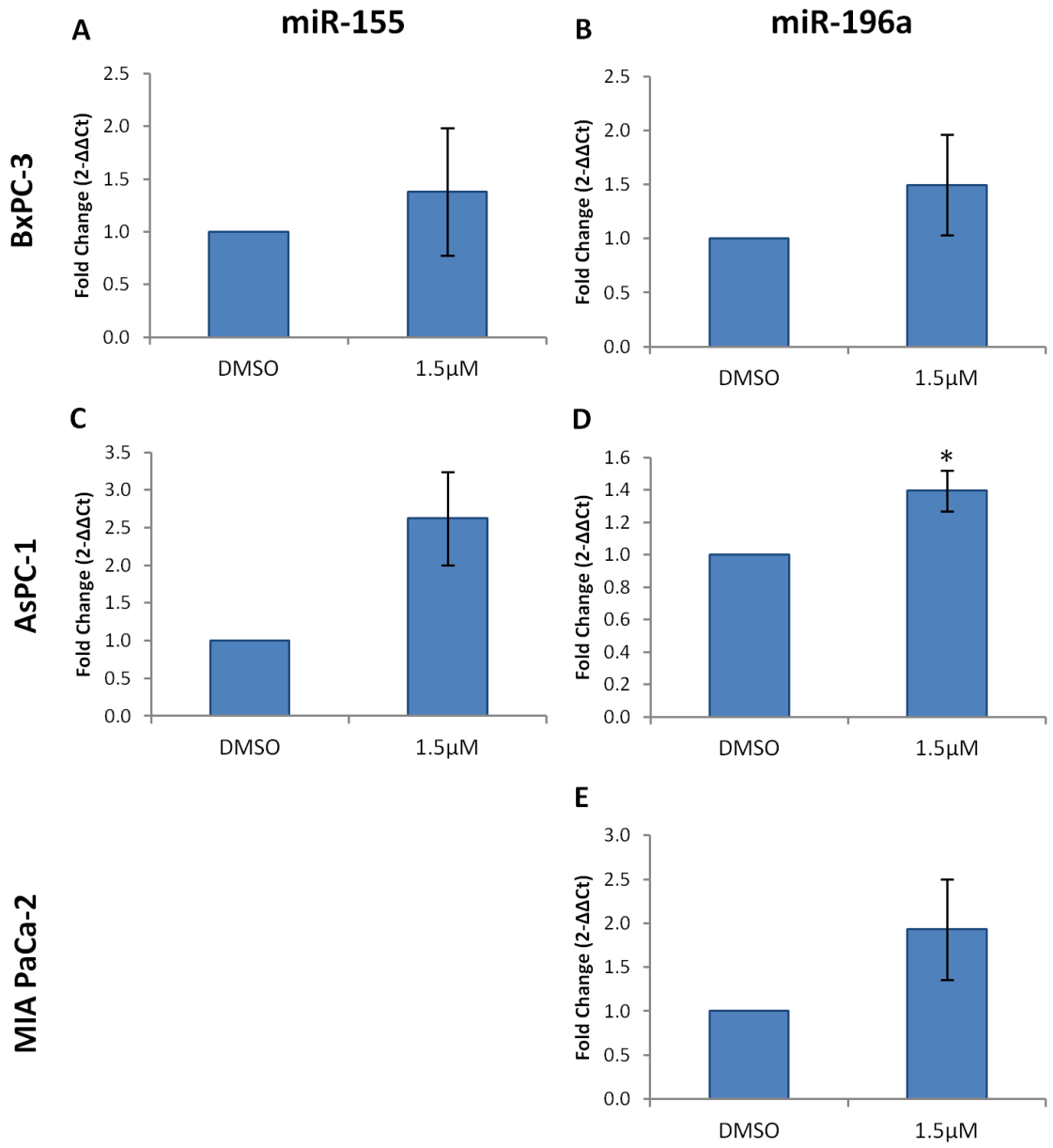

Figure 5.12: miScript SYBR® Green RT-qPCR Analysis used to Validate Microarray Profiling PC Associated Data. PC cells were treated with 1.5µM curcumin or DMSO (control) for 96 hours and analysed for **(A, C, E)** miR-155 and **(B, D, E)** miR-196a. RT-qPCR data were normalised against RNU6B for MIA PaCa-2 samples, miR-15a for BxPC-3 samples and an average of RNU6B and miR-15a for AsPC-1 cells and represent the mean ± SEM (n=4) (paired T-test, *$p<0.05$).

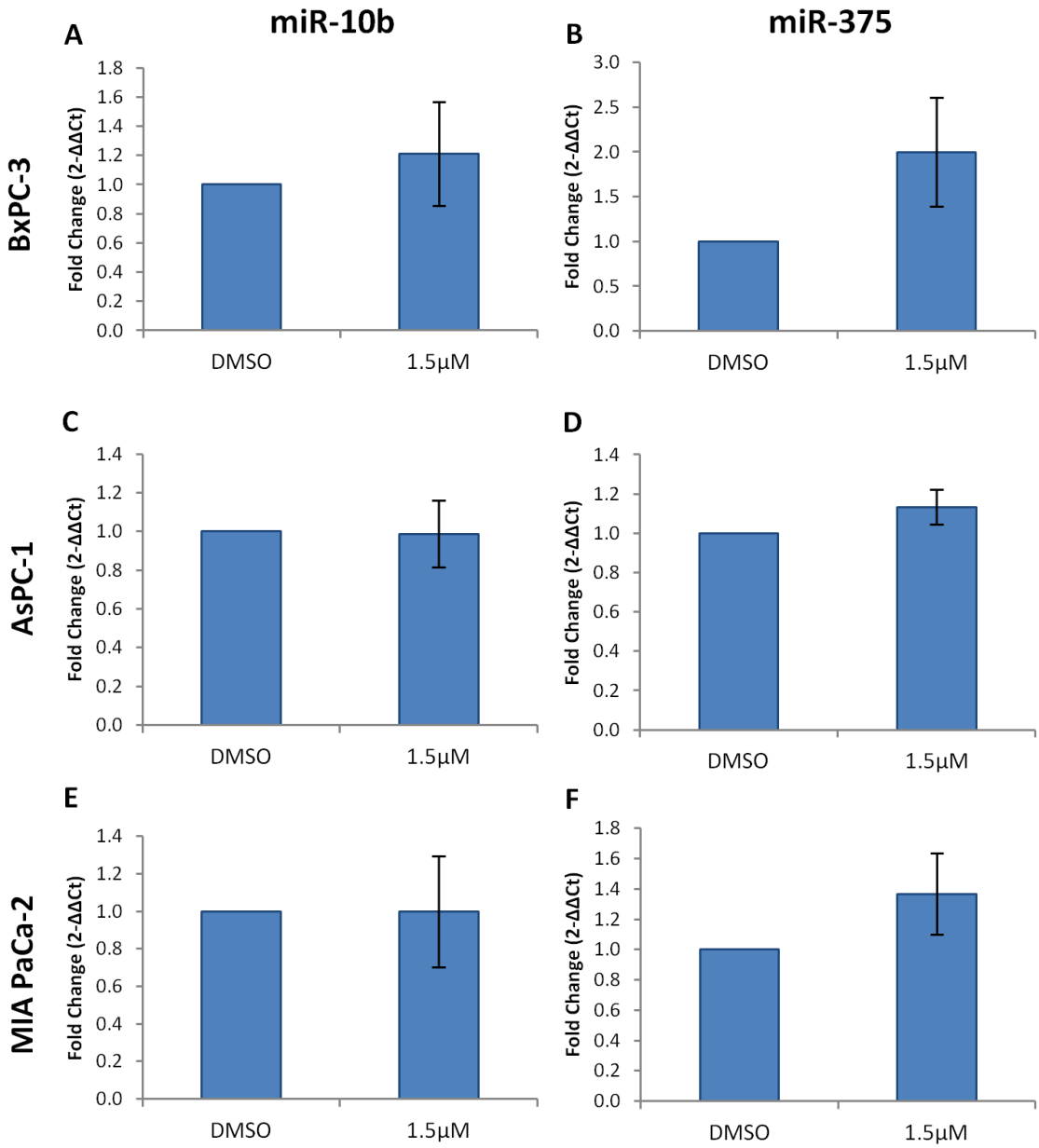

Figure 5.13: miScript SYBR® Green RT-qPCR Analysis used to Validate Microarray Profiling PC Associated Data. PC cells were treated with 1.5µM curcumin or DMSO (control) for 96 hours and analysed for **(A, C, E)** miR-10b and **(B, D, E)** miR-375. RT-qPCR data were normalised against RNU6B for MIA PaCa-2 samples, miR-15a for BxPC-3 samples and an average of RNU6B and miR-15a for AsPC-1 cells and represent the mean ± SEM (n=4) (paired T-test).

5.2.8. Target Gene Analysis by RT-qPCR

To determine if longer treatment with curcumin could modulate key proteins implicated in the progression of PC, the mRNA levels of Notch2/3, RREB1, EZH2 and c-Myc (already described in Chapter 3) were assessed using SensiMix SYBR Green RT-qPCR analysis. No change in mRNA expression was observed for Notch2 or Notch3 following curcumin treatment of AsPC-1 or BxPC-3 cells (Figure 5.14). However, in MIA PaCa-2

cells a small statistically significant decrease (fold change of 0.89) was observed (Figure 5.14F). Expression levels for RREB1, EZH2 and c-Myc remained generally unaffected in the three PC cell lines following treatment (Figure 5.15 and 5.16).

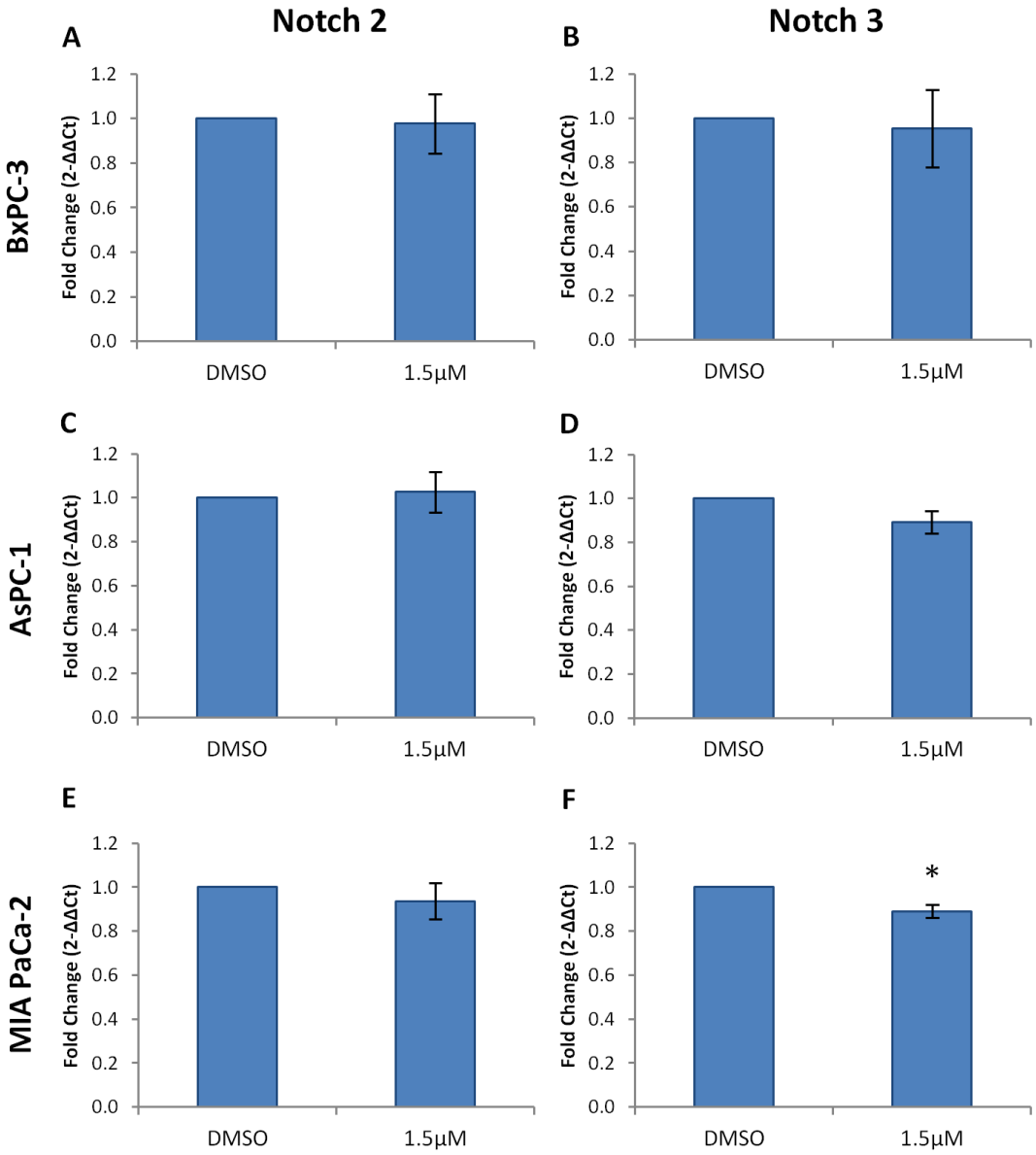

Figure 5.14: SensiMix SYBR Green RT-qPCR Analysis of Notch2/3. Cells were treated as shown for 96 hours and analysed for Notch 2 and Notch 3 mRNA expression. RT-qPCR data were normalised against 18S RNA and represent the mean ± SEM (n=4) (paired T-test, *p<0.05).

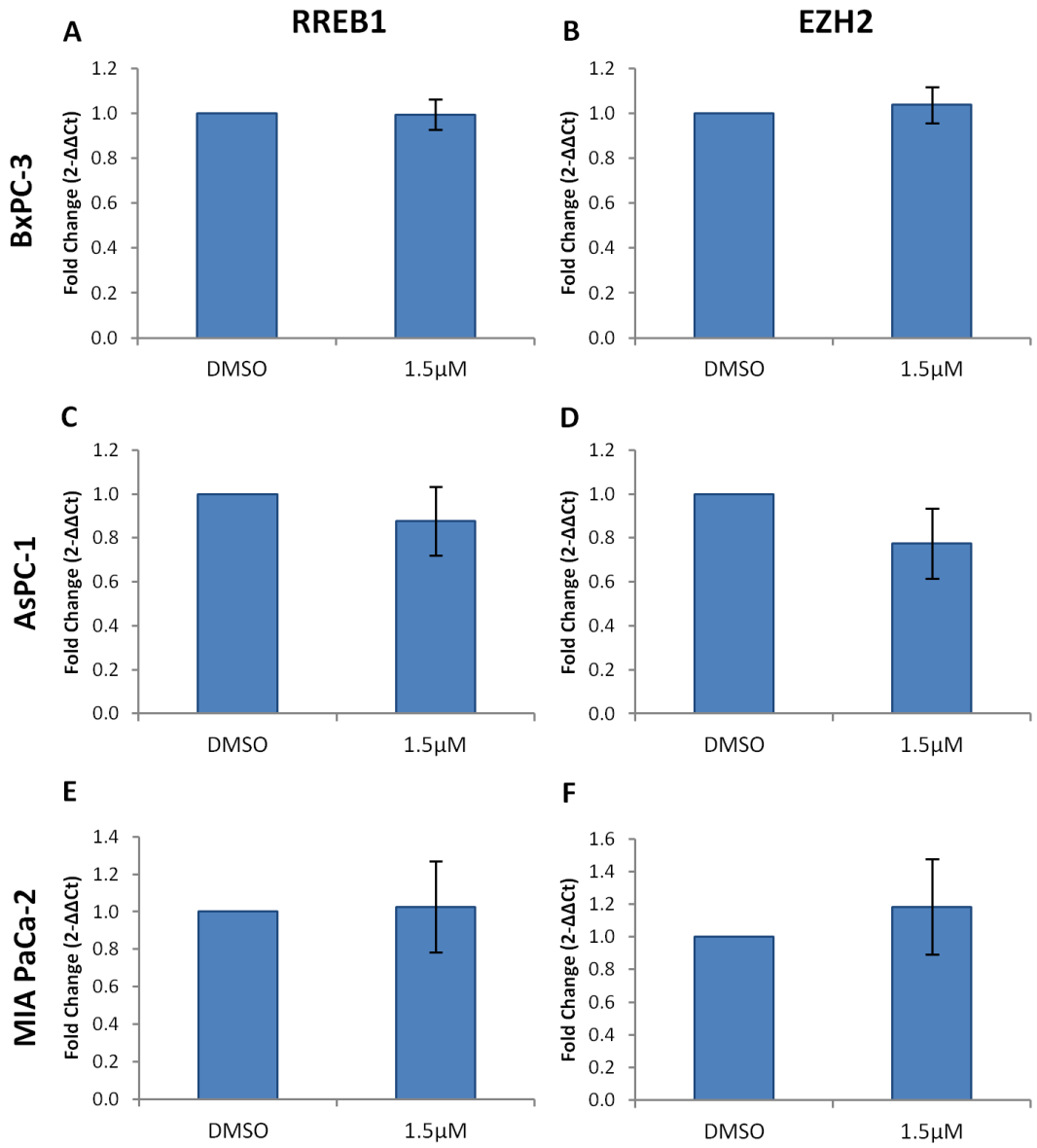

Figure 5.15: SensiMix SYBR Green RT-qPCR Analysis of RREB1 and EZH2. Cells were treated as shown for 96 hours and analysed for RREB1 and EZH2 mRNA expression. RT-qPCR data were normalised against 18S RNA and represent the mean ± SEM (n=4) (paired T-test).

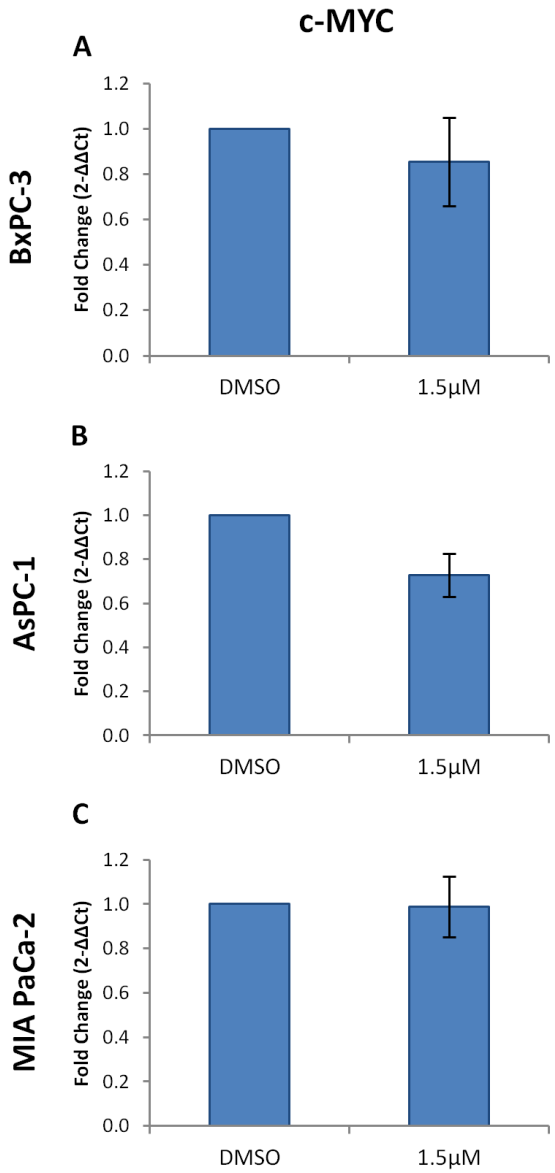

Figure 5.16: SensiMix SYBR Green RT-qPCR Analysis of c-Myc. Cells were treated as shown for 96 hours and analysed for c-Myc mRNA expression. RT-qPCR data were normalised against 18S RNA and represent the mean ± SEM (n=4) (paired T-test).

5.2.9. Analysis of Agilent miRNA Microarray Data Using Partek Software

5.2.9.1. Differential miRNA Expression Following Curcumin Treatment

Attempts to manually normalise and assess the microarray data in order to identify any significant changes in miRNA expression following curcumin treatment could not be independently validated by RT-qPCR. When analysed using Agilent Technologies GeneSpring GX software, top tables were produced containing differentially expressed miRNAs following curcumin treatment with a log2 fold change of >1 or <-1 and a p-value of ≤0.5 (Appendix 5). However, although some miRNAs appeared to have significant ($p<0.05$) fold changes in miRNA expression when treated with curcumin,

when factoring in the corrected p-value, none of the changes to miRNAs in these top tables were significant. It could be assumed therefore, that curcumin may not have an effect on miRNA expression. Since analysis of microarray data is notoriously complex, in order to determine whether the above conclusion was valid, the microarray data were further analysed by the Bioinformatics and Biostatistics Analysis Support Hub (B/BASH, University of Leicester). Data were processed and normalised (quartile normalisation) using Partek Genomics Suite software, with boxplots produced pre and post-normalisation for the gTotalGeneSignal (the name used in Partek for qMeanSignal) (Figure 5.17). These boxplots indicated that all samples were successfully normalised (Figure 5.17).

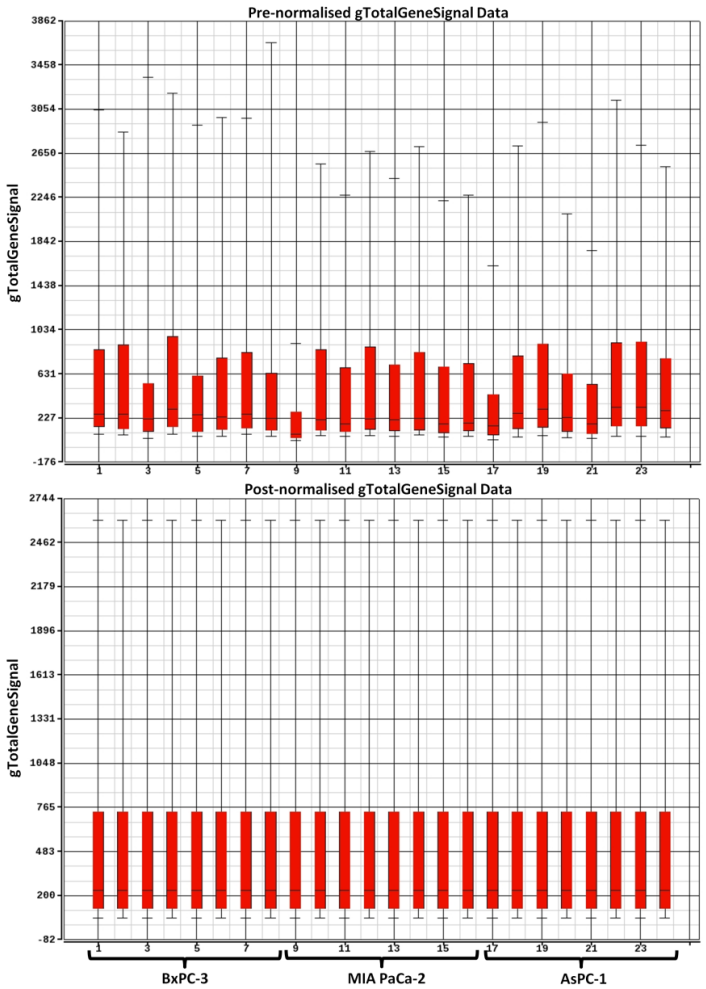

Figure 5.17: Boxplots for Pre and Post-normalisation using Partek Software. Boxplots can be used to show the distribution of a data set in relation to its central (median) value, and therefore can be used to see the variability within a dataset. The median value for each sample varies as does the distribution of each dataset pre-normalisation (top boxplot), however, post-normalisation (bottom boxplot), all median values align as does the distribution of each dataset.

A PCA plot was also produced post-normalisation using Partek software for the three experiments (MIA PaCa-2, AsPC-1 or BxPC-3 cells) in order to determine the data quality and expression variation between samples (Figure 5.18). This plot showed that generally, irrespective of treatment type (curcumin or DMSO), all samples from the same cell lines were grouped. In the PCA plots produced by both the GeneSpring GX (Figure 5.7) and Partek (Figure 5.18) software, variability was observed between some of the biological repeats within each experiment which could be labelled as outliers. Interclass correlation coefficient (ICC), was used to measure the similarity (linear correlation) between the four biological repeats within each experimental grouping (e.g. curcumin or DMSO treated) to determine how the biological repeats correlated. The statistical analysis programme SPSS was used to calculate the ICC, with values close to 1 indicating total positive correlation, values close to -1 indicating total negative correlation and values close to zero indicating no correlation. The biological repeats produced following treatment of the MIA PaCa-2, AsPC-1 and BxPC-3 cells when analysed using ICC were given values of 0.979, 0.996 and 0.951 respectively (Appendix 6). Therefore for each set of biological repeats there was a high level of positive correlation, indicating high levels of similarity between these samples.

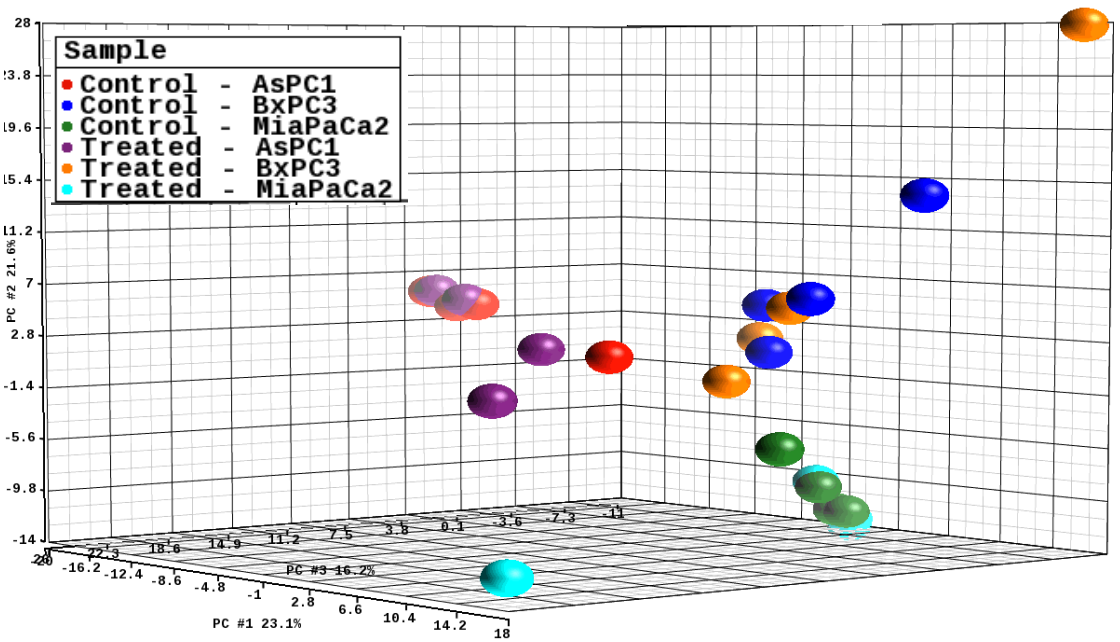

Figure 5.18: A PCA Plot for All Pancreatic Cancer Cell Lines Following Partek Normalisation. A PCA plot shows how data are separated in regard to expression variation and can be used in quality assessment to identify outliers and to observe grouping of samples.

Significance analysis of microarrays (SAM) was also carried out on the Partek normalised microarray data using MultiExperiment Viewer (MeV) software. SAM is a commonly used statistical technique applied to microarray data in order to determine whether changes in miRNA expression identified by the microarray are statistically significant. No significant changes in miRNA expression following curcumin treatment were identified for any of the PC cell lines using SAM (Figure 5.19).

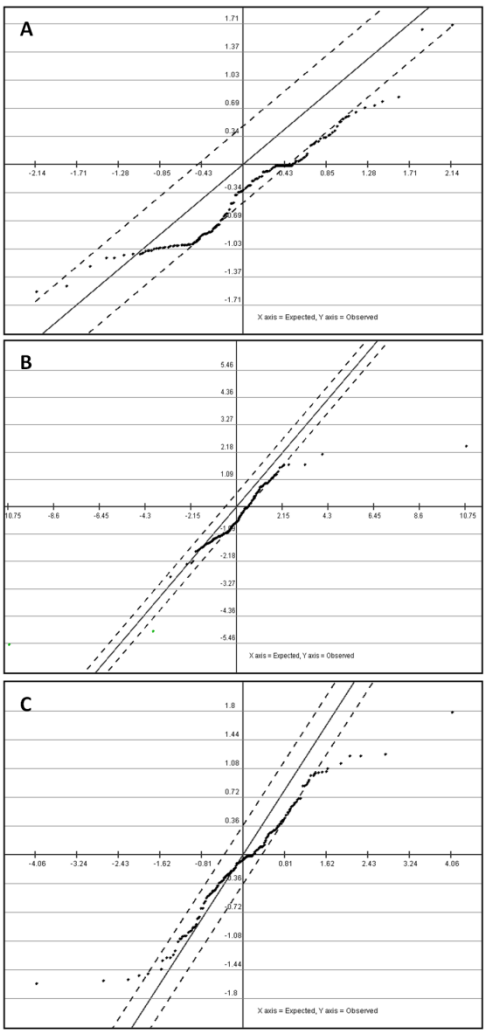

Figure 5.19: Significance Analysis of Microarrays (SAM). SAM analysis of **(A)** MIA PaCa-2, **(B)** AsPC-1 and **(C)** BxPC-3 cell lines was used to identify miRNAs that were significantly differentially expressed following treatment with 1.5µM curcumin for 96 hours when compared to DMSO (control) treated cells. The 90th percentile (as shown by the two dotted lined on each plot) false discovery rate for all SAM analysis was zero. Red data points would report miRNAs which are significantly differentially expressed, but none were observed in any of the three experiments.

Once normalised, the data processed using Partek were analysed. Top tables containing miRNAs with a log2 fold change >1 or <-1 and a p-value of <0.5 were produced for MIA PaCa-2, AsPC-1 and BxPC-3 cells following curcumin treatment (Appendix 7). A

comparison was carried out between the top tables produced using the GeneSpring and the Partek software (Appendix 9). A high percentage of miRNAs were identified as differentially expressed using both forms of analysis for the three PC cell lines, MIA PaCa-2 (88-94%), AsPC-1 (56-92%) and BxPC-3 (80-85%). To further check the consistency and reliability of the Agilent microarray platform, expression data produced for the three PC cell lines using Partek were compared against a set of data obtained from the NCBI Gene Expression Omnibus (GEO) database. This dataset (series GSE29542) also used the Agilent human miRNA microarray platform (although a slightly earlier series, G4470B) to assess miRNA expression in a number of PC cell lines and tumour samples including MIA PaCa-2, AsPC-1 and BxPC-3. The log2 gTotalGeneSignal for the twenty most highly expressed miRNAs in MIA PaCa-2, AsPC-1 and BxPC-3 cells from both experiments were compared (Table 5.3, 5.4 and 5.5). The linear relationship between these two sets of data was then assessed using the correlation coefficient (Excel), with a positive correlation between both sets of values indicated when the correlation coefficient value is closest to 1. Values >0.8 indicated a strong correlation between the two datasets, and values <0.5 indicated a weak correlation between two datasets. Correlation coefficient values of 0.812, 0.776 and 0.821 were obtained for the dataset comparisons in MIA PaCa-2, AsPC-1 and BxPC-3 cells respectively.

Table 5.3: A Comparison in miRNA gTotalGeneSignal Between Two Independent Agilent Microarray Experiments for MIA PaCa-2 Cells

	GEO dataset (GSE29542)	Agilent Microarray
Name	**gTotalGeneSignal (log2)**	**gTotalGeneSignal (log2)**
hsa-miR-21	12.49	13.07
hsa-miR-27a	10.25	10.04
hsa-miR-29b	10.07	10.25
hsa-miR-886-3p	9.83	10.96
hsa-miR-29a	9.60	10.96
hsa-let-7i	9.48	10.83
hsa-miR-24	8.98	9.82
hsa-miR-16	8.87	10.70
hsa-miR-15b	8.72	10.52
hsa-let-7a	8.70	10.99
hsa-miR-19b	8.44	9.73
hsa-let-7f	8.40	10.72
hsa-miR-23a	8.22	9.98
hsa-miR-106b	8.17	9.05
hsa-miR-20a	8.11	9.48
hsa-miR-130a	8.06	8.74
hsa-let-7b	7.90	9.78
hsa-miR-22	7.59	7.85
hsa-miR-103	7.49	9.61
hsa-miR-19a	7.41	8.86

The correlation coefficient for the comparison of these two datasets is 0.812.

Table 5.4: A Comparison in miRNA gTotalGeneSignal Between Two Independent Agilent Microarray Experiments for AsPC-1 Cells

	GEO dataset (GSE29542)	Agilent Microarray
Name	**gTotalGeneSignal (log2)**	**gTotalGeneSignal (log2)**
hsa-miR-21	13.33	13.07
hsa-miR-29b	10.77	9.48
hsa-miR-29a	10.22	10.42
hsa-let-7a	9.47	10.84
hsa-miR-16	9.31	9.95
hsa-let-7b	9.15	9.39
hsa-miR-24	9.14	10.82
hsa-miR-200b	8.94	8.97
hsa-let-7f	8.88	9.95
hsa-miR-27a	8.83	11.29
hsa-miR-15b	8.71	9.68
hsa-miR-20a	8.65	9.99
hsa-miR-19b	8.63	10.05
hsa-let-7i	8.55	7.78
hsa-miR-27b	8.36	7.82
hsa-miR-19a	7.41	8.52
hsa-miR-107	7.41	7.81
hsa-miR-15a	7.29	7.38
hsa-miR-17	7.27	9.21
hsa-miR-96	7.20	6.55

The correlation coefficient for the comparison of these two datasets is 0.776.

Table 5.5: A Comparison in miRNA gTotalGeneSignal Between Two Independent Agilent Microarray Experiments for BxPC-3 Cells

	GEO dataset (GSE29542)	Agilent Microarray
Name	**gTotalGeneSignal (log2)**	**gTotalGeneSignal (log2)**
hsa-miR-21	13.34	12.38
hsa-miR-27a	10.95	10.70
hsa-miR-205	10.64	12.48
hsa-miR-141	10.49	10.58
hsa-let-7a	10.11	10.81
hsa-miR-24	9.83	10.74
hsa-miR-29b	9.49	9.45
hsa-miR-200c	9.45	9.59
hsa-miR-200b	9.44	8.85
hsa-miR-16	9.34	9.57
hsa-let-7b	9.31	9.51
hsa-miR-23a	9.10	10.08
hsa-miR-29a	9.07	10.01
hsa-let-7f	9.03	10.11
hsa-miR-19b	8.92	9.54
hsa-miR-27b	8.86	9.02
hsa-let-7i	8.79	8.75
hsa-miR-20a	8.70	9.70
hsa-miR-15b	8.69	8.54
hsa-miR-106b	8.65	8.67

The correlation coefficient for the comparison of these two datasets is 0.821

5.2.9.2. Differential miRNA Expression Between Pancreatic Cancer Cell Lines

SAM was also used to establish if any miRNAs were significantly differentially expressed between the untreated MIA PaCa-2, AsPC-1 and BxPC-3 cell lines (Figure 5.20). Interestingly, 55 miRNAs were found to be differentially expressed. The expression levels of those miRNAs were represented using hierarchical clustering analysis (Figure 5.21).

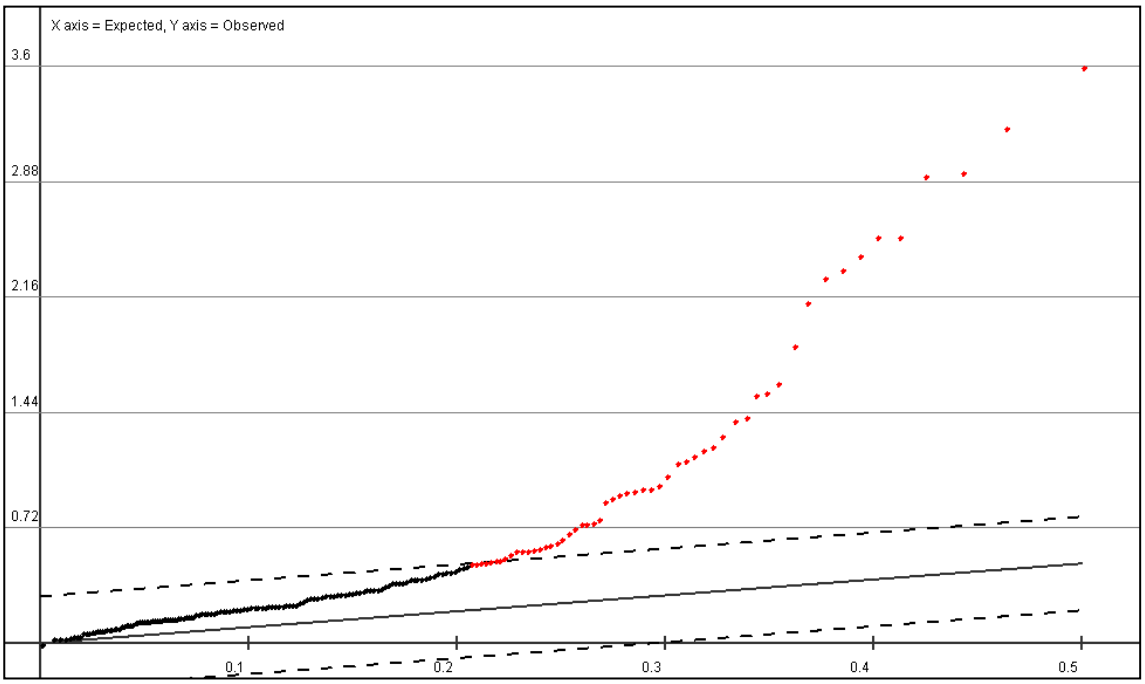

Figure 5.20: SAM Analysis Comparing MIA PaCa-2, AsPC-1 and BxPC-3 Cell Lines. SAM analysis comparing all three PC cell lines (MIA PaCa-2, AsPC-1 and BxPC-3) was used to identify miRNAs that were significantly differentially expressed. The 90th percentile (as shown by the two dotted lined on the plot) false discovery rate for SAM analysis was zero. Red data points indicate miRNAs which are significantly differentially expressed.

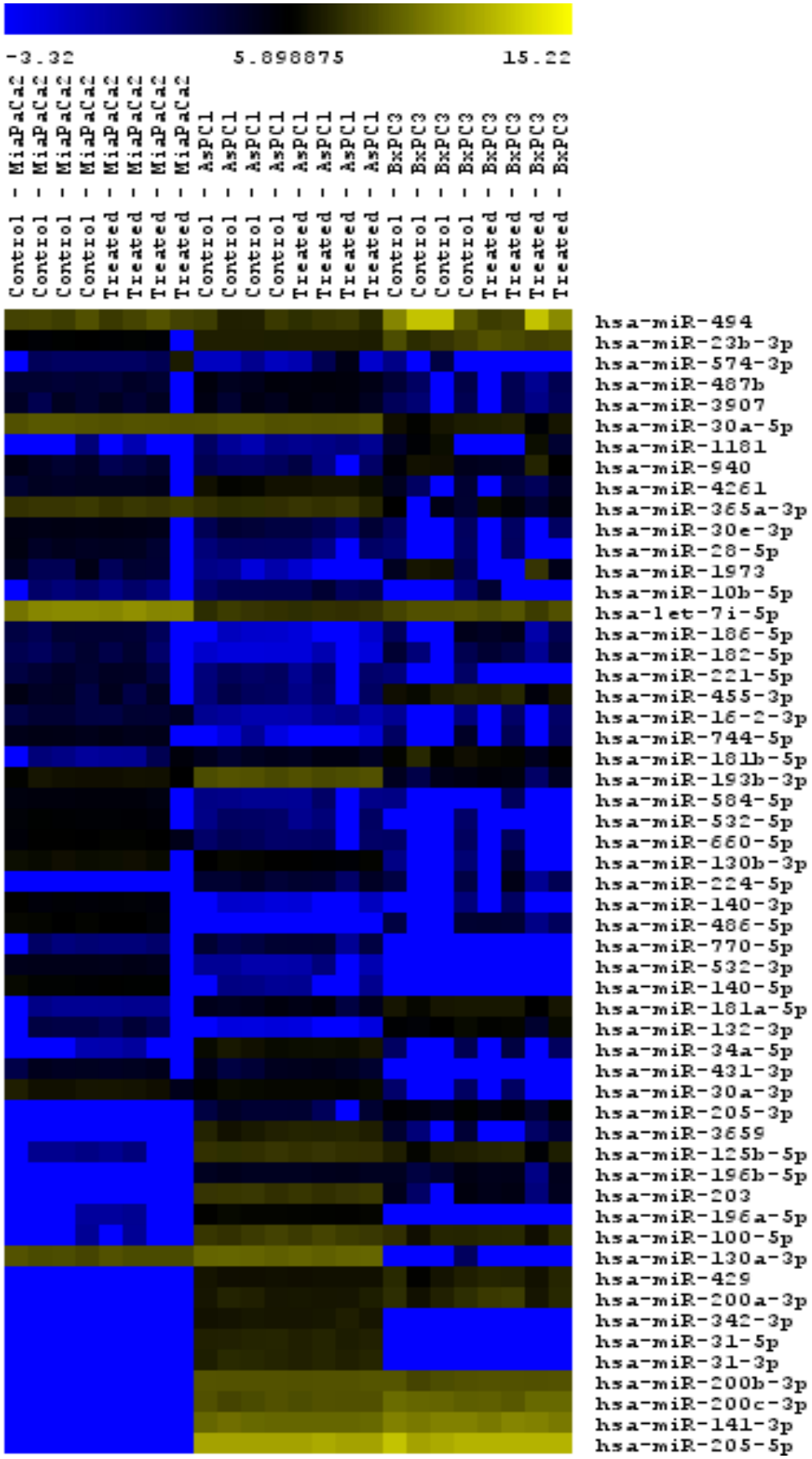

Figure 5.21: Hierarchical Clustering of Differentially Expressed miRNAs Identified by SAM Analysis. Relative expression levels of the 55 miRNAs identified using SAM when comparing expression between the PC cell lines.

5.3. Discussion

The work described in this chapter aimed to identify miRNAs regulated by a longer biologically effective treatment with curcumin in the PC cell lines. Although microarrays are commonly used for miRNA profile analysis there are a number of drawbacks to this method. Not only is there an increased chance of observing false discoveries, but there are many variables which can affect the reproducibility, quality and reliability of the data produced (Baker, 2010; Pritchard et al, 2012). This second attempt at microarray analysis of MIA PaCa-2, AsPC-1 and BxPC-3 cells following curcumin treatment was again unable to successfully identify differentially expressed miRNAs which could be validated by RT-qPCR. However, a number of miRNAs, previously shown in the literature to be dysregulated in PC were found to be significantly altered in expression by RT-qPCR following treatment with 1.5μM curcumin for 96 hours.

As discussed in chapter 3, the TRI-reagent® method of RNA isolation was chosen because of its ability to extract total RNA, enabling miRNA and mRNA expression to be assessed from within the same sample (Pritchard et al, 2012). The importance of RNA quality for successful microarray profile analysis as described in the literature is somewhat unclear. Although RNA is recommended to have a ratio of absorbance at A260/280 and A260/230 of ≥2 and RIN values of ≥7, some studies have deemed low RIN values as having little or no effect on miRNA results and have described them as poor predictors of experimental success (Fleige et al, 2006; Jung et al, 2010; Lee et al, 2007; Hall et al, 2012). Even though the traditional TRI-reagent® RNA extraction protocol was adapted (method A) in chapter 3 in order to improve the isolation of miRNAs, these changes were not sufficient to obtain total RNA fitting the recommended criteria. As a result of this, total RNA samples with RIN values ≥4 were used for profile analysis, however the differentially expressed miRNAs detected by the microarray could not be successfully validated. Some studies suggest that in order to carry out reliable microarray analysis, high quality RNA is necessary (Mraz et al, 2009). Therefore, further changes to the TRI-reagent® RNA extraction protocol were made (method B) in an attempt to improve RNA quality and yield for use in further miRNA microarray analysis. These changes included; the increased volume of TRI-reagent®, the increased use of glycogen and alterations to the ratio of isopropanol used to precipitate RNA. TRI-reagent® is used to homogenise and isolate RNA, DNA and protein from

within a sample. Increasing the volume of TRI-reagent® used should in theory improve the complete lysis of a sample and therefore potentially improve the yield. Glycogen acts as a carrier for nucleic acid precipitation and can improve the level of RNA precipitation. Isopropanol, like ethanol, prevents the solubilisation of RNA encouraging its aggregation and enabling it to pellet following centrifugation. These modifications appeared to greatly improve the RIN values (≥8.3) for all samples, indicating the successful adaptation of this RNA isolation protocol (Table 5.1).

Although deep-sequencing and qPCR are frequently used techniques for identifying differentially expressed miRNAs, microarrays are more commonly employed when screening several samples in the hope of finding a few target miRNAs which alter in expression (Baker, 2010). With increasing interest in the field of miRNA expression and its involvement in disease progression, the commercial options for expression platforms have grown. However, with significant variation often observed between studies using different platforms, research has been carried out to determine which microarray technologies perform the best. When comparing criteria such as hybridisation performance and effectiveness when detecting differential expression, studies suggested that different manufacturers produced platforms with different strengths. Agilent, although not without faults, was highly rated throughout (Git et al, 2010; Sah et al, 2010). Therefore, in an attempt to improve the reliability of the microarray analysis of curcumin-treated samples, Agilent SurePrint G3 human v16 miRNA arrays were used instead of the in-house microarrays.

Spike-in solutions contain known RNA transcripts which are used as controls to differentiate between genuine biological data and processing issues. These are recommended for the assessment of RNA labelling and sample hybridisation when using Agilent microarrays. Following scanning, each Agilent Sureprint array was evaluated and a QC report produced. This report incorporated data associated with these spike-in controls in order to assess labelling and hybridisation efficiency, in addition to other data conferring the reliability of the array (Figure 5.1). Four paired biological samples were assessed for each PC cell line, as it is necessary, when comparing individual microarrays, that data be both reliable and reproducible, which is why QC analysis is carried out before the microarray data are analysed. Microarrays which do

not reach the required criteria are often removed from an experiment. The microarray samples for all PC cell lines were satisfactory and were included for further assessment.

Having previously observed a decrease in miRNA expression following treatment with 5μM curcumin for 24 hours (chapter 3) it was surprising to witness a general increase in miRNA expression for MIA PaCa-2 and AsPC-1 cells when treated with 1.5μM for 96 hours. To regulate such a large number of miRNAs in one direction, curcumin must affect a pathway which modulates many of these non-coding RNAs. The effect of curcumin on drosha and dicer expression was therefore assessed due to the involvement of these enzymes in miRNA biogenesis and their association with poor prognosis (Vaksman et al, 2012). Assessment in MIAPaCa-2 and AsPC-1 cells showed no significant changes in drosha or dicer expression (Figure 5.2C-J).However, treatment of the BxPC-3 cell line resulted in a significant ($p<0.05$) downregulation in drosha mRNA expression (Figure 5.2A). As observed in chapter 3, mRNA levels of drosha and dicer are elevated in MIA PaCa-2 and AsPC-1 cell lines when compared to NP mRNA (Figure 3.8). Increased mRNA expression was also observed in untreated BxPC-3 cells when compared with NP levels to the same extent as the other PC cell lines. Although drosha mRNA levels were significantly reduced following curcumin treatment in BxPC-3 cells, it was concluded from these data that curcumin does not appear to consistently regulate drosha or dicer expression.

To determine if the differentially expressed miRNAs identified by manual analysis of the miRNA data were involved in any common regulatory networks, pathway analysis was carried out. The pancreatic adenocarcinoma signalling pathway was recognised as the second most significantly enriched network by the IPA software (Table 5.2.), with 36 of the 128 mRNA target encoding genes involved in this pathway targeted by one or more of the differentially expressed miRNAs (Figure 5.3). Although the changes in expression observed for these miRNAs following curcumin treatment could not be validated, the implication that small changes within these five miRNAs could together result in the modulation of 36 signalling molecules within the pancreatic adenocarcinoma pathway supports the notion that curcumin could modulate a network of associated molecules involved in PC through changes to miRNAs.

Stringent criteria were initially used to analyse the microarray data, however it was not possible to identify many significant changes in miRNA expression following curcumin treatment. Manual microarray analysis based on log2 fold change (>1 or <-1) and p-values (<0.5) produced five candidates for differential expression (miR-29b-3p, miR-34b-5p, miR-30b-5p, miR-30c-5p and miR-128a) However, when assessed by RT-qPCR the previously observed effects of curcumin could not be validated (Figure 5.4, 5.5 and 5.6). Manual analysis of the data was initially performed due to the lack of availability of the GeneSpring GX software at the time. In retrospect the data were also analysed using this software in the hope that either more significantly differentially expressed miRNAs could be identified, or to support those miRNAs identified following manual microarray analysis. Although miR-128a and miR-34b-5p were observed within the top tables (log2 fold change >1 or <-1, p-value <0.5) produced using the GeneSpring GX analysed data (Appendix 5), none of the other miRNAs were identified. It is common for a manufacturer to produce analytical software to be used for the analysis of their microarray platforms, however, this does not mean microarray data cannot be analysed by other methods. A study assessing the performance of various commercial miRNA microarrays independently of the analytical tools provided for by each manufacturer used the raw probe-level (gTotalMeanSignal) for each miRNA (Sah et al, 2010). However, this was not possible for the Agilent data as the analysis is based on the repeated measurement of two probes per miRNA, whereby data are summarised through the use of a proprietary algorithm by the Agilent GeneSpring software. Therefore using the raw probe-level data for analysis or normalisation is not recommended.

To further assess the capacity of curcumin in modulating miRNA expression, a number of miRNA and mRNA targets previously recognised in the literature as aberrantly expressed in PC were evaluated following treatment with 1.5μM for 96 hours. Significant changes in miRNA expression were observed in the MIA PaCa-2 (miR-148a, miR-145 and miR-196a) and AsPC-1 (miR-206, miR-155 and miR-196a) cell lines (Figure 5.8-5.13). Although not statistically significant, a greater number of these miRNAs were altered in expression following curcumin treatment in BxPC-3 cells when compared to the other PC cell lines (Figure 5.8-5.13). Data described in chapter 4 showed that of the three PC cell lines, the differentiated BxPC-3 cell line was the most sensitive to curcumin treatment (Sipos et al, 2003). This suggests that curcumin may

have a greater capacity to modulate miRNA expression in the earlier stages of PC progression. Surprisingly, no changes in mRNA expression were observed (Figure 5.14-5.16).

When the microarray data was further analysed by BBASH using Partek software, as with GeneSpring GX analysis, no consistent changes in miRNA expression across the cell lineswere detected. This was further confirmed by SAM analysis (Figure 5.19). PCA plots produced by GeneSpring GX and Partek for the microarray data showed that curcumin and DMSO treated biological repeats did not independently cluster, however they did show some variability between the biological repeats indicating potential outliers (Figure 5.7 and 5.18). Variation in the biological repeats could conceal or falsely highlight changes in miRNA expression not related to the curcumin treatment. However, reassuringly ICC analysis showed high levels of positive correlation for each set of biological repeats indicating a high level of similarity between biological samples. To check the consistency of the samples produced for microarray analysis the raw expression data as calculated by the Partek software were compared to a dataset which also used the Agilent platform (Table 5.3, 5.4 and 5.5). ICC analysis within all three PC cell lines showed a strong positive correlation between this dataset and the externally obtained dataset, giving confidence in the reliability of sample production and execution of the microarray experiment. The Partek analysed data were also used to compare miRNA expression profiles between the three PC cell lines. SAM identified 55 miRNAs that were differentially expressed between MIA PaCa-2, AsPC-1 and BxPC-3 cell lines (Figure 5.20). The relative expression of each miRNA in comparison to the other cell lines was then represented using hierarchical clustering analysis, with patterns of increased and decreased expression observed for each miRNA (Figure 5.21). A number of miRNAs including the miR-200 family and miR-196a were differentially expressed between the three cell lines. Increasing levels of expression of the miR-200 family are observed in BxPC-3<AsPC-1<MIA PaCa-2 cells (Figure 5.21). This correlated with previous characterisation of these cell lines which determined BxPC-3 and AsPC-1 cells to be moderately differentiated and MIA PaCa-2 cells to be poorly differentiated (Sipos et al, 2003).

The effect of 1.5μM curcumin for 96 hours on miRNA expression in PC cell lines as assessed by the Agilent microarray platform showed no significant changes in

expression. When evaluating the effect of curcumin on miRNAs known to be deregulated in PC, various miRNAs were found to be significantly regulated. Without further assessment of both the capacity of curcumin to elicit an effect on miRNA expression, and the reliability of this microarray platform, a conclusion cannot be made in regard to the ability of curcumin to modulate miRNAs in PC.

Chapter 6. General Discussion

PC is a highly aggressive disease characterised by a lack of specific symptoms and validated diagnostic markers. Consequently, early detection is extremely difficult, with disease diagnosis often unattainable until the presentation of aggressive local invasion and metastatic disease (Park et al, 2011a). Existing screening modalities used to identify PC tend to lack in sensitivity and specificity, further exacerbating the problem (Ansari et al, 2011; Cleary et al, 2004; Hanbidge, 2002; Ballehaninna and Chamberlain, 2013). It comes as no surprise that at advanced-stage presentation existing treatments for PC are ineffective, disease recurrence is frequent and overall prognosis is dismal with only 5% of patients diagnosed with PC surviving for >5 years (Hanbidge, 2002; Warshaw and Fernandez-Del Castillo, 1992).

Various microarray profiling studies have shown that miRNA expression is often deregulated in PC (Lee et al, 2007; Kent et al, 2009; Wang et al, 2009a; Jamieson et al, 2012; Gong et al, 2011; Szafranska et al, 2007). Due to their ability to control multiple targets, and therefore many biological processes, altered miRNAs are believed to play a significant role in promoting disease progression (Karius et al, 2012; Dykxhoorn, 2010). Curcumin also has the potential to regulate multiple molecular targets in cancer progression and has been shown to increase sensitivity of cancer cells to current chemotherapeutics through the modulation of differentially expressed miRNAs (Ali et al, 2010; Iwagami et al, 2013; Zhao et al, 2013; Hamada et al, 2012). Research to date has shown the feasibility of using miRNAs as biomarkers; in spite of this a unique diagnostic miRNA profile for PC has yet to be identified.

The work presented in this thesis aimed to identify novel aberrantly expressed miRNAs which could potentially be used as diagnostic markers for PC, and to ascertain if curcumin could modulate their expression. Additionally, possible mechanisms by which curcumin may regulate the expression of key miRNAs in PC cells when compared to non-transformed cells were also examined. The results have demonstrated that, despite a lack of validation of the differential expression of various miRNAs identified by microarray analysis, curcumin did appear to modulate the expression of a number of miRNAs known to be deregulated in PC.

Initial microarray experiments using in-house arrays identified several significantly differentially expressed miRNAs; validation of these changes by RT-qPCR did not generate the same results (Chapter 3). This suggested that either the execution and/or analysis of the microarray experiments were unsuccessful, or that the curcumin treatment used was ineffective in regard to altering miRNA expression. The ability of curcumin to modulate various biological responses in PC cell lines was reassessed (Chapter 4), and a longer treatment chosen for further experiments.

These were carried out using Agilent SurePrint G3 Human v16 microRNA Arrays (Chapter 5) after addressing various limitations found to affect the quality and reproducibility of the Genisphere labelled array (Chapter 3). Alterations to the RNA extraction protocol were successfully carried out, greatly improving sample quality. A major limitation when performing a microarray experiment is the labelling of RNA. The methods used to label each miRNA are often biased, as enzymes such as RNA ligase which are commonly involved in this process favour some miRNA sequences over others (Baker, 2010; Pritchard et al, 2012; Nelson et al, 2008). Spike-in solutions were used as controls to differentiate between genuine biological data and processing issues within the Agilent microarrays. QC reports were produced and incorporated spike-in data in order to assess labelling and hybridisation efficiency in addition to other data conferring the reliability of the array (Figure 5.1) (Pritchard et al, 2012).

Differentially expressed miRNAs were identified by manual analysis of the Agilent arrays; however, once again these changes could not be reproduced following RT-qPCR validation. Although percentile normalisation was applied to these data; it is probable that this analysis was inadequate for the genuine identification of differentially expressed miRNA (Sah et al, 2010). The normalisation of microarray data is essential in order to obtain accurate results, as it manipulates the data to remove variation observed across samples that does not correspond to the biological effect being assessed**.** Discrepancies observed between profiling studies are quite likely owing to the use of different types of normalisation (Pritchard et al, 2012).

Assessment of the data was also carried out using both the Agilent GeneSpring GX and Partek software, with similar results. Unlike Limma/R used in the analysis of the in-house (Genisphere) microarrays (Chapter 3), GeneSpring GX and Partek software

provided a guided workflow to assist in normalisation and analysis of the microarray data. This workflow used default parameter settings whereby the software selected the most appropriate parameters for the data and analysis being carried out.

Multiple controls are recommended when performing microarray analysis, the most commonly being the global measure of miRNA expression within an experiment. The application of quantile or percentile normalisation can achieve this, based on the theory that most miRNAs will remain unaltered. The normalisation of the microarray data would therefore correct for any technical or sample quality differences (Baker, 2010; Pritchard et al, 2012).

PCA plots for GeneSpring and Partek (Chapter 5) showed considerable variability between biological repeats. However, ICC analysis showed a strong positive correlation for all sets of biological replicates, indicating high levels of similarity (Baker, 2010). Having normalised the microarray data as recommended, and not observing any change in miRNA expression following curcumin treatment, it was assumed that there were no reproducible changes in miRNA expression in PC cell lines following treatment with curcumin.

Sample variability cannot be held accountable for the opposing results observed between the two microarray platforms. When labelling total RNA for use in microarray, the types of RNA are not discriminated between, so not only do the mature miRNAs get labelled, but also pre-miRNA and pri-miRNA. Most microarray platforms do not use probes which discriminate between these forms of small non-coding RNAs, and therefore all forms of miRNA are assessed. The RT-qPCR platforms used in this research were mature miRNA specific, so if this was the case it could help to explain the discrepancies during validation (Agranat-Tamir et al, 2014). However, the Agilent probes are mature miRNA specific, so the changes observed by RT-qPCR and by microarray analysis should be comparable, at least in the second set of data.

Although negatively expressed miRNAs are factored in when processing by GeneSpring and Partek, these values are still present in the final analysis. When producing top tables for GeneSpring many of the greatest and most significant fold changes were actually small difference but in low expressing miRNAs. The same was

also observed for the Partek analysed data. It was assumed when producing the top tables using this software that this would have been factored in, but it was not the case.

In parallel with the broad approach of microarray, individual miRNAs and mRNAs shown to be aberrantly expressed in PC were also assessed. Although no mRNAs were significantly altered following curcumin treatment some miRNAs were, with significant changes in the MIA PaCa-2 (miR-148a, miR-145 and miR-196a) and AsPC-1 (miR-206, miR-155 and miR-196a) cell lines.

Finally, the expression of several proteins known to be involved with aberrant signalling in PC were examined. Although some changes in c-Myc expression were observed, these effects were not reproducible in all experiments. This lack of consistency was also observed when assessing the effects of curcumin on the signalling protein MK5 which acts upstream of c-Myc (Kress et al, 2011). Attempts at producing data in triplicate for each experimental condition were unsuccessful, and therefore statistical significance for some changes could not be determined.

It has been suggested that supradietary doses of phytochemicals may exert different effects to those observed when a physiologically relevant dose is administered (Scott et al, 2009). The maximum physiological concentration achievable for curcumin in the human colon is 10μM/L. However much higher doses are often used when assessing the response to this phytochemical (Garcea et al, 2005a; Howells et al, 2007; Huang et al, 1991; Gandhy et al, 2012). If a dose cannot be achieved clinically in the target tissue, then the response observed in relation to that dose is unlikely to be applicable *in vivo*.

Data showed that longer exposure to lower doses of curcumin in the PC cell lines could potentially be as efficient as higher doses for shorter periods of time with respect to cell growth and induction of apoptosis. Chemopreventive agents administered clinically are also usually taken over a long period of time (Scott et al, 2009). Interestingly, it was also demonstrated that BxPC-3 cells were the most sensitive and MIA PaCa-2 cells the least sensitive in response to curcumin. This correlates with previous characterisation of various PC cell lines which determined BxPC-3 cells to be moderately differentiated and MIA PaCa-2 cells to be poorly differentiated (Sipos et al, 2003).

It has been shown that curcumin has a significant biological effect on cells at the concentrations used for microarray analysis (Chapter 4). It has also been shown that curcumin can affect the expression of various miRNAs known to be aberrantly expressed in PC (Chapter 5). However, no differentially expressed miRNAs were observed using microarray analysis following curcumin treatment. It is possible therefore that the microarray platform used was not sensitive enough to identify differential miRNA expression as a result of curcumin treatment. However, from the data acquired, it seems unlikely the initial hypothesis that curcumin may modulate many different signalling pathways in PC through changes to miRNA expression may be correct.

Although the work described here has been unable to elucidate any novel miRNAs to be used as biomarkers, various miRNAs known to be deregulated in PC have been shown to alter in expression following curcumin treatment. Further assessment of these changes and the potential downstream responses to the modulation of these miRNAs could be investigated *in vitro*, for example using AMOs to downregulate miRNA expression and using a qPCR array to identify potential mRNA targets. A key objective of this project was to establish a curcumin treatment which would most effectively modulate changes in relevant miRNAs and proteins, either independently or in combination with other treatments. Further work assessing the effects of curcumin on miRNA expression when administered in combination with the first line chemotherapeutic Gemcitabine would hopefully result in a more substantial change in miRNA expression.

References

Abraham, S.C., Wu, T.T., Klimstra, D.S., Finn, L.S., Lee, J.H., Yeo, C.J., Cameron, J.L. and Hruban, R.H., 2001. Distinctive molecular genetic alterations in sporadic and familial adenomatous polyposis-associated pancreatoblastomas : frequent alterations in the APC/beta-catenin pathway and chromosome 11p. *The American Journal of Pathology,* 159(5), pp. 1619-1627.

Abrams, R.A., Lowy, A.M., O'Reilly, E.M., Wolff, R.A., Picozzi, V.J. and Pisters, P.W., 2009. Combined modality treatment of resectable and borderline resectable pancreas cancer: expert consensus statement. *Annals of Surgical Oncology,* 16(7), pp. 1751-1756.

Adhikary, S. and Eilers, M., 2005. Transcriptional regulation and transformation by Myc proteins. *Nature Reviews.Molecular Cell Biology,* 6(8), pp. 635-645.

Aggarwal, B.B., Sundaram, C., Malani, N. and Ichikawa, H., 2007. Curcumin: The Indian Solid Gold. In: Aggarwal, B.B., Surh, Y. and Shishodia, S. eds, *The Molecular Targets and Therapeutic uses of Curcumin in Health and Disease.* New York: Springer, pp. 1.

Aggarwal, B.B. and Shishodia, S., 2006. Molecular targets of dietary agents for prevention and therapy of cancer. *Biochemical Pharmacology,* 71(10), pp. 1397-1421.

Agranat-Tamir, L., Shomron, N., Sperling, J. and Sperling, R., 2014. Interplay between pre-mRNA splicing and microRNA biogenesis within the supraspliceosome. *Nucleic Acids Research,* 42(7), pp. 4640-4651.

Aguirre, A.J., Bardeesy, N., Sinha, M., Lopez, L., Tuveson, D.A., Horner, J., Redston, M.S. and Depinho, R.A., 2003. Activated Kras and Ink4a/Arf deficiency cooperate to produce metastatic pancreatic ductal adenocarcinoma. *Genes & Development,* 17(24), pp. 3112-3126.

Akao, Y., Nakagawa, Y. and Naoe, T., 2006. MicroRNAs 143 and 145 are possible common onco-microRNAs in human cancers. *Oncology Reports,* 16(4), pp. 845-850.

Ali, S., Ahmad, A., Banerjee, S., Padhye, S., DominiakK, K., Schaffert, J.M., Wang, Z., Philip, P.A. and Sarkar, F.H., 2010. Gemcitabine sensitivity can be induced in pancreatic cancer cells through modulation of miR-200 and miR-21 expression by curcumin or its analogue CDF. *Cancer Research,* 70(9), pp. 3606-3617.

Ali, S., Ahmad, A., Aboukameel, A., Bao, B., Padhye, S., Philip, P.A. and Sarkar, F.H., 2012. Increased Ras GTPase activity is regulated by miRNAs that can be attenuated by CDF treatment in pancreatic cancer cells. *Cancer Letters,* 319(2), pp. 173-181.

American Institute for Cancer Research, World Cancer Research Fund and Potter, J., D., 1997. *Food, Nutrition and the Prevention of Cancer: a Global Perspective.* London: World Cancer Research Fund/American Institute for Cancer Research.

Ammon, H.P. and Wahl, M.A., 1991. Pharmacology of Curcuma longa. *Planta Medica,* 57(1), pp. 1-7.

Ansari, D., Rosendahl, A., Elebro, J. and Andersson, R., 2011. Systematic review of immunohistochemical biomarkers to identify prognostic subgroups of patients with pancreatic cancer. *The British Journal of Surgery,* 98(8), pp. 1041-1055.

Arbiser, J.L., Klauber, N., Rohan, R., Van Leeuwen, R., Huang, M.T., Fischer, C., Flynn, E. and Byers, H.R., 1998. Curcumin is an in vivo inhibitor of angiogenesis. *Molecular Medicine,* 4(6), pp. 376-383.

Asano, T., Yao, Y.X., Zhu, J.J., Li, D.H., Abbruzzese, J.L. and Reddy, S.A.G., 2004. The PI 3-kinase/Akt signaling pathway is activated due to aberrant Pten expression and targets transcription factors NF-kappa B and c-Myc in pancreatic cancer cells. *Oncogene,* 23(53), pp. 8571-8580.

Ayaz, L., Cayan, F., Balci, S., Gorur, A., Akbayir, S., Yildirim Yaroglu, H., Dogruer Unal, N. and Tamer, L., 2014. Circulating microRNA expression profiles in ovarian cancer. *Journal of Obstetrics and Gynaecology,* 34(7) , pp. 620-624.

Azmi, A.S., Ahmad., Banerjee, S., Rangnekar, V.M., Mohammad, R.M. and Sarkar, F.H., 2008. Chemoprevention of pancreatic cancer: characterization of Par-4 and its modulation by 3,3' diindolylmethane (DIM). *Pharmaceutical Research,* 25(9), pp. 2117-2124.

Azmi, A.S., Ali, S., Banerjee, S., Bao, B., Maitah, M.N., Padhye, S., Philip, P.A., Mohammad, R.M. and Sarkar, F.H., 2011. Network modeling of CDF treated pancreatic cancer cells reveals a novel c-myc-p73 dependent apoptotic mechanism. *American Journal of Translational Research,* 3(4), pp. 374-382.

Baker, M., 2010. MicroRNA profiling: separating signal from noise. *Nature Methods,* 7(9), pp. 687-692.

Ballehaninna, U.K. and Chamberlain, R.S., 2013. Biomarkers for pancreatic cancer: promising new markers and options beyond CA 19-9. *Tumour Biology,* 34(6), pp. 3279-3292.

Bao, B., Ali, S., Wang, Z., Ahmad, A., Azmi, A.S., Sarkar, S.H., Banerjee, S., Kong, D., Li, Y., Thakur, S. and Sarkar, F.H., 2011. Metformin Inhibits Cell Proliferation, Migration and Invasion by Attenuating CSC Function Mediated by Deregulating miRNAs in Pancreatic Cancer Cells. *Pancreas,* 40(8), pp. 1313-1313.

Bao, B., Ali, S., Banerjee, S., Wang, Z., Logna, F., Azmi, A.S., Kong, D., Ahmad, A., Li, Y., Padhye, S. and Sarkar, F.H., 2012. Curcumin Analogue CDF Inhibits Pancreatic Tumor Growth by Switching on Suppressor microRNAs and Attenuating EZH2 Expression. *Cancer Research,* 72(1), pp. 335-345.

Bao, B., Ali, S., Kong, D., Sarkar, S.H., Wang, Z., Banerjee, S., Aboukameel, A., Padhye, S., Philip, P.A. and Sarkar, F.H., 2011. Anti-Tumor Activity of a Novel Compound-CDF Is Mediated by Regulating miR-21, miR-200, and PTEN in Pancreatic Cancer. *Plos One,* 6(3), pp. e17850.

Bardeesy, N., Aguirre, A.J., Chu, G.C., Cheng, K.H., Lopez, L.V., Hezel, A.F., Feng, B., Brennan, C., Weissleder, R., Mahmood, U., Hanahan, D., Redston, M.S., Chin, L. and Depinho, R.A., 2006. Both p16(Ink4a) and the p19(Arf)-p53 pathway constrain progression of pancreatic adenocarcinoma in the mouse. *Proceedings of the National Academy of Sciences of the United States of America,* 103(15), pp. 5947-5952.

Bardeesy, N. and Depinho, R.A., 2002. Pancreatic cancer biology and genetics. *Nature Reviews Cancer,* 2(12), pp. 897-909.

Bartel, B. and Bartel, D.P., 2003. MicroRNAs: at the root of plant development? *Plant Physiology,* 132(2), pp. 709-717.

Bartel, D.P., 2004. MicroRNAs: genomics, biogenesis, mechanism, and function. *Cell,* 116(2), pp. 281-297.

Behm-Ansmant, I., Rehwinkel, J., Doerks, T., Stark, A., Bork, P. and Izaurralde, E., 2006. mRNA degradation by miRNAs and GW182 requires both CCR4:NOT deadenylase and DCP1:DCP2 decapping complexes. *Genes & Development,* 20(14), pp. 1885-1898.

Benes, V. and Castoldi, M., 2010. Expression profiling of microRNA using real-time quantitative PCR, how to use it and what is available. *Methods,* 50(4), pp. 244-249.

Bera, A., Venkatasubbarao, K., Manoharan, M.S., Hill, P. and Freeman, J.W., 2014. A miRNA Signature of Chemoresistant Mesenchymal Phenotype Identifies Novel Molecular Targets Associated with Advanced Pancreatic Cancer. *PloS One,* 9(9), pp. e106343.

Bergmann, F., Esposito, I., Herpel, E. and Schirmacher, P., 2007. Pancreatic cancer - Pathology. *Chinese-German Journal of Clinical Oncology,* 6, pp. 95-101.

Bhattacharyya, S.N., Habermacher, R., Martine, U., Closs, E.I. and Filipowicz, W., 2006. Relief of microRNA-mediated translational repression in human cells subjected to stress. *Cell,* 125(6), pp. 1111-1124.

Bhatti, I., Lee, A., James, V., Hall, R.I., Lund, J.N., Tufarelli, C., Lobo, D.N. and Larvin, M., 2011. Knockdown of microRNA-21 inhibits proliferation and increases cell death by targeting programmed cell death 4 (PDCD4) in pancreatic ductal adenocarcinoma. *Journal of Gastrointestinal Surgery,* 15(1), pp. 199-208.

Blahna, M.T. and Hata, A., 2013. Regulation of miRNA biogenesis as an integrated component of growth factor signaling. *Current Opinion in Cell Biology,* 25(2), pp. 233-240.

Bloomston, M., Frankel, W.L., Petrocca, F., Volinia, S., Alder, H., Hagan, J.P., Liu, C.G., Bhatt, D., Tacciolo, C. and Croce, C.M., 2007. MicroRNA expression patterns to differentiate pancreatic adenocarcinoma from normal pancreas and chronic pancreatitis. T*he Journal of the American Medical Association,* 297(17), pp. 1901-1908.

Boominathan, L.P., 2010. Curcumin Functions as a Positive Regulator of miRNA Processing & a Negative Regulator of Cancer Stem Cell Proliferation. *Nature Precedings.*

Brouk, B., 1975. *Plants Consumed by Man.* London: Academic Press.

Buchholz, M., Schatz, A., Wagner, M., Michl, P., Linhart, T., Adler, G., Gress, T.M. and Ellenrieder, V., 2006. Overexpression of c-myc in pancreatic cancer caused by ectopic activation of NFATc1 and the Ca2+/calcineurin signaling pathway. *The EMBO Journal,* 25(15), pp. 3714-3724.

Burk, U., Schubert, J., Wellner, U., Schmalhofer, O., Vincan, E., Spaderna, S. and Brabletz, T., 2008. A reciprocal repression between ZEB1 and members of the miR-200 family promotes EMT and invasion in cancer cells. *EMBO Reports,* 9(6), pp. 582-589.

Bustin, S. A., Benes, V., Garson, J.A., Hellemans, J., Huggett, J., Kubista, M., Mueller, R., Nola, T., Pfaffl, M. W., Shipley, G.L., Vandesompele, J. and Wittwer, C.T., 2009. The MIQE Guidelines: Minimum Information for Publication of Quantitative Real-Time PCR Experiments. *Clinical Chemistry*, 55(4), pp. 611-622.

Cairns, S.R., Scholefield, J.H., Steele, R.J., Dunlop, M.G., Thomas, H.J.W., Evans, G.D., Eaden, J.A., Rutter, M.D., Atkin, W.P., Saunders, B.P., Lucassen, A., Jenkins, P., Fairclough, P.D., Woodhouse, C.R.J. and Developed on Behalf of the British Society of Gastroenterology, and the Association of Coloproctology for Great Britain and Ireland, 2010. Guidelines for colorectal cancer screening and surveillance in moderate and high risk groups (update from 2002). *Gut,* 59(5), pp. 666-689.

Caldas, C., Hahn, S.A., Da Costa, L.T., Redston, M.S., Schutte, M., Seymour, A.B., Weinstein, C.L., Hruban, R.H., Yeo, C.J. and Kern, S.E., 1994. Frequent somatic mutations and homozygous deletions of the p16 (MTS1) gene in pancreatic adenocarcinoma. *Nature Genetics,* 8(1), pp. 27-32.

Calin, G.A., Dumitru, C.D., Shimizu, M., Bichi, R., Zupo, S., Noch, E., Alder, H., Rattan, S., Keating, M., Rai, K., Rassenti, L., Kipps, T., Negrini, M., Bullrich, F. and Croce, C.M., 2002. Frequent deletions and down-regulation of micro- RNA genes miR15 and miR16 at 13q14 in chronic lymphocytic leukemia. *Proceedings of the National Academy of Sciences of the United States of America,* 99(24), pp. 15524-15529.

Calin, G.A., Sevignani, C., Dumitru, C.D., Hyslop, T., Noch, E., Yendamuri, S., Shimizu, M., Rattan, S., Bullrich, F., Negrini, M. and Croce, C.M., 2004. Human microRNA genes are frequently located at fragile sites and genomic regions involved in cancers. *Proceedings of the National Academy of Sciences of the United States of America,* 101(9), pp. 2999-3004.

Cancer Research UK, 2014a, All Cancers Combined Key Facts. Available from: http://www.cancerresearchuk.org/cancer-info/cancerstats/keyfacts/Allcancerscombined/ [Accessed: 16th June 2014].

Cancer Research UK, 2014b, Pancreatic Cancer Statisitcs. Available from: http://www.cancerresearchuk.org/cancer-info/cancerstats/types/pancreas/?script=true [Accessed: 9th April 2014].

Cannell, I.G. and Bushell, M., 2010. Regulation of Myc by miR-34c: A mechanism to prevent genomic instability? *Cell Cycle,* 9(14), pp. 2726-2730.

Cannell, I.G., Kong, Y.W., Johnston, S.J., Chen, M.L., Collins, H.M., Dobbyn, H.C., Elia, A., Kress, T.R., Dickens, M., Clemens, M.J., Heery, D.M., Gaestel, M., Eilers, M., Willis, A.E. and Bushell, M., 2010. p38 MAPK/MK2-mediated induction of miR-34c following DNA damage prevents Myc-dependent DNA replication. *Proceedings of the National Academy of Sciences of the United States of America,* 107(12), pp. 5375-5380.

Cardiff, R.D., 2005. Epithelial to Mesenchymal Transition Tumors: Fallacious or Snail's Pace? *Clinical Cancer Research,* 11(24 Pt 1), pp. 8534-8537.

Carroll, R.E., Benya, R.V., Turgeon, D.K., Vareed, S., Neuman, M., Rodriguez, L., Kakarala, M., Carpenter, P.M., Mclaren, C., Meyskens, F.L.,JR and Brenner, D.E., 2011. Phase IIa clinical trial of curcumin for the prevention of colorectal neoplasia. *Cancer Prevention Research,* 4(3), pp. 354-364.

Chan, E., Estevez Prado, D. and Barnes Weidhaas, J., 2011. Cancer microRNAs: From subtype profiling to predictors of response to therapy. *Cell Press,* 17, pp. 235-243.

Chan, J.A., Krichevsky, A.M. and Kosik, K.S., 2005. MicroRNA-21 is an antiapoptotic factor in human glioblastoma cells. *Cancer Research,* 65(14), pp. 6029-6033.

Chang, T.C., Wentzel, E.A., Kent, O.A., Ramachandran, K., Mullendore, M., Lee, K.H., Feldmann, G., Yamakuchi, M., Ferlito, M., Lowenstein, C.J., Arking, D.E., Beer, M.A., Maitra, A. and Mendell, J.T., 2007. Transactivation of miR-34a by p53 broadly influences gene expression and promotes apoptosis. *Molecular Cell,* 26(5), pp. 745-752.

Chen, H.W. and Huang, H.C., 1998. Effect of curcumin on cell cycle progression and apoptosis in vascular smooth muscle cells. *British Journal of Pharmacology,* 124(6), pp. 1029-1040.

Cheng, A.L., Hsu, C.H., Lin, J.K., Hsu, M.M., Ho, Y.F., Shen, T.S., Ko, J.Y., Lin, J.T., Lin, B.R., Wu, M.S., Yu, H.S., Jee, S.H., Chen, G.S., Chen, T.M., Chen, C.A., Lai, M.K., Pu, Y.S., Pan, M.H., Wang, Y.J., Tsai, C.C. and Hsieh, C.Y., 2001. Phase I clinical trial of curcumin, a chemopreventive agent, in patients with high-risk or pre-malignant lesions. *Anticancer Research,* 21(4B), pp. 2895-2900.

Chivukula, R.R., Shi, G., Acharya, A., Mills, E.W., Zeitels, L.R., Anandam, J.L., Abdelnaby, A.A., Balch, G.C., Mansour, J.C., Yopp, A.C., Maitra, A. and Mendell, J.T., 2014. An Essential Mesenchymal Function for miR-143/145 in Intestinal Epithelial Regeneration. *Cell,* 157(5), pp. 1104-1116.

Ciafre, S.A., Galardi, S., Mangiola, A., Ferracin, M., Liu, C.G., Sabatino, G., Negrini, M., Maira, G., Croce, C.M. and Farace, M.G., 2005. Extensive modulation of a set of microRNAs in primary glioblastoma. *Biochemical and Biophysical Research Communications,* 334(4), pp. 1351-1358.

Ciolino, H.P., Daschner, P.J., Wang, T.T. and Yeh, G.C., 1998. Effect of curcumin on the aryl hydrocarbon receptor and cytochrome P450 1A1 in MCF-7 human breast carcinoma cells. *Biochemical Pharmacology,* 56(2), pp. 197-206.

Ciolino, H.P. and Yeh, G.C., 1999. Inhibition of aryl hydrocarbon-induced cytochrome P-450 1A1 enzyme activity and CYP1A1 expression by resveratrol. *Molecular Pharmacology,* 56(4), pp. 760-767.

Cleary, S.P., Gryfe, R., Guindi, M., Greig, P., Smith, L., Mackenzie, R., Strasberg, S., Hanna, S., Taylor, B., Langer, B. and Gallinger, S., 2004. Prognostic factors in resected pancreatic adenocarcinoma: analysis of actual 5-year survivors. *Journal of the American College of Surgeons,* 198(5), pp. 722-731.

Colvin, E.K. and Scarlett, C.J., 2014. A historical perspective of pancreatic cancer mouse models. *Seminars in Cell & Developmental Biology,* 27, pp. 96-105.

Craig, R. and Mindell, J., 2012, Health Survey for England 2011. Volume 1. Health, social care and lifestyles. [Homepage of The Health and Social Care Information Centre], [Online]. Available: www.ic.nhs.uk/pubs/hse11report [Accessed: 3rd Janurary 2014].

Croce, C.M., 2009. Causes and consequences of microRNA dysregulation in cancer. *Nature Reviews. Genetics,* 10(10), pp. 704-714.

Dalton, T.P., Shertzer, H.G. and Puga, A., 1999. Regulation of gene expression by reactive oxygen. *Annual Review of Pharmacology and Toxicology,* 39, pp. 67-101.

Dandawate, P.R., Vyas, A., Ahmad, A., Banerjee, S., Deshpande, J., Swamy, K.V., Jamadar, A., Dumhe-Klaire, A.C., Padhye, S. and Sarkar, F.H., 2012. Inclusion Complex of Novel Curcumin Analogue CDF and beta-Cyclodextrin (1:2) and Its Enhanced In Vivo Anticancer Activity Against Pancreatic Cancer. *Pharmaceutical Research,* 29(7), pp. 1775-1786.

Dhillon, N., Aggarwal, B.B., Newman, R.A., Wolff, R.A., Kunnumakkara, A.B., Abbruzzese, J.L., Ng, C.S., Badmaev, V. and Kurzrock, R., 2008. Phase II trial of curcumin in patients with advanced pancreatic cancer. *Clinical Cancer Research,* 14(14), pp. 4491-4499.

Dimeo, T.A., Anderson, K., Phadke, P., Fan, C., Perou, C.M., Naber, S. and Kuperwasser, C., 2009. A novel lung metastasis signature links Wnt signaling with cancer cell self-renewal and epithelial-mesenchymal transition in basal-like breast cancer. *Cancer Research,* 69(13), pp. 5364-5373.

Dominguez-Bendala, J. and Springerlink (Online Service), 2009. *Pancreatic Stem Cells.* Totowa, NJ: Humana Press.

Doucas, H., Mann, C.D., Sutton, C.D., Garcea, G., Neal, C.P., Berry, D.P. and Manson, M.M., 2008. Expression of nuclear Notch3 in pancreatic adenocarcinomas is associated with adverse clinical features, and correlates with the expression of STAT3 and phosphorylated akt. *Journal of Surgical Oncology,* 97(1), pp. 63-68.

Duell, E.J., Lucenteforte, E., Olson, S.H., Bracci, P.M., Li, D., Risch, H.A., Silverman, D.T., Ji, B.T., Gallinger, S., Holly, E.A., Fontham, E.H., Maisonneuve, P., Bueno-de-Mesquita, H.B., Ghadirian, P., Kurtz, R.C., Ludwig, E., Yu, H., Lowenfels, A.B., Seminara, D., Petersen, G.M., La Vecchia, C. and Boffetta, P., 2012. Pancreatitis and pancreatic cancer risk: a pooled analysis in the International Pancreatic Cancer Case-Control Consortium (PanC4). *Annals of Oncology,* 23(11), pp. 2964-2970.

Dweep, H., Sticht, C., Pandey, P. and Gretz, N., 2011. miRWalk--database: prediction of possible miRNA binding sites by "walking" the genes of three genomes. *Journal of Biomedical Informatics,* 44(5), pp. 839-847.

Dykxhoorn, D.M., 2010. MicroRNAs and metastasis: little RNAs go a long way. *Cancer Research,* 70(16), pp. 6401-6406.

Eis, P.S., Tam, W., Sun, L., Chadburn, A., Li, Z., Gomez, M.F., Lund, E. and Dahlberg, J.E., 2005. Accumulation of miR-155 and BIC RNA in human B cell lymphomas. *Proceedings of the National Academy of Sciences of the United States of America,* 102(10), pp. 3627-3632.

Elena, J.W., Steplowski, E., Yu, K., Hartge, P., Tobias, G.S., Brotzman, M.J., Chanock, S.J., Stolzenberg-Solomon, R.Z., Arslan, A.A., Bueno-de-Mesquita, H.B., Helzlsouer, K., Jacobs, E.J., Lacroix, A., Petersen, G., Zheng, W., Albanes, D., Allen, N.E., Amundadottir, L., Bao, Y., Boeing, H., Boutron-Ruault, M.C., Buring, J.E., Gaziano, J.M., Giovannucci, E.L., Duell, E.J., Hallmans, G., Howard, B.V., Hunter, D.J., Hutchinson, A., Jacobs, K.B., Kooperberg, C., Kraft, P., Mendelsohn, J.B., Michaud, D.S., Palli, D., Phillips, L.S., Overvad, K., Patel, A.V., Sansbury, L., Shu, X.O., Simon, M.S., Slimani, N., Trichopoulos, D., Visvanathan, K., Virtamo, J., Wolpin, B.M., Zeleniuch-Jacquotte, A., Fuchs, C.S., Hoover, R.N. and Gross, M., 2013. Diabetes and risk of pancreatic cancer: a pooled analysis from the pancreatic cancer cohort consortium. *Cancer Causes & Control,* 24(1), pp. 13-25.

Elliman, S.J., Howley, B.V., Mehta, D.S., Fearnhead, H.O., Kemp, D.M. and Barkley, L.R., 2014. Selective repression of the oncogene cyclin D1 by the tumor suppressor miR-206 in cancers. *Oncogenesis,* 3(8), pp. e113.

Epelbaum, R., Schaffer, M., Vizel, B., Badmaev, V. and Bar-Sela, G., 2010. Curcumin and Gemcitabine in Patients With Advanced Pancreatic Cancer. *Nutrition and Cancer-an International Journal,* 62(8), pp. 1137-1141.

Fernandez, P.C., Frank, S.R., Wang, L., Schroeder, M., Liu, S., Greene, J., Cocito, A. and Amati, B., 2003. Genomic targets of the human c-Myc protein. *Genes & Development,* 17(9), pp. 1115-1129.

Filipowicz, W., Bhattacharyya, S.N. and Sonenberg, N., 2008. Mechanisms of post-transcriptional regulation by microRNAs: are the answers in sight? *Nature Reviews.Genetics,* 9(2), pp. 102-114.

Fire, A., Xu, S., Montgomery, M.K., Kostas, S.A., Driver, S.E. and Mello, C.C., 1998. Potent and specific genetic interference by double-stranded RNA in Caenorhabditis elegans. *Nature,* 391(6669), pp. 806-811.

Fleige, S., Walf, V., Huch, S., Prgomet, C., Sehm, J. and Pfaffl, M.W., 2006. Comparison of relative mRNA quantification models and the impact of RNA integrity in quantitative real-time RT-PCR. *Biotechnology Letters,* 28(19), pp. 1601-1613.

Fluiter, K., Ten Asbroek, A.L., De Wissel, M.B., Jakobs, M.E., Wissenbach, M., Olsson, H., Olsen, O., Oerum, H. and Baas, F., 2003. In vivo tumor growth inhibition and biodistribution studies of locked nucleic acid (LNA) antisense oligonucleotides. *Nucleic Acids Research,* 31(3), pp. 953-962.

Gandhy, S.U., Kim, K., Larsen, L., Rosengren, R.J. and Safe, S., 2012. Curcumin and synthetic analogs induce reactive oxygen species and decreases specificity protein (Sp) transcription factors by targeting microRNAs. *BMC Cancer,* 12, pp. 564.

Garcea, G., Berry, D.P., Jones, D.J., Singh, R., Dennison, A.R., Farmer, P.B., Sharma, R.A., Steward, W.P. and Gescher, A.J., 2005. Consumption of the putative chemopreventive agent curcumin by cancer patients: assessment of curcumin levels in the colorectum and their pharmacodynamic consequences. *Cancer Epidemiology, Biomarkers & Prevention,* 14(1), pp. 120-125.

Garcea, G., Neal, C.P., Pattenden, C.J., Steward, W.P. and Berry, D.P., 2005. Molecular prognostic markers in pancreatic cancer: a systematic review. *European Journal of Cancer,* 41(15), pp. 2213-2236.

Garte, S., Gaspari, L., Alexandrie, A.K., Ambrosone, C., Autrup, H., Autrup, J.L., Baranova, H., Bathum, L., Benhamou, S., Boffetta, P., Bouchardy, C., Breskvar, K., Brockmoller, J., Cascorbi, I., Clapper, M.L., Coutelle, C., Daly, A., Dell'omo, M., Dolzan, V., Dresler, C.M., Fryer, A., Haugen, A., Hein, D.W., Hildesheim, A., Hirvonen, A., Hsieh, L.L., Ingelman-Sundberg, M., Kalina, I., Kang, D., Kihara, M., Kiyohara, C., Kremers, P., Lazarus, P., Le Marchand, L., Lechner, M.C., Van Lieshout, E.M., London, S., Manni, J.J., Maugard, C.M., Morita, S., Nazar-Stewart, V., Noda, K., Oda, Y., Parl, F.F., Pastorelli, R., Persson, I., Peters, W.H., Rannug, A., Rebbeck T., Risch, A., Roelandt, L., Romkes, M., Ryberg, D., Salagovic, J., Schoket, B., Seidegard, J., Shields, P.G., Sim, E., Sinnet, D., Strange, R.C., Stucker, I., Sugimura, H., To-Figueras, J., Vineis, P., Yu, M.C. and Taioli, E., 2001. Metabolic gene polymorphism frequencies in control populations. *Cancer Epidemiology, Biomarkers & Prevention,* 10(12), pp. 1239-1248.

Gescher, A.J., Sharma, R.A. and Steward, W.P., 2001. Cancer chemoprevention by dietary constituents: a tale of failure and promise. *The Lancet Oncology,* 2(6), pp. 371-379.

Gibbons, D.L., Lin, W., Creighton, C.J., Rizvi, Z.H., Gregory, P.A., Goodall, G.J., Thilaganathan, N., Du, L., Zhang, Y., Pertsemlidis, A. and Kurie, J.M., 2009. Contextual extracellular cues promote tumor cell EMT and metastasis by regulating miR-200 family expression. *Genes & Development,* 23(18), pp. 2140-2151.

Git, A., Dvinge, H., Salmon-Divon, M., Osborne, M., Kutter, C., Hadfield, J., Bertone, P. and Caldas, C., 2010. Systematic comparison of microarray profiling, real-time PCR, and next-generation sequencing technologies for measuring differential microRNA expression. *RNA,* 16(5), pp. 991-1006.

Goggins, M., 2011. Markers of pancreatic cancer: working toward early detection. *Clinical Cancer Research,* 17(4), pp. 635-637.

Gong, X., Wu R., Wang, H., Guo, X., Wang, D., Gu, Y., Zhang, Y., Zhao, W., Cheng, L., Wang, C. and Guo, Z., 2011. Evaluating the consistency of differential expression of microRNA detected in human cancers. *Molecular Cancer Therapeutics,* 10(5), pp. 752-760.

Goonetilleke, K.S. and Siriwardena, A.K., 2007. Systematic review of carbohydrate antigen (CA 19-9) as a biochemical marker in the diagnosis of pancreatic cancer. *European Journal of Surgical Oncology,* 33(3), pp. 266-270.

Grace, P.B., Taylor, J.I., Low, Y., Luben, R.N., Mulligan, A.A., Botting, N.P., Dowsett, M., Welch, A.A., Khaw, K., Wareham, N.J., Day, N.E. and Bingham, S.A., 2004. Phytoestrogen Concentrations in Serum and Spot Urine as Biomarkers for Dietary Phytoestrogen Intake and Their Relation to Breast Cancer Risk in European Prospective Investigation of Cancer and Nutrition-Norfolk. *Cancer Epidemiology Biomarkers & Prevention,* 13(5), pp. 698-708.

Greenwald, P., Kelloff G., Burch-Whitman, C. and Kramer, B.S., 1995. Chemoprevention. *CA: A Cancer Journal for Clinicians,* 45(1), pp. 31-49.

Greither, T., Grochola, L.F., Udelnow, A., Lautenschlager, C., Wurl, P. and Taubert, H., 2010. Elevated expression of microRNAs 155, 203, 210 and 222 in pancreatic tumors is associated with poorer survival. *International Journal of Cancer,* 126(1), pp. 73-80.

Griffiths-Jones, S., 2004. The microRNA Registry. *Nucleic Acids Research,* 32(Database issue), pp. D109-111.

Grippo, P.J., Nowlin, P.S., Demeure, M.J., Longnecker, D.S. and Sandgren, E.P., 2003. Preinvasive pancreatic neoplasia of ductal phenotype induced by acinar cell targeting of mutant Kras in transgenic mice. *Cancer Research,* 63(9), pp. 2016-2019.

Guengoer, C., Zander, H., Effenberger, K.E., Vashist, Y.K., Kalinina, T., Izbicki, J.R., Yekebas, E. and Bockhorn, M., 2011. Notch Signaling Activated by Replication Stress-Induced Expression of Midkine Drives Epithelial-Mesenchymal Transition and Chemoresistance in Pancreatic Cancer. *Cancer Research,* 71(14), pp. 5009-5019.

Gullo, L., Tomassetti, P., Migliori, M., Casadei, R. and Marrano, D., 2001. Do early symptoms of pancreatic cancer exist that can allow an earlier diagnosis? *Pancreas,* 22(2), pp. 210-213.

Gupta, S.C., Kismali, G. and Aggarwal, B.B., 2013. Curcumin, a component of turmeric: from farm to pharmacy. *BioFactors,* 39(1), pp. 2-13.

Gupta, S.C., Patchva, S. and Aggarwal, B.B., 2013. Therapeutic roles of curcumin: lessons learned from clinical trials. *The AAPS Journal,* 15(1), pp. 195-218.

Gusscott, S., Kuchenbauer, F., Humphries, R.K. and Weng, A.P., 2012. Notch-mediated repression of miR-223 contributes to IGF1R regulation in T-ALL. *Leukemia Research,* 36(7), pp. 905-911.

Hall, J.S., Taylor, J., Valentine, H.R., Irlam, J.J., Eustace, A., Hoskin, P.J., Miller, C.J. and West, C.M., 2012. Enhanced stability of microRNA expression facilitates classification of FFPE tumour samples exhibiting near total mRNA degradation. *British Journal of Cancer,* 107(4), pp. 684-694.

Hamada, S., Satoh, K., Fujibuchi, W., Hirota, M., Kanno, A., Unno, J., Masamune, A., Kikuta, K., Kume, K. and Shimosegawa, T., 2012. MiR-126 Acts as a Tumor Suppressor in Pancreatic Cancer Cells via the Regulation of ADAM9. *Molecular Cancer Research,* 10(1), pp. 3-10.

Hamilton, S.R., Aaltonen, L.A., Switzerland. Bundesamt Für Gesundheit, International Academy of Pathology, International Agency for Research on Cancer and World Health Organisation, 2000. *Pathology and Genetics of Tumours of the Digestive System.* Lyon: IARC Press.

Han, L., Witmer, P.D., Casey, E., Valle, D. and Sukumar, S., 2007. DNA methylation regulates MicroRNA expression. *Cancer Biology & Therapy,* 6(8), pp. 1284-1288.

Han, S.S., Keum, Y.S., Seo, H.J. and Surh, Y.J., 2002. Curcumin suppresses activation of NF-kappaB and AP-1 induced by phorbol ester in cultured human promyelocytic leukemia cells. *Journal of Biochemistry and Molecular Biology,* 35(3), pp. 337-342.

Han, Y., Liu, Y., Gui, Y. and Cai, Z., 2013. Inducing cell proliferation inhibition and apoptosis via silencing Dicer, Drosha, and Exportin 5 in urothelial carcinoma of the bladder. *Journal of Surgical Oncology,* 107(2), pp. 201-205.

Hanbidge, A.E., 2002. Cancer of the pancreas: the best image for early detection--CT, MRI, PET or US? *Canadian Journal of Gastroenterology,* 16(2), pp. 101-105.

Harrison, S. and Benziger, H., 2011. The molecular biology of colorectal carcinoma and its implications: A review. *The Surgeon,* 9(4), pp. 200-210.

Hastert, T.A., Beresford, S.A.A., Sheppard, L. and White, E., 2014. Adherence to the WCRF/AICR cancer prevention recommendations and cancer-specific mortality: results from the Vitamins and Lifestyle (VITAL) Study. *Cancer Causes & Control,* 25(5), pp. 541-552.

Hatcher, H., Planalp, R., Cho, J., Torti F.M. and Torti, S.V., 2008. Curcumin: from ancient medicine to current clinical trials. *Cellular and Molecular Life Sciences,* 65(11), pp. 1631-1652.

Hayes, J.D. and McMahon, M., 2001. Molecular basis for the contribution of the antioxidant responsive element to cancer chemoprevention, *Cancer Letters,* 174(2), pp. 103-113.

He, L. and Hannon, G.J., 2004. MicroRNAs: small RNAs with a big role in gene regulation. *Nature Reviews.Genetics,* 5(7), pp. 522-531.

He, L., He, X., Lim, L.P., De Stanchina, E., Xuan, Z., Liang, Y., Xue, W., Zender, L., Magnus, J., Ridzon, D., Jackson, A.L., Linsley, P.S., Chen, C., Lowe, S.W., Cleary, M.A. and Hannon, G.J., 2007. A microRNA component of the p53 tumour suppressor network. *Nature,* 447(7148), pp. 1130-1134.

Hemminki, K., Li, X., Sundquist, J. and Sundquist, K., 2009. Cancer risks in Crohn disease patients. *Annals of Oncology,* 20(3), pp. 574-580.

Hemminki, K., LI, X., Sundquist, J. and Sundquist, K., 2008. Cancer risks in ulcerative colitis patients. *International Journal of Cancer,* 123(6), pp. 1417-1421.

Hermeking, H., 2010. The miR-34 family in cancer and apoptosis. *Cell Death and Differentiation,* 17(2), pp. 193-199.

Hernández, G., 2012. On the Emergence and Evolution of the Eukaryotic Translation Apparatus. In: Biyani, M. ed, *Cell-Free Protein Synthesis.* http://www.intechopen.com/books/cell-free-protein-synthesis/on-the-emergence-and-evolution-of-the-eukaryotic-translation-apparatus: InTech, pp. 31.

Hezel, A.F., Kimmelman, A.C., Stanger, B.Z., Bardeesy, N. and Depinho, R.A., 2006. Genetics and biology of pancreatic ductal adenocarcinoma. *Genes & Development,* 20(10), pp. 1218-1249.

Hingorani, S.R., Petricoin, E.F., Maitra, A., Rajapakse, V., King, C., Jacobetz, M.A., Ross, S., Conrads, T.P., Veenstra, T.D., Hitt, B.A., Kawaguchi, Y., Johann, D., Liotta, L.A., Crawford, H.C., Putt, M.E., Jacks, T., Wright, C.V., Hruban, R.H., Lowy, A.M. and Tuveson, D.A., 2003. Preinvasive and invasive ductal pancreatic cancer and its early detection in the mouse. *Cancer Cell,* 4(6), pp. 437-450.

Hingorani, S.R., Wang, L., Multani, A.S., Combs, C., Deramaudt, T.B., Hruban, R.H., Rustgi, A.K., Chang, S. and Tuveson, D.A., 2005. Trp53R172H and KrasG12D cooperate to promote chromosomal instability and widely metastatic pancreatic ductal adenocarcinoma in mice. *Cancer Cell,* 7(5), pp. 469-483.

Holder, G.M., Plummer, J.L. and Ryan, A.J., 1978. The metabolism and excretion of curcumin (1,7-bis-(4-hydroxy-3-methoxyphenyl)-1,6-heptadiene-3,5-dione) in the rat. *Xenobiotica,* 8(12), pp. 761-768.

Holland, P.M., Abramson, R.D., Watson, R. and Gelfand, D.H., 1991. Detection of specific polymerase chain reaction product by utilizing the 5'----3' exonuclease activity of Thermus aquaticus DNA polymerase. *Proceedings of the National Academy of Sciences of the United States of America,* 88(16), pp. 7276-7280.

Hour, T.C., Chen, J., Huang, C.Y., Guan, J.Y., Lu, S.H. and Pu, Y.S., 2002. Curcurnin enhances cytotoxicity of chemotherapeutic agents in prostate cancer cells by inducing p21(WAF1/CIP1) and C/EBP beta expressions and suppressing NF-kappa B activation. *Prostate,* 51(3), pp. 211-218.

Howells, L.M., Moiseeva, E.P., Neal, C.P., Foreman, B.E., Andreadi, C.K., Sun, Y.Y., Hudson, E.A. and Manson, M.M., 2007. Predicting the physiological relevance of in vitro cancer preventive activities of phytochemicals. *Acta Pharmacologica Sinica,* 28(9), pp. 1274-1304.

Hruban, R.H., Maitra, A., Schulick, R., Laheru, D., Herman, J., Kern, S.E. and Goggins, M., 2008. Emerging Molecular Biology of Pancreatic Cancer. *Gastrointestinal Cancer Research,* 2, pp. 10-15.

Hruban, R.H., Canto, M.I., Goggins, M., Schulick, R. and Klein, A.P., 2010. Update on familial pancreatic cancer. *Advances in Surgery,* 44, pp. 293-311.

Hruban, R.H., Maitra, A. and Goggins, M., 2008. Update on pancreatic intraepithelial neoplasia. *International Journal of Clinical and Experimental Pathology,* 1(4), pp. 306-316.

Hruban, R.H., Maitra, A., Kern, S.E. and Goggins, M., 2007. Precursors to pancreatic cancer. *Gastroenterology Clinics of North America,* 36(4), pp. 831-49, vi.

Hsu, C.-. and Cheng, A.-., 2007. Clinical Studies with Curcumin. In: Aggarwal, B.B., Surh, Y. and Shishodia, S. eds, *The Molecular Targets and Therapeutic uses of Curcumin in Health and Disease.* New York: Springer, pp. 471.

Hsu, J.B., Chiu, C.M., Hsu, S.D., Huang, W.Y., Chien, C.H., Lee, T.Y. and Huang, H.D., 2011. miRTar: an integrated system for identifying miRNA-target interactions in human. *BMC Bioinformatics,* 12, pp. 300.

Hu, J., Qiu, M., Jiang, F., Zhang, S., Yang, X., Wang, J., Xu, L. and Yin, R., 2014. MiR-145 regulates cancer stem-like properties and epithelial-to-mesenchymal transition in lung adenocarcinoma-initiating cells. *Tumour Biology,* Epub ahead of print.

Huang, C.S., Fan, Y.E., Lin, C.Y. and Hu, M.L., 2007. Lycopene inhibits matrix metalloproteinase-9 expression and down-regulates the binding activity of nuclear factor-kappa B and stimulatory protein-1. *The Journal of Nutritional Biochemistry,* 18(7), pp. 449-456.

Huang, H.C., Nguyen, T. and Pickett, C.B., 2000. Regulation of the antioxidant response element by protein kinase C-mediated phosphorylation of NF-E2-related factor 2. *Proceedings of the National Academy of Sciences of the United States of America,* 97(23), pp. 12475-12480.

Huang, M.T., Lysz, T., Ferraro, T., Abidi, T.F., Laskin, J.D. and Conney, A.H., 1991. Inhibitory Effects of Curcumin on Invitro Lipoxygenase and Cyclooxygenase Activities in Mouse Epidermis. *Cancer Research,* 51(3), pp. 813-819.

Huang, S. and Chen, L., 2014. miR-888 regulates side population properties and cancer metastasis in breast cancer cells. *Biochemical and Biophysical Research Communications,* 450(4), pp. 1234-1240.

Hurst, D.R., Edmonds, M.D. and Welch, D.R., 2009. Metastamir: the field of metastasis-regulatory microRNA is spreading. *Cancer Research,* 69(19), pp. 7495-7498.

Hurteau, G.J., Carlson, J.A., Roos, E. and Brock, G.J., 2009. Stable expression of miR-200c alone is sufficient to regulate TCF8 (ZEB1) and restore E-cadherin expression. *Cell Cycle,* 8(13), pp. 2064-2069.

Hurteau, G.J., Spivack, S.D. and Brock, G.J., 2006. Potential mRNA degradation targets of hsa-miR-200c, identified using informatics and qRT-PCR. *Cell Cycle,* 5(17), pp. 1951-1956.

Ibberson, D., Benes, V., Muckenthaler, M.U. and Castoldi, M., 2009. RNA degradation compromises the reliability of microRNA expression profiling. *BMC Biotechnology,* 9, pp. 102.

Ireson, C., Orr, S., Jones, D.J., Verschoyle, R., Lim, C.K., Luo, J.L., Howells, L., Plummer, S., Jukes, R., Williams, M., Steward, W.P. and Gescher, A., 2001. Characterization of metabolites of the chemopreventive agent curcumin in human and rat hepatocytes and in the rat in vivo, and evaluation of their ability to inhibit phorbol ester-induced prostaglandin E2 production. *Cancer Research,* 61(3), pp. 1058-1064.

Iwagami, Y., Eguchi, H., Nagano, H., Akita, H., Hama, N., Wada, H., Kawamoto, K., Kobayashi, S., Tomokuni, A., Tomimaru, Y., Mori, M. and Doki, Y., 2013. miR-320c regulates gemcitabine-resistance in pancreatic cancer via SMARCC1. *British Journal of Cancer,* 109(2), pp. 502-511.

Jackson, R.J. and Standart, N., 2007. How do microRNAs regulate gene expression? *Science's STKE,* 2007(367), pp. re1.

Jamieson, N.B., Morran, D.C., Morton, J.P., Ali, A., Dickson, E.J., Carter, C.R., Sansom, O.J., Evans, T.R., McKay, C.J. and Oien, K.A., 2012. MicroRNA molecular profiles associated with diagnosis, clinicopathologic criteria, and overall survival in patients with resectable pancreatic ductal adenocarcinoma. *Clinical Cancer Research,* 18(2), pp. 534-545.

Janssen, H.L., Reesink, H.W., Lawitz, E.J., Zeuzem, S., Rodriguez-Torres, M., Patel, K., Van Der Meer, A.J., Patick, A.K., Chen, A., Zhou, Y., Persson, R., King, B.D., Kauppinen, S., Levin, A.A. and Hodges, M.R., 2013. Treatment of HCV infection by targeting microRNA. *The New England Journal of Medicine,* 368(18), pp. 1685-1694.

Jazieh, K.A., Foote, M.B. and Diaz, L.A.,JR, 2014. The clinical utility of biomarkers in the management of pancreatic adenocarcinoma. *Seminars in Radiation Oncology,* 24(2), pp. 67-76.

Jemal, A., Siegel, R., Xu, J. and Ward, E., 2010. Cancer Statistics, 2010. *CA: A Cancer Journal for Clinicians,* 60(5), pp. 277-300.

Ji, Q., Hao, X., Zhang, M., Tang, W., Yang, M., Li, L., Xiang, D., Desano, J.T., Bommer, G.T., Fan, D., Fearon, E.R., Lawrence, T.S. and XU, L., 2009. MicroRNA miR-34 inhibits human pancreatic cancer tumor-initiating cells. *PloS One,* 4(8), pp. e6816.

Jiang, J., Lee, E.J., Gusev, Y. and Schmittgen, T.D., 2005. Real-time expression profiling of microRNA precursors in human cancer cell lines. *Nucleic Acids Research,* 33(17), pp. 5394-5403.

Jiang, X.T., Tao, H.Q. and Zou, S.C., 2004. Detection of serum tumor markers in the diagnosis and treatment of patients with pancreatic cancer. *Hepatobiliary & Pancreatic Diseases International,* 3(3), pp. 464-468.

Jonckheere, N., Skrypek, N. and Vab Seuningen, I., 2010. Mucins and Pancreatic Cancer. *Cancers*, 2(4), pp.1794-1812.

Jung, M., Schaffer, A., Steiner, I., Kempkensteffen, C., Stephan, C., Erbersdobler, A. and Jung, K., 2010. Robust microRNA stability in degraded RNA preparations from human tissue and cell samples. *Clinical Chemistry,* 56(6), pp. 998-1006.

Kanai, M., Yoshimura, K., Asada, M., Imaizumi, A., Suzuki, C., Matsumoto, S., Nishimura, T., Mori, Y., Masui, T., Kawaguchi, Y., Yanagihara, K., Yazumi, S., Chiba, T., Guha, S. and Aggarwal, B.B., 2011. A phase I/II study of gemcitabine-based chemotherapy plus curcumin for patients with gemcitabine-resistant pancreatic cancer. *Cancer Chemotherapy and Pharmacology,* 68(1), pp. 157-164.

Kang, N., Wang, M., Wang, Y., Zhang, Z., Cao, H., Lv, Y., Yang, Y., Fan, P., Qiu, F. and Gao, X., 2014. Tetrahydrocurcumin induces G2/M cell cycle arrest and apoptosis involving p38 MAPK activation in human breast cancer cells. *Food and Chemical Toxicology,* 67, pp. 193-200.

Kanwar, S.S., Yu, Y., Nautiyal, J., Patel, B.B., Padhye, S., Sarkar, F.H. and Majumdar, A.P.N., 2011. Difluorinated-Curcumin (CDF): A Novel Curcumin Analog is a Potent Inhibitor of Colon Cancer Stem-Like Cells. *Pharmaceutical Research,* 28(4), pp. 827-838.

Karius, T., Schnekenburger, M., Dicato, M. and Diederich, M., 2012. MicroRNAs in cancer management and their modulation by dietary agents. *Biochemical Pharmacology,* 83(12), pp. 1591-1601.

Katiyar, S.K., Afaq, F., Azizuddin, K. and Mukhtar, H., 2001. Inhibition of UVB-induced oxidative stress-mediated phosphorylation of mitogen-activated protein kinase signaling pathways in cultured human epidermal keratinocytes by green tea polyphenol (-)-epigallocatechin-3-gallate. *Toxicology and Applied Pharmacology,* 176(2), pp. 110-117.

Katz, M.H., Wang, H., Fleming, J.B., Sun, C.C., Hwang, R.F., Wolff, R.A., Varadhachary, G., Abbruzzese, J.L., Crane, C.H., Krishnan, S., Vauthey, J.N., Abdalla, E.K., Lee, J.E., Pisters, P.W. and Evans, D.B., 2009. Long-term survival after multidisciplinary management of resected pancreatic adenocarcinoma. *Annals of Surgical Oncology,* 16(4), pp. 836-847.

Kawaguchi, T., Komatsu, S., Ichikawa, D., Morimura, R., Tsujiura, M., Konishi, H., Takeshita, H., Nagata, H., Arita, T., Hirajima, S., Shiozaki, A., Ikoma H., Okamoto, K., Ochiai, T., Taniguchi, H. and Otsuji, E., 2013. Clinical impact of circulating miR-221 in plasma of patients with pancreatic cancer. *British Journal of Cancer,* 108(2), pp. 361-369.

Kelly, M.E. and Conlon, K.C., 2014. Pancreatic Adenocarcinoma. In: Garden, O.J. and Parks, R.W., eds, *A Companion to specialist surgical practice: Hepatobiliary and Pancreatic Surgery.* 5th Edition edn. Edinburgh: Saunders Elsevier, pp. 275.

Kent, O.A., Chivukula, R.R., Mullendore, M., Wentzel, E.A., Feldmann, G., Lee, K.H., Liu, S., Leach, S.D., Maitra, A. and Mendell, J.T., 2010. Repression of the miR-143/145 cluster by oncogenic Ras initiates a tumor-promoting feed-forward pathway. *Genes & Development,* 24(24), pp. 2754-2759.

Kent, O.A., Mullendore, M., Wentzel, E.A., Lopez-Romero, P., Tan, A.C., Alvarez, H., West, K., Ochs, M.F., Hidalgo, M., Arking, D.E., Maitra, A. and Mendell, J.T., 2009. A resource for analysis of microRNA expression and function in pancreatic ductal adenocarcinoma cells. *Cancer Biology & Therapy,* 8(21), pp. 2013-2024.

Kent, O.A., McCall, M.N., Cornish, T.C. and Halushka, M.K., 2014. Lessons from miR-143/145: the importance of cell-type localization of miRNAs. *Nucleic Acids Research,* 42(12), pp. 7528-7538.

Khan, S.G., Katiyar, S.K., Agarwal, R. and Mukhtar, H., 1992. Enhancement of antioxidant and phase II enzymes by oral feeding of green tea polyphenols in drinking water to SKH-1 hairless mice: possible role in cancer chemoprevention. *Cancer Research,* 52(14), pp. 4050-4052.

Kim, S.O., Kundu, J.K., Shin, Y.K., Park, J.H., Cho, M.H., Kim, T.Y. and Surh, Y.J., 2005. [6]-Gingerol inhibits COX-2 expression by blocking the activation of p38 MAP kinase and NF-kappaB in phorbol ester-stimulated mouse skin. *Oncogene,* 24(15), pp. 2558-2567.

Kim, V.N. and Nam, J.W., 2006. Genomics of microRNA. *Trends in Genetics,* 22(3), pp. 165-173.

Kim, V.N., Han, J. and Siomi, M.C., 2009. Biogenesis of small RNAs in animals. *Nature Reviews Molecular Cell Biology,* 10(2), pp. 126-139.

Klein, A.P., Brune, K.A., Petersen, G.M., Goggins, M., Tersmette, A.C., Offerhaus, G.J., Griffin, C., Cameron, J.L., Yeo, C.J., Kern, S. and Hruban, R.H., 2004. Prospective risk of pancreatic cancer in familial pancreatic cancer kindreds. *Cancer Research,* 64(7), pp. 2634-2638.

Klein, C.A., 2009. Parallel progression of primary tumours and metastases. *Nature Reviews. Cancer,* 9(4), pp. 302-312.

Kong, A.N., Yu, R., Hebbar, V., Chen, C., Owuor, E., Hu, R., Ee, R. and Mandlekar, S., 2001. Signal transduction events elicited by cancer prevention compounds. *Mutation Research,* 480-481, pp. 231-241.

Koorstra, J.B., Hustinx, S.R., Offerhaus, G.J. and Maitra, A., 2008. Pancreatic carcinogenesis *Pancreatology,* 8(2), pp. 110-125.

Korc, M., 1998. Role of growth factors in pancreatic cancer. *Surgical Oncology Clinics of North America,* 7(1), pp. 25-41.

Kress, T.R., Cannell, I.G., Brenkman, A.B., Samans, B., Gaestel, M., Roepman, P., Burgering, B.M., Bushell, M., Rosenwald, A. and Eilers, M., 2011. The MK5/PRAK kinase and Myc form a negative feedback loop that is disrupted during colorectal tumorigenesis. *Molecular Cell,* 41(4), pp. 445-457.

Krutzfeldt, J., Rajewsky, N., Braich, R., Rajeev, K.G., Tuschl, T., Manoharan, M. and Stoffel, M., 2005. Silencing of microRNAs in vivo with 'antagomirs'. *Nature,* 438(7068), pp. 685-689.

Kulig, P., Pach, R. and Kulig, J., 2014. Role of abdominal ultrasonography in clinical staging of pancreatic carcinoma: a tertiary center experience. *Polskie Archiwum Medycyny Wewnetrznej,* 124(5), pp. 225-232.

Kulshreshtha, R., Ferracin, M., Wojcik, S.E., Garzon, R., Alder, H., Agosto-Perez, F.J., Davuluri, R., Liu, C.G., Croce, C.M., Negrini, M., Calin, G.A. and Ivan, M., 2007. A microRNA signature of hypoxia *Molecular and Cellular Biology,* 27(5), pp. 1859-1867.

Kunnumakkara, A.B., Guha, S., Krishnan, S., Diagaradjane, P., Gelovani, J. and Aggarwal, B.B., 2007. Curcumin potentiates antitumor activity of gemcitabine in an orthotopic model of pancreatic cancer through suppression of proliferation, angiogenesis, and inhibition of nuclear factor-kappaB-regulated gene products. *Cancer Research,* 67(8), pp. 3853-3861.

Kushwaha, R., Thodima, V., Tomishima, M.J., Bosl, G.J. and Chaganti, R.S.K., 2014. miR-18b and miR-518b Target FOXN1 During Epithelial Lineage Differentiation in Pluripotent Cells. *Stem Cells and Development,* 23(10), pp. 1149-1156.

Lagos-Quintana, M., Rauhut, R., Lendeckel, W. and Tuschl, T., 2001. Identification of novel genes coding for small expressed RNAs. *Science,* 294(5543), pp. 853-858.

Landis-Piwowar, K.R. and Iyer, N.R., 2014. Cancer chemoprevention: current state of the art. *Cancer Growth and Metastasis,* 7, pp. 19-25.

Lao, C.D., Ruffin, M.T., Normolle, D., Heath, D.D., Murray, S.I., Bailey, J.M., Boggs, M.E., Crowell, J., Rock, C.L. and Brenner, D.E., 2006. Dose escalation of a curcuminoid formulation. *BMC Complementary and Alternative Medicine,* 6, pp. 10.

Lau, N.C., Lim, L.P., Weinstein, E.G. and Bartel, D.P., 2001. An abundant class of tiny RNAs with probable regulatory roles in Caenorhabditis elegans. *Science,* 294(5543), pp. 858-862.

Lee, E.J., Gusev, Y., Jiang, J., Nuovo, G.J., Lerner, M.R., Frankel, W.L., Morgan, D.L., Postier, R.G., Brackett, D.J. and Schmittgen, T.D., 2007. Expression profiling identifies microRNA signature in pancreatic cancer. *International Journal of Cancer,* 120(5), pp. 1046-1054.

Lee, J.M., Hanson, J.M., Chu, W.A. and Johnson, J.A., 2001. Phosphatidylinositol 3-kinase, not extracellular signal-regulated kinase, regulates activation of the antioxidant-responsive element in IMR-32 human neuroblastoma cells. *The Journal of Biological Chemistry,* 276(23), pp. 20011-20016.

Lee, R.C. and Ambros, V., 2001. An extensive class of small RNAs in Caenorhabditis elegans. *Science,* 294(5543), pp. 862-864.

Lee, R.C., Feinbaum, R.L. and Ambros, V., 1993. The C. elegans heterochronic gene lin-4 encodes small RNAs with antisense complementarity to lin-14. *Cell,* 75(5), pp. 843-854.

Lee, T.Y., Lee, K.C., Chen, S.Y. and Chang, H.H., 2009. 6-Gingerol inhibits ROS and iNOS through the suppression of PKC-alpha and NF-kappaB pathways in lipopolysaccharide-stimulated mouse macrophages. *Biochemical and Biophysical Research Communications,* 382(1), pp. 134-139.

Leung, A.K. and Sharp, P.A., 2010. MicroRNA Functions in Stress Responses. *Molecular Cell,* 40(2), pp. 205-215.

Levayer, R. and Lecuit, T., 2008. Breaking down EMT. *Nature Cell Biology,* 10(7), pp. 757-759.

Lewis, B.P., Burge, C.B. and Bartel, D.P., 2005. Conserved seed pairing, often flanked by adenosines, indicates that thousands of human genes are microRNA targets. *Cell,* 120(1), pp. 15-20.

Li, C., Heidt, D.G., Dalerba, P., Burant, C.F., Zhang, L., Adsay, V., Wicha, M., Clarke, M.F. and Simeone, D.M., 2007. Identification of Pancreatic Cancer Stem Cells. *Cancer Research,* 3, pp. 1030-1037.

Li, C.H., To, K., Tong, J.H., Xiao, Z., Xia, T., Lai, P.B.S., Chow, S.C., Zhu, Y., Chan, S.L., Marquez, V.E. and Chen, Y., 2013. Enhancer of Zeste Homolog 2 Silences MicroRNA-218 in Human Pancreatic Ductal Adenocarcinoma Cells by Inducing Formation of Heterochromatin. *Gastroenterology,* 144(5), pp. 1086-1097.

Li, J., Guo, Y., Liang, X., Sun, M., Wang, G., De, W. and Wu, W., 2012. MicroRNA-223 functions as an oncogene in human gastric cancer by targeting FBXW7/hCdc4. *Journal of Cancer Research and Clinical Oncology,* 138(5), pp. 763-774.

Li, L., Braiteh, F.S. and Kurzrock, R., 2005. Liposome-encapsulated curcumin: in vitro and in vivo effects on proliferation, apoptosis, signalling, and angiogenesis. *Cancer,* 104(6), pp. 1322-1331.

Li, Y., Kong, D., Wang, Z. and Sarkar, F.H., 2010. Regulation of microRNAs by natural agents: an emerging field in chemoprevention and chemotherapy research. *Pharmaceutical Research,* 27(6), pp. 1027-1041.

Li, Y. and Sarkar, F.H., 2002. Inhibition of nuclear factor kappaB activation in PC3 cells by genistein is mediated via Akt signaling pathway *Clinical Cancer Research,* 8(7), pp. 2369-2377.

Li, Y., Vandenboom, T.G., Kong, D., Wang, Z., Ali, S., Philip, P.A. and Sarkar, F.H., 2009. Up-regulation of miR-200 and let-7 by natural agents leads to the reversal of epithelial-to-mesenchymal transition in gemcitabine-resistant pancreatic cancer cells. *Cancer Research,* 69 (16), pp. 6704-6712.

Lin, W.C., Rajbhandari, N., Liu, C., Sakamoto, K., Zhang, Q., Triplett, A.A., Batra, S.K., Opavsky, R., Felsher, D.W., Dimaio, D.J., Hollingsworth, M.A., Morris, J.P., Hebrok, M., Witkiewicz, A.K., Brody, J.R., Rui, H. and Wagner, K.U., 2013. Dormant cancer cells contribute to residual disease in a model of reversible pancreatic cancer. *Cancer Research,* 73(6), pp. 1821-1830.

Link, A., Balaguer, F. and Goel, A., 2010. Cancer chemoprevention by dietary polyphenols: Promising role for epigenetics. *Biochemical Pharmacology,* 80(12), pp. 1771-1792.

Liu, C.G., Calin, G.A., Meloon, B., Gamliel, N., Sevignani, C., Ferracin, M., Dumitru, C.D., Shimizu, M., Zupo, S., Dono, M., Alder, H., Bullrich, F., Negrini, M. and Croce, C.M., 2004. An oligonucleotide microchip for genome-wide microRNA profiling in human and mouse tissues. *Proceedings of the National Academy of Sciences of the United States of America,* 101(26), pp. 9740-9744.

Liu, J., Valencia-Sanchez, M.A., Hannon, G.J. and Parker, R., 2005. MicroRNA-dependent localization of targeted mRNAs to mammalian P-bodies. *Nature Cell Biology,* 7(7), pp. 719-723.

Liu, Q., Chen, J., Wang, J., Amos, C., Killary, A.M., Sen, S., Wei, C. and Frazier, M.L., 2014. Putative tumor suppressor gene SEL1L was downregulated by aberrantly upregulated hsa-mir-155 in human pancreatic ductal adenocarcinoma. *Molecular Carcinogenesis,* 53(9), pp. 711-721.

Liu, W., Xu, C., Wan, H., Liu, C., Wen, C., Lu, H. and Wan, F., 2014. MicroRNA-206 overexpression promotes apoptosis, induces cell cycle arrest and inhibits the migration of human hepatocellular carcinoma HepG2 cells. *International Journal of Molecular Medicine,* 34(2), pp. 420-428.

Livak, K.J. and Schmittgen, T,D., 2002. Analysis of relative gene expression data using real-time quantitative PCR and the 2(-Delta Delta C(T)) Method. *Methods,* 25(4), pp. 402-408.

Lo, S.-., Hung, P.-., Chen, J.-., Tu, H.-., Fang, W.-., Chen, C.-., Chen, W.-., Gong, N.-. and Wu, C.-., 2012. Overexpression of miR-370 and downregulation of its novel target TGF beta-RII contribute to the progression of gastric carcinoma. *Oncogene,* 31(2), pp. 226-237.

Lodes, M.J., Caraballo, M., Suciu, D., Munro, S., Kumar, A. and Anderson, B., 2009. Detection of cancer with serum miRNAs on an oligonucleotide microarray *PloS One,* 4(7), pp. e6229.

Lotterman, C.D., Kent, O.A. and Mendell, J.T., 2008. Functional integration of microRNAs into oncogenic and tumor suppressor pathways. *Cell Cycle,* 7(16), pp. 2493-2499.

Lowenfels, A.B., Maisonneuve, P., Cavallini, G., Ammann, R.W., Lankisch, P.G., Andersen, J.R., Dimagno, E.P., Andren-Sandberg, A. and Domellof, L., 1993. Pancreatitis and the risk of pancreatic cancer. International Pancreatitis Study Group. *The New England Journal of Medicine,* 328(20), pp. 1433-1437.

Lu, J., Getz, G., Miska, E.A., Alvarez-Saavedra, E., Lamb, J., Peck, D., Sweet-Cordero, A., Ebert, B.L., Mak, R.H., Ferrando, A.A., Downing, J.R., Jacks, T., Horvitz, H.R. and Golub, T.R., 2005. MicroRNA expression profiles classify human cancers. *Nature,* 435(7043), pp. 834-838.

Luo, J., Nordenvall, C., Nyren, O., Adami, H.O., Permert, J. and Ye, W., 2007. The risk of pancreatic cancer in patients with gastric or duodenal ulcer disease. *International Journal of Cancer,* 120(2), pp. 368-372.

Ma, Z., Swede, H., Cassarino, D., Fleming, E., Fire, A. and Dadras, S.S., 2011. Up-Regulated Dicer Expression in Patients with Cutaneous Melanoma. *Plos One,* 6(6), pp. e20494.

Macfarlane, L.A. and Murphy, P.R., 2010. MicroRNA: Biogenesis, Function and Role in Cancer. *Current Genomics,* 11(7), pp. 537-561.

Maitra, A., Adsay, N.V., Argani, P., Iacobuzio-Donahue, C., De Marzo, A., Cameron, J.L., Yeo, C.J. and Hruban, R.H., 2003. Multicomponent analysis of the pancreatic adenocarcinoma progression model using a pancreatic intraepithelial neoplasia tissue microarray. *Modern Pathology,* 16(9), pp. 902-912.

Mann, C.D., Bastianpillai, C., Neal, C.P., Masood, M.M., Jones, D.J., Teichert, F., Singh. R., Karpova, E., Berry, D.P. and Manson, M.M., 2012. Notch3 and HEY-1 as prognostic biomarkers in pancreatic adenocarcinoma. *PloS One,* 7(12), pp. e51119.

Mann, C.D., Neal, C.P., Garcea, G., Manson, M.M., Dennison, A.R. and Berry, D.P., 2009. Phytochemicals as potential chemopreventive and chemotherapeutic agents in hepatocarcinogenesis. *European Journal of Cancer Prevention,* 18(1), pp. 13-25.

Manna, S.K., Mukhopadhyay, A. and Aggarwal, B.B., 2000. Resveratrol suppresses TNF-induced activation of nuclear transcription factors NF-kappa B, activator protein-1, and apoptosis: potential role of reactive oxygen intermediates and lipid peroxidation. *Journal of Immunology,* 164(12), pp. 6509-6519.

Manson, M.M., 2003. Cancer prevention -- the potential for diet to modulate molecular signalling. *Trends in Molecular Medicine,* 9(1), pp. 11-18.

Maragkakis, M., Reczko, M., Simossis, V.A., Alexiou, P., Papadoppulos, G.L., Dalamagas, T., Giannopoulos, G., Goumas, G., Koukis, E., Kourtis, K., Vergoulis, T., Koziris, N., Sellis, T., Tsanakas, P. and Hatzigeorgiou, A.G., 2009. DIANA-microT web server: elucidating microRNA functions through target prediction. *Nucleic Acids Research,* 37(Web Server issue), pp. W273-276.

Margulies, M., Egholm, M., Altman, W.E., Attiya, S., Bader, J.S., Bemben, L.A., Berka, J., Braverman, M.S., Chen, Y.J., Chen, Z., Dewell, S.B., Du, L., Fierro, J.M., Gomes, X.V., Godwin, B.C., He, W., Helgesen, S., Ho, C.H., Irzyk, G.P., Jando, S.C., Alenquer, M.L., Jarvie, T.P., Jirage, K.B., Kim, J.B., Knight, J.R., Lanza, J.R., Leamon, J.H., Lefkowitz, S.M., Lei, M., Li, J., Lohman, K.L., Lu, H., Makhijani, V.B., McDade, K.E., McKenna, M.P., Myers, E.W., Nickerson, E., Nobile, J.R., Plant, R., Puc B.P., Ronan, M.T., Roth, G.T., Sarkis, G.J., Simons, J.F., Simpson, J.W., Srinicasan, M., Tartaro, K.R., Tomasz, A., Vogt, K.A., Volkmer, G.A., Wang, S.H., Wang, Y., Weiner, M.P., Yu, P., Begley, R.F. and Rothberg, J.M., 2005. Genome sequencing in microfabricated high-density picolitre reactors. *Nature,* 437(7057), pp. 376-380.

Masala, G., Ceroti, M., Pala, V., Krogh, V., Vineis, P., Sacerdote, C., Saieva, C., Salvini, S., Sieri, S., Berrino, F., Panico, S., Mattiello, A., Tumino, R., Giurdanella, M.C., Bamia, C., Trichopoulou, A., Riboli, E. and Palli, D., 2007. A dietary pattern rich in olive oil and raw vegetables is associated with lower mortality in Italian elderly subjects. *The British Journal of Nutrition,* 98(2), pp. 406-415.

Mescher, A.L. and Junqueira, L.C.U., 2013. *Junqueira's basic histology: text and atlas.* London; New York, N.Y: McGraw-Hill Medical.

Messina, M.J., Persky, V., Setchell, K.D. and Barnes, S., 1994. Soy intake and cancer risk: a review of the in vitro and in vivo data. *Nutrition and Cancer,* 21(2), pp. 113-131.

Michaud, D.S., Liu, Y., Meyer, M., Giovannucci, E. and Joshipura, K., 2008. Periodontal disease, tooth loss, and cancer risk in male health professionals: a prospective cohort study. *The Lancet Oncology,* 9(6), pp. 550-558.

Milner, J.A., 2006. Diet and cancer: facts and controversies. *Nutrition and Cancer,* 56(2), pp. 216-224.

Milner, J.A., McDonald, S.S., Anderson, D.E. and Greenwald, P., 2001. Molecular targets for nutrients involved with cancer prevention. *Nutrition and Cancer,* 41(1-2), pp. 1-16.

Min, W., Wang, B., LI, J., Han, J., Zhao, Y., Su, W., Dai, Z., Wang, X. and Ma, Q., 2014. The expression and significance of five types of miRNAs in breast cancer. *Medical Science Monitor Basic Research,* 20, pp. 97-104.

Mitchell, P.S., Parkin, R.K., Kroh, E.M., Fritz, B.R., Wyman, S.K., Pogosova-Agadjanyan, E.L., Peterson, A., Noteboom, J., O'Briant, K.C., Allen, A., Lin, D.W., Urban, N., Drescher, C.W., Knudsen, B.S., Stirewalt, D.L., Gentleman, R., Vessella, R.L., Nelson, P.S., Martin, D.B. and Tewari, M., 2008. Circulating microRNAs as stable blood-based markers for cancer detection. *Proceedings of the National Academy of Sciences of the United States of America,* 105(30), pp. 10513-10518.

Moiseeva, E.P. and Manson, M.M., 2009. Dietary chemopreventive phytochemicals: too little or too much? *Cancer Prevention Research,* 2(7), pp. 611-616.

Morton, J.P., Timpson, P., Karim, S.A., Ridgway, R.A., Athineos, D., Doyle, B., Jamieson, N.B., Oien, K.A., Lowy, A.M., Brunton, V.G., Frame, M.C., Evans, T.R. and Sansom, O.J., 2010. Mutant p53 drives metastasis and overcomes growth arrest/senescence in pancreatic cancer. *Proceedings of the National Academy of Sciences of the United States of America,* 107(1), pp. 246-251.

Mraz, M., Malinova, K., Mayer, J. and Pospisilova, S., 2009. MicroRNA isolation and stability in stored RNA samples. *Biochemical and Biophysical Research Communications,* 390(1), pp. 1-4.

Muralidhar, B., Winder, D., Murray, M., Palmer, R., Barbosa-Morais, N., Saini, H., Roberts, I., Pett, M. and Coleman, N., 2011. Functional evidence that Drosha overexpression in cervical squamous cell carcinoma affects cell phenotype and microRNA profiles. *The Journal of Pathology,* 224(4), pp. 496-507.

Muto, S., Fujita, K., Yamazaki, Y. and Kamataki, T., 2001. Inhibition by green tea catechins of metabolic activation of procarcinogens by human cytochrome P450. *Mutation Research,* 479(1-2), pp. 197-206.

Myant, K. and Sansom, O.J., 2011. More, more, more: downregulation of a MK5-FoxO3a-mir34b/c pathway further increases c-Myc levels in colorectal cancer. *Molecular Cell,* 41(4), pp. 369-370.

Neergheen, V.S., Bahorun, T., Taylor, E.W., Jen, L.S. and Aruoma, O.I., 2010. Targeting specific cell signaling transduction pathways by dietary and medicinal phytochemicals in cancer chemoprevention. *Toxicology,* 278(2), pp. 229-241.

Negrini, M., Ferracin, M., Sabbioni, S. and Croce, C.M., 2007. MicroRNAs in human cancer: from research to therapy. *Journal of Cell Science,* 120(Pt 11), pp. 1833-1840.

Nelson, P.T., Wang, W.X., Wilfred, B.R. and Tang, G., 2008. Technical variables in high-throughput miRNA expression profiling: much work remains to be done. *Biochimica et Biophysica Acta,* 1779(11), pp. 758-765.

Neoptolemos, J.P., Stocken, D.D., Bassi, C., Ghaneh, P., Cunningham, D., Goldstein, D., Padbury, R., Moore, M.J., Gallinger, S., Mariette, C., Wente, M.N., Izbicki, J.R., Friess, H., Lerch, M.M., Dervenis, C., Olah, A., Butturini, G., Doi, R., Lind, P.A., Smith, D., Valle, J.W., Palmer, D.H., Buckels, J.A., Thompson, J., McKay, C.J., Rawcliffe, C.L., Buchler, M.W. and European Study Group for Pancreatic Cancer, 2010. Adjuvant chemotherapy with fluorouracil plus folinic acid vs gemcitabine following pancreatic cancer resection: a randomized controlled trial. *JAMA,* 304(10), pp. 1073-1081.

Neoptolemos, J.P., Stocken, D.D., Friess, H., Bassi, C., Dunn, J.A., Hickey, H., Beger, H., Fernandez-Cruz, L., Dervenis, C., Lacaine, F., Falconi, M., Pederzoli, P., Pap, A., Spooner, D., Kerr, D.J., Buchler, M.W. and European Study Group for Pancreatic Cancer, 2004. A randomized trial of chemoradiotherapy and chemotherapy after resection of pancreatic cancer. *The New England Journal of Medicine,* 350(12), pp. 1200-1210.

Neoptolemos, J.P., Stocken, D.D., Tudur Smith, C., Bassi, C., Ghaneh, P., Owen, E., Moore, M., Padbury, R., Doi, R., Smith, D. and Buchler, M.W., 2009. Adjuvant 5-fluorouracil and folinic acid vs observation for pancreatic cancer: composite data from the ESPAC-1 and -3(v1) trials. *British Journal of Cancer,* 100(2), pp. 246-250.

Neuhouser, M.L., 2004. Dietary flavonoids and cancer risk: evidence from human population studies. *Nutrition and Cancer,* 50(1), pp. 1-7.

Newman, D.J. and Cragg, G.M., 2012. Natural products as sources of new drugs over the 30 years from 1981 to 2010. *Journal of Natural Products,* 75(3), pp. 311-335.

Ni, X.G., Bai, X.F., Mao, Y.L., Shao, Y.F., Wu, J.X., Shan, Y., Wang, C.F., Wang, J., Tian, Y.T., Liu, Q., Xu, D.K. and Zhao, P., 2005. The clinical value of serum CEA, CA19-9, and CA242 in the diagnosis and prognosis of pancreatic cancer. *European Journal of Surgical Oncology,* 31(2), pp. 164-169.

Ojajarvi, I.A., Partanen, T.J., Ahlbom, A., Boffetta, P., Hakulinen, T., Jourenkova, N., Kauppinen, T.P., Kogevinas, M., Porta, M., Vainio, H.U., Weiderpass, E. and Wesseling, C.H., 2000. Occupational exposures and pancreatic cancer: a meta-analysis. *Occupational and Environmental Medicine,* 57(5), pp. 316-324.

Oyagbemi, A.A., Azeez, O.I. and Saba, A.B., 2009. Interactions between reactive oxygen species and cancer: the roles of natural dietary antioxidants and their molecular mechanisms of action. *Asian Pacific Journal of Cancer Prevention,* 10(4), pp. 535-544.

Oyebode, O., Gordon-Dseagu, V., Walker, A. and Mindell, J.S., 2014. Fruit and vegetable consumption and all-cause, cancer and CVD mortality: analysis of Health Survey for England data. *Journal of Epidemiology and Community Health,* 68(9), pp. 856-862.

Padhye, S., Chavan, D., Pandey, S., Deshpande, J., Swamy, K.V. and Sarkar, F.H., 2010. Perspectives on chemopreventive and therapeutic potential of curcumin analogs in medicinal chemistry. *Mini Reviews in Medicinal Chemistry,* 10(5), pp. 372-387.

Padhye, S., Banerjee, S., Chavan, D., Pandye, S., Swamy, K.V., Ali, S., Li, J., Dou, Q.P. and Sarkar, F.H., 2009. Fluorocurcumins as Cyclooxygenase-2 Inhibitor: Molecular Docking, Pharmacokinetics and Tissue Distribution in Mice. *Pharmaceutical Research,* 26(11), pp. 2438-2445.

Padhye, S., Yang, H., Jamadar, A., Cui, Q.C., Chavan, D., Dminiak, K., McKinney, J., Banerjee, S., Dou, Q.P. and Sarkar, F.H., 2009. New Difluoro Knoevenagel Condensates of Curcumin, Their Schiff Bases and Copper Complexes as Proteasome Inhibitors and Apoptosis Inducers in Cancer Cells. *Pharmaceutical Research,* 26(8), pp. 1874-1880.

Pal, A., Sung, B., Bhanu Prasad, B.A., Schuber, P.T.,JR, Prasad, S., Aggarwal, B.B. and Bornmann, W.G., 2014. Curcumin glucuronides: assessing the proliferative activity against human cell lines. *Bioorganic & Medicinal Chemistry,* 22(1), pp. 435-439.

Pancreatic Cancer Action, 2014, Abraxane [Homepage of Pancreatic Cancer Action], [Online]. Available from: https://pancreaticcanceraction.org/pancreatic-cancer/treatment/chemotherapy/chemotherapy-drugs-treat-cancer/abraxane/ [Available: 6th January 2014].

Parasramka, M.A., Ho, E., Williams, D.E. and Dashwood, R.H., 2012. MicroRNAs, diet, and cancer: new mechanistic insights on the epigenetic actions of phytochemicals. *Molecular Carcinogenesis,* 51(3), pp. 213-230.

Park, J.Y., Helm, J., Coppola, D., Kim, D., Malafa, M. and Kim, S.J., 2011. MicroRNAs in pancreatic ductal adenocarcinoma. *World Journal of Gastroenterology,* 17(7), pp. 817-827.

Park, J., Henry, J.C., Jiang, J., Esau, C., Gusev, Y., Lerner, M.R., Postier, R.G., Brackett, D.J. and Schmittgen, T.D., 2011. miR-132 and miR-212 are increased in pancreatic cancer and target the retinoblastoma tumor suppressor. *Biochemical and Biophysical Research Communications,* 406(4), pp. 518-523.

Parkin, D.M., 2011. 2. Tobacco-attributable cancer burden in the UK in 2010. *British Journal of Cancer,* 105 Suppl 2, pp. S6-S13.

Pasquinelli, A.E., Reinhart, B.J., Slack, F., Martindale, M.Q., Kuroda, M.I., Maller, B., Hayward, D.C., Ball, E.E., Degnan, B., Muller, P., Spring, J., Srinivasan, A., Fishman, M., Finnerty, J., Corbo, J., Levine, M., Leahy, P., Davidson, E. and Ruvkun, G., 2000. Conservation of the sequence and temporal expression of let-7 heterochronic regulatory RNA. *Nature,* 408(6808), pp. 86-89.

Pelengaris, S., Khan, M. and Evan, G., 2002. c-MYC: more than just a matter of life and death. *Nature Reviews. Cancer,* 2(10), pp. 764-776.

Peltier, H.J. and Latham, G.J., 2008. Normalization of microRNA expression levels in quantitative RT-PCR assays: identification of suitable reference RNA targets in normal and cancerous human solid tissues. *RNA,* 14(5), pp. 844-852.

Peng, Y., Liu, Y.M., Li, L.C., Wang, L.L. and Wu, X.L., 2014. microRNA-503 inhibits gastric cancer cell growth and epithelial-to-mesenchymal transition. *Oncology Letters,* 7(4), pp. 1233-1238.

PerkinElmer, 2013, ATPlite Luminescence ATP Detection Assay System [Homepage of PerkinElmer], [Online]. Available from: http://www.perkinelmer.co.uk/CMSResources/Images/44-157882MAN_ATPlite.pdf [Available: 3rd January 2014].

Pestova, T.V., Hellen, C.U. and Shatsky, I.N., 1996. Canonical eukaryotic initiation factors determine initiation of translation by internal ribosomal entry. *Molecular and Cellular Biology,* 16(12), pp. 6859-6869.

Pham, H., Rodriguez, C.E., Donald, G.W., Hertzer, K.M., Jung, X.S., Chang, H., Moro, A., Reber, H.A., Hines, O.J. and Eibl, G., 2013. miR-143 decreases COX-2 mRNA stability and expression in pancreatic cancer cells. *Biochemical and Biophysical Research Communications,* 439(1), pp. 6-11.

Pillai, R.S., Bhattacharyya, S.N. and Filipowicz, W., 2007. Repression of protein synthesis by miRNAs: how many mechanisms? *Trends in Cell Biology,* 17(3), pp. 118-126.

Plummer, S.M., Holloway, K.A., Manson, M.M., Munks, R.J., Kaptein, A., Farrow, S. and Howells, L., 1999. Inhibition of cyclo-oxygenase 2 expression in colon cells by the chemopreventive agent curcumin involves inhibition of NF-kappaB activation via the NIK/IKK signalling complex. *Oncogene,* 18(44), pp. 6013-6020.

Podolska, A., Kaczkowski, B., Litman, T., Fredholm, M. and Cirera, S., 2011. How the RNA isolation method can affect microRNA microarray results. *Acta Biochimica Polonica,* 58(4), pp. 535-540.

Pramanik, D., Campbell, N.R., Karikari, C., Chivukula, R., Kent, O.A., Mendell, J.T. and Maitra, A., 2011. Restitution of Tumor Suppressor MicroRNAs Using a Systemic Nanovector Inhibits Pancreatic Cancer Growth in Mice. *Molecular Cancer Therapeutics,* 10(8), pp. 1470-1480.

Pritchard, C.C., Cheng, H.H. and Tewari, M., 2012. MicroRNA profiling: approaches and considerations. *Nature Reviews. Genetics,* 13(5), pp. 358-369.

Priyadarsini, R.V. and Nagini, S., 2012. Cancer chemoprevention by dietary phytochemicals: promises and pitfalls. *Current Pharmaceutical Biotechnology,* 13(1), pp. 125-136.

Public Health England, 2013, NHS Cancer Screening Programmes [Homepage of Public Health England], [Online]. Available from: http://www.cancerscreening.nhs.uk/ [Available: 5th January 2014].

Qiao, Q., Jiang, Y. and Li, G., 2013. Inhibition of the PI3K/AKT-NF-kappaB pathway with curcumin enhanced radiation-induced apoptosis in human Burkitt's lymphoma. *Journal of Pharmacological Sciences,* 121(4), pp. 247-256.

Radtke, F. and Raj, K., 2003. The role of Notch in tumorigenesis: oncogene or tumour suppressor? *Nature Reviews. Cancer,* 3(10), pp. 756-767.

Ravindranath, V. and Chandrasekhara, N., 1981a. Invitro Studies on the Intestinal-Absorption of Curcumin in Rats. *Toxicology,* 20(2-3), pp. 251-257.

Ravindranath, V. and Chandrasekhara, N., 1981b. Metabolism of curcumin--studies with [3H]curcumin. *Toxicology,* 22(4), pp. 337-344.

Rayner, M. and Scarborough, P., 2005. The burden of food related ill health in the UK. *Journal of Epidemiology and Community Health,* 59(12), pp. 1054-1057.

Redmond, K.J., Wolfgang, C.L., Sugar, E.A., Ahn, J., Nathan, H., Laheru, D., Edil, B.H., Choti, M.A., Pawlik, T.M., Hruban, R.H., Cameron, J.L. and Herman, J.M., 2010. Adjuvant chemoradiation therapy for adenocarcinoma of the distal pancreas. *Annals of Surgical Oncology,* 17(12), pp. 3112-3119.

Reichert, M., Saur, D., Hamacher, R., Schmid, R.M. and Schneider, G., 2007. Phosphoinositide-3-kinase signaling controls S-phase kinase-associated protein 2 transcription via E2F1 in pancreatic ductal adenocarcinoma cells. *Cancer Research,* 67(9), pp. 4149-4156.

Reinhart, B.J., Slack, F.J., Basson, M., Pasquinelli, A.E., Bettinger, J.C., Rougvie, A.E., Horvitz, H.R. and Ruvkun, G., 2000. The 21-nucleotide let-7 RNA regulates developmental timing in Caenorhabditis elegans. *Nature,* 403(6772), pp. 901-906.

Ren, J., Huang, H.J., Gong, Y., Yue, S., Tang, L.M. and Cheng, S.Y., 2014. MicroRNA-206 suppresses gastric cancer cell growth and metastasis. *Cell & Bioscience,* 4, pp. 26.

Reuland, D.J., Khademi, S., Castle, C.J., Irwin, D.C., McCord, J.M., Miller, B.F. and Hamilton, K.L., 2013. Upregulation of phase II enzymes through phytochemical activation of Nrf2 protects cardiomyocytes against oxidant stress. *Free Radical Biology & Medicine,* 56, pp. 102-111.

Roughley, P.J. and Whiting, D.A., 1973. Experiments in Biosynthesis of Curcumin. *Journal of the Chemical Society-Perkin Transactions 1,* (20), pp. 2379-2388.

Roy, S., Levi, E., Majumdar, A.P. and Sarkar, F.H., 2012. Expression of miR-34 is lost in colon cancer which can be re-expressed by a novel agent CDF. *Journal of Hematology & Oncology,* 5, pp. 58.

Rubie, C., Kruse, B., Frick, V.O., Kolsch, K., Ghadjar, P., Wagner, M., Grasser, F., Wagenpfeil, S. and Glanemann, M., 2014. Chemokine receptor CCR6 expression is regulated by miR-518a-5p in colorectal cancer cells. *Journal of Translational Medicine,* 12, pp. 48.

Russo, S.M., Ove, R. and Saif, M.W., 2011. Identification of prognostic and predictive markers in pancreatic adenocarcinoma. Highlights from the "2011 ASCO Gastrointestinal Cancers Symposium". San Francisco, CA, USA. January 20-22, 2011. *Journal of the Pancreas,* 12(2), pp. 92-95.

Sah, S., McCall, M.N., Eveleigh, D., Wilson, M. and Irizarry, R.A., 2010. Performance evaluation of commercial miRNA expression array platforms. *BMC Research Notes,* 3, pp. 80.

Sarkar, F.H., Li, Y., Wang, Z. and Kong, D., 2009. Cellular signaling perturbation by natural products. *Cellular Signalling,* 21(11), pp. 1541-1547.

Sarkar, F.H., Li, Y., Wang, Z., Kong, D. and Ali, S., 2010. Implication of microRNAs in drug resistance for designing novel cancer therapy. *Drug Resistance Updates,* 13(3), pp. 57-66.

Sassen, S., Miska, E.A. and Caldas, C., 2008. MicroRNA: implications for cancer *Virchows Archiv,* 452(1), pp. 1-10.

Schonleben, F., Qiu, W., Ciau, N.T., Ho, D.J., Li, X., Allendorf, J.D., Remotti, H.E. and Su, G.H., 2006. PIK3CA mutations in intraductal papillary mucinous neoplasm/carcinoma of the pancreas. *Clinical Cancer Research,* 12(12), pp. 3851-3855.

Schutte, M., Hruban, R.H., Geradts, J., Maynard, R., Hilgers, W., Rabindran, S.K., Moskaluk, C.A., Hahn, S.A., Schwarte-Waldhoff, I., Schmiegel, W., Baylin, S.B., Kern, S.E. and Herman, J.G., 1997. Abrogation of the Rb/p16 tumor-suppressive pathway in virtually all pancreatic carcinomas. *Cancer Research,* 57(15), pp. 3126-3130.

Schwartz, A.M. and Henson, D.E., 2007. Familial and sporadic pancreatic carcinoma, epidemiologic concordance. *The American Journal of Surgical Pathology,* 31(4), pp. 645-646.

Scott, E.N., Gescher, A.J., Steward, W.P. and Brown, K., 2009. Development of dietary phytochemical chemopreventive agents: biomarkers and choice of dose for early clinical trials. *Cancer Prevention Research,* 2(6), pp. 525-530.

Setoyama, T., Zhang, X., Natsugoe, S. and Calin, G.A., 2011. microRNA-10b: A New Marker or the Marker of Pancreatic Ductal Adenocarcinoma? *Clinical Cancer Research,* 17(17), pp. 5527-5529.

Sharma, R.A., Euden, S.A., Platton, S.L., Cooke, D.N., Shafayat, A., Hewitt, H.R., Marczylo, T.H., Morgan, B., Hemingway, D., Plummer, S.M., Pirmohamed, M., Gescher, A.J. and Steward, W.P., 2004. Phase I clinical trial of oral curcumin: biomarkers of systemic activity and compliance. *Clinical Cancer Research,* 10(20), pp. 6847-6854.

Sharma, R.A., Gescher, A.J. and Steward, W.P., 2005. Curcumin: the story so far. *European Journal of Cancer,* 41(13), pp. 1955-1968.

Sharma, R.A., McClelland, H.R., Hill, K.A., Ireson, C.R., Euden, S.A., Manson, M.M., Pirmohamed, M., Marnett, L.J., Gescher, A.J. and Steward, W.P., 2001. Pharmacodynamic and pharmacokinetic study of oral Curcuma extract in patients with colorectal cancer. *Clinical Cancer Research,* 7(7), pp. 1894-1900.

Shen, M., Boffetta, P., Olsen, J.H., Andersen, A., Hemminki, K., Pukkala, E., Tracey, E., Brewster, D.H., McBride, M.L., Pompe-Kirn, V., Kliewer, E.V., Tonita, J.M., Chia, K.S., Martos, C., Jonasson, J.G., Colin, D., Scelo, G. and Brennan, P., 2006. A pooled analysis of second primary pancreatic cancer. *American Journal of Epidemiology,* 163(6), pp. 502-511.

Shi, C., Hruban, R.H. and Klein, A.P., 2009. Familial pancreatic cancer. *Archives of Pathology & Laboratory Medicine,* 133(3), pp. 365-374.

Shishodia, S., Chaturvedi, M.M. and Aggarwal, B.B., 2007. Role of curcumin in cancer therapy. *Current Problems in Cancer,* 31(4), pp. 243-305.

Shoba, G., Joy, D., Joseph, T., Majeed, M., Rajendran, R. and Srinivas, P.S.S.R., 1998. Influence of piperine on the pharmacokinetics of curcumin in animals and human volunteers. *Planta Medica,* 64(4), pp. 353-356.

Shureiqi, I. and Baron, J.A., 2011. Curcumin Chemoprevention: The Long Road to Clinical Translation. *Cancer Prevention Research,* 4(3), pp. 296-298.

Siegel, R., Naishadham, D. and Jemal, A., 2013. Cancer Statistics, 2013. *CA: A Cancer Journal for Clinicians,* 63(1), pp.11-30.

Sipos, B., Moser, S., Kalthoff, H., Torok, V., Lohr, M. and Kloppel, G., 2003. A comprehensive characterization of pancreatic ductal carcinoma cell lines: towards the establishment of an in vitro research platform. *Virchows Archiv,* 442(5), pp. 444-452.

Slater, E.P., Strauch, K., Rospleszcz, S., Ramaswamy, A., Esposito, I., Kloppel, G., Matthai, E., Heeger, K., Fendrich, V., Langer, P. and Bartsch, D.K., 2014. MicroRNA-196a and -196b as Potential Biomarkers for the Early Detection of Familial Pancreatic Cancer. *Translational Oncology,* 7(4), pp. 464-471.

Sporn, M.B., 1976. Approaches to prevention of epithelial cancer during the preneoplastic period. *Cancer Research,* 36(7 PT 2), pp. 2699-2702.

Stanger, B.Z. and Dor, Y., 2006. Dissecting the cellular origins of pancreatic cancer. *Cell Cycle,* 5(1), pp. 43-46.

Su, G.H., ed, 2003. *Pancreatic Cancer: Methods and Protocols.* 2nd Edition edn. New York: Springer.

Subramaniam, D., Ponnurangam, S., Ramamoorthy, P., Standing, D., Battfarano, R.J., Anant, S. and Sharma, P., 2012. Curcumin Induces Cell Death in Esophageal Cancer Cells through Modulating Notch Signaling. *Plos One,* 7(2), pp. e30590.

Sun, M., Estrov, Z., Ji, Y., Coombes, K.R., Harris, D.H. and Kurzrock, R., 2008. Curcumin (diferuloylmethane) alters the expression profiles of microRNAs in human pancreatic cancer cells. *Molecular Cancer Therapeutics,* 7(3), pp. 464-473.

Sun, T., Kong, X., Du, Y. and Li, Z., 2014. Aberrant MicroRNAs in Pancreatic Cancer: Researches and Clinical Implications. *Gastroenterology Research and Practice,* 487(16), pp. 386561-386561.

Surh, Y.-. and Chun, K.-., 2007. Cancer Chemoprevention Effects of Curcumin. In: Aggarwal, B.B., Surh, Y. and Shishodia, S., eds, *The Molecular Targets and Therapeutic uses of Curcumin in Health and Disease.* New York: Springer.

Surh, Y., 2003. Cancer chemoprevention with dietary phytochemicals. *Nature Reviews Cancer,* 3(10), pp. 768.

Szafranska, A.E., Davison, T.S., John, J., Cannon, T., Sipos, B., Maghnouj, A., Labourier, E. and Hahn, S.A., 2007. MicroRNA expression alterations are linked to tumorigenesis and non-neoplastic processes in pancreatic ductal adenocarcinoma. *Oncogene,* 26(30), pp. 4442-4452.

Tang, D., Shen, Y., Wang, M., Yang, R., Wang, Z., Sui, A., Jiao, W. and Wang, Y., 2013. Identification of plasma microRNAs as novel noninvasive biomarkers for early detection of lung cancer. *European Journal of Cancer Prevention,* 22(6), pp. 540-548.

Tarin, D., Thompson, E.W. and Newgreen, D.F., 2005. The fallacy of epithelial mesenchymal transition in neoplasia. *Cancer Research,* 65(14), pp. 5996-6001.

Tavani, A. and La Vecchia, C., 1995. Fruit and vegetable consumption and cancer risk in a Mediterranean population. *The American Journal of Clinical Nutrition,* 61(6 Suppl), pp. 1374S-1377S.

Tel-Aviv Sourasky Medcial Center, 2007, Phase III Trial of Gemcitabine, Curcumin and Celebrex in Patients With Advance or Inoperable Pancreatic Cancer. Available from: http://clinicaltrials.gov/ct2/show/NCT00486460 [Available: 28th June 2014].

Thiery, J.P., Acloque, H., Huang, R.Y. and Nieto, M.A., 2009. Epithelial-mesenchymal transitions in development and disease. *Cell,* 139(5), pp. 871-890.

Thompson, E.W., Newgreen, D.F. and Tarin, D., 2005. Carcinoma invasion and metastasis: a role for epithelial-mesenchymal transition? *Cancer Research,* 65(14), pp. 5991-5995.

Thomson, J.M., Newman, M., Parker, J.S., Morin-Kensicki, E.M., Wright, T. and Hammond, S.M., 2006. Extensive post-transcriptional regulation of microRNAs and its implications for cancer. *Genes & Development,* 20(16), pp. 2202-2207.

Thomson, J.M., Parker, J., Perou, C.M. and Hammond, S.M., 2004. A custom microarray platform for analysis of microRNA gene expression. *Nature Methods,* 1(1), pp. 47-53.

Tilak, J.C., Banerjee, M., Mohan, H. and Devasagayam, T.P., 2004. Antioxidant availability of turmeric in relation to its medicinal and culinary uses. *Phytotherapy Research,* 18(10), pp. 798-804.

Tili, E., Michaille, J., Alder, H., Volinia, S., Delmas, D., Latruffe, N. and Croce, C.M., 2010. Resveratrol modulates the levels of microRNAs targeting genes encoding tumor-suppressors and effectors of TGFβ signaling pathway in SW480 cells. *Biochemical Pharmacology,* 80(12), pp. 2057-2065.

Tonnesen, H.H., Karlsen, J. and Van Henegouwen, G.B., 1986. Studies on curcumin and curcuminoids. VIII. Photochemical stability of curcumin. *Zeitschrift fur Lebensmittel-Untersuchung und -Forschung,* 183(2), pp. 116-122.

Tuveson, D.A. and Neoptolemos, J.P., 2012. Understanding metastasis in pancreatic cancer: a call for new clinical approaches. *Cell,* 148(1-2), pp. 21-23.

University of Leicester, 2014, Combining Curcumin With FOLFOX Chemotherapy in Patients With Inoperable Colorectal Cancer (CUFOX). Available from: http://clinicaltrials.gov/show/NCT01490996 [Available: 28th June 2014].

University of Liverpool, 2014, EUROPAC [Homepage of University of Liverpool], [Online]. Available from: http://www.europac-org.eu/ [Available: 1st April 2014].

Vaksman, O., Hetland, T.E., Trope', C.G., Reich, R. and Davidson, B., 2012. Argonaute, Dicer, and Drosha are up-regulated along tumor progression in serous ovarian carcinoma. *Human Pathology,* 43(11), pp. 2062-2069.

Valadi, H., Ekstrom, K., Bossios, A., Sjostrand, M., Lee, J.J. and Lotvall, J.O., 2007. Exosome-mediated transfer of mRNAs and microRNAs is a novel mechanism of genetic exchange between cells. *Nature Cell Biology,* 9(6), pp. 654-672.

Valerio, L.G.,JR, Kepa, J.K., Pickwell, G.V. and Quattrochi, L.C., 2001. Induction of human NAD(P)H:quinone oxidoreductase (NQO1) gene expression by the flavonol quercetin. *Toxicology Letters,* 119(1), pp. 49-57.

Vallejo, D.M., Caparros, E. and Dominguez, M., 2011. Targeting Notch signalling by the conserved miR-8/200 microRNA family in development and cancer cells. *Embo Journal,* 30(4), pp. 756-769.

Van Der Heijden, M.S., Brody, J.R., Dezentje, D.A., Gallmeier, E., Cunningham, S.C., Swartz, M.J., Demarzo, A.M., Offerhaus, G.J., Isacoff, W.H., Hruban, R.H. and Kern, S.E., 2005. In vivo therapeutic responses contingent on Fanconi anemia/BRCA2 status of the tumor. *Clinical Cancer Research,* 11(20), pp. 7508-7515.

Van Heek, N.T., Meeker, A.K., Kern, S.E., Yeo, C.J., Lillemoe, K.D., Cameron, J.L., Offerhaus, G.J., Hicks, J.L., Wilentz, R.E., Goggins, M.G., De Marzo, A.M., Hruban, R.H. and Maitra, A., 2002.

Telomere shortening is nearly universal in pancreatic intraepithelial neoplasia. *The American Journal of Pathology,* 161(5), pp. 1541-1547.

Verma, S.P., Salamone, E. and Goldin, B., 1997. Curcumin and genistein, plant natural products, show synergistic inhibitory effects on the growth of human breast cancer MCF-7 cells induced by estrogenic pesticides. *Biochemical and Biophysical Research Communications,* 233(3), pp. 692-696.

Vincent, A., Herman, J., Schulick, R., Hruban, R.H. and Goggins, M., 2011. Pancreatic cancer. *Lancet,* 378(9791), pp. 607-620.

Vogt, M., Munding, J., Gruner, M., Liffers, S.T., Verdoodt, B., Hauk, J., Steinstraesser, L., Tannapeel, A. and Hermeking, H., 2011. Frequent concomitant inactivation of miR-34a and miR-34b/c by CpG methylation in colorectal, pancreatic, mammary, ovarian, urothelial, and renal cell carcinomas and soft tissue sarcomas. *Virchows Archiv,* 458(3), pp. 313-322.

Von Hoff, D.D., Ervin, T., Arena, F.P., Chiorean, E.G., Infante, J., Moore, M., Seay, T., Tjulandin, S.A., Ma, W.W., Saleh, M.N., Harris, M., Reni, M., Dowden, S., Laheru, D., Bahary, N., Ramanathan, R.K., Tabernero, J., Hidalgo, M., Goldstein, D., Van Cutsem, E., Wei, X., Iglesias, J. and Renschler, M.F., 2013. Increased survival in pancreatic cancer with nab-paclitaxel plus gemcitabine. *The New England Journal of Medicine,* 369(18), pp. 1691-1703.

Von Hoff, D.D., Ramanathan, R.K., Borad, M.J., Laheru, D.A., Smith, L.S., Wood, T.E., Korn, R.L., Desai, N., Trieu, V., Iglesias, J.L., Zhang, H., Soon-Shiong, P., Shi, T., Rajeshkumar, N.V., Maitra, A. and Hidalgo, M., 2011. Gemcitabine plus nab-paclitaxel is an active regimen in patients with advanced pancreatic cancer: a phase I/II trial. *Journal of Clinical Oncology,* 29(34), pp. 4548-4554.

Wang, J., Chen, J., Chang, P., LeBlanc, A., Li, D., Abbruzzesse, J.L., Frazier, M.L., Killary, A.M. and Sen, S., 2009. MicroRNAs in plasma of pancreatic ductal adenocarcinoma patients as novel blood-based biomarkers of disease. *Cancer Prevention Research,* 2(9), pp. 807-813.

Wang, W., Liu, L., Li, G., Chen, Y., Li, C., Jin, D. and Wang, X., 2013. Combined Serum CA19-9 and miR-27a-3p in Peripheral Blood Mononuclear Cells to Diagnose Pancreatic Cancer. *Cancer Prevention Research,* 6(4), pp. 331-338.

Wang, Y.J., Pan, M.H., Cheng, A.L., Lin, L.I., Ho, Y.S., Hsieh, C.Y. and Lin, J.K., 1997. Stability of curcumin in buffer solutions and characterization of its degradation products. *Journal of Pharmaceutical and Biomedical Analysis,* 15(12), pp. 1867-1876.

Wang, Z., Li, Y., Ahmad, A., Azmi, A.S., Kong, D., Banerjee, S. and Sarkar, F.H., 2010. Targeting miRNAs involved in cancer stem cell and EMT regulation: An emerging concept in overcoming drug resistance. *Drug Resistance Updates,* 13(4-5), pp.109-118.

Wang, Z., Li, Y., Kong, D., Banerjee, S., Ahmad, A., Azmi, A.S., Ali, S., Abbruzzese, J.L., Gallick, G.E. and Sarkar, F.H., 2009. Acquisition of epithelial-mesenchymal transition phenotype of gemcitabine-resistant pancreatic cancer cells is linked with activation of the notch signaling pathway. *Cancer Research,* 69(6), pp. 2400-2407.

Wang, Z.W., Zhang, Y.X., Banerjee, S., Li, Y.W. and Sarkar, F.H., 2006. Notch-1 down-regulation by curcumin is associated with the inhibition of cell growth and the induction of apoptosis in pancreatic cancer cells. *Cancer,* 106(11), pp. 2503-2513.

Wang, Z., Banerjee, S., Ahmad, A., Li, Y., Azmi, A.S., Gunn, J.R., Kong, D., Bao, B., Ali, S., Gao, J., Mohammad, R.M., Miele, L., Korc, M. and Sarkar, F.H., 2011. Activated K-ras and INK4a/Arf Deficiency Cooperate During the Development of Pancreatic Cancer by Activation of Notch and NF-kappa B Signaling Pathways. *Plos One,* **6**(6), pp. e20537.

Wang, Z., Li, Y., Kong, D., Ahmad, A., Banerjee, S. and Sarkar, F.H., 2010. Cross-talk between miRNA and Notch signaling pathways in tumor development and progression. *Cancer Letters,* 292(2), pp. 141-148.

Warshaw, A.L. and Fernandez-Del Castillo, C., 1992. Pancreatic carcinoma. *The New England Journal of Medicine,* 326(7), pp. 455-465.

Watson, J.L., Hill, R., Yaffe, P.B., Greenshields, A., Walsh, M., Lee, P.W., Giacomantonio, C.A. and Hoskin, D.W., 2010. Curcumin causes superoxide anion production and p53-independent apoptosis in human colon cancer cells. *Cancer Letters,* 297(1), pp. 1-8.

Wattenberg, L.W., 1985. Chemoprevention of cancer. *Cancer Research,* 45(1), pp. 1-8.

Weinberg, R.A., 2013. *The Biology of Cancer.* Second Edition edn. USA: Garland Science, Taylor & Francis Group, LLC.

Wicha, M.S., 2011. Stemming a tumor with a little miR. *Nature Medicine,* 17(2), pp. 162-164.

Wiencke, J.K., 2004. Impact of race/ethnicity on molecular pathways in human cancer. *Nature Reviews Cancer,* 4(1), pp. 79-81.

Winston, J., C., 1997. Phytochemicals: Guardians of our Health. *Journal of the American Dietetic Association,* 97(10), pp. S199-S204.

Wolfer, A., Wittner, B.S., Irimia, D., Flavin, R.J., Lupien, M., Gunawardane, R.N., Meyer, C.A., Lightcap, E.S., Tamayo, P., Mesirov, J.P., Liu, X.S., Shioda, T., Toner, M., Loda, M., Brown, M., Brugge, J.S. and Ramaswamy, S., 2010. MYC regulation of a "poor-prognosis" metastatic cancer cell state. *Proceedings of the National Academy of Sciences of the United States of America,* 107(8), pp. 3698-3703.

Woodson, K., Ratnasinghe, D., Bhat, N.K., Stewart, C., Tangrea, J.A., Hartman, T.J., Stolzenberg-Solomon, R., Virtamo, J., Taylor, P.R. and Albanes, D., 1999. Prevalence of disease-related DNA polymorphisms among participants in a large cancer prevention trial. *European Journal of Cancer Prevention,* 8(5), pp. 441-447.

World Cancer Research Fund/American Institute for Cancer Research, 2007. *Food, Nutrition, Physical Activity, and the Prevention of Cancer: a Global Perspective.* Washington DC: AICR.

World Health Organisation, 2002. *Reducing Risks, Promoting Healthy Life.* Geneva: World Health Organisation.

World Health Organisation, 1990. *Diet, Nutrition, and the Prevention of Chronic Diseases.* Geneva: World Health Organisation.

Wu, M.L., Li, H., Yu, L.J., Chen, X.Y., Kong, Q.Y., Song, X., Shu, X.H. and Liu, J., 2014. Short-term resveratrol exposure causes in vitro and in vivo growth inhibition and apoptosis of bladder cancer cells. *PloS One,* 9(2), pp. e89806.

Xi, Y., Nakajima, G., Gavin, E., Morris, C.G., Kudo, K., Hayashi, K. and JU, J., 2007. Systematic analysis of microRNA expression of RNA extracted from fresh frozen and formalin-fixed paraffin-embedded samples. *RNA,* 13(10), pp. 1668-1674.

Yang, C.H., Yue, J., Sims, M. and Pfeffer, L.M., 2013. The Curcumin Analog EF24 Targets NF-kappa B and miRNA-21, and Has Potent Anticancer Activity In Vitro and In Vivo. *Plos One,* 8(8), pp. e71130.

Yang, J., Cao, Y., Sun, J. and Zhang, Y., 2010. Curcumin reduces the expression of Bcl-2 by upregulating miR-15a and miR-16 in MCF-7 cells. *Medical Oncology,* 27(4), pp. 1114-1118.

Yang, L., Belaguli, N. and Berger, D.H., 2009. MicroRNA and colorectal cancer. *World Journal of Surgery,* 33(4), pp. 638-646.

Yang, Y., Liu, L., Zhang, Y., Guan, H., Wu, J., Zhu, X., Yuan, J. and Li, M., 2014. MiR-503 targets PI3K p85 and IKK-beta and suppresses progression of non-small cell lung cancer. *International Journal of Cancer,* 135(7), pp. 1531-1542.

Ye, T.T., Yang, Y.L., Liu, X.Y., Ji, Q.Q., Pan, Y.F. and Xiang, Y.Q., 2014. Prognostic value of circulating microRNA-21 in digestive system cancers: a meta-analysis. *International Journal of Clinical and Experimental Medicine,* 7(4), pp. 873-878.

Yokota, J., 2000. Tumor progression and metastasis. *Carcinogenesis,* 21(3), pp. 497-503.

Yu, J., Li, A., Hong, S., Hruban, R.H. and Goggins, M., 2012. MicroRNA Alterations of Pancreatic Intraepithelial Neoplasias. *Clinical Cancer Research,* 18(4), pp. 981-992.

Yu, R., Chen, C., Mo, Y.Y., Hebbar, V., Owuor, E.D., Tan, T.H. and Kong, A.N., 2000. Activation of mitogen-activated protein kinase pathways induces antioxidant response element-mediated gene expression via a Nrf2-dependent mechanism. *The Journal of Biological Chemistry,* 275(51), pp. 39907-39913.

Yu, R., Mandlekar, S., Lei, W., Fahl, W.E., Tan, T.H. and Kong, A.N., 2000. p38 mitogen-activated protein kinase negatively regulates the induction of phase II drug-metabolizing enzymes that detoxify carcinogens. *The Journal of Biological Chemistry,* 275(4), pp. 2322-2327.

Zekri, L., Huntzinger, E., Heimstadt, S. and Izaurralde, E., 2009. The silencing domain of GW182 interacts with PABPC1 to promote translational repression and degradation of microRNA targets and is required for target release. *Molecular and Cellular Biology,* 29(23), pp. 6220-6231.

Zhang, J., Zhang, T., Ti, X., Shi, J., Wu, C., Ren, X. and Yin, H., 2010. Curcumin promotes apoptosis in A549/DDP multidrug-resistant human lung adenocarcinoma cells through an miRNA signaling pathway. *Biochemical and Biophysical Research Communications,* 399(1), pp. 1-6.

Zhang, M., Zhou, S., Zhang, L., Zhang, J., Cai, H., Zhu, J., Huang, C. and Wang, J., 2012. miR-518b is down-regulated, and involved in cell proliferation and invasion by targeting Rap1b in esophageal squamous cell carcinoma. *FEBS letters,* 586(19), pp. 3508-3521.

Zhang, S., Hao, J., Xie, F., Hu, X., Liu, C., Tong, J., Zhou, J., Wu, J. and Shao, C., 2011. Downregulation of miR-132 by promoter methylation contributes to pancreatic cancer development. *Carcinogenesis,* 32(8), pp. 1183-1189.

Zhang, Y., 2004. Cancer-preventive isothiocyanates: measurement of human exposure and mechanism of action. *Mutation Research,* 555(1-2), pp. 173-190.

Zhang, Y., Li, M., Wang, H., Fisher, W.E., Lin, P.H., Yao, Q. and Chen, C., 2009. Profiling of 95 microRNAs in pancreatic cancer cell lines and surgical specimens by real-time PCR analysis. *World Journal of Surgery,* 33(4), pp. 698-709.

Zhao, G., Deng, S., Zhu, S., Wang, B., Li, X., Liu, Y., Qin, Q., Gong, Q., Niu, Y., Xiang, C., Chen, J., Yan, J., Deng, S., Yin, T., Yang, M., Wu, H. and Wang, C., 2014. Chronic pancreatitis and pancreatic cancer demonstrate active epithelial-mesenchymal transition profile, regulated by miR-217-SIRT1 pathway. *Cancer Letters,* Epub ahead of print.

Zhao, G., Zhang, J., Liu, Y., Qin, Q., Wang, B., Tian, K., Liu, L., Li, X., Niu, Y., Deng, S. and Wang, C., 2013. miR-148b Functions as a Tumor Suppressor in Pancreatic Cancer by Targeting AMPK alpha 1. *Molecular Cancer Therapeutics,* 12(1), pp. 83-93.

Zheng, Y.B., Luo, H.P., Shi, Q., Hao, Z.N., Ding, Y., Wang, Q.S., Li, S.B., Xiao, G.C. and Tong, S.L., 2014. miR-132 inhibits colorectal cancer invasion and metastasis via directly targeting ZEB2. *World Journal of Gastroenterology,* 20(21), pp. 6515-6522.

Zhou, J., Tao, Y., Peng, C., Gu, P. and Wang, W., 2014. miR-503 regulates metastatic function through Rho guanine nucleotide exchanger factor 19 in hepatocellular carcinoma. *The Journal of Surgical Research,* 188(1), pp. 129-136.

Zipper, H., Brunner, H., Bernhagen, J. and Vitzthum, F., 2004. Investigations on DNA intercalation and surface binding by SYBR Green I, its structure determination and methodological implications. *Nucleic Acids Research,* 32(12), pp. e103.

Appendices

Appendix 1: Buffers, Reagents and Cell lines

SDS-PAGE Separating and Stacking Gel Recipes

	10% Separating (ml)	12% Separating (ml)	5% Stacking (ml)
dH_2O	4.000	3.300	2.700
30% Acrylamide	3.300	4.000	0.670
1.5M Tris-HCL pH8.8	2.500	2.500	-----
1M Tris-HCL pH6.8	-----	-----	0.500
10% SDS	0.100	0.100	0.040
10% APS	0.100	0.100	0.040
TEMED	0.004	0.004	0.004
TOTAL	10.000	10.000	4.000

Pancreatic Cancer Cell Line Information

Cell Type	**AsPC-1**	**BxPC-3**	**MIA PaCa-2**
Differentiation Status	moderate	moderate	poorly
Source of Tumour	Ascites	Primary Tumour	Primary Tumour
Histology & Grade 1° Tumour	PDAC G2	PDAC G2	PDAC G2
K-Ras	Mut (p.m.)	w.t.	Mut (p.m.)
p53	Mut (Frameshift)	Mut (p.m.)	Mut (p.m.)
p16	Mut (Frameshift)	Mut (no gene product detected)	Mut (h.d.)
DPC4/Smad4	w.t/Mut (p.m.)	Mut (h.d.)	w.t.
Effect of Curcumin	Moderate Sensitivity	High Sensitivity	Low Sensitivity

Key: Point Mutation (p.m.), Wild Type (w.t.), Homozygous Deletion (h.d.), Mutated (Mut). (Sipos et al, 2003)

Appendix 2: Linear Regression Analysis

Linear Regression Plots MIA PaCa-2:

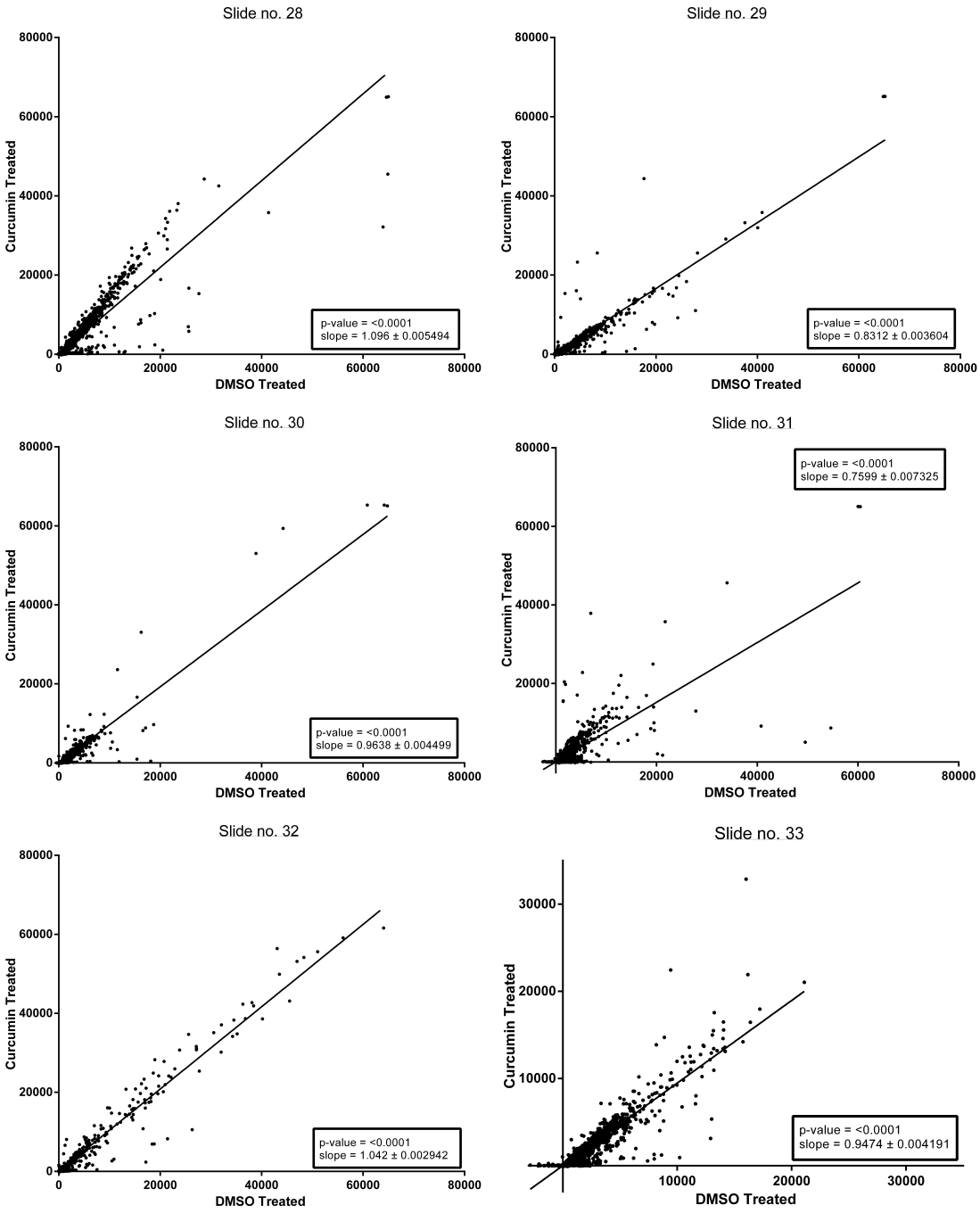

Slide no. 34

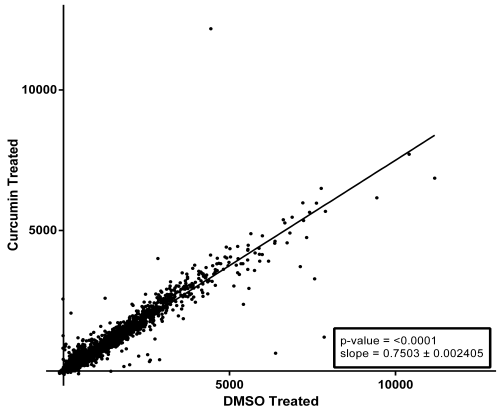

Slide no. 35

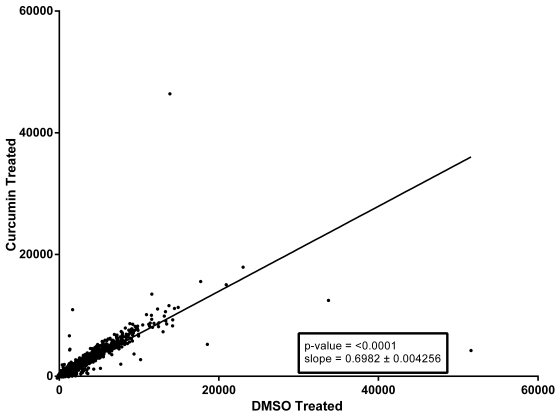

Slide no. 36

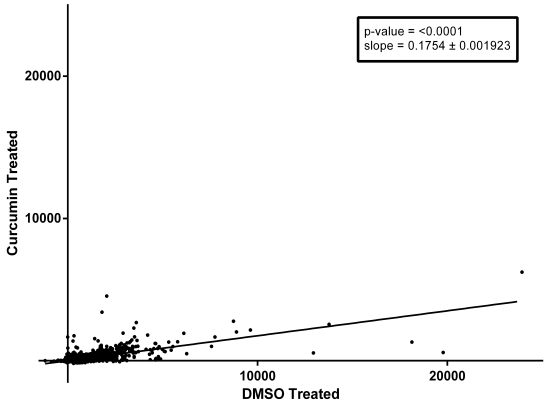

Slide no. 37

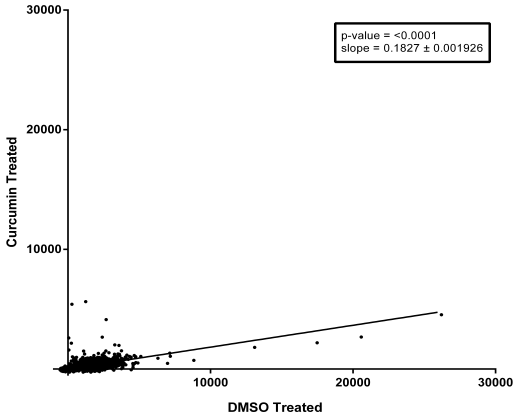

Slide no. 48

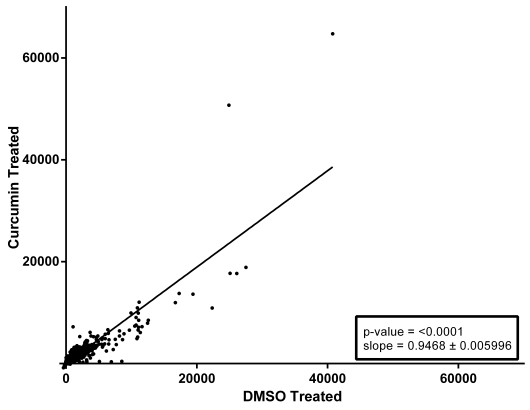

Slide no. 49

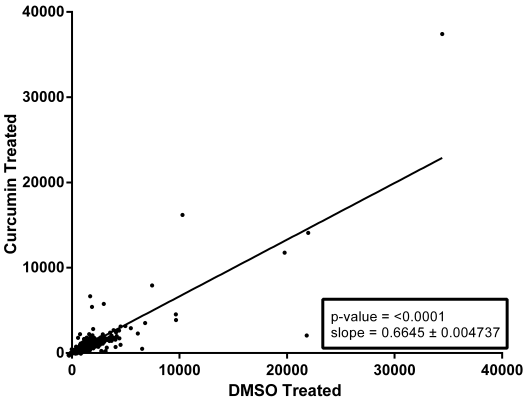

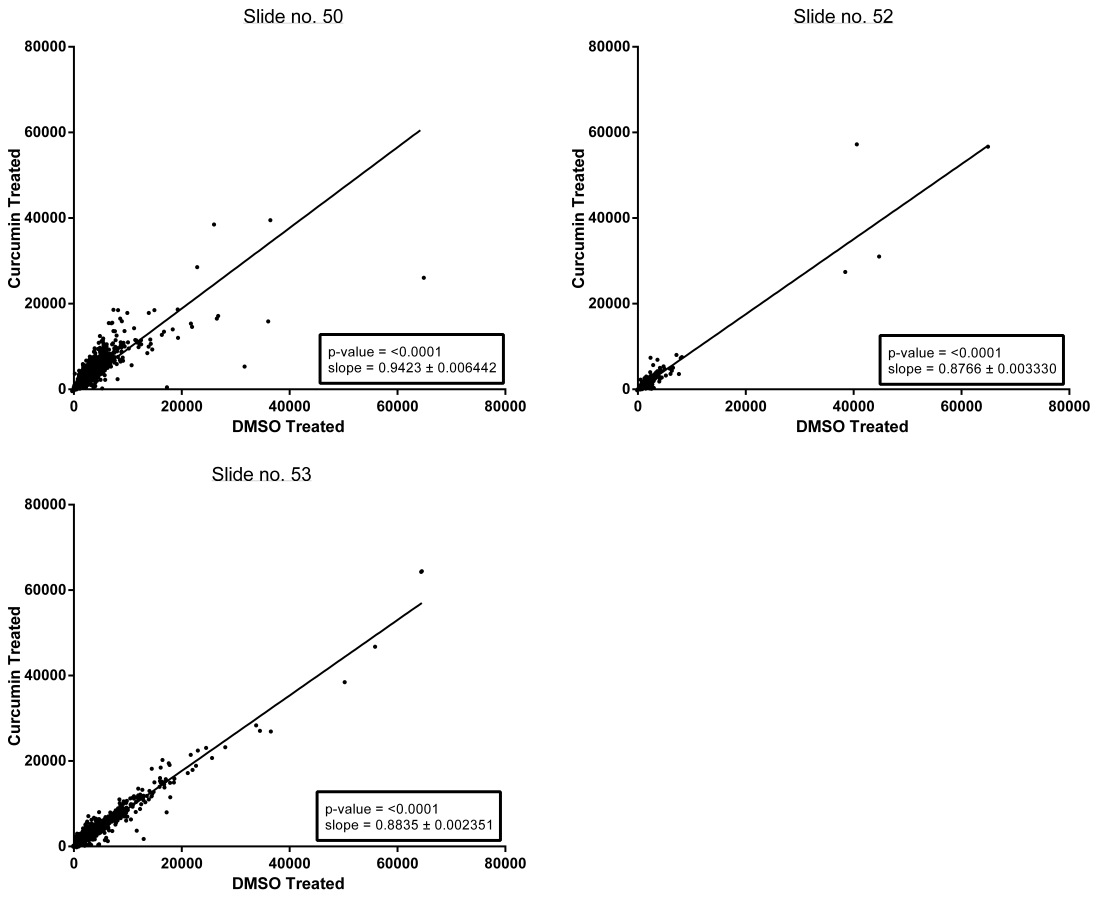

Linear regression plots for Cy3(DMSO treated) and Cy5 (curcumin treated) labelled RNA samples obtained from MIA PaCa-2 cells following in-house (Genisphere) microarray hybridisation. The slope of each linear regression is given ± SEM in addition to the significance of the data as the p-value.

Linear Regression Plots AsPC-1:

Slide no. 23

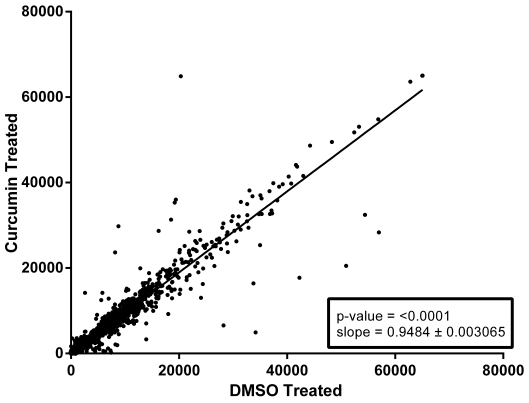

Slide no. 24

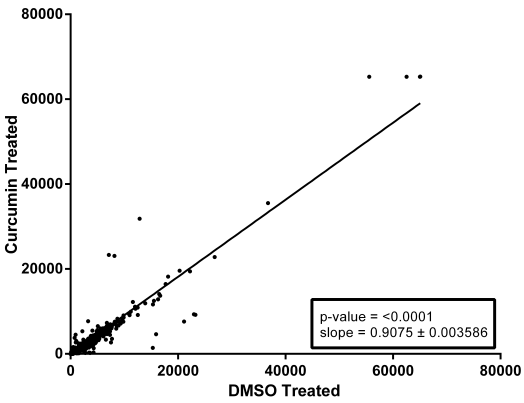

Slide no. 25

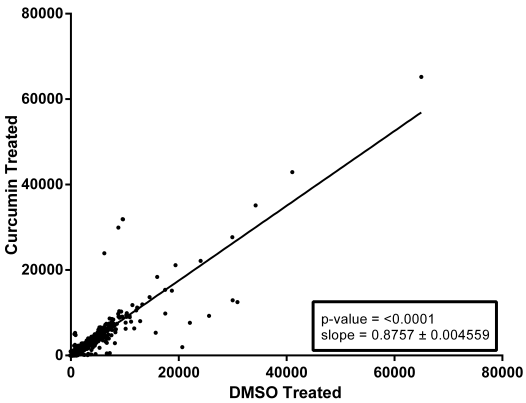

Slide no. 26

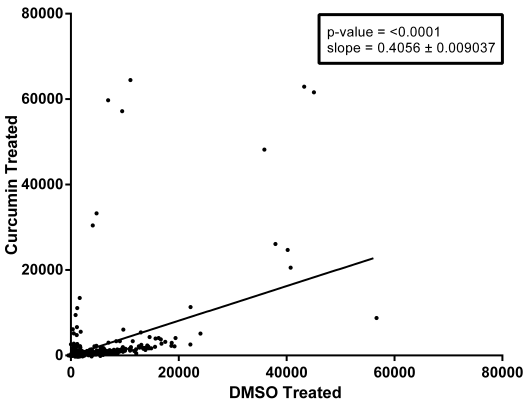

Slide no. 27

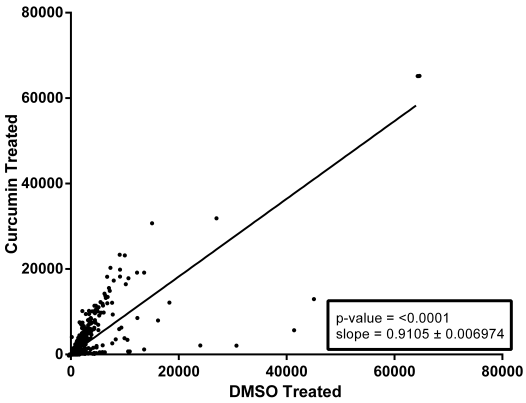

Slide no. 38

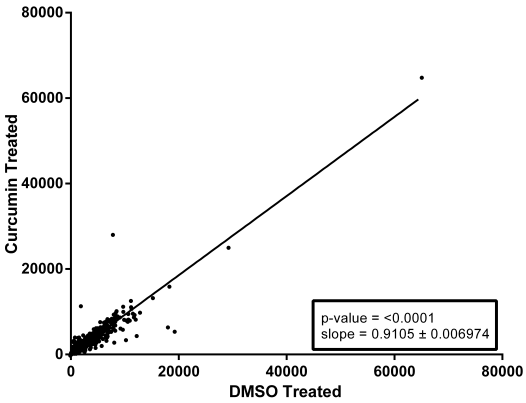

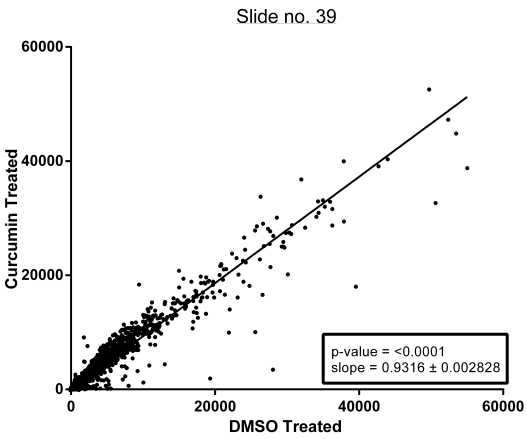
Slide no. 39
Curcumin Treated
DMSO Treated
p-value = <0.0001
slope = 0.9316 ± 0.002828

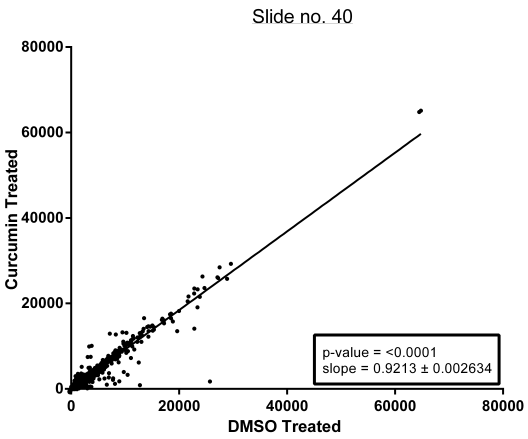
Slide no. 40
Curcumin Treated
DMSO Treated
p-value = <0.0001
slope = 0.9213 ± 0.002634

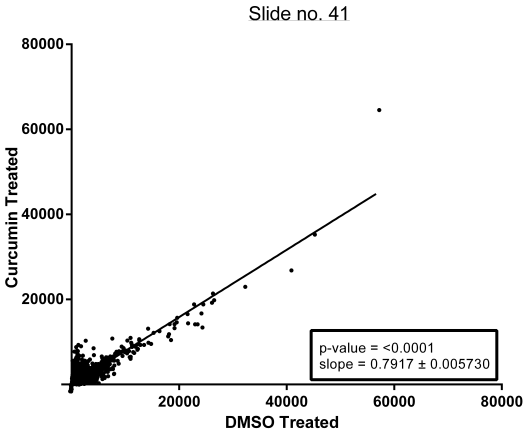
Slide no. 41
Curcumin Treated
DMSO Treated
p-value = <0.0001
slope = 0.7917 ± 0.005730

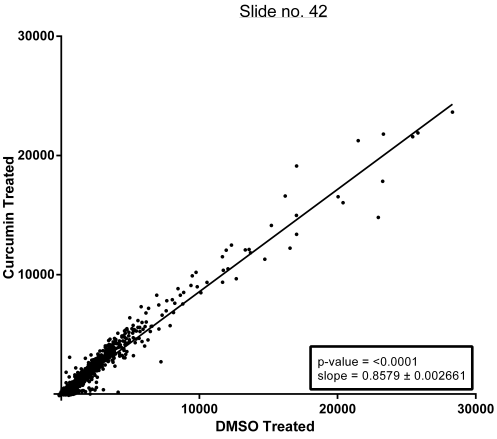
Slide no. 42
Curcumin Treated
DMSO Treated
p-value = <0.0001
slope = 0.8579 ± 0.002661

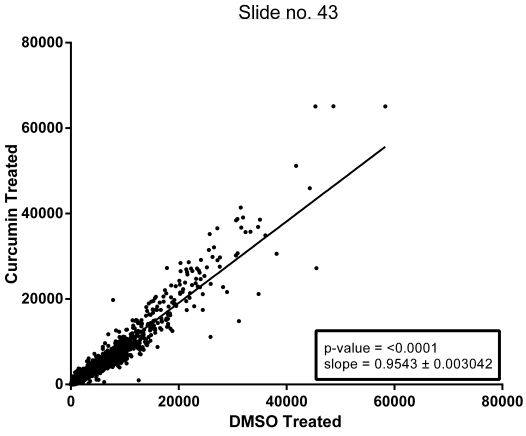
Slide no. 43
Curcumin Treated
DMSO Treated
p-value = <0.0001
slope = 0.9543 ± 0.003042

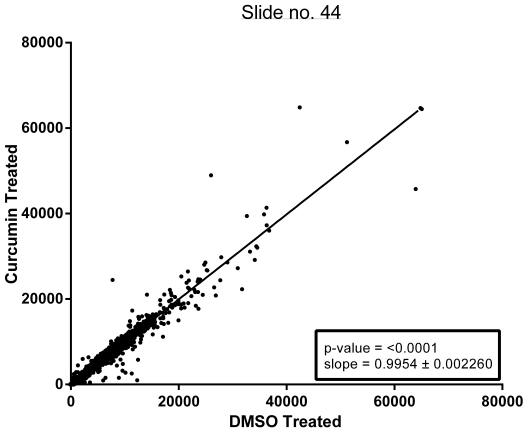
Slide no. 44
Curcumin Treated
DMSO Treated
p-value = <0.0001
slope = 0.9954 ± 0.002260

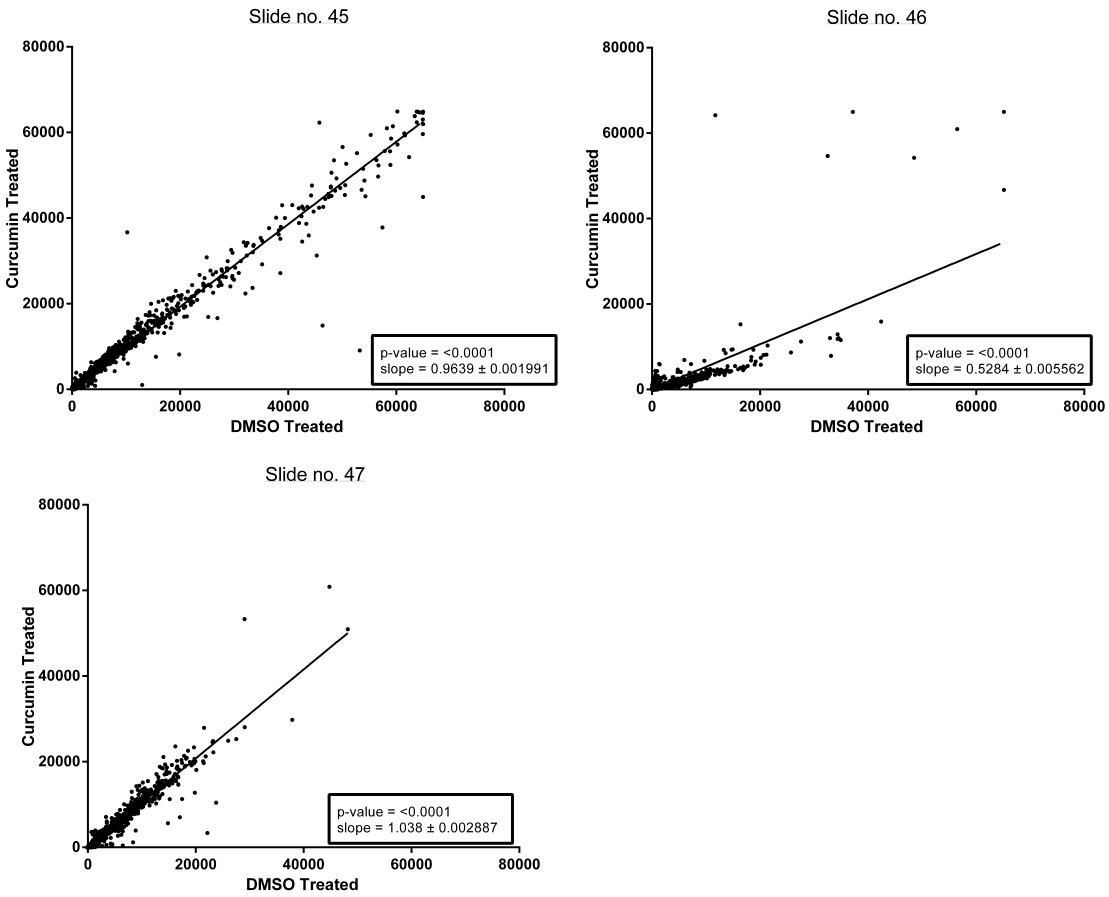

Linear regression plots for Cy3 (DMSO treated) and Cy5 (curcumin treated) labelled RNA samples obtained from AsPC-1 cells following in-house (Genisphere) microarray hybridisation. The slope of each linear regression is given ± SEM in addition to the significance of the data as the p-value.

Appendix 3: Limma Commands

The Limma commands used to process and normalise the in-house (Genisphere) microarray data are outlined below. ***(Explanation of commands in bold italics)***

library(limma)

targets<-readTargets("Targets.txt") ***becomes targets frame***

RG<-

read.maimages(targets,source="genepix.median",wt.fun=wtflags(weight=0,cutoff=-5),

annotation=c("Block","Row","Column","ID","Name","description")) ***foreground and background intensities are read into the RG (red green) list using this command***

backgroundCorrect(RG,method="normexp",offset=50) ***subtracts background intensity from foreground intensity***

MA<-normalizeWithinArrays(RG,method="printtiploess") ***adjusts foreground adaptively for background intensities (required for traditional log ratio analysis of 2 colour array data)***

MA.s<-normalizeBetweenArrays(MA,method="quantile") ***separate channel normalisation method***

fit<-lmFit(MA.s) ***estimates fold change and standard error by fitting linear model for each miRNA***

fit<-eBayes(fit) ***applies empirical Bayes smoothing to standard errors***

tt<-topTable(fit,number=nrow(fit)) ***shows statistics and fold change for differentially expressed miRNAs***

write.table(tt,file="table",sep=",")

Graph commands: ***(explanation of commands in bold italics)***

(X is interchangeable for RG, MA, MA.s or fit)

plotMA(X) ***plots an MA scattergraph***

plotDensities(X) ***plots a density graph of red vs green. Smoothed empirical densities for individual green and red channels on all arrays.***

plotPrintTipLoess(X) ***plots an MA plot for each print tip group on the array along with a loess curve (which should be flat through 0 on each print tip)***

(plotMA, plotDensities and plotPrintTipLoess can all be used to show normalisation of the array data)

Volcanoplot(fit) ***plots the fold change against the p-value***

Appendix 4: MA Plots Showing Intra and Inter-Normalisation of In-house (Genisphere) Microarray Data

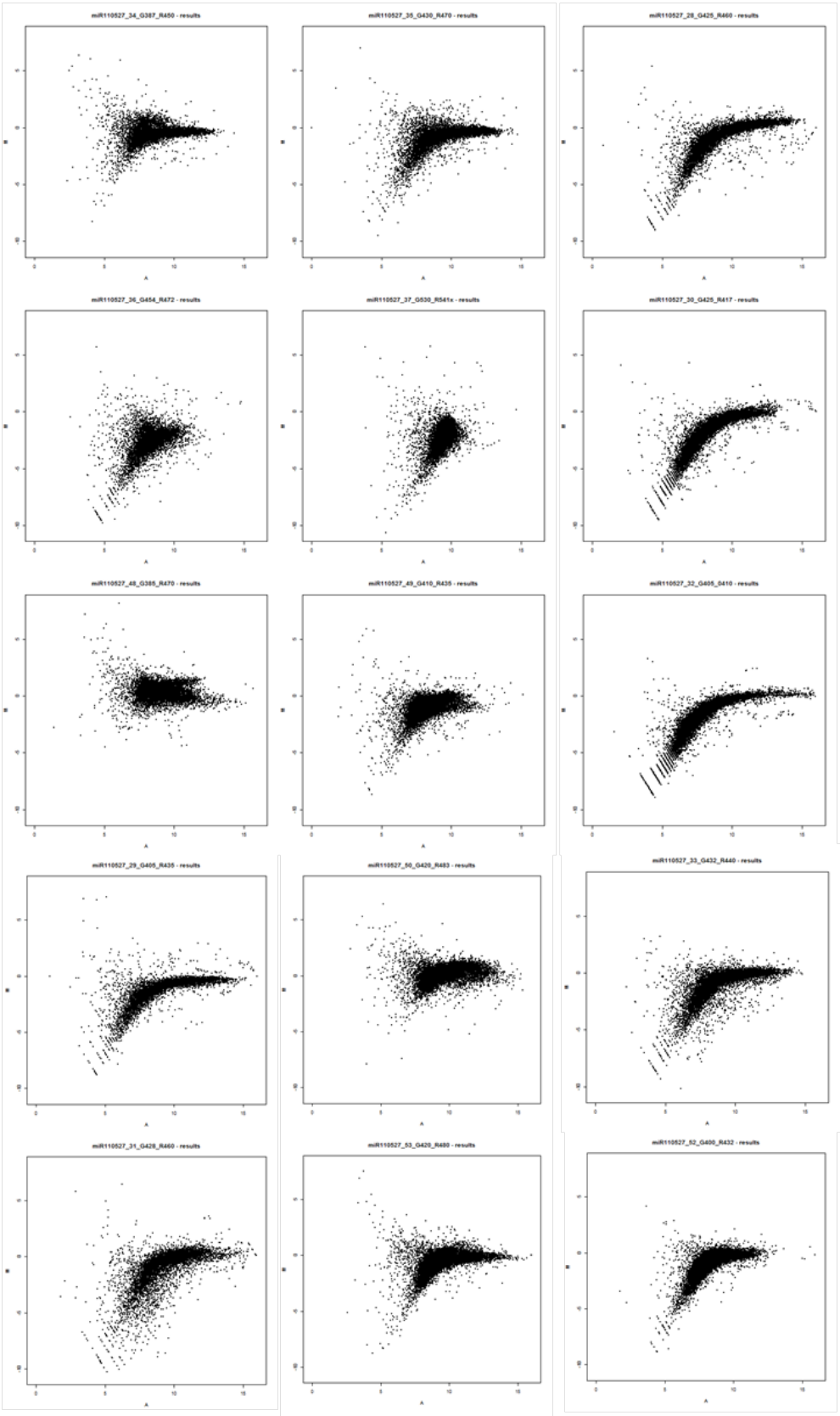

MA plots were produced for the pre-normalised raw data for each microarray slide containing curcumin and DMSO treated MIA PaCa-2 samples.

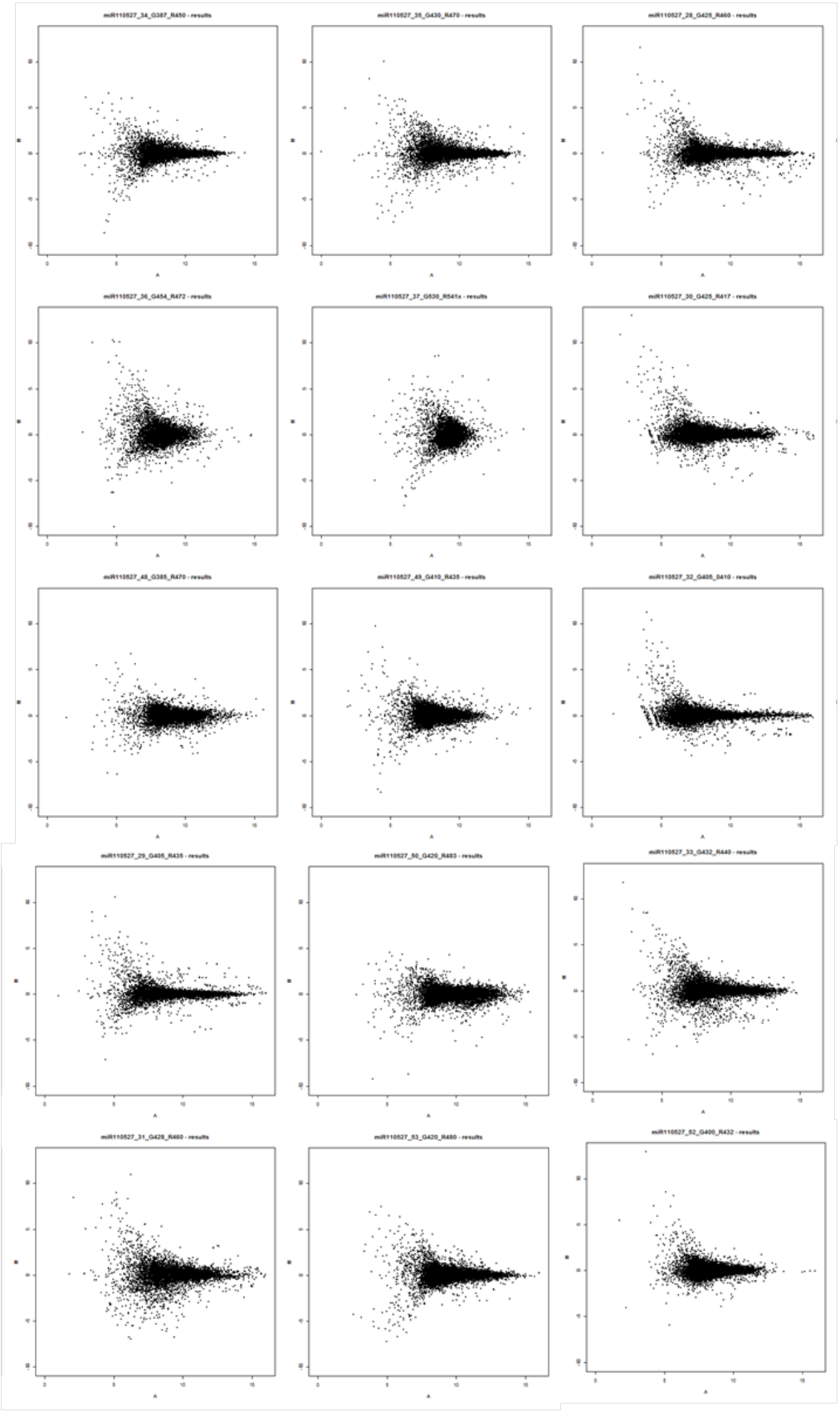

MA plots were produced following intra-normalisation (within array normalisation) of data for each microarray slide containing curcumin and DMSO treated MIA PaCa-2 samples.

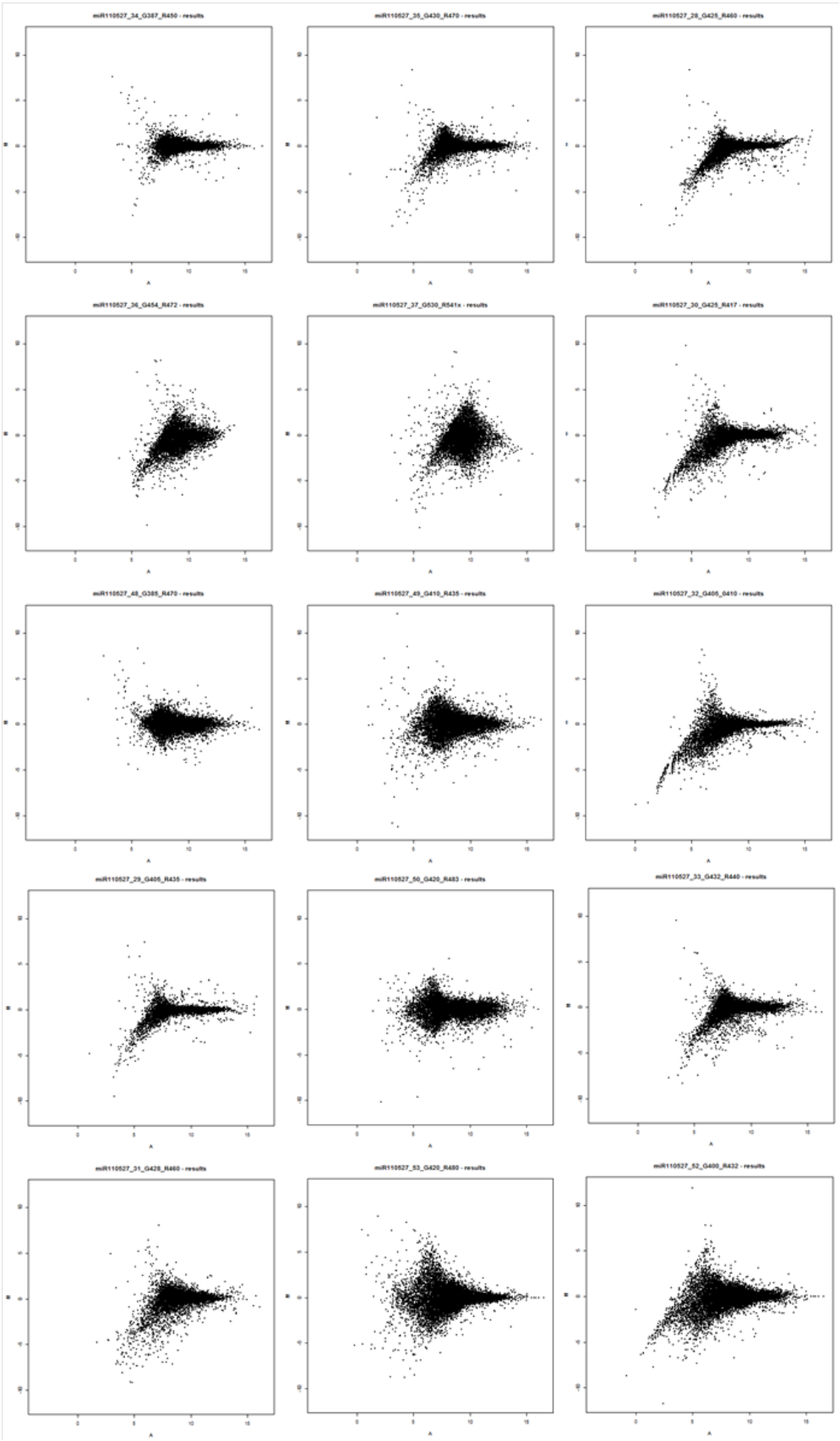

MA plots were produced following inter-normalisation (between array normalisation) of data for each microarray slide containing curcumin and DMSO treated MIA PaCa-2 samples.

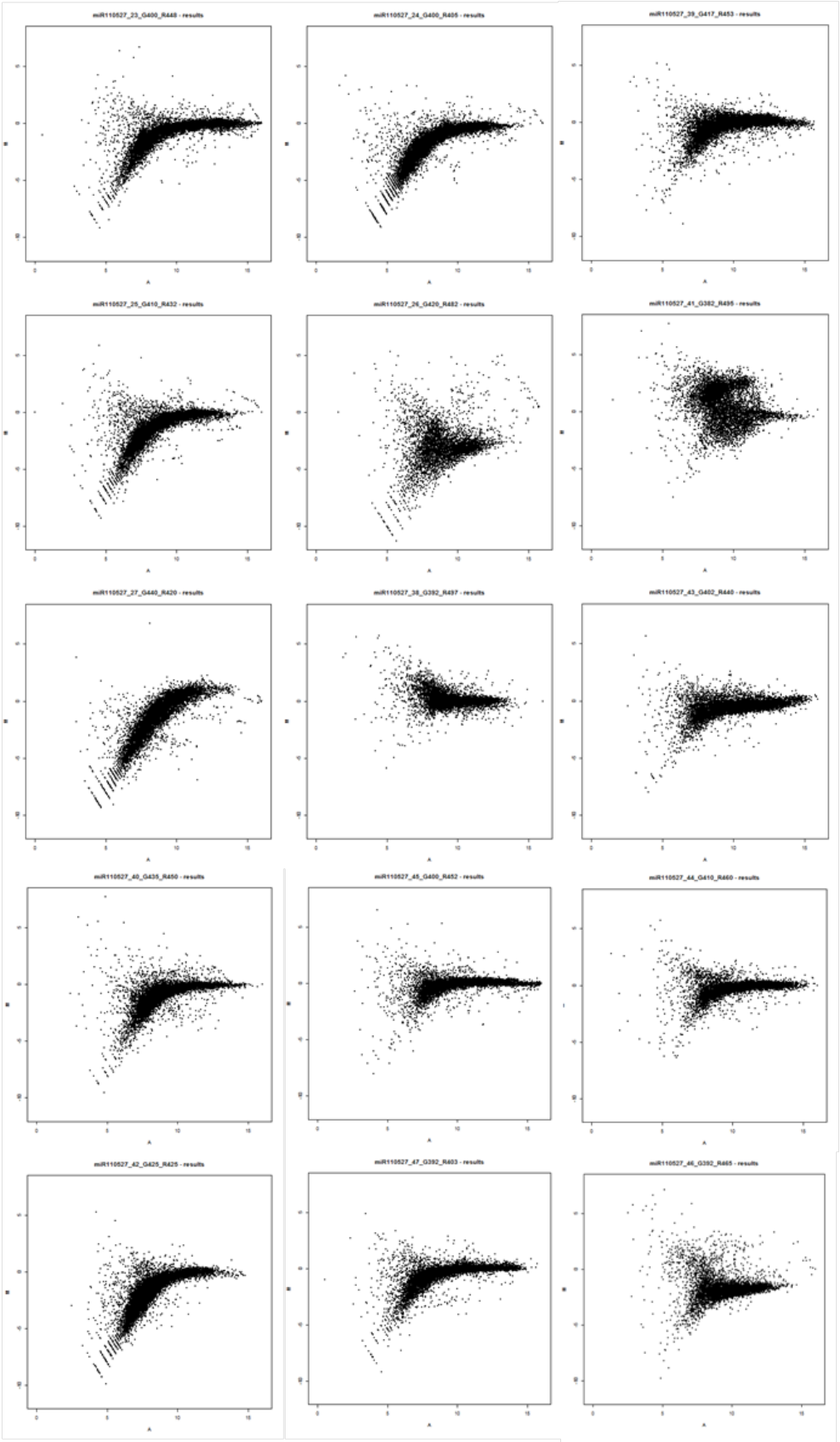

MA plots were produced for the pre-normalised raw data for each microarray slide containing curcumin and DMSO treated AsPC-1 samples.

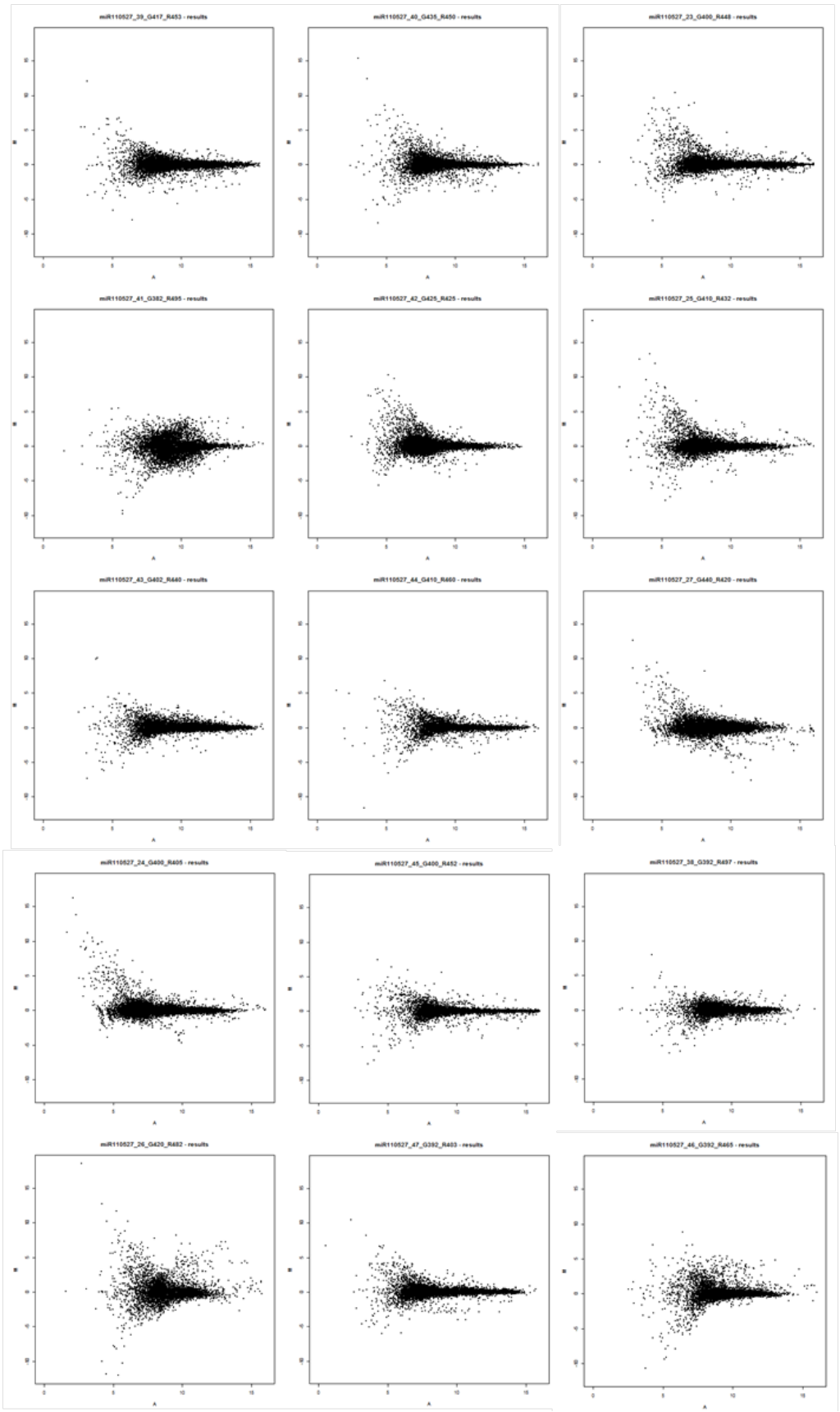

MA plots were produced following intra-normalisation (within array normalisation) of data for each microarray slide containing curcumin and DMSO treated AsPC-1 samples.

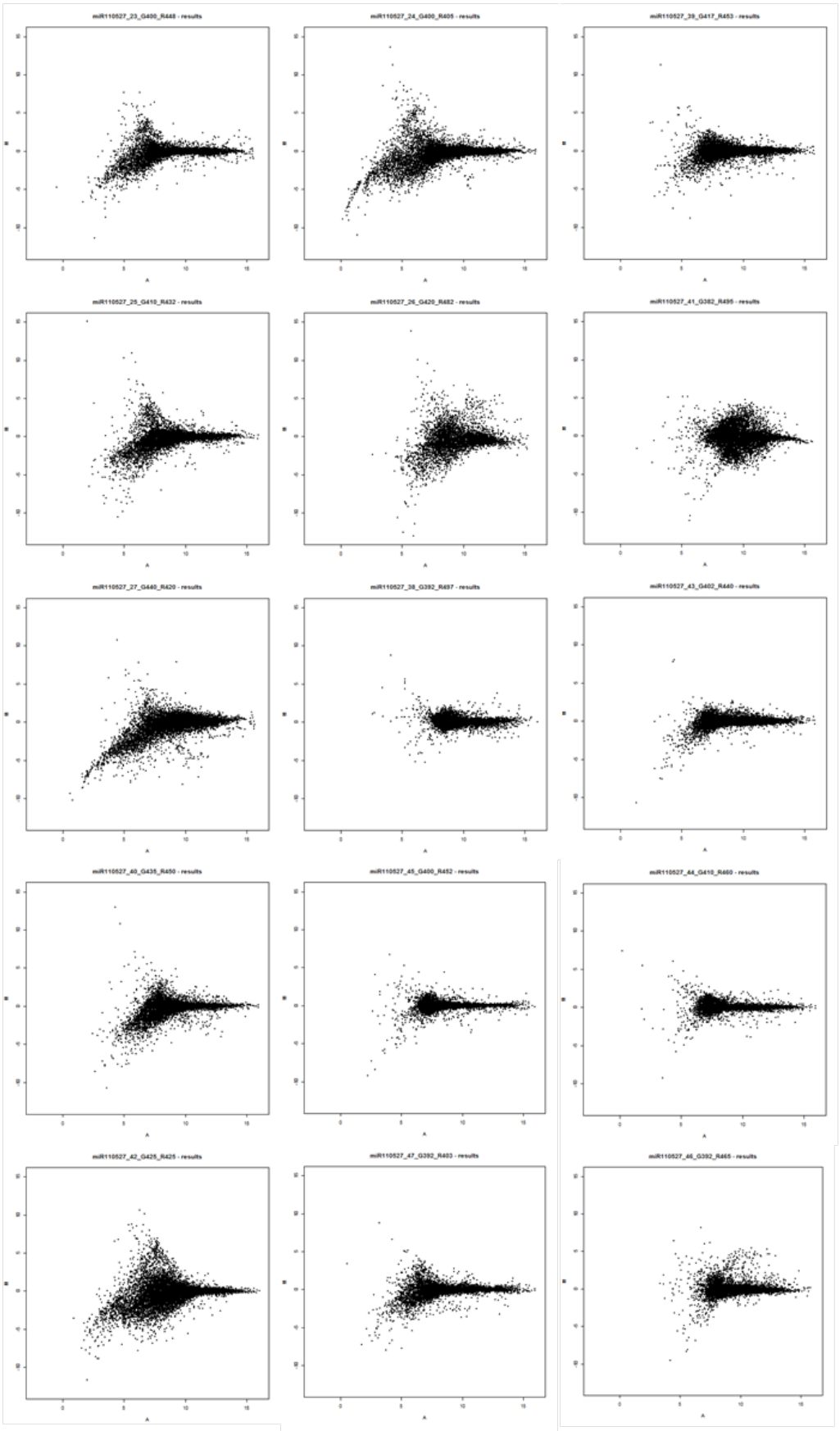

MA plots were produced following inter-normalisation (between array normalisation) of data for each microarray slide containing curcumin and DMSO treated AsPC-1 samples.

Appendix 5: GeneSpring Top Tables

MIA PaCa-2 miRNA Microarray GeneSpring Analysed Top Table

Name	FC	Log FC	p-value (Corr)	p-value
hsa-miR-885-5p	4.591	2.199	0.403	0.348
hsa-miR-328	4.304	2.106	0.403	0.352
hsa-miR-449b-3p	4.268	2.094	0.403	0.352
hsa-let-7d-3p	4.237	2.083	0.403	0.352
hsa-let-7b-3p	4.156	2.055	0.403	0.353
hsa-miR-664a-3p	4.103	2.037	0.403	0.150
hsa-miR-299-5p	4.088	2.031	0.403	0.354
hsa-miR-574-3p	4.075	2.027	0.403	0.154
hsa-miR-3940-3p	4.031	2.011	0.403	0.355
hsa-miR-4312	3.942	1.979	0.403	0.357
hsa-miR-204-5p	3.930	1.975	0.403	0.357
hsa-miR-181b-5p	3.925	1.973	0.403	0.111
hsa-miR-595	3.887	1.959	0.403	0.357
hsa-miR-335-3p	3.818	1.933	0.403	0.359
hsa-let-7f-1-3p	3.774	1.916	0.403	0.359
hsa-miR-337-3p	3.771	1.915	0.403	0.359
hsa-miR-34b-3p	3.769	1.914	0.403	0.359
hsa-miR-3613-3p	3.723	1.897	0.403	0.360
hsa-miR-211-5p	3.701	1.888	0.403	0.361
hsa-miR-181d	3.693	1.885	0.403	0.361
hsa-miR-3935	3.691	1.884	0.403	0.361
hsa-miR-483-3p	3.676	1.878	0.403	0.361
hsa-miR-766-3p	3.641	1.864	0.403	0.362
hsa-miR-1227-3p	3.335	1.738	0.403	0.368
hsa-miR-1296	3.302	1.723	0.403	0.369
hsa-miR-937-3p	3.220	1.687	0.403	0.371
hsa-miR-1976	3.211	1.683	0.403	0.371
hsa-miR-631	3.176	1.667	0.403	0.372
hsa-miR-744-3p	3.160	1.660	0.403	0.373
hsa-miR-654-3p	3.130	1.646	0.403	0.374
hsa-miR-605	3.126	1.644	0.403	0.374
hsa-miR-3714	3.099	1.632	0.403	0.374
hsa-miR-1236-3p	3.094	1.629	0.403	0.375
hsa-miR-1539	3.079	1.622	0.403	0.375
hsa-let-7e-3p	3.076	1.621	0.403	0.375
hsa-miR-4323	3.076	1.621	0.403	0.375
hsa-miR-634	3.073	1.620	0.403	0.375
hsa-miR-3646	3.072	1.619	0.403	0.375
hsa-miR-196b-3p	3.064	1.615	0.403	0.375

High	2.199
NC	0
Low	-2.669

hsa-miR-4324	2.859	1.515	0.403	0.382
hsa-miR-150-5p	2.770	1.470	0.403	0.385
hsa-miR-615-3p	2.743	1.456	0.403	0.386
hsa-miR-3685	2.739	1.454	0.403	0.387
hsa-miR-640	2.737	1.453	0.403	0.387
hsa-miR-1226-3p	2.642	1.402	0.403	0.391
hsa-miR-130b-5p	2.610	1.384	0.403	0.392
hsa-miR-7-2-3p	2.564	1.358	0.403	0.394
hsa-miR-19b-1-5p	-2.760	-1.465	0.403	0.281
hsa-miR-15b-3p	-2.795	-1.483	0.403	0.337
hsa-miR-301b	-2.811	-1.491	0.403	0.344
hsa-miR-183-3p	-2.827	-1.499	0.403	0.353
hsa-let-7a-3p	-2.831	-1.501	0.403	0.303
hsa-miR-501-5p	-2.861	-1.517	0.403	0.102
hsa-miR-135a-3p	-2.884	-1.528	0.403	0.103
hsa-miR-431-3p	-2.887	-1.529	0.429	0.426
hsa-miR-892b	-2.935	-1.553	0.403	0.337
hsa-miR-513b	-2.962	-1.567	0.403	0.321
hsa-miR-935	-3.010	-1.590	0.403	0.099
hsa-miR-339-3p	-3.043	-1.606	0.403	0.330
hsa-miR-423-3p	-3.171	-1.665	0.403	0.283
hsa-miR-3907	-3.211	-1.683	0.403	0.367
hsa-miR-874	-3.247	-1.699	0.403	0.312
hsa-miR-221-5p	-3.269	-1.709	0.403	0.355
hsa-miR-497-5p	-3.317	-1.730	0.403	0.330
hsa-miR-1305	-3.337	-1.738	0.411	0.406
hsa-miR-182-5p	-3.376	-1.755	0.403	0.315
hsa-miR-652-3p	-3.378	-1.756	0.403	0.280
hsa-miR-3648	-3.385	-1.759	0.403	0.119
hsa-miR-642b-3p	-3.405	-1.768	0.403	0.331
hsa-miR-487b	-3.416	-1.772	0.403	0.331
hsa-miR-4261	-3.420	-1.774	0.403	0.349
hsa-miR-4298	-3.429	-1.778	0.403	0.121
hsa-miR-126-5p	-3.435	-1.780	0.403	0.121
hsa-miR-195-5p	-3.438	-1.781	0.403	0.292
hsa-miR-450a-5p	-3.450	-1.787	0.403	0.121
hsa-miR-500a-3p	-3.540	-1.824	0.403	0.305
hsa-miR-501-3p	-3.552	-1.829	0.403	0.284
hsa-miR-125b-5p	-3.569	-1.835	0.403	0.315
hsa-miR-186-5p	-3.571	-1.836	0.403	0.300
hsa-miR-33a-5p	-3.595	-1.846	0.403	0.234
hsa-miR-486-3p	-3.597	-1.847	0.403	0.300
hsa-miR-574-5p	-3.611	-1.852	0.403	0.347

hsa-miR-29b-1-5p	-3.614	-1.854	0.403	0.305
hsa-miR-183-5p	-3.724	-1.897	0.403	0.337
hsa-miR-32-5p	-3.782	-1.919	0.403	0.291
hsa-miR-362-3p	-3.844	-1.943	0.403	0.337
hsa-miR-148b-3p	-4.019	-2.007	0.403	0.332
hsa-miR-1973	-4.030	-2.011	0.403	0.270
hsa-miR-638	-4.033	-2.012	0.403	0.303
hsa-miR-212-3p	-4.087	-2.031	0.403	0.289
hsa-miR-423-5p	-4.122	-2.043	0.403	0.333
hsa-miR-98-5p	-4.136	-2.048	0.403	0.357
hsa-miR-762	-4.152	-2.054	0.403	0.270
hsa-miR-455-3p	-4.263	-2.092	0.403	0.271
hsa-miR-532-3p	-4.304	-2.106	0.403	0.285
hsa-miR-4306	-4.361	-2.125	0.403	0.300
hsa-miR-744-5p	-4.449	-2.153	0.403	0.276
hsa-miR-28-5p	-4.505	-2.172	0.403	0.254
hsa-miR-101-3p	-4.576	-2.194	0.403	0.264
hsa-miR-584-5p	-4.582	-2.196	0.403	0.289
hsa-miR-1207-5p	-4.593	-2.199	0.403	0.266
hsa-miR-30e-3p	-4.599	-2.201	0.403	0.272
hsa-miR-362-5p	-4.620	-2.208	0.403	0.271
hsa-miR-128	-4.724	-2.240	0.403	0.336
hsa-miR-1290	-4.750	-2.248	0.403	0.291
hsa-miR-3665	-4.764	-2.252	0.403	0.284
hsa-miR-1915-3p	-4.772	-2.254	0.403	0.271
hsa-miR-210	-4.850	-2.278	0.403	0.272
hsa-miR-185-5p	-4.857	-2.280	0.403	0.294
hsa-miR-135b-5p	-4.860	-2.281	0.403	0.296
hsa-miR-4291	-4.898	-2.292	0.403	0.266
hsa-miR-424-5p	-4.910	-2.296	0.403	0.271
hsa-miR-940	-4.948	-2.307	0.403	0.210
hsa-miR-532-5p	-4.973	-2.314	0.403	0.278
hsa-miR-140-3p	-4.978	-2.315	0.403	0.275
hsa-miR-3132	-5.085	-2.346	0.403	0.301
hsa-miR-1225-5p	-5.106	-2.352	0.403	0.264
hsa-miR-23b-3p	-5.132	-2.360	0.403	0.272
hsa-miR-126-3p	-5.140	-2.362	0.403	0.297
hsa-miR-1275	-5.167	-2.369	0.403	0.286
hsa-miR-3195	-5.207	-2.380	0.403	0.288
hsa-miR-30d-5p	-5.266	-2.397	0.403	0.252
hsa-miR-301a-3p	-5.288	-2.403	0.403	0.280
hsa-miR-140-5p	-5.308	-2.408	0.403	0.266
hsa-miR-151a-3p	-5.368	-2.424	0.403	0.277

hsa-miR-17-3p	-5.371	-2.425	0.403	0.257
hsa-miR-130b-3p	-5.476	-2.453	0.403	0.280
hsa-miR-590-5p	-5.681	-2.506	0.403	0.270
hsa-miR-486-5p	-5.862	-2.551	0.403	0.240
hsa-miR-361-5p	-5.988	-2.582	0.403	0.262
hsa-miR-378_v17.0	-6.056	-2.598	0.403	0.252
hsa-miR-1238-3p	-6.067	-2.601	0.403	0.067
hsa-miR-3196	-6.360	-2.669	0.403	0.262

A table of the top miRNAs demonstrating an average Log2 fold change (Log FC) of > 1 (red) or < -1 (blue) and a corrected p-value of <0.5 (corr p-value) following treatment for 96 hours with 1.5μM curcumin in MIA PaCa-2 cells. The fold change (FC) and p-value prior to correction (p-value) are also given. (Key: NC= no change, High = increased fold change, Low = decreased fold change)

AsPC-1 miRNA Microarray GeneSpring Analysed Top Table.

Name	FC	Log FC	p-value (Corr)	p-value
hsa-miR-328	18.523	4.211	0.408	0.101
hsa-miR-885-5p	18.195	4.186	0.408	0.101
hsa-miR-766-3p	15.899	3.991	0.408	0.101
hsa-let-7d-3p	15.568	3.960	0.408	0.102
hsa-let-7b-3p	15.526	3.957	0.408	0.103
hsa-miR-3940-3p	15.466	3.951	0.408	0.101
hsa-miR-664a-3p	15.403	3.945	0.408	0.101
hsa-miR-449b-3p	13.144	3.716	0.408	0.107
hsa-miR-4323	11.896	3.572	0.408	0.105
hsa-miR-204-5p	9.979	3.319	0.408	0.105
hsa-miR-4313	9.764	3.288	0.408	0.071
hsa-miR-1249	9.537	3.254	0.408	0.075
hsa-miR-615-3p	9.195	3.201	0.408	0.109
hsa-miR-3646	9.162	3.196	0.408	0.104
hsa-miR-296-5p	7.687	2.942	0.408	0.070
hsa-miR-636	6.676	2.739	0.408	0.108
hsa-miR-1825	5.763	2.527	0.408	0.311
hsa-miR-483-3p	4.291	2.101	0.408	0.300
hsa-let-7f-1-3p	4.243	2.085	0.408	0.300
hsa-miR-4312	4.205	2.072	0.408	0.300
hsa-miR-299-5p	4.117	2.042	0.408	0.300
hsa-miR-3714	4.115	2.041	0.408	0.300
hsa-miR-3613-3p	4.110	2.039	0.408	0.300
hsa-miR-211-5p	4.095	2.034	0.408	0.300
hsa-miR-3605-3p	4.032	2.012	0.408	0.300
hsa-miR-3622a-3p	3.978	1.992	0.408	0.300
hsa-miR-3620-3p	3.969	1.989	0.408	0.300
hsa-miR-1307-3p	3.833	1.938	0.449	0.380

High	4.211
NC	0
Low	-4.614

hsa-miR-4324	3.764	1.912	0.434	0.353
hsa-miR-1227-3p	3.752	1.908	0.408	0.301
hsa-miR-595	3.682	1.881	0.408	0.301
hsa-miR-1296	3.638	1.863	0.408	0.301
hsa-miR-485-3p	3.477	1.798	0.408	0.302
hsa-miR-631	3.464	1.793	0.408	0.302
hsa-miR-1976	3.417	1.773	0.408	0.302
hsa-miR-937-3p	3.407	1.768	0.408	0.302
hsa-miR-337-3p	3.395	1.763	0.408	0.302
hsa-miR-1236-3p	3.390	1.761	0.408	0.302
hsa-miR-196b-3p	3.342	1.741	0.408	0.303
hsa-let-7e-3p	3.319	1.731	0.408	0.303
hsa-miR-3622b-3p	3.298	1.721	0.408	0.303
hsa-miR-605	3.297	1.721	0.408	0.303
hsa-miR-1539	3.287	1.717	0.408	0.303
hsa-miR-154-5p	3.277	1.712	0.408	0.303
hsa-miR-3935	3.259	1.704	0.408	0.303
hsa-miR-150-5p	2.990	1.580	0.408	0.304
hsa-miR-1226-3p	2.891	1.531	0.408	0.305
hsa-miR-130b-5p	2.837	1.504	0.408	0.305
hsa-miR-15a-3p	2.811	1.491	0.408	0.164
hsa-miR-541-5p	2.794	1.482	0.408	0.306
hsa-miR-629-3p	2.793	1.482	0.408	0.306
hsa-let-7g-3p	2.767	1.468	0.408	0.306
hsa-miR-1281	2.685	1.425	0.408	0.277
hsa-miR-3679-3p	2.585	1.370	0.408	0.277
hsa-miR-197-3p	2.312	1.209	0.408	0.079
hsa-miR-574-3p	2.072	1.051	0.408	0.155
hsa-miR-100-3p	2.057	1.040	0.478	0.476
hsa-miR-23b-5p	-2.047	-1.033	0.408	0.287
hsa-miR-147b	-2.073	-1.052	0.464	0.446
hsa-miR-135a-3p	-2.095	-1.067	0.408	0.290
hsa-let-7a-3p	-2.106	-1.074	0.464	0.459
hsa-miR-200c-5p	-2.238	-1.162	0.456	0.421
hsa-miR-182-5p	-2.290	-1.195	0.425	0.338
hsa-miR-934	-2.336	-1.224	0.445	0.373
hsa-miR-500a-3p	-2.394	-1.260	0.464	0.458
hsa-miR-4327	-2.419	-1.275	0.408	0.288
hsa-miR-1226-5p	-2.461	-1.300	0.408	0.285
hsa-miR-455-5p	-2.462	-1.300	0.408	0.270
hsa-miR-181c-5p	-2.463	-1.301	0.408	0.270
hsa-miR-1285-3p	-2.473	-1.306	0.464	0.459
hsa-miR-4257	-2.478	-1.309	0.464	0.453

hsa-miR-874	-2.518	-1.332	0.435	0.360
hsa-miR-24-1-5p	-2.519	-1.333	0.408	0.285
hsa-miR-20a-3p	-2.543	-1.347	0.464	0.448
hsa-miR-339-3p	-2.570	-1.362	0.425	0.341
hsa-miR-30b-3p	-2.581	-1.368	0.463	0.439
hsa-miR-140-3p	-2.582	-1.368	0.464	0.459
hsa-miR-32-5p	-2.586	-1.371	0.456	0.409
hsa-miR-301b	-2.603	-1.380	0.456	0.399
hsa-miR-532-3p	-2.616	-1.387	0.421	0.331
hsa-miR-3653	-2.622	-1.390	0.422	0.334
hsa-miR-484	-2.629	-1.395	0.434	0.356
hsa-miR-584-5p	-2.630	-1.395	0.434	0.357
hsa-miR-1972	-2.642	-1.401	0.456	0.423
hsa-miR-718	-2.654	-1.408	0.462	0.436
hsa-miR-132-3p	-2.654	-1.408	0.456	0.415
hsa-miR-421	-2.679	-1.422	0.456	0.423
hsa-miR-622	-2.703	-1.434	0.449	0.380
hsa-miR-361-3p	-2.712	-1.439	0.408	0.285
hsa-miR-193b-5p	-2.716	-1.442	0.440	0.366
hsa-miR-4287	-2.722	-1.444	0.454	0.387
hsa-miR-19b-1-5p	-2.739	-1.453	0.408	0.294
hsa-miR-22-5p	-2.753	-1.461	0.456	0.411
hsa-miR-330-3p	-2.767	-1.468	0.462	0.432
hsa-miR-517a-3p	-2.838	-1.505	0.464	0.450
hsa-miR-186-5p	-2.857	-1.515	0.456	0.412
hsa-miR-34c-5p	-2.903	-1.538	0.456	0.411
hsa-miR-3126-5p	-2.907	-1.539	0.456	0.417
hsa-miR-200a-5p	-2.950	-1.561	0.408	0.310
hsa-miR-423-3p	-2.954	-1.563	0.408	0.258
hsa-miR-625-5p	-2.981	-1.576	0.456	0.411
hsa-miR-4317	-2.983	-1.577	0.408	0.293
hsa-miR-3200-3p	-2.986	-1.578	0.456	0.400
hsa-miR-505-3p	-2.992	-1.581	0.408	0.272
hsa-miR-29b-1-5p	-3.057	-1.612	0.421	0.329
hsa-miR-193a-5p	-3.089	-1.627	0.408	0.295
hsa-miR-4270	-3.089	-1.627	0.456	0.402
hsa-miR-1290	-3.130	-1.646	0.421	0.330
hsa-miR-30c-2-3p	-3.147	-1.654	0.408	0.306
hsa-miR-630	-3.158	-1.659	0.456	0.397
hsa-miR-23a-5p	-3.195	-1.676	0.408	0.255
hsa-miR-140-5p	-3.242	-1.697	0.462	0.434
hsa-miR-513b	-3.300	-1.723	0.408	0.205
hsa-miR-532-5p	-3.354	-1.746	0.408	0.271

hsa-miR-202-3p	-3.369	-1.752	0.408	0.306
hsa-miR-4298	-3.381	-1.757	0.434	0.356
hsa-miR-152	-3.398	-1.765	0.408	0.287
hsa-miR-483-5p	-3.411	-1.770	0.416	0.321
hsa-miR-28-5p	-3.418	-1.773	0.408	0.271
hsa-miR-1183	-3.461	-1.791	0.408	0.313
hsa-miR-335-5p	-3.494	-1.805	0.408	0.268
hsa-miR-218-5p	-3.514	-1.813	0.408	0.299
hsa-miR-642b-3p	-3.518	-1.815	0.408	0.299
hsa-miR-650	-3.524	-1.817	0.408	0.234
hsa-miR-940	-3.527	-1.819	0.408	0.276
hsa-miR-378b	-3.543	-1.825	0.456	0.415
hsa-miR-660-5p	-3.549	-1.827	0.408	0.262
hsa-miR-503-5p	-3.594	-1.846	0.408	0.237
hsa-miR-126-3p	-3.646	-1.866	0.408	0.258
hsa-miR-221-5p	-3.658	-1.871	0.408	0.241
hsa-miR-125a-3p	-3.666	-1.874	0.408	0.274
hsa-miR-3911	-3.754	-1.908	0.408	0.230
hsa-miR-455-3p	-3.983	-1.994	0.408	0.216
hsa-miR-1288	-3.995	-1.998	0.408	0.277
hsa-miR-324-5p	-4.037	-2.013	0.408	0.294
hsa-miR-4306	-4.145	-2.051	0.408	0.267
hsa-miR-205-3p	-4.158	-2.056	0.408	0.263
hsa-miR-101-3p	-4.270	-2.094	0.408	0.225
hsa-miR-892b	-4.273	-2.095	0.408	0.183
hsa-miR-3127-5p	-4.308	-2.107	0.408	0.240
hsa-miR-378_v17.0	-4.314	-2.109	0.408	0.245
hsa-miR-501-5p	-4.315	-2.109	0.408	0.263
hsa-miR-513c-5p	-4.366	-2.126	0.408	0.121
hsa-miR-182-3p	-4.431	-2.148	0.408	0.112
hsa-miR-3679-5p	-4.490	-2.167	0.408	0.199
hsa-miR-93-3p	-4.541	-2.183	0.408	0.068
hsa-miR-545-3p	-4.682	-2.227	0.408	0.067
hsa-miR-30d-3p	-4.730	-2.242	0.408	0.109
hsa-miR-3125	-4.851	-2.278	0.408	0.238
hsa-miR-15b-3p	-4.933	-2.302	0.408	0.065
hsa-miR-1228-3p	-5.312	-2.409	0.408	0.202
hsa-miR-141-5p	-5.478	-2.454	0.408	0.095
hsa-miR-516a-5p	-6.119	-2.613	0.408	0.069
hsa-miR-362-3p	-6.175	-2.626	0.408	0.097
hsa-miR-138-2-3p	-6.384	-2.675	0.408	0.083
hsa-miR-3176	-6.446	-2.688	0.408	0.079
hsa-miR-342-5p	-6.470	-2.694	0.408	0.069

hsa-miR-188-5p	-6.494	-2.699	0.408	0.074
hsa-miR-3648	-6.524	-2.706	0.408	0.111
hsa-miR-652-3p	-6.555	-2.713	0.408	0.114
hsa-miR-219-5p	-6.776	-2.760	0.408	0.069
hsa-miR-362-5p	-6.842	-2.774	0.408	0.104
hsa-miR-1234-3p	-6.900	-2.787	0.408	0.127
hsa-miR-1287	-7.162	-2.840	0.408	0.129
hsa-miR-1224-5p	-7.208	-2.850	0.408	0.111
hsa-miR-454-3p	-7.237	-2.855	0.408	0.084
hsa-miR-519e-5p	-7.350	-2.878	0.408	0.138
hsa-miR-744-5p	-7.353	-2.878	0.408	0.116
hsa-miR-517c-3p	-7.593	-2.925	0.408	0.086
hsa-miR-33a-5p	-7.980	-2.996	0.408	0.089
hsa-miR-572	-8.609	-3.106	0.408	0.108
hsa-miR-3141	-9.242	-3.208	0.408	0.100
hsa-miR-500a-5p	-9.383	-3.230	0.408	0.097
hsa-miR-371a-5p	-9.830	-3.297	0.408	0.093
hsa-miR-663a	-10.424	-3.382	0.408	0.062
hsa-miR-34b-5p	-10.966	-3.455	0.408	0.082
hsa-miR-513a-5p	-11.188	-3.484	0.408	0.050
hsa-miR-3156-5p	-12.517	-3.646	0.408	0.078
hsa-miR-1973	-24.481	-4.614	0.408	0.006

A table of the top miRNAs demonstrating an average Log2 fold change (Log FC) of > 1 (red) or < -1 (blue) and a corrected p-value of <0.5 (corr p-value) following treatment for 96 hours with 1.5μM curcumin in AsPC-1 cells. The fold change (FC) and p-value prior to correction (p-value) are also given. (Key: NC= no change, High = increased fold change, Low = decreased fold change)

BxPC-3 miRNA Microarray GeneSpring Analysed Top Table.

Name	FC	Log FC	p-value (Corr)	p-value
hsa-miR-148b-3p	18.132	4.181	0.463	0.092
hsa-miR-7-1-3p	12.265	3.616	0.463	0.134
hsa-miR-128	11.413	3.513	0.463	0.139
hsa-miR-186-5p	11.349	3.505	0.463	0.135
hsa-miR-101-3p	11.282	3.496	0.463	0.138
hsa-miR-486-5p	10.703	3.420	0.463	0.137
hsa-miR-191-3p	8.845	3.145	0.463	0.073
hsa-miR-148a-3p	7.170	2.842	0.463	0.198
hsa-miR-892b	6.655	2.734	0.463	0.066
hsa-miR-365a-3p	6.518	2.704	0.463	0.219
hsa-miR-374b-5p	4.702	2.233	0.463	0.291
hsa-miR-2276	4.554	2.187	0.463	0.256
hsa-miR-3663-3p	4.304	2.106	0.463	0.255
hsa-miR-211-5p	4.258	2.090	0.463	0.331

High	4.181
NC	0
Low	-4.149

hsa-miR-134	4.255	2.089	0.463	0.255
hsa-miR-203a	4.236	2.083	0.463	0.295
hsa-miR-3911	4.029	2.010	0.463	0.253
hsa-let-7b-3p	3.965	1.987	0.463	0.333
hsa-miR-3610	3.941	1.978	0.463	0.253
hsa-miR-671-5p	3.883	1.957	0.463	0.253
hsa-miR-424-3p	3.865	1.950	0.463	0.253
hsa-miR-3682-3p	3.819	1.933	0.463	0.252
hsa-miR-622	3.801	1.927	0.463	0.252
hsa-miR-3137	3.797	1.925	0.463	0.252
hsa-miR-662	3.745	1.905	0.463	0.252
hsa-miR-3138	3.736	1.902	0.463	0.252
hsa-miR-3692-5p	3.733	1.900	0.463	0.252
hsa-miR-3654	3.715	1.894	0.463	0.252
hsa-miR-98-5p	3.548	1.827	0.463	0.311
hsa-miR-664a-3p	3.500	1.807	0.463	0.338
hsa-miR-449b-3p	3.482	1.800	0.463	0.338
hsa-miR-182-5p	3.451	1.787	0.463	0.305
hsa-miR-765	3.297	1.721	0.463	0.249
hsa-miR-564	3.288	1.717	0.463	0.249
hsa-miR-3176	3.275	1.712	0.463	0.248
hsa-miR-1281	3.229	1.691	0.463	0.248
hsa-miR-516a-5p	3.205	1.680	0.463	0.248
hsa-miR-509-3-5p	3.172	1.666	0.463	0.248
hsa-miR-1238-3p	3.137	1.650	0.463	0.295
hsa-miR-33a-5p	3.099	1.632	0.463	0.300
hsa-miR-615-3p	3.079	1.623	0.463	0.343
hsa-miR-3174	3.079	1.622	0.463	0.247
hsa-miR-718	3.071	1.619	0.463	0.247
hsa-miR-3926	3.064	1.615	0.463	0.247
hsa-miR-192-5p	3.061	1.614	0.463	0.300
hsa-miR-345-5p	3.054	1.611	0.463	0.246
hsa-miR-378b	3.022	1.595	0.463	0.246
hsa-miR-4313	3.008	1.589	0.463	0.246
hsa-miR-921	2.971	1.571	0.463	0.246
hsa-miR-602	2.751	1.460	0.463	0.243
hsa-miR-494	-2.105	-1.074	0.463	0.341
hsa-let-7a-3p	-2.390	-1.257	0.463	0.328
hsa-miR-105-5p	-2.433	-1.282	0.463	0.327
hsa-miR-106b-3p	-2.453	-1.294	0.463	0.326
hsa-miR-200c-5p	-2.461	-1.299	0.463	0.289
hsa-miR-19b-1-5p	-2.504	-1.324	0.463	0.325
hsa-miR-339-3p	-2.601	-1.379	0.463	0.289

hsa-miR-132-5p	-2.892	-1.532	0.463	0.319
hsa-miR-532-5p	-2.894	-1.533	0.463	0.319
hsa-miR-99b-3p	-2.936	-1.554	0.463	0.261
hsa-miR-874	-2.946	-1.559	0.463	0.340
hsa-miR-24-1-5p	-2.957	-1.564	0.463	0.318
hsa-miR-130a-3p	-3.099	-1.632	0.463	0.317
hsa-miR-4317	-3.104	-1.634	0.463	0.287
hsa-miR-3679-5p	-3.495	-1.805	0.463	0.348
hsa-miR-423-5p	-3.553	-1.829	0.463	0.283
hsa-miR-1288	-3.583	-1.841	0.463	0.299
hsa-miR-3188	-3.732	-1.900	0.463	0.264
hsa-miR-1914-3p	-3.827	-1.936	0.463	0.309
hsa-miR-1180	-3.938	-1.977	0.463	0.265
hsa-miR-3663-5p	-3.975	-1.991	0.463	0.265
hsa-miR-575	-4.117	-2.042	0.463	0.302
hsa-miR-595	-4.158	-2.056	0.463	0.266
hsa-miR-155-5p	-4.220	-2.077	0.463	0.232
hsa-miR-3917	-4.301	-2.105	0.463	0.266
hsa-miR-574-5p	-4.383	-2.132	0.463	0.265
hsa-miR-4322	-4.414	-2.142	0.463	0.266
hsa-miR-3132	-4.469	-2.160	0.463	0.271
hsa-miR-1307-3p	-4.477	-2.163	0.463	0.266
hsa-miR-1306-3p	-4.492	-2.167	0.463	0.266
hsa-miR-432-5p	-4.557	-2.188	0.463	0.267
hsa-miR-623	-5.076	-2.344	0.463	0.268
hsa-miR-1207-5p	-5.471	-2.452	0.463	0.246
hsa-miR-642b-3p	-5.653	-2.499	0.463	0.243
hsa-miR-181d	-6.155	-2.622	0.463	0.269
hsa-miR-572	-7.359	-2.879	0.463	0.215
hsa-miR-181a-3p	-8.253	-3.045	0.463	0.098
hsa-miR-221-5p	-8.884	-3.151	0.463	0.098
hsa-miR-152	-9.187	-3.200	0.463	0.097
hsa-miR-652-3p	-9.207	-3.203	0.463	0.097
hsa-miR-513b	-9.289	-3.215	0.463	0.158
hsa-miR-574-3p	-10.865	-3.442	0.463	0.085
hsa-miR-125a-3p	-12.908	-3.690	0.463	0.106
hsa-miR-3656	-14.755	-3.883	0.463	0.143
hsa-miR-1973	-15.163	-3.922	0.463	0.159
hsa-miR-513a-5p	-17.735	-4.149	0.463	0.115

A table of the top miRNAs demonstrating an average Log2 fold change (Log FC) of > 1 (red) or < -1 (blue) and a corrected p-value of <0.5 (corr p-value) following treatment for 96 hours with 1.5µM curcumin in BxPC-3 cells. The fold change (FC) and p-value prior to correction (p-value) are also given. (Key: NC= no change, High = increased fold change, Low = decreased fold change)

Appendix 6: Interclass Correlation Coefficient Analysis of Agilent Microarray Data

Reliability Statistics

Cronbach's Alpha	Cronbach's Alpha Based on Standardized Items	N of Items
.979	.984	4

Case Processing Summary

		N	%
Cases	Valid	188	100.0
	Excluded[a]	0	.0
	Total	188	100.0

Inter-Item Correlation Matrix

	Control_MiaPaCa2_1	Control_MiaPaCa2_2	Control_MiaPaCa2_3	Control_MiaPaCa2_4
Control_MiaPaCa2_1	1.000	.892	.900	.902
Control_MiaPaCa2_2	.892	1.000	.981	.974
Control_MiaPaCa2_3	.900	.981	1.000	.987
Control_MiaPaCa2_4	.902	.974	.987	1.000

Summary Item Statistics

	Mean	Minimum	Maximum	Range	Maximum / Minimum	Variance	N of Items
Item Means	5.297	4.753	5.554	.801	1.169	.135	4
Item Variances	16.872	13.816	22.928	9.112	1.660	16.996	4
Inter-Item Covariances	15.556	14.147	17.016	2.868	1.203	1.281	4
Inter-Item Correlations	.939	.892	.987	.094	1.106	.002	4

Intraclass Correlation Coefficient

	Intraclass Correlation[b]	95% Confidence Interval		F Test with True Value 0			
		Lower Bound	Upper Bound	Value	df1	df2	Sig
Single Measures	.922[a]	.904	.938	48.288	187	561	.000
Average Measures	.979[c]	.974	.984	48.288	187	561	.000

Two-way mixed effects model where people effects are random and measures effects are fixed.

a. The estimator is the same, whether the interaction effect is present or not.

b. Type C intraclass correlation coefficients using a consistency definition. The between-measure variance is excluded from the denominator variance.

c. This estimate is computed assuming the interaction effect is absent, because it is not estimable otherwise.

Interclass correlation coefficient (ICC) analysis was carried out on all MIA PaCa-2 samples using SPSS software.

Reliability Statistics

Cronbach's Alpha	Cronbach's Alpha Based on Standardized Items	N of Items
.996	.996	4

Case Processing Summary

		N	%
Cases	Valid	188	100.0
	Excluded[a]	0	.0
	Total	188	100.0

Inter-Item Correlation Matrix

	Control_AsPC1_1	Control_AsPC1_2	Control_AsPC1_3	Control_AsPC1_4
Control_AsPC1_1	1.000	.971	.974	.988
Control_AsPC1_2	.971	1.000	.990	.987
Control_AsPC1_3	.974	.990	1.000	.990
Control_AsPC1_4	.988	.987	.990	1.000

Summary Item Statistics

	Mean	Minimum	Maximum	Range	Maximum / Minimum	Variance	N of Items
Item Means	5.770	5.739	5.790	.051	1.009	.001	4
Item Variances	10.862	10.668	11.290	.622	1.058	.083	4
Inter-Item Covariances	10.678	10.579	10.899	.320	1.030	.013	4
Inter-Item Correlations	.983	.971	.990	.019	1.020	.000	4

Intraclass Correlation Coefficient

	Intraclass Correlation[b]	95% Confidence Interval		F Test with True Value 0			
		Lower Bound	Upper Bound	Value	df1	df2	Sig
Single Measures	.983[a]	.979	.987	233.292	187	561	.000
Average Measures	.996[c]	.995	.997	233.292	187	561	.000

Two-way mixed effects model where people effects are random and measures effects are fixed.

a. The estimator is the same, whether the interaction effect is present or not.

b. Type C intraclass correlation coefficients using a consistency definition. The between-measure variance is excluded from the denominator variance.

c. This estimate is computed assuming the interaction effect is absent, because it is not estimable otherwise.

Interclass correlation coefficient (ICC) analysis was carried out on all AsPC-1 samples using SPSS software.

Reliability Statistics

Cronbach's Alpha	Cronbach's Alpha Based on Standardized Items	N of Items
.951	.959	4

Case Processing Summary

		N	%
Cases	Valid	188	100.0
	Excluded[a]	0	.0
	Total	188	100.0

Inter-Item Correlation Matrix

	Control_BxPC3_1	Control_BxPC3_2	Control_BxPC3_3	Control_BxPC3_4
Control_BxPC3_1	1.000	.878	.912	.851
Control_BxPC3_2	.878	1.000	.809	.899
Control_BxPC3_3	.912	.809	1.000	.776
Control_BxPC3_4	.851	.899	.776	1.000

Summary Item Statistics

	Mean	Minimum	Maximum	Range	Maximum / Minimum	Variance	N of Items
Item Means	5.071	4.367	5.660	1.293	1.296	.433	4
Item Variances	18.366	13.021	25.820	12.799	1.983	40.065	4
Inter-Item Covariances	15.219	11.951	21.136	9.185	1.769	9.093	4
Inter-Item Correlations	.854	.776	.912	.135	1.174	.003	4

Intraclass Correlation Coefficient

	Intraclass Correlation[b]	95% Confidence Interval		F Test with True Value 0			
		Lower Bound	Upper Bound	Value	df1	df2	Sig
Single Measures	.829[a]	.792	.862	20.341	187	561	.000
Average Measures	.951[c]	.938	.961	20.341	187	561	.000

Two-way mixed effects model where people effects are random and measures effects are fixed.

a. The estimator is the same, whether the interaction effect is present or not.

b. Type C intraclass correlation coefficients using a consistency definition. The between-measure variance is excluded from the denominator variance.

c. This estimate is computed assuming the interaction effect is absent, because it is not estimable otherwise.

Interclass correlation coefficient (ICC) analysis was carried out on all BxPC-3 samples using SPSS software.

Appendix 7: Partek Top Tables

MIA PaCa-2 miRNA Microarray Partek Analysed Top Table.

Name	p-value	Log2 Ratio
hsa-miR-885-5p	0.306	2.835
hsa-miR-328	0.323	2.731
hsa-miR-449b-3p	0.242	2.722
hsa-let-7d-3p	0.312	2.683
hsa-let-7b-3p	0.271	2.651
hsa-miR-574-3p	0.143	2.613
hsa-miR-299-5p	0.184	2.599
hsa-miR-3940-3p	0.202	2.577
hsa-miR-4312	0.191	2.545
hsa-miR-204-5p	0.282	2.534
hsa-miR-595	0.221	2.507
hsa-miR-181b-5p	0.020	2.505
hsa-miR-335-3p	0.129	2.478
hsa-let-7f-1-3p	0.201	2.426
hsa-miR-337-3p	0.149	2.418
hsa-miR-34b-3p	0.100	2.411
hsa-miR-3613-3p	0.195	2.403
hsa-miR-211-5p	0.281	2.381
hsa-miR-181d	0.263	2.373
hsa-miR-3935	0.133	2.366
hsa-miR-483-3p	0.210	2.354
hsa-miR-766-3p	0.353	2.342
hsa-miR-664-3p	0.266	2.314
hsa-miR-1227	0.180	2.266
hsa-miR-1296	0.173	2.240
hsa-miR-937	0.159	2.201
hsa-miR-1976	0.160	2.194
hsa-miR-631	0.164	2.177
hsa-miR-744-3p	0.100	2.169
hsa-miR-654-3p	0.100	2.154
hsa-miR-605	0.141	2.147
hsa-miR-3714	0.217	2.139
hsa-miR-1236	0.161	2.127
hsa-miR-1539	0.142	2.117
hsa-let-7e-3p	0.149	2.111
hsa-miR-4323	0.214	2.103
hsa-miR-634	0.100	2.097
hsa-miR-3646	0.329	2.090
hsa-miR-196b-3p	0.152	2.069

High	2.835
NC	0
Low	-2.726

hsa-miR-4324	0.146	2.043
hsa-miR-150-5p	0.139	2.032
hsa-miR-615-3p	0.273	2.019
hsa-miR-3685	0.100	2.012
hsa-miR-640	0.100	2.006
hsa-miR-1226-3p	0.140	1.974
hsa-miR-130b-5p	0.140	1.964
hsa-miR-7-2-3p	0.100	1.953
hsa-miR-629-3p	0.218	1.620
hsa-miR-4317	0.438	1.021
hsa-miR-892b	0.465	-1.006
hsa-miR-15b-3p	0.143	-1.251
hsa-miR-183-3p	0.100	-1.511
hsa-miR-3907	0.362	-1.552
hsa-let-7a-3p	0.127	-1.555
hsa-miR-339-3p	0.192	-1.579
hsa-miR-19b-1-5p	0.153	-1.594
hsa-miR-431-3p	0.196	-1.608
hsa-miR-652-3p	0.201	-1.691
hsa-miR-221-5p	0.302	-1.701
hsa-miR-874	0.262	-1.726
hsa-miR-182-5p	0.250	-1.748
hsa-miR-1305	0.189	-1.777
hsa-miR-487b	0.304	-1.778
hsa-miR-423-3p	0.113	-1.785
hsa-miR-4261	0.343	-1.821
hsa-miR-29b-1-5p	0.325	-1.839
hsa-miR-186-5p	0.312	-1.840
hsa-miR-195-5p	0.050	-1.857
hsa-miR-1238	0.132	-1.884
hsa-miR-500a-3p	0.088	-1.901
hsa-miR-486-3p	0.209	-1.919
hsa-miR-642b-3p	0.342	-1.931
hsa-miR-32-5p	0.233	-1.931
hsa-miR-362-3p	0.148	-1.952
hsa-miR-501-3p	0.042	-1.954
hsa-miR-574-5p	0.270	-1.960
hsa-miR-148b-3p	0.314	-1.983
hsa-miR-98	0.286	-1.984
hsa-miR-638	0.130	-1.990
hsa-miR-183-5p	0.155	-1.999
hsa-miR-212-3p	0.109	-2.004
hsa-miR-1973	0.346	-2.023

hsa-miR-33a-5p	0.148	-2.042
hsa-miR-423-5p	0.238	-2.050
hsa-miR-532-3p	0.140	-2.057
hsa-miR-455-3p	0.154	-2.096
hsa-miR-4306	0.368	-2.098
hsa-miR-744-5p	0.310	-2.098
hsa-miR-30e-3p	0.260	-2.151
hsa-miR-101-3p	0.298	-2.161
hsa-miR-1290	0.195	-2.162
hsa-miR-584-5p	0.243	-2.163
hsa-miR-362-5p	0.125	-2.170
hsa-miR-1207-5p	0.245	-2.195
hsa-miR-1915-3p	0.111	-2.208
hsa-miR-762	0.114	-2.210
hsa-miR-128	0.291	-2.212
hsa-miR-210	0.295	-2.221
hsa-miR-28-5p	0.240	-2.244
hsa-miR-185-5p	0.145	-2.248
hsa-miR-3665	0.107	-2.251
hsa-miR-424-5p	0.100	-2.259
hsa-miR-135b-5p	0.131	-2.261
hsa-miR-4291	0.094	-2.272
hsa-miR-1225-5p	0.122	-2.310
hsa-miR-532-5p	0.186	-2.323
hsa-miR-23b-3p	0.096	-2.331
hsa-miR-140-3p	0.194	-2.333
hsa-miR-3132	0.231	-2.333
hsa-miR-126-3p	0.292	-2.345
hsa-miR-1275	0.115	-2.347
hsa-miR-3195	0.126	-2.353
hsa-miR-151a-3p	0.129	-2.357
hsa-miR-140-5p	0.157	-2.377
hsa-miR-301a-3p	0.141	-2.385
hsa-miR-17-3p	0.109	-2.390
hsa-miR-30d-5p	0.078	-2.398
hsa-miR-130b-3p	0.226	-2.418
hsa-miR-590-5p	0.139	-2.421
hsa-miR-361-5p	0.102	-2.500
hsa-miR-486-5p	0.179	-2.560
hsa-miR-378_v17.0	0.151	-2.594
hsa-miR-3196	0.094	-2.621
hsa-miR-940	0.067	-2.727

A table of the top miRNAs demonstrating an average Log2 fold change (Log2 Ratio) of > 1 (red) or < -1 (blue) and a p-value of <0.5 (p-value) following treatment for 96 hours with 1.5µM curcumin in MIA PaCa-2 cells. (Key: NC= no change, High = increased fold change, Low = decreased fold change)

AsPC-1 miRNA Microarray Partek Analysed Top Table.

Name	p-value	Log2 Ratio
hsa-miR-328	0.149	4.053
hsa-miR-885-5p	0.156	3.985
hsa-miR-766-3p	0.144	3.752
hsa-let-7b-3p	0.132	3.690
hsa-let-7d-3p	0.170	3.682
hsa-miR-3940-3p	0.078	3.637
hsa-miR-664-3p	0.090	3.612
hsa-miR-1825	0.016	3.215
hsa-miR-449b-3p	0.173	3.188
hsa-miR-4323	0.084	2.984
hsa-miR-204-5p	0.299	2.448
hsa-miR-615-3p	0.223	2.255
hsa-miR-574-3p	0.231	2.112
hsa-miR-1307-3p	0.225	2.107
hsa-miR-483-3p	0.268	2.069
hsa-miR-3646	0.335	2.064
hsa-let-7f-1-3p	0.281	2.032
hsa-miR-4312	0.297	2.012
hsa-miR-197-3p	0.352	1.973
hsa-miR-4313	0.021	1.967
hsa-miR-299-5p	0.310	1.964
hsa-miR-3714	0.258	1.953
hsa-miR-3613-3p	0.290	1.949
hsa-miR-211-5p	0.396	1.864
hsa-miR-3605-3p	0.100	1.845
hsa-miR-3622a-3p	0.100	1.823
hsa-miR-3620	0.100	1.805
hsa-miR-1249	0.037	1.739
hsa-miR-1227	0.319	1.665
hsa-miR-4324	0.253	1.589
hsa-miR-595	0.435	1.578
hsa-miR-1296	0.334	1.566
hsa-miR-3656	0.410	1.564
hsa-miR-636	0.012	1.543
hsa-miR-485-3p	0.100	1.442
hsa-miR-631	0.356	1.422

High	4.053
NC	0
Low	-3.309

hsa-miR-15a-3p	0.097	1.402
hsa-miR-1976	0.368	1.381
hsa-miR-937	0.372	1.370
hsa-miR-337-3p	0.406	1.364
hsa-miR-1236	0.365	1.352
hsa-miR-196b-3p	0.393	1.212
hsa-let-7e-3p	0.407	1.188
hsa-miR-335-3p	0.468	1.155
hsa-miR-3622b-3p	0.100	1.116
hsa-miR-605	0.437	1.109
hsa-miR-1539	0.434	1.103
hsa-miR-154-5p	0.100	1.087
hsa-miR-3935	0.480	1.083
hsa-miR-296-5p	0.014	1.023
hsa-miR-150-5p	0.449	1.015
hsa-miR-1226-3p	0.442	1.004
hsa-miR-200a-5p	0.455	-1.014
hsa-miR-630	0.494	-1.064
hsa-miR-590-5p	0.476	-1.139
hsa-miR-140-5p	0.478	-1.167
hsa-miR-4317	0.372	-1.177
hsa-miR-517a-3p	0.020	-1.234
hsa-miR-193a-5p	0.309	-1.271
hsa-miR-30c-2-3p	0.413	-1.272
hsa-miR-1290	0.432	-1.293
hsa-miR-513b	0.459	-1.320
hsa-miR-362-5p	0.320	-1.379
hsa-miR-4298	0.432	-1.399
hsa-miR-335-5p	0.357	-1.403
hsa-miR-23a-5p	0.049	-1.428
hsa-miR-1287	0.106	-1.448
hsa-miR-1234	0.466	-1.468
hsa-miR-454-3p	0.162	-1.469
hsa-miR-152	0.410	-1.470
hsa-miR-483-5p	0.372	-1.529
hsa-miR-501-5p	0.023	-1.548
hsa-miR-202-3p	0.123	-1.573
hsa-miR-218-5p	0.106	-1.575
hsa-miR-28-5p	0.404	-1.577
hsa-miR-940	0.273	-1.582
hsa-miR-519e-5p	0.145	-1.586
hsa-miR-660-5p	0.309	-1.595
hsa-miR-378b	0.137	-1.596

hsa-miR-532-5p	0.351	-1.621
hsa-miR-1183	0.099	-1.674
hsa-miR-126-3p	0.443	-1.693
hsa-miR-125a-3p	0.399	-1.708
hsa-miR-642b-3p	0.399	-1.711
hsa-miR-650	0.026	-1.760
hsa-miR-221-5p	0.286	-1.762
hsa-miR-33a-5p	0.202	-1.787
hsa-miR-3911	0.298	-1.826
hsa-miR-517c-3p	0.008	-1.846
hsa-miR-1288	0.367	-1.877
hsa-miR-455-3p	0.194	-1.900
hsa-miR-324-5p	0.138	-1.922
hsa-miR-4306	0.382	-2.034
hsa-miR-503	0.192	-2.105
hsa-miR-101-3p	0.306	-2.123
hsa-miR-205-3p	0.058	-2.148
hsa-miR-378_v17.0	0.226	-2.168
hsa-miR-572	0.157	-2.211
hsa-miR-3127-5p	0.303	-2.220
hsa-miR-892b	0.111	-2.259
hsa-miR-3679-5p	0.294	-2.261
hsa-miR-3125	0.369	-2.285
hsa-miR-500a-5p	0.049	-2.432
hsa-miR-3141	0.176	-2.529
hsa-miR-371a-5p	0.237	-2.605
hsa-miR-1973	0.203	-2.758
hsa-miR-34b-5p	0.005	-2.938
hsa-miR-663a	0.112	-2.947
hsa-miR-513a-5p	0.150	-3.192
hsa-miR-3156-5p	0.135	-3.309

A table of the top miRNAs demonstrating an average Log2 fold change (Log2 Ratio) of > 1 (red) or < -1 (blue) and a p-value of <0.5 (p-value) following treatment for 96 hours with 1.5µM curcumin in AsPC-1 cells. (Key: NC= no change, High = increased fold change, Low = decreased fold change)

BxPC-3 miRNA Microarray Partek Analysed Top Table.

Name	p-value	Log2 Ratio
hsa-miR-148b-3p	0.089	3.446
hsa-miR-7-1-3p	0.143	2.862
hsa-miR-128	0.177	2.857
hsa-miR-186-5p	0.135	2.767
hsa-miR-148a-3p	0.162	2.762
hsa-miR-101-3p	0.189	2.751

High	3.445
NC	0
Low	-3.978

hsa-miR-486-5p	0.156	2.710
hsa-miR-365a-3p	0.074	2.390
hsa-miR-374b-5p	0.095	2.211
hsa-miR-191-3p	0.019	2.178
hsa-miR-211-5p	0.329	2.147
hsa-let-7b-3p	0.383	2.090
hsa-miR-892b	0.148	2.033
hsa-miR-2276	0.100	1.981
hsa-miR-664-3p	0.368	1.859
hsa-miR-449b-3p	0.423	1.845
hsa-miR-3663-3p	0.100	1.823
hsa-miR-203	0.168	1.813
hsa-miR-615-3p	0.324	1.810
hsa-miR-134	0.100	1.795
hsa-miR-98	0.390	1.587
hsa-miR-3911	0.374	1.552
hsa-miR-182-5p	0.308	1.543
hsa-miR-3127-5p	0.475	1.530
hsa-miR-1234	0.449	1.528
hsa-miR-3610	0.100	1.468
hsa-miR-671-5p	0.100	1.448
hsa-miR-1238	0.241	1.448
hsa-miR-424-3p	0.100	1.435
hsa-miR-33a-5p	0.302	1.435
hsa-miR-3682-3p	0.100	1.428
hsa-miR-622	0.124	1.422
hsa-miR-3137	0.100	1.415
hsa-miR-192-5p	0.369	1.407
hsa-miR-662	0.100	1.381
hsa-miR-3138	0.100	1.364
hsa-miR-3692-5p	0.100	1.358
hsa-miR-3654	0.100	1.352
hsa-miR-224-5p	0.437	1.238
hsa-miR-30c-5p	0.027	1.216
hsa-miR-146a-5p	0.420	1.161
hsa-miR-765	0.100	1.097
hsa-miR-564	0.100	1.083
hsa-miR-3176	0.128	1.076
hsa-miR-1281	0.281	1.072
hsa-miR-516a-5p	0.114	1.010
hsa-let-7a-3p	0.285	-1.072
hsa-miR-105-5p	0.100	-1.083
hsa-miR-106b-3p	0.266	-1.092

hsa-miR-19b-1-5p	0.313	-1.109
hsa-miR-1273e	0.480	-1.136
hsa-miR-99b-3p	0.100	-1.188
hsa-miR-22-5p	0.496	-1.193
hsa-miR-874	0.419	-1.234
hsa-miR-28-5p	0.505	-1.257
hsa-miR-99a-5p	0.318	-1.311
hsa-miR-503	0.398	-1.344
hsa-miR-494	0.157	-1.344
hsa-miR-30a-3p	0.298	-1.349
hsa-miR-132-5p	0.100	-1.358
hsa-miR-4317	0.305	-1.358
hsa-miR-532-5p	0.431	-1.364
hsa-miR-660-5p	0.381	-1.368
hsa-miR-24-1-5p	0.107	-1.411
hsa-miR-3188	0.100	-1.453
hsa-miR-130a-3p	0.102	-1.453
hsa-miR-1228-3p	0.502	-1.527
hsa-miR-1180	0.100	-1.578
hsa-miR-3663-5p	0.100	-1.665
hsa-miR-3659	0.269	-1.684
hsa-miR-595	0.397	-1.716
hsa-miR-630	0.256	-1.785
hsa-miR-1288	0.386	-1.800
hsa-miR-3679-5p	0.395	-1.824
hsa-miR-3917	0.100	-1.845
hsa-miR-1914-3p	0.373	-1.898
hsa-miR-4322	0.100	-1.953
hsa-miR-423-5p	0.255	-1.975
hsa-miR-1307-3p	0.249	-1.999
hsa-miR-575	0.350	-2.014
hsa-miR-1306-3p	0.100	-2.019
hsa-miR-432-5p	0.100	-2.053
hsa-miR-1224-5p	0.392	-2.054
hsa-miR-3132	0.259	-2.196
hsa-miR-623	0.100	-2.201
hsa-miR-574-5p	0.217	-2.203
hsa-miR-181a-3p	0.008	-2.223
hsa-miR-1181	0.288	-2.345
hsa-miR-572	0.127	-2.394
hsa-miR-181d	0.240	-2.501
hsa-miR-1207-5p	0.184	-2.522
hsa-miR-642b-3p	0.210	-2.570

hsa-miR-155-5p	0.025	-2.603
hsa-miR-221-5p	0.120	-2.610
hsa-miR-513b	0.139	-2.699
hsa-miR-574-3p	0.121	-2.771
hsa-miR-152	0.128	-2.785
hsa-miR-652-3p	0.041	-2.798
hsa-miR-125a-3p	0.099	-3.438
hsa-miR-1973	0.094	-3.689
hsa-miR-3656	0.060	-3.717
hsa-miR-513a-5p	0.077	-3.978

A table of the top miRNAs demonstrating an average Log2 fold change (Log2 Ratio) of > 1 (red) or < -1 (blue) and a p-value of <0.5 (p-value) following treatment for 96 hours with 1.5μM curcumin in BxPC-3 cells. (Key: NC= no change, High = increased fold change, Low = decreased fold change)

Appendix 8: Ingenuity Pathway Analysis

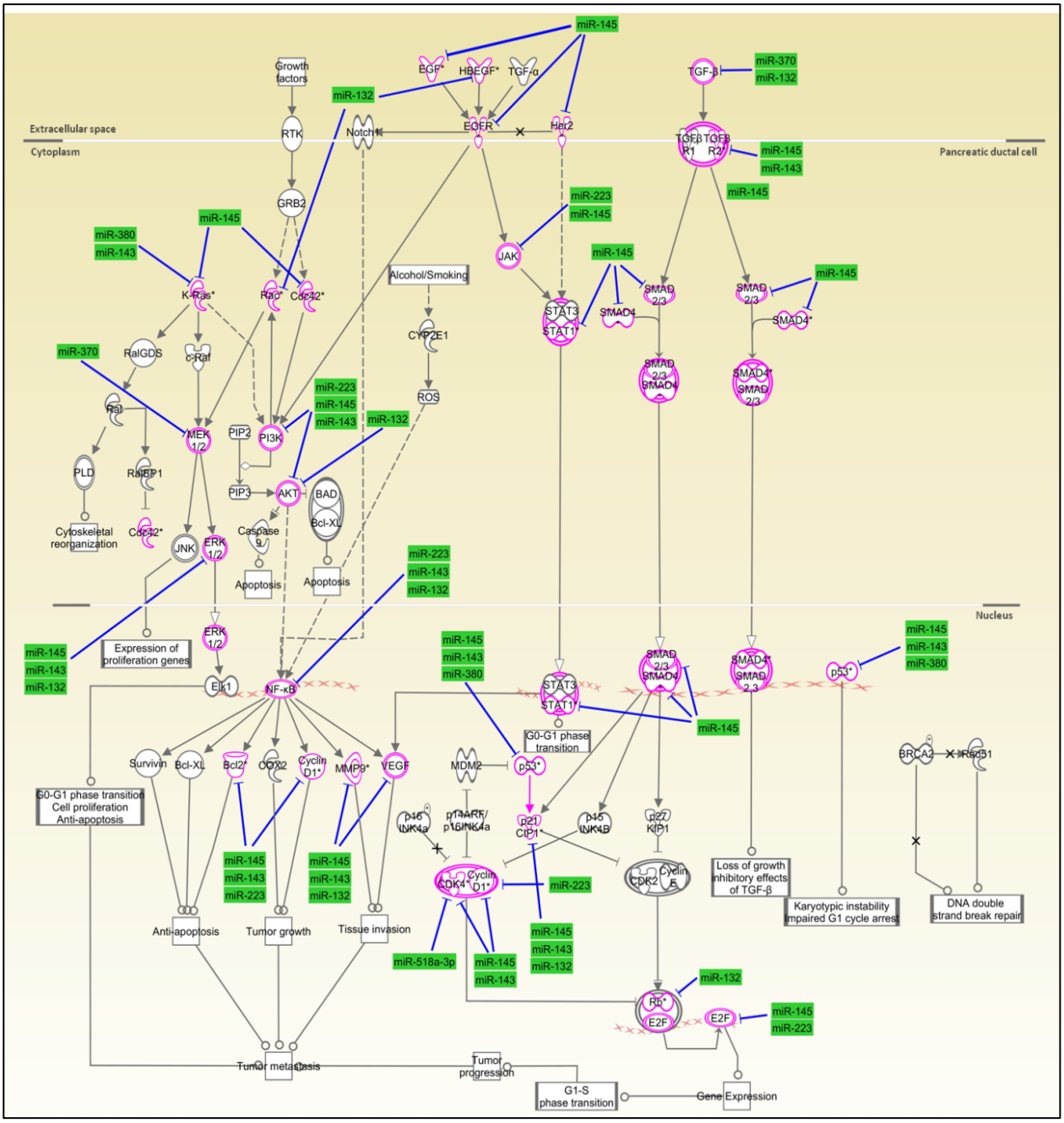

An enlarged image of Figure 3.9.

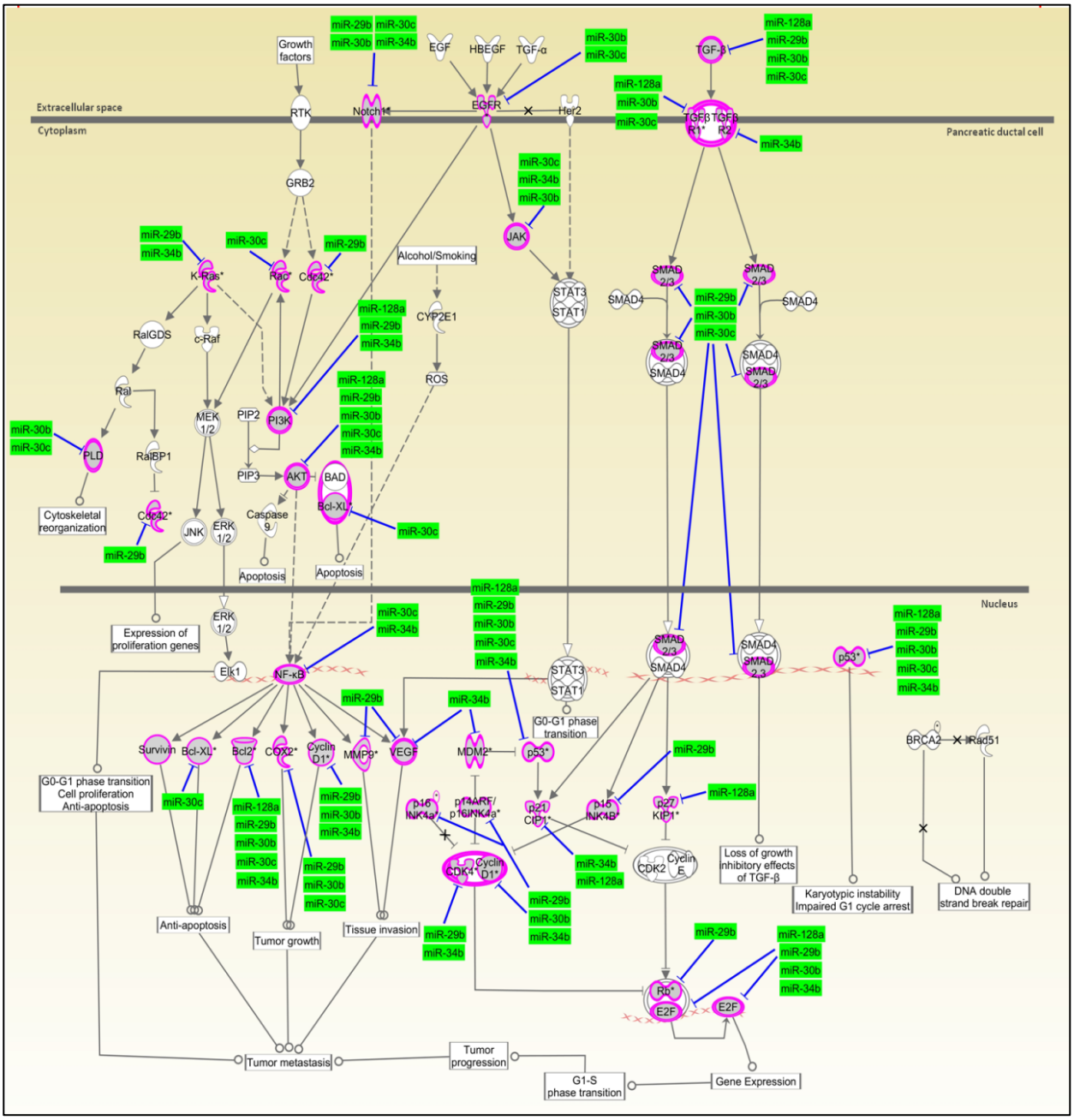

An enlarged image of Figure 5.3.

Appendix 9: Comparison of GeneSpring and Partek Top Tables

MIA PaCa-2 miRNA Microarray GeneSpring and Partek Comparison Table.

Name	Log FC		p-value	
	GeneSpring	Partek	GeneSpring	Partek
hsa-let-7a-3p	-1.501	-1.555	0.303	0.127
hsa-let-7b-3p	2.055	2.651	0.353	0.271
hsa-let-7d-3p	2.083	2.683	0.352	0.312
hsa-let-7e-3p	1.621	2.111	0.375	0.149
hsa-let-7f-1-3p	1.916	2.426	0.359	0.201
hsa-miR-101-3p	-2.194	-2.161	0.264	0.298
hsa-miR-1207-5p	-2.199	-2.195	0.266	0.245
hsa-miR-1225-5p	-2.352	-2.31	0.264	0.122
hsa-miR-1226-3p	1.402	1.974	0.391	0.14
hsa-miR-126-3p	-2.362	-2.345	0.297	0.292
hsa-miR-1275	-2.369	-2.347	0.286	0.115
hsa-miR-128	-2.24	-2.212	0.336	0.291
hsa-miR-1290	-2.248	-2.162	0.291	0.195
hsa-miR-1296	1.723	2.24	0.369	0.173
hsa-miR-1305	-1.738	-1.777	0.406	0.189
hsa-miR-130b-3p	-2.453	-2.418	0.28	0.226
hsa-miR-130b-5p	1.384	1.964	0.392	0.14
hsa-miR-135b-5p	-2.281	-2.261	0.296	0.131
hsa-miR-140-3p	-2.315	-2.333	0.275	0.194
hsa-miR-140-5p	-2.408	-2.377	0.266	0.157
hsa-miR-148b-3p	-2.007	-1.983	0.332	0.314
hsa-miR-150-5p	1.47	2.032	0.385	0.139
hsa-miR-151a-3p	-2.424	-2.357	0.277	0.129
hsa-miR-1539	1.622	2.117	0.375	0.142
hsa-miR-15b-3p	-1.483	-1.251	0.337	0.143
hsa-miR-17-3p	-2.425	-2.39	0.257	0.109
hsa-miR-181b-5p	1.973	2.505	0.111	0.02
hsa-miR-181d	1.885	2.373	0.361	0.263
hsa-miR-182-5p	-1.755	-1.748	0.315	0.25
hsa-miR-183-3p	-1.499	-1.511	0.353	0.1
hsa-miR-183-5p	-1.897	-1.999	0.337	0.155
hsa-miR-185-5p	-2.28	-2.248	0.294	0.145
hsa-miR-186-5p	-1.836	-1.84	0.3	0.312
hsa-miR-1915-3p	-2.254	-2.208	0.271	0.111
hsa-miR-195-5p	-1.781	-1.857	0.292	0.05
hsa-miR-196b-3p	1.615	2.069	0.375	0.152
hsa-miR-1973	-2.011	-2.023	0.27	0.346
hsa-miR-1976	1.683	2.194	0.371	0.16
hsa-miR-19b-1-5p	-1.465	-1.594	0.281	0.153

hsa-miR-204-5p	1.975	2.534	0.357	0.282
hsa-miR-210	-2.278	-2.221	0.272	0.295
hsa-miR-211-5p	1.888	2.381	0.361	0.281
hsa-miR-212-3p	-2.031	-2.004	0.289	0.109
hsa-miR-221-5p	-1.709	-1.701	0.355	0.302
hsa-miR-23b-3p	-2.36	-2.331	0.272	0.096
hsa-miR-28-5p	-2.172	-2.244	0.254	0.24
hsa-miR-299-5p	2.031	2.599	0.354	0.184
hsa-miR-29b-1-5p	-1.854	-1.839	0.305	0.325
hsa-miR-301a-3p	-2.403	-2.385	0.28	0.141
hsa-miR-30d-5p	-2.397	-2.398	0.252	0.078
hsa-miR-30e-3p	-2.201	-2.151	0.272	0.26
hsa-miR-3132	-2.346	-2.333	0.301	0.231
hsa-miR-3195	-2.38	-2.353	0.288	0.126
hsa-miR-3196	-2.669	-2.621	0.262	0.094
hsa-miR-32-5p	-1.919	-1.931	0.291	0.233
hsa-miR-328	2.106	2.731	0.352	0.323
hsa-miR-335-3p	1.933	2.478	0.359	0.129
hsa-miR-337-3p	1.915	2.418	0.359	0.149
hsa-miR-339-3p	-1.606	-1.579	0.33	0.192
hsa-miR-33a-5p	-1.846	-2.042	0.234	0.148
hsa-miR-34b-3p	1.914	2.411	0.359	0.1
hsa-miR-3613-3p	1.897	2.403	0.36	0.195
hsa-miR-361-5p	-2.582	-2.5	0.262	0.102
hsa-miR-362-3p	-1.943	-1.952	0.337	0.148
hsa-miR-362-5p	-2.208	-2.17	0.271	0.125
hsa-miR-3646	1.619	2.09	0.375	0.329
hsa-miR-3665	-2.252	-2.251	0.284	0.107
hsa-miR-3685	1.454	2.012	0.387	0.1
hsa-miR-3714	1.632	2.139	0.374	0.217
hsa-miR-378_v17.0	-2.598	-2.594	0.252	0.151
hsa-miR-3907	-1.683	-1.552	0.367	0.362
hsa-miR-3935	1.884	2.366	0.361	0.133
hsa-miR-3940-3p	2.011	2.577	0.355	0.202
hsa-miR-423-3p	-1.665	-1.785	0.283	0.113
hsa-miR-423-5p	-2.043	-2.05	0.333	0.238
hsa-miR-424-5p	-2.296	-2.259	0.271	0.1
hsa-miR-4261	-1.774	-1.821	0.349	0.343
hsa-miR-4291	-2.292	-2.272	0.266	0.094
hsa-miR-4306	-2.125	-2.098	0.3	0.368
hsa-miR-4312	1.979	2.545	0.357	0.191
hsa-miR-431-3p	-1.529	-1.608	0.426	0.196
hsa-miR-4323	1.621	2.103	0.375	0.214

hsa-miR-4324	1.515	2.043	0.382	0.146
hsa-miR-449b-3p	2.094	2.722	0.352	0.242
hsa-miR-455-3p	-2.092	-2.096	0.271	0.154
hsa-miR-483-3p	1.878	2.354	0.361	0.21
hsa-miR-486-3p	-1.847	-1.919	0.3	0.209
hsa-miR-486-5p	-2.551	-2.56	0.24	0.179
hsa-miR-487b	-1.772	-1.778	0.331	0.304
hsa-miR-500a-3p	-1.824	-1.901	0.305	0.088
hsa-miR-501-3p	-1.829	-1.954	0.284	0.042
hsa-miR-532-3p	-2.106	-2.057	0.285	0.14
hsa-miR-532-5p	-2.314	-2.323	0.278	0.186
hsa-miR-574-3p	2.027	2.613	0.154	0.143
hsa-miR-574-5p	-1.852	-1.96	0.347	0.27
hsa-miR-584-5p	-2.196	-2.163	0.289	0.243
hsa-miR-590-5p	-2.506	-2.421	0.27	0.139
hsa-miR-595	1.959	2.507	0.357	0.221
hsa-miR-605	1.644	2.147	0.374	0.141
hsa-miR-615-3p	1.456	2.019	0.386	0.273
hsa-miR-631	1.667	2.177	0.372	0.164
hsa-miR-634	1.62	2.097	0.375	0.1
hsa-miR-638	-2.012	-1.99	0.303	0.13
hsa-miR-640	1.453	2.006	0.387	0.1
hsa-miR-642b-3p	-1.768	-1.931	0.331	0.342
hsa-miR-652-3p	-1.756	-1.691	0.28	0.201
hsa-miR-654-3p	1.646	2.154	0.374	0.1
hsa-miR-664a-3p	2.037	2.314	0.15	0.266
hsa-miR-7-2-3p	1.358	1.953	0.394	0.1
hsa-miR-744-3p	1.66	2.169	0.373	0.1
hsa-miR-744-5p	-2.153	-2.098	0.276	0.31
hsa-miR-762	-2.054	-2.21	0.27	0.114
hsa-miR-766-3p	1.864	2.342	0.362	0.353
hsa-miR-874	-1.699	-1.726	0.312	0.262
hsa-miR-885-5p	2.199	2.835	0.348	0.306
hsa-miR-892b	-1.553	-1.006	0.337	0.465
hsa-miR-940	-2.307	-2.727	0.21	0.067

An overlap for differentially expressed miRNA of 88% and 94% following GeneSpring and Partek analysis respectively was observed for MIA PaCa-2 cells following treatment with 1.5μM curcumin for 96 hours.

AsPC-1 miRNA Microarray GeneSpring and Partek Comparison Table.

Name	Log FC		p-value	
	GeneSpring	Partek	GeneSpring	Partek
hsa-let-7b-3p	3.957	3.69	0.103	0.132
hsa-let-7d-3p	3.96	3.682	0.102	0.17

hsa-let-7e-3p	1.731	1.188	0.303	0.407
hsa-let-7f-1-3p	2.085	2.032	0.3	0.281
hsa-miR-101-3p	-2.094	-2.123	0.225	0.306
hsa-miR-1183	-1.791	-1.674	0.313	0.099
hsa-miR-1226-3p	1.531	1.004	0.305	0.442
hsa-miR-1249	3.254	1.739	0.075	0.037
hsa-miR-125a-3p	-1.874	-1.708	0.274	0.399
hsa-miR-126-3p	-1.866	-1.693	0.258	0.443
hsa-miR-1287	-2.84	-1.448	0.129	0.106
hsa-miR-1288	-1.998	-1.877	0.277	0.367
hsa-miR-1290	-1.646	-1.293	0.33	0.432
hsa-miR-1296	1.863	1.566	0.301	0.334
hsa-miR-1307-3p	1.938	2.107	0.38	0.225
hsa-miR-140-5p	-1.697	-1.167	0.434	0.478
hsa-miR-150-5p	1.58	1.015	0.304	0.449
hsa-miR-152	-1.765	-1.47	0.287	0.41
hsa-miR-1539	1.717	1.103	0.303	0.434
hsa-miR-154-5p	1.712	1.087	0.303	0.1
hsa-miR-15a-3p	1.491	1.402	0.164	0.097
hsa-miR-1825	2.527	3.215	0.311	0.016
hsa-miR-193a-5p	-1.627	-1.271	0.295	0.309
hsa-miR-196b-3p	1.741	1.212	0.303	0.393
hsa-miR-1973	-4.614	-2.758	0.006	0.203
hsa-miR-197-3p	1.209	1.973	0.079	0.352
hsa-miR-1976	1.773	1.381	0.302	0.368
hsa-miR-200a-5p	-1.561	-1.014	0.31	0.455
hsa-miR-202-3p	-1.752	-1.573	0.306	0.123
hsa-miR-204-5p	3.319	2.448	0.105	0.299
hsa-miR-205-3p	-2.056	-2.148	0.263	0.058
hsa-miR-211-5p	2.034	1.864	0.3	0.396
hsa-miR-218-5p	-1.813	-1.575	0.299	0.106
hsa-miR-221-5p	-1.871	-1.762	0.241	0.286
hsa-miR-23a-5p	-1.676	-1.428	0.255	0.049
hsa-miR-28-5p	-1.773	-1.577	0.271	0.404
hsa-miR-296-5p	2.942	1.023	0.07	0.014
hsa-miR-299-5p	2.042	1.964	0.3	0.31
hsa-miR-30c-2-3p	-1.654	-1.272	0.306	0.413
hsa-miR-3125	-2.278	-2.285	0.238	0.369
hsa-miR-3127-5p	-2.107	-2.22	0.24	0.303
hsa-miR-3141	-3.208	-2.529	0.1	0.176
hsa-miR-3156-5p	-3.646	-3.309	0.078	0.135
hsa-miR-324-5p	-2.013	-1.922	0.294	0.138
hsa-miR-328	4.211	4.053	0.101	0.149

hsa-miR-335-5p	-1.805	-1.403	0.268	0.357
hsa-miR-337-3p	1.763	1.364	0.302	0.406
hsa-miR-33a-5p	-2.996	-1.787	0.089	0.202
hsa-miR-34b-5p	-3.455	-2.938	0.082	0.005
hsa-miR-3605-3p	2.012	1.845	0.3	0.1
hsa-miR-3613-3p	2.039	1.949	0.3	0.29
hsa-miR-3622a-3p	1.992	1.823	0.3	0.1
hsa-miR-3622b-3p	1.721	1.116	0.303	0.1
hsa-miR-362-5p	-2.774	-1.379	0.104	0.32
hsa-miR-3646	3.196	2.064	0.104	0.335
hsa-miR-3679-5p	-2.167	-2.261	0.199	0.294
hsa-miR-3714	2.041	1.953	0.3	0.258
hsa-miR-371a-5p	-3.297	-2.605	0.093	0.237
hsa-miR-378_v17.0	-2.109	-2.168	0.245	0.226
hsa-miR-378b	-1.825	-1.596	0.415	0.137
hsa-miR-3911	-1.908	-1.826	0.23	0.298
hsa-miR-3935	1.704	1.083	0.303	0.48
hsa-miR-3940-3p	3.951	3.637	0.101	0.078
hsa-miR-4298	-1.757	-1.399	0.356	0.432
hsa-miR-4306	-2.051	-2.034	0.267	0.382
hsa-miR-4312	2.072	2.012	0.3	0.297
hsa-miR-4313	3.288	1.967	0.071	0.021
hsa-miR-4317	-1.577	-1.177	0.293	0.372
hsa-miR-4323	3.572	2.984	0.105	0.084
hsa-miR-4324	1.912	1.589	0.353	0.253
hsa-miR-449b-3p	3.716	3.188	0.107	0.173
hsa-miR-454-3p	-2.855	-1.469	0.084	0.162
hsa-miR-455-3p	-1.994	-1.9	0.216	0.194
hsa-miR-483-3p	2.101	2.069	0.3	0.268
hsa-miR-483-5p	-1.77	-1.529	0.321	0.372
hsa-miR-485-3p	1.798	1.442	0.302	0.1
hsa-miR-500a-5p	-3.23	-2.432	0.097	0.049
hsa-miR-501-5p	-2.109	-1.548	0.263	0.023
hsa-miR-513a-5p	-3.484	-3.192	0.05	0.15
hsa-miR-513b	-1.723	-1.32	0.205	0.459
hsa-miR-517a-3p	-1.505	-1.234	0.45	0.02
hsa-miR-517c-3p	-2.925	-1.846	0.086	0.008
hsa-miR-519e-5p	-2.878	-1.586	0.138	0.145
hsa-miR-532-5p	-1.746	-1.621	0.271	0.351
hsa-miR-572	-3.106	-2.211	0.108	0.157
hsa-miR-574-3p	1.051	2.112	0.155	0.231
hsa-miR-595	1.881	1.578	0.301	0.435
hsa-miR-605	1.721	1.109	0.303	0.437

hsa-miR-615-3p	3.201	2.255	0.109	0.223
hsa-miR-630	-1.659	-1.064	0.397	0.494
hsa-miR-631	1.793	1.422	0.302	0.356
hsa-miR-636	2.739	1.543	0.108	0.012
hsa-miR-642b-3p	-1.815	-1.711	0.299	0.399
hsa-miR-650	-1.817	-1.76	0.234	0.026
hsa-miR-660-5p	-1.827	-1.595	0.262	0.309
hsa-miR-663a	-3.382	-2.947	0.062	0.112
hsa-miR-664a-3p	3.945	3.612	0.101	0.09
hsa-miR-766-3p	3.991	3.752	0.101	0.144
hsa-miR-885-5p	4.186	3.985	0.101	0.156
hsa-miR-892b	-2.095	-2.259	0.183	0.111

An overlap for differentially expressed miRNA of 56% and 92% following GeneSpring and Partek analysis respectively was observed for AsPC-1 cells following treatment with 1.5μM curcumin for 96 hours.

BxPC-3 miRNA Microarray GeneSpring and Partek Comparison Table.

Name	Log FC		p-value	
	GeneSpring	Partek	GeneSpring	Partek
hsa-let-7a-3p	-1.257	-1.072	0.328	0.285
hsa-let-7b-3p	1.987	2.09	0.333	0.383
hsa-miR-101-3p	3.496	2.751	0.138	0.189
hsa-miR-105-5p	-1.282	-1.083	0.327	0.1
hsa-miR-106b-3p	-1.294	-1.092	0.326	0.266
hsa-miR-1180	-1.977	-1.578	0.265	0.1
hsa-miR-1207-5p	-2.452	-2.522	0.246	0.184
hsa-miR-125a-3p	-3.69	-3.438	0.106	0.099
hsa-miR-128	3.513	2.857	0.139	0.177
hsa-miR-1281	1.691	1.072	0.248	0.281
hsa-miR-1288	-1.841	-1.8	0.299	0.386
hsa-miR-1306-3p	-2.167	-2.019	0.266	0.1
hsa-miR-1307-3p	-2.163	-1.999	0.266	0.249
hsa-miR-130a-3p	-1.632	-1.453	0.317	0.102
hsa-miR-132-5p	-1.532	-1.358	0.319	0.1
hsa-miR-134	2.089	1.795	0.255	0.1
hsa-miR-148a-3p	2.842	2.762	0.198	0.162
hsa-miR-148b-3p	4.181	3.446	0.092	0.089
hsa-miR-152	-3.2	-2.785	0.097	0.128
hsa-miR-155-5p	-2.077	-2.603	0.232	0.025
hsa-miR-181a-3p	-3.045	-2.223	0.098	0.008
hsa-miR-181d	-2.622	-2.501	0.269	0.24
hsa-miR-182-5p	1.787	1.543	0.305	0.308
hsa-miR-186-5p	3.505	2.767	0.135	0.135

hsa-miR-191-3p	3.145	2.178	0.073	0.019
hsa-miR-1914-3p	-1.936	-1.898	0.309	0.373
hsa-miR-192-5p	1.614	1.407	0.3	0.369
hsa-miR-1973	-3.922	-3.689	0.159	0.094
hsa-miR-19b-1-5p	-1.324	-1.109	0.325	0.313
hsa-miR-211-5p	2.09	2.147	0.331	0.329
hsa-miR-221-5p	-3.151	-2.61	0.098	0.12
hsa-miR-2276	2.187	1.981	0.256	0.1
hsa-miR-24-1-5p	-1.564	-1.411	0.318	0.107
hsa-miR-3132	-2.16	-2.196	0.271	0.259
hsa-miR-3137	1.925	1.415	0.252	0.1
hsa-miR-3138	1.902	1.364	0.252	0.1
hsa-miR-3176	1.712	1.076	0.248	0.128
hsa-miR-3188	-1.9	-1.453	0.264	0.1
hsa-miR-33a-5p	1.632	1.435	0.3	0.302
hsa-miR-3610	1.978	1.468	0.253	0.1
hsa-miR-3654	1.894	1.352	0.252	0.1
hsa-miR-3656	-3.883	-3.717	0.143	0.06
hsa-miR-365a-3p	2.704	2.39	0.219	0.074
hsa-miR-3663-3p	2.106	1.823	0.255	0.1
hsa-miR-3663-5p	-1.991	-1.665	0.265	0.1
hsa-miR-3679-5p	-1.805	-1.824	0.348	0.395
hsa-miR-3682-3p	1.933	1.428	0.252	0.1
hsa-miR-3692-5p	1.9	1.358	0.252	0.1
hsa-miR-374b-5p	2.233	2.211	0.291	0.095
hsa-miR-3911	2.01	1.552	0.253	0.374
hsa-miR-3917	-2.105	-1.845	0.266	0.1
hsa-miR-423-5p	-1.829	-1.975	0.283	0.255
hsa-miR-424-3p	1.95	1.435	0.253	0.1
hsa-miR-4317	-1.634	-1.358	0.287	0.305
hsa-miR-4322	-2.142	-1.953	0.266	0.1
hsa-miR-432-5p	-2.188	-2.053	0.267	0.1
hsa-miR-449b-3p	1.8	1.845	0.338	0.423
hsa-miR-486-5p	3.42	2.71	0.137	0.156
hsa-miR-494	-1.074	-1.344	0.341	0.157
hsa-miR-513a-5p	-4.149	-3.978	0.115	0.077
hsa-miR-513b	-3.215	-2.699	0.158	0.139
hsa-miR-516a-5p	1.68	1.01	0.248	0.114
hsa-miR-532-5p	-1.533	-1.364	0.319	0.431
hsa-miR-564	1.717	1.083	0.249	0.1
hsa-miR-572	-2.879	-2.394	0.215	0.127

hsa-miR-574-3p	-3.442	-2.771	0.085	0.121
hsa-miR-574-5p	-2.132	-2.203	0.265	0.217
hsa-miR-575	-2.042	-2.014	0.302	0.35
hsa-miR-595	-2.056	-1.716	0.266	0.397
hsa-miR-615-3p	1.623	1.81	0.343	0.324
hsa-miR-622	1.927	1.422	0.252	0.124
hsa-miR-623	-2.344	-2.201	0.268	0.1
hsa-miR-642b-3p	-2.499	-2.57	0.243	0.21
hsa-miR-652-3p	-3.203	-2.798	0.097	0.041
hsa-miR-662	1.905	1.381	0.252	0.1
hsa-miR-664a-3p	1.807	1.859	0.338	0.368
hsa-miR-671-5p	1.957	1.448	0.253	0.1
hsa-miR-7-1-3p	3.616	2.862	0.134	0.143
hsa-miR-765	1.721	1.097	0.249	0.1
hsa-miR-874	-1.559	-1.234	0.34	0.419
hsa-miR-892b	2.734	2.033	0.066	0.148
hsa-miR-99b-3p	-1.554	-1.188	0.261	0.1

An overlap for differentially expressed miRNA of 85% and 80% following GeneSpring and Partek analysis respectively was observed for BxPC-3 cells following treatment with 1.5μM curcumin for 96 hours.